THREE-DIMENSIONAL VECTOR MODELING AND RESTORATION OF FLAT FINITE WAVE TANK RADIOMETRIC MEASUREMENTS

by

William M. Truman

Constantine A. Balanis

FINAL REPORT

Prepared by

Department of Electrical Engineering
West Virginia University
Morgantown, West Virginia 26506

For

National Aeronautics and Space Administration
Langley Research Center
Hampton, Virginia 23665

Grant No. NGR 49-001-056

May 15, 1977

Acknowledgement

The authors would like to thank John J. Holmes of the Department of Electrical Engineering, West Virginia University, for his two-dimensional calculations and helpful recommendations. Also we wish to thank J.W. Johnson, Dr. W.L. Jones, B.M. Kendall, and Dr. C.T. Swift of NASA, Langley Research Center for their interest, availability of measurements, and valuable discussions throughout the project.

The project was supported by NASA, Langley Research Center, Hampton, Virginia, under Grant No. NGR 49-001-056.

TABLE OF CONTENTS

Page

LIST OF FIGURES

Figure Page

Figure | Page

LIST OF TABLES

Table		Page

Table		Page

Table | Page

Table		Page
XXXVII	Restored antenna temperatures for finite wave tank with random error, interpolation, and one restoration (antenna = 12λ horn, ρ = 13 feet, f = 10.69 GHz, T_m = 284°K, S = 0 o/oo)	143
XXXVIII	Restored antenna temperatures for finite wave tank with random error, interpolation, and three restorations (antenna = 12λ horn, ρ = 13 feet, f = 10.69 GHz, T_m = 284°K, S = 0 o/oo)....	144
XXXIX	Restored antenna temperatures for finite wave tank with random error, interpolation, and one restoration (antenna = 8λ horn, ρ = 13 feet, f = 10.69 GHz, T_m = 284°K, S = 0 o/oo)	145
XL	Restored antenna temperatures for finite wave tank with random error, interpolation, and three restorations (antenna = 8λ horn, ρ = 13 feet, f = 10.69 GHz, T_m = 284°K, S = 0 o/oo)....	146
XLI	Restored antenna temperatures for finite wave tank with random error, interpolation, and one restoration (antenna = 12λ horn, ρ = 26 feet, f = 10.69 GHz, T_m = 284°K, S = 0 o/oo)	147
XLII	Restored antenna temperatures for finite wave tank with random error, interpolation, and three restorations (antenna = 12λ horn, ρ = 26 feet, f = 10.69 GHz, T_m = 284°K, S = 0 o/oo)..........	148
XLIII	Restored antenna temperatures for finite wave tank with random error, interpolation, and one restoration (antenna = 8λ horn, ρ = 26 feet, f = 10.69 GHz, T_m = 284°K, S = 0 o/oo)	149
XLIV	Restored antenna temperatures for finite wave tank with random error, interpolation, and three restorations (antenna = 8λ horn, ρ = 26 feet, f = 10.69 GHz, T_m = 284°K, S = 0 o/oo)	150
XLV	Optimum restoration for the finite wave tank with the 12λ horn antenna and the 13 foot boom..	157
XLVI	Optimum restoration for the finite wave tank with the 8λ horn antenna and the 13 foot boom...	158

Table		Page
XLVII	Optimum restoration for the finite wave tank with the 12λ horn antenna and the 26 foot boom ...	159
XLVIII	Optimum restoration for the finite wave tank with the 8λ horn antenna and the 26 foot boom	160
XLIX	Antenna temperatures for the finite wave tank with cross-polarization (antenna = 12λ horn, ρ = 13 feet, f = 10.69 GHz, T_m = 284°K, S = 0 o/oo)	162
L	Antenna temperatures for the finite wave tank with cross-polarization (antenna = 8λ horn, ρ = 13 feet, f = 10.69 GHz, T_m = 284°K, S = 0 o/oo)	163
LI	Antenna temperatures for the finite wave tank with cross-polarization (antenna = 12λ horn, ρ = 26 feet, f = 10.69 GHz, T_m = 284°K, S = 0 o/oo)	164
LII	Antenna temperatures for the finite wave tank with cross-polarization (antenna = 8λ horn, ρ = 26 feet, f = 10.69 GHz, T_m = 284°K, S = 0 o/oo)	165
LIII	Restored antenna temperatures for finite wave tank with -20 dB cross-polarization and three restorations (antenna = 12λ horn, ρ = 13 feet, f = 10.69 GHz, T_m = 284°K, S = 0 o/oo)	166
LIV	Restored antenna temperatures for finite wave tank with -20 dB cross-polarization and three restorations (antenna = 8λ horn, ρ = 13 feet, f = 10.69 GHz, T_m = 284°K, S = 0 o/oo)	168
LV	Restored antenna temperatures for finite wave tank with -20 dB cross-polarization and three restorations (antenna = 12λ horn, ρ = 26 feet, f = 10.69 GHz, T_m = 284°K, S = 0 o/oo)	169
LVI	Restored antenna temperatures for finite wave tank with -20 dB cross-polarization and three restorations (antenna = 8λ horn, ρ = 26 feet, f = 10.69 GHz, T_m = 284°K, S = 0 o/oo)	170

Table Page

I. Introduction

For years man had desired the capability to remotely monitor various phenomenon in his environment. For example, the measurement of ocean wave and wind conditions are of vital interest to many marine industries and government agencies. Furthermore, the knowledge of ocean-surface temperature on a global, all-weather, and day-night basis is also of importance to the fishery and marine transport industries, as well as the oceanographers and marine meterorologists, and weather forcasters. In recent years, the microwave radiometer has proven itself to be a feasible remote sensing device. To monitor the environment on an all-weather basis, microwave sensing has the immediate advantage of being affected less by fog and rain than infrared. In addition, microwave radiometers have been designed [1] that can measure the incident radiation to an accuracy of $\pm$ 0.1 $^{\circ}$K and remain calibrated, unattended, for a year or more. In fact, small, lightweight, automated radiometer systems have recently been flown by NASA on the Nimbus satellite program [2]. There is presently a great deal of research and development being conducted in the area of microwave remote sensing from satellites.

In order to make precise measurements of the radiometric brightness temperature of a target (and thereby infer certain physical parameters) one must be able to mathematically model the interaction between the electromagnetic radiation properties of the antenna and the incident radiation from the environment. This interaction can be described by Fredholm integral equations of the first kind which are extremely unstable. This instability has been studied in considerable detail by investigators in many fields. Twomey [3] and Phillips [4] have devised matrix filtering techniques to stabilize the solution. Although these matrix methods are not without merit, Bracewell and Roberts [5] have demonstrated the value of a successive substitution solution. Assuming that the intensity of the emitted radiation of the environment can be represented in scalar form, they have shown that the antenna is only capable of responding to those frequency components of the function representing the environment below a cut-off determined by the antenna aperture. The high frequency components of the emission function are invisible to the antenna. The low frequency components are accepted but their relative magnitude is altered according to the system (antenna) frequency characteristics. Inversion through the method of successive restorations leads to the principal solution [5], in which frequency components accepted by the antenna have been restored to their original values, but the rejected components are not represented in the solution. The work done by Bracewell and Roberts was, however, more applicable to astronomical observations than to general microwave radiometric measurements. They assumed that the antenna was very efficient and that the sidelobes and backlobes could be neglected, which is not always the case. They also used a scalar representation of the interaction between the antenna radiation characteristics and the emission by the target.

The interaction between the emitted radiation from a water surface and the radiation characteristics of an antenna is a vector relationship. As the sidelobe and backlobe levels of the system (antenna) weighting function become more intense, and the major lobe beamwidth more wide, the vector model interaction becomes more important. Classen and Fung [6] have vectorially modeled the viewing of the ocean using matrix techniques. Their representation, however, assumes that the observed environment is circularly symmetric and infinite in extent. It should also be pointed out that computer time using the matrix modeling would be quite extensive as compared to some other types of numerical techniques.

To study the radiometric signature of a controlled water surface, a wave tank system has been constructed at NASA Langley Research Center, Hampton, Virginia. For the wave tank geometry, the environment is of finite extent and is no longer circularly symmetric. The response of the radiometer for this system was first modeled by Fisher [7], using a two-dimensional scalar approximation. This approximation works well for high efficiency antennas. The direct inversion used by Fisher [7] was, however, sensitive to errors. Holmes [8], by applying the iteration techniques of Bracewell and Roberts [5] to this problem, was able to restore, with acceptable accuracy, the brightness temperature (scalar emission function) of the water from measurements that contained error. Both Holmes [8] and Fisher [7] used the Fast Fourier Transform techniques, with an algorithm reported by Fisher [9], to perform their computations.

The first three-dimensional modeling of the NASA wave tank was done by Beck [10]. He was able to formulate and calculate the antenna response of the system given the emission characteristics of the surroundings. Beck's formulation requires numerical integration for direct computation of the antenna temperature and is not convenient for inversion processes nor can it be modified conveniently for efficient and economic restoration computations.

The classical design consideration of a radiometer antenna is the compromise between resolution and system design constraints (size, frequency, etc.). Only after the inversion process has been studied is the true resolution of the antenna known and can the design for the particular application be made. The study of this inversion for the wave tank geometry is the subject of this dissertation. A three-dimensional inversion scheme is described which takes into account the interaction between the radiation characteristics of the antenna and emitted radiation from the wave tank (vector representation), and computations are performed using the efficient and economical Fast Fourier Transform algorithm. The inherent instabilities of the inversion are overcome by the adoption of the filtering properties of the restoration method.

II. Theory

A. Brightness Temperature

All matter above absolute zero temperature emits electromagnetic radiation due to the thermal motion of its atoms/molecules. The brightness temperature of a given substance is a standard measure of the intensity of this radiation. By definition, the brightness temperature of a perfect black body radiator is equal to its molecular temperature. For the perfect black body radiator, none of the electromagnetic radiation generated from within the body is reflected back at the interface between the radiating surface and the surrounding transmission media. For all passive physical objects, however, the transmission coefficients for the radiating surface are less than unity. Consequently, the brightness temperature will be less than the molecular temperature. The transmission coefficient is often called the emissivity, and the brightness and molecular temperatures are related by

$$T_b = \varepsilon T_m \qquad (1)$$

where T_b is the brightness temperature, T_m the molecular temperature, and ε the emissivity or transmission coefficient.

For a flat semi-infinite radiating surface the emissivity can be found from the complex dielectric properties of the radiator. The emissivity is also a function of both the incidence angle at which the interface is viewed and the polarization of the emitted wave. Stogryn [11] and Holmes [8] have shown how the emissivity is related to the complex permittivity of the radiator. For the perpendicular (horizontal) polarization the E-field is perpendicular to the plane of incidence and the emissivity is given as [8]

$$\varepsilon_h(\theta'') = \frac{4\,p\cos\theta''}{(\cos\theta'' + p)^2 + q^2} \tag{2}$$

where

$$\gamma = \frac{1}{2}\tan^{-1}\left(\frac{\varepsilon''}{\varepsilon' - \sin^2\theta''}\right)$$

$\theta'' \equiv$ incidence angle

$p = \sqrt{r}\cos\gamma$

$q = \sqrt{r}\sin\gamma$

$$r = \sqrt{(\varepsilon' - \sin^2\theta'')^2 + \varepsilon''^2} \tag{3}$$

$\varepsilon' = \mathrm{Re}[\varepsilon_r]$

$\varepsilon'' = \mathrm{Im}[\varepsilon_r]$

$\varepsilon_r \equiv$ complex dielectric constant of the radiator

For the parallel (vertical) polarization the E-field is parallel to the plane of incidence and the emissivity is expressed as

$$\varepsilon_v(\theta'') = \frac{4\,p\,\varepsilon'\cos\theta'' + 4\,q\,\varepsilon''\cos\theta''}{(\varepsilon'\cos\theta'' + p)^2 + (\varepsilon''\cos\theta'' + q)^2} \tag{4}$$

Through (2) and (4), the radiation is being described as two orthogonal, linearly polarized waves. The radiation from the surface of the water can be described in this manner if the dielectric properties of the water are known. Stogryn [11] has concluded that the dielectric constant ε_r for sea water may be adequately represented by the following equation of the Debye form

$$\varepsilon_r = \varepsilon_\infty + \frac{\varepsilon_0 - \varepsilon_\infty}{1 - j\, 2\pi\, \tau\, f} + \frac{j\sigma}{2\pi\, \varepsilon_0^*\, f} \tag{5}$$

where ε_0 and ε_∞ are, respectively, the static and high frequency dielectric constants of the solvent, τ the relaxation time, ε_0^* the permittivity of free space (= 8.854×10^{-12} farads/m), σ the ionic conductivity of the dissolved salt in mhos/m, and f the electromagnetic frequency.

In order to evaluate (5), the variations of ε_0, τ, and σ as functions of salinity, frequency, and temperature need to be known. By using resonant cavity techniques, Stogryn [11] reported, through numerous measurements, empirical equations to evaluate the variables.

The high frequency dielectric constant ε_∞ is considered to be a constant (=0.48). The low frequency dielectric constant ε_0 and the relaxation time τ are expressed as

$$\varepsilon_0(T,N) = \varepsilon_0(T,0)\ a(N) \tag{6}$$

$$2\pi\tau(T,N) = 2\pi\tau(T,0)\ b(T,N) \tag{7}$$

where T is the water temperature in $^\circ$C and N is the normality of the solution. The series expansions used to evaluate (6) and (7) for $0 \le T \le 40^{\circ}C$ and $0 \le N \le 3$ are

$$a(N) = 1.0 - 0.2551\,N + 5.151 \times 10^{-2} N^{2} - 6.889 \times 10^{-3} N^{3} \tag{8}$$

$$b(N,T) = 1.463 \times 10^{-3}\,N\,T + 1.0 - 0.04896\,N - 0.02967\,N^{2} + 5.644 \times 10^{-3} N^{3} \tag{9}$$

$$\varepsilon_{0}(T,0) = 87.74 - 0.40008\,T + 9.398 \times 10^{-4} T^{2} + 1.410 \times 10^{-6} T^{3} \tag{10}$$

$$2\pi\tau(T,0) = 1.1109 \times 10^{-10} - 3.824 \times 10^{-12} T + 6.938 \times 10^{-14} T^{2} - 5.096 \times 10^{-16} T^{3} \tag{11}$$

Given the salinity in parts per thousand, the normality can be found as

$$N = S\,(1.707 \times 10^{-2} + 1.205 \times 10^{-5} S + 4.058 \times 10^{-9} S^{2}) \tag{12}$$

The series is valid for $0 \le S \le 260$. The expression reported for the conductivity σ of sea water is

$$\sigma(T,S) = \sigma(25,S)\,e^{-\Delta\zeta} \tag{13}$$

where $\Delta = 25 - T$ and

$$\zeta = 2.033 \times 10^{-2} + 1.266 \times 10^{-4} \Delta + 2.464 \times 10^{-6} \Delta - S\,(1.849 \times 10^{-5} - 2.551 \times 10^{-7} \Delta + 2.551 \times 10^{-8} \Delta^{2}) \tag{14}$$

$$\sigma(25,S) = S(0.182521 - 1.46192 \times 10^{-3} S + 2.09324 \times 10^{-5} S^2 - 1.28205 \times 10^{-7} S^3) \quad (15)$$

in the range $0 \leq S \leq 40$.

Using (6) - (15) we can obtain ε' and ε'' from (5). With ε' and ε'', $\varepsilon_h(\theta'')$ and $\varepsilon_v(\theta'')$ are found by the use of (2), (3), and (4). As seen by (1), the horizontal and vertical brightness temperatures of the polarized radiation emitted by the water are

$$T_{bwh}(\theta'') = \varepsilon_h(\theta'')T_m \quad (16a)$$

$$T_{bwv}(\theta'') = \varepsilon_v(\theta'')T_m \quad (16b)$$

Equations (16a) and (16b) yield the intensities of two linearly polarized, orthogonal waves that are needed to describe the radiation emitted from the water.

Brightness temperatures of the earth and sky were also part of this investigation. These brightness temperatures have been found (experimentally) to be nearly randomly polarized and therefore related to molecular temperature by (1). For the sky, Peake [12] expressed the brightness temperature as

$$T_{bs}(\theta_s) = T_{eff}[1 - e^{-\tau_o \sec\theta_s}] \quad (17)$$

where

$$T_{eff} = 1.12\ T_m - 50 \quad (18)$$

$$\tau_0 = -\log_e(1-3/T_{eff}) \tag{19}$$

The angle θ_s is the angle measured from zenith. For the lack of a more accurate brightness temperature model, the earth emissions are usually assumed to be constant and unpolarized. If a more accurate polarized brightness temperature model were known, it could be utilized in the analysis and computations.

In addition to its own generated radiation, the water surface reflects the incident sky radiation and directs it toward the receiving antenna. To account for this reflection, (16a) and (16b) can be modified as

$$T_{bwh}(\theta'') = \varepsilon_h(\theta'')T_m + (1-\varepsilon_h)T_{bs}(\theta_s=\theta'') \tag{20a}$$

$$T_{bwv}(\theta'') = \varepsilon_v(\theta'')T_m + (1-\varepsilon_v)T_{bs}(\theta_s=\theta'') \tag{20b}$$

In Figure 1, we have plotted T_{bwh} and T_{bwv} as functions of incidence angle for $T_m = 284^\circ K$, S = 0 ‰, and f = 10.69 GHz. The shape of the plots are basically the same for any temperature, salinity, and frequency. The peak in the T_{bwv} curve occurs when the water is viewed at the Brewster angle ($\varepsilon_v = 1$). At this angle, T_{bwv} is equal to the molecular temperature of the water.

B. Antenna Temperature

The antenna temperature measured by a radiometer is the brightness temperature of the observed environment weighted by the power pattern of the antenna. We shall define $T_b(\theta,\phi)$ as the

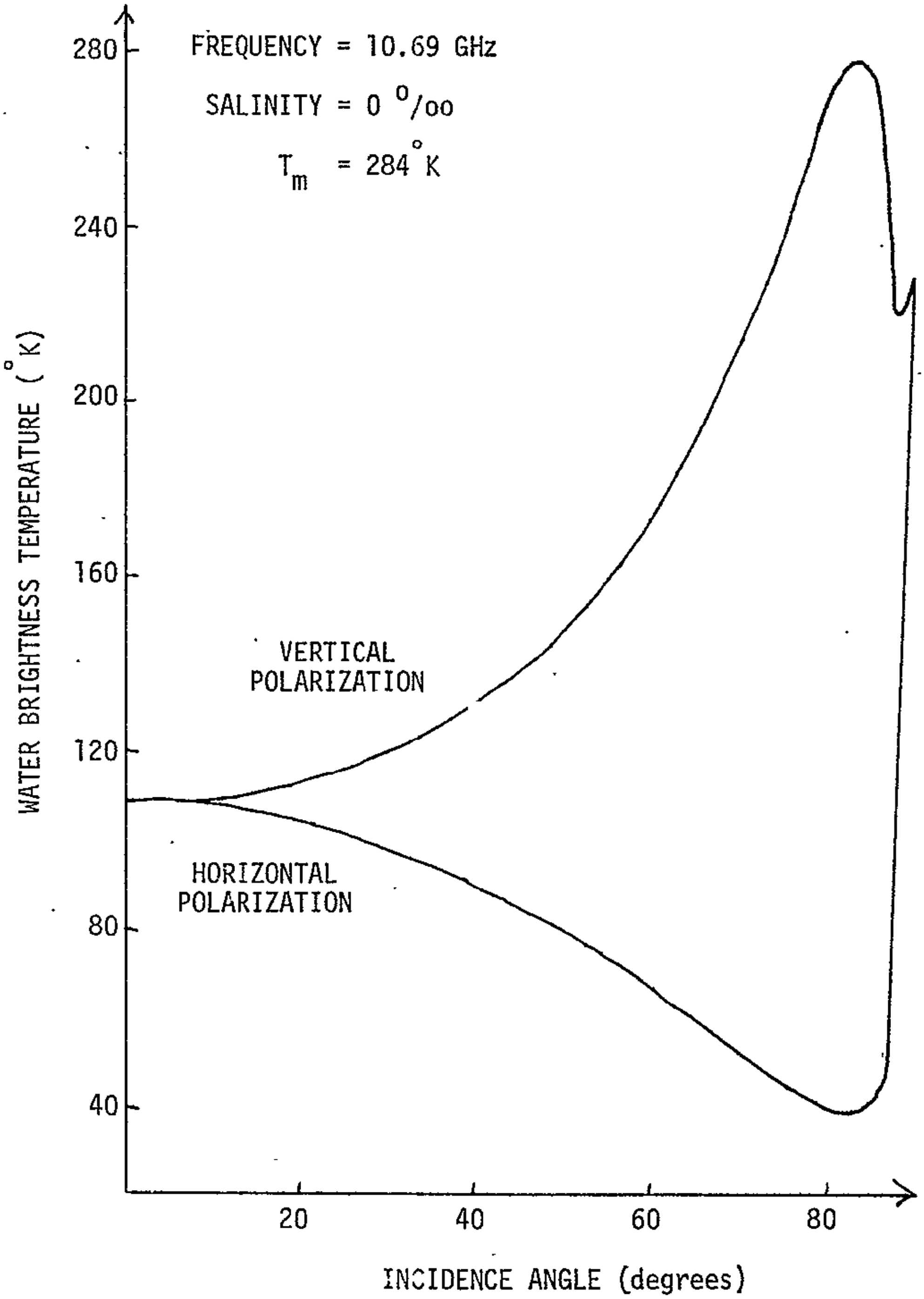

Fig. 1. Water brightness temperatures.

unpolarized brightness temperature of the environment, T_a the measured antenna temperature, and $G(\theta,\emptyset)$ the antenna power pattern which has been normalized so that the integral of $G(\theta,\emptyset)$ over the entire solid angle is equal to unity. The variables are related by the following relationship

$$T_a = \int_0^{2\pi} \int_0^{\pi} T_b(\theta,\emptyset)\; G(\theta,\emptyset)\; \sin\theta \; d\theta \; d\emptyset \qquad (21)$$

If $G(\theta,\emptyset)$ were a delta function $\delta(\theta-\theta_o,\emptyset-\emptyset_o)$, T_a would then equal $T_b(\theta_o,\emptyset_o)$. Practical antennas, however, do not have such convenient radiation characteristics, and T_a is generally not equal to the T_b at boresight.

If a significant fraction of the emitted radiation from the observed environment (brightness temperature) is polarized, such as that emitted by the water surface, (21) is no longer a valid expression to be used to calculate the antenna temperature. To explain the coupling between the radiation properties of the antenna and emitted polarized radiation from the environment as well as the concept of partial and total antenna temperatures, let us assume that the radiometer system is over the ocean in clear atmospheric surroundings. Since the observed environment is the water and sky, the total antenna temperature T_a is equal to the contributions from the water T_{aw} and sky T_{as}. Assuming that the radiation from the sky is unpolarized, T_{as} is expressed as

$$T_{as} = \iint\limits_{\substack{\text{over} \\ \text{sky}}} T_{bs}(\theta,\emptyset)\ G(\theta,\emptyset)\ \sin\theta\ d\theta\ d\emptyset \qquad (22)$$

Since the radiation emitted from the water is polarized, to find its antenna temperature contribution,the weight of the gain function $G(\theta,\emptyset)$ needs to be found at each integration point in directions perpendicular and parallel to the plane of incidence. To do this, we form the unit vectors $\hat{h}(\theta,\emptyset)$ and $\hat{v}(\theta,\emptyset)$ within the water integration limits. The vector $\hat{h}(\theta,\emptyset)$ is perpendicular to the plane of incidence formed at the integration point on the water surface, and $\hat{v}(\theta,\emptyset)$ is orthogonal to $\hat{h}(\theta,\emptyset)$ and $\hat{r}(\theta,\emptyset)$, where $\hat{r}(\theta,\emptyset)$ is the radial unit vector. For a given antenna, the normalized electric field intensities in the $\hat{\theta}(\theta,\emptyset)$ and $\hat{\emptyset}(\theta,\emptyset)$ directions, $E_\theta(\theta,\emptyset)$ and $E_\emptyset(\theta,\emptyset)$, can also be found. In turn, the power intensities, at each integration point, for the horizontal and vertical polarizations, G^h and G^V, are then formulated as

$$G^h(\theta,\emptyset) = [\hat{h} \cdot \hat{\theta}\ E_\theta + \hat{h} \cdot \hat{\emptyset}\ E_\emptyset]^2 \qquad (23)$$

$$G^V(\theta,\emptyset) = [\hat{v} \cdot \hat{\theta}\ E_\theta + \hat{v} \cdot \hat{\emptyset}\ E_\emptyset]^2 \qquad (24)$$

The antenna temperature contribution from the water can then be expressed as

$$T_{aw} = \iint_{\substack{\text{over}\\\text{water}}} T_{bwh}(\theta,\emptyset)\ G^{h}(\theta,\emptyset)\ \sin\theta\ d\theta\ d\emptyset$$

$$+ \iint_{\substack{\text{over}\\\text{water}}} T_{bwv}(\theta,\emptyset)\ G^{v}(\theta,\emptyset)\ \sin\theta\ d\theta\ d\emptyset \qquad (25)$$

The total temperature measured by the radiometer is

$$T_a = T_{as} + T_{aw} \qquad (26)$$

Equations (22) and (25) define the relationships between the power pattern of the antenna, the brightness temperature functions of the observed environment, and the measured antenna temperature for both unpolarized and polarized emissions.

C. Wave Tank Geometry and Theory

In order to obtain the microwave emission signature of a water surface in a controlled environment, a wave tank system has been constructed at NASA Langley Research Center, Hampton, Virginia. The model, as illustrated in Figure 2, consists of a fourteen foot square tank with the antenna and radiometer placed at the end of a boom over the tank. The antenna and radiometer can move along a circular arc above the tank and can be scanned, at each position, through a complete 360° in a plane which bisects the wave tank. The angle β is the scanning angle and α describes the position of the boom.

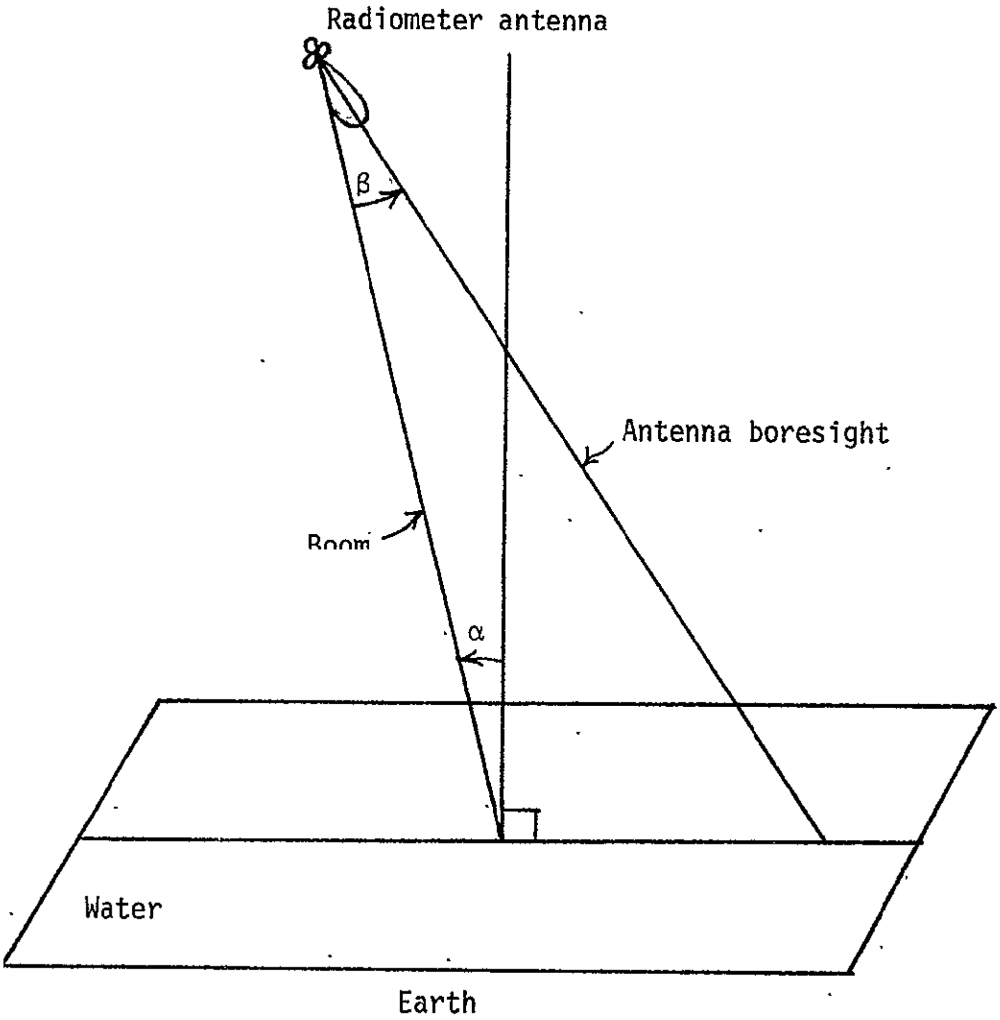

Fig. 2. Radiometer and Finite Wave Tank Configuration at NASA Langley Research Center, Hampton, Virginia.

For the wave tank measurements, the total antenna temperature is composed of three partial antenna temperatures; namely that of the water, earth, and sky. The partial antenna temperatures are of the same form as (22) and (25) and are given by

$$T_{aw} = \iint\limits_{\substack{\text{over}\\ \text{water}}} T_{bwh}(\theta,\phi)\, G^h(\theta,\phi)\, \sin\theta\, d\theta\, d\phi$$

$$+ \iint\limits_{\substack{\text{over}\\ \text{water}}} T_{bwv}(\theta,\phi)\, G^v(\theta,\phi)\, \sin\theta\, d\theta\, d\phi \qquad (27)$$

$$T_{ae} = \iint\limits_{\substack{\text{over}\\ \text{earth}}} T_{be}(\theta,\phi)\, G(\theta,\phi)\, \sin\theta\, d\theta\, d\phi \qquad (28)$$

$$T_{as} = \iint\limits_{\substack{\text{over}\\ \text{sky}}} T_{bs}(\theta,\phi)\, G(\theta,\phi)\, \sin\theta\, d\theta\, d\phi \qquad (29)$$

where G^h and G^v are defined by (23) and (24), respectively. The total antenna temperature T_a is then equal to $T_{aw} + T_{ae} + T_{as}$.

1. Z-Axis Normal to Radiometer Antenna Aperture

Patterns from directional antennas used in radiometry, such as horns, are nearly circular symmetric about the boresight. It would therefore be convenient to express the gain functions in a coordinate system which uses the z-axis as the boresight. The problem was originally formulated in this manner by Beck [10]. The coordinate systems used are illustrated in Figures 3 and 4. The origin of the x,y,z coordinate system is the phase center of the antenna and the origin of the x', y', z' coordinate system is the center of the wave tank. Although the radiometer antenna may be of any type, let us assume one with an aperture E-field polarized in the $\hat{x}$ direction (aperture E-field parallel to the x-z or $x' - z'$ plane of Figure 3). This type of antenna has a strongly polarized pattern. As the antenna is scanned parallel to the x-z plane, as shown in Figure 3, the antenna will principally see the vertically polarized emissions from the water. When scanned parallel to the y-z plane, as shown in Figure 4, the horizontal polarization will predominate. In the system implementation, if the boom is allowed to move only along one plane, the system polarization can be changed by simply rotating the antenna aperture 90° about the z-axis. The system at NASA has, however, the capacity to move along either plane. To describe both rotations, shown in Figures 3 and 4, with one set of functions, a fictitious constant ϕ_0 is introduced which is set equal to zero when the rotation is as shown in Figure 3 (vertical polarization scan) and equal to $\pi/2$ for the scanning displayed in Figure 4 (horizontal polarization scan).

The two variable brightness temperature profiles in (27), $T_{bwh}(\theta,\phi)$ and $T_{bwv}(\theta,\phi)$, can be expressed as a function of a single incidence angle variable θ''. To find θ'', one begins with the relationship between the primed and unprimed rectangular unit vectors of

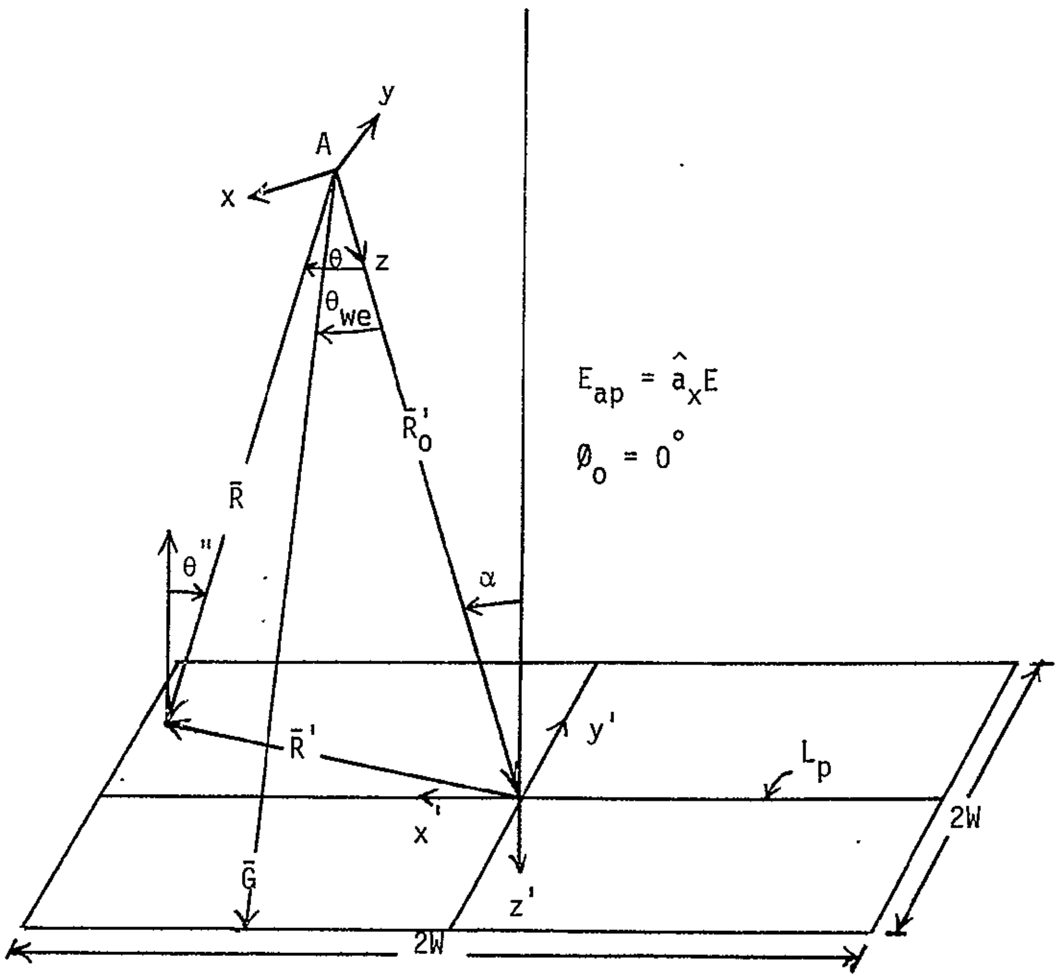

Fig. 3. Z-axis Coordinate System Orientation for Vertical Polarization.

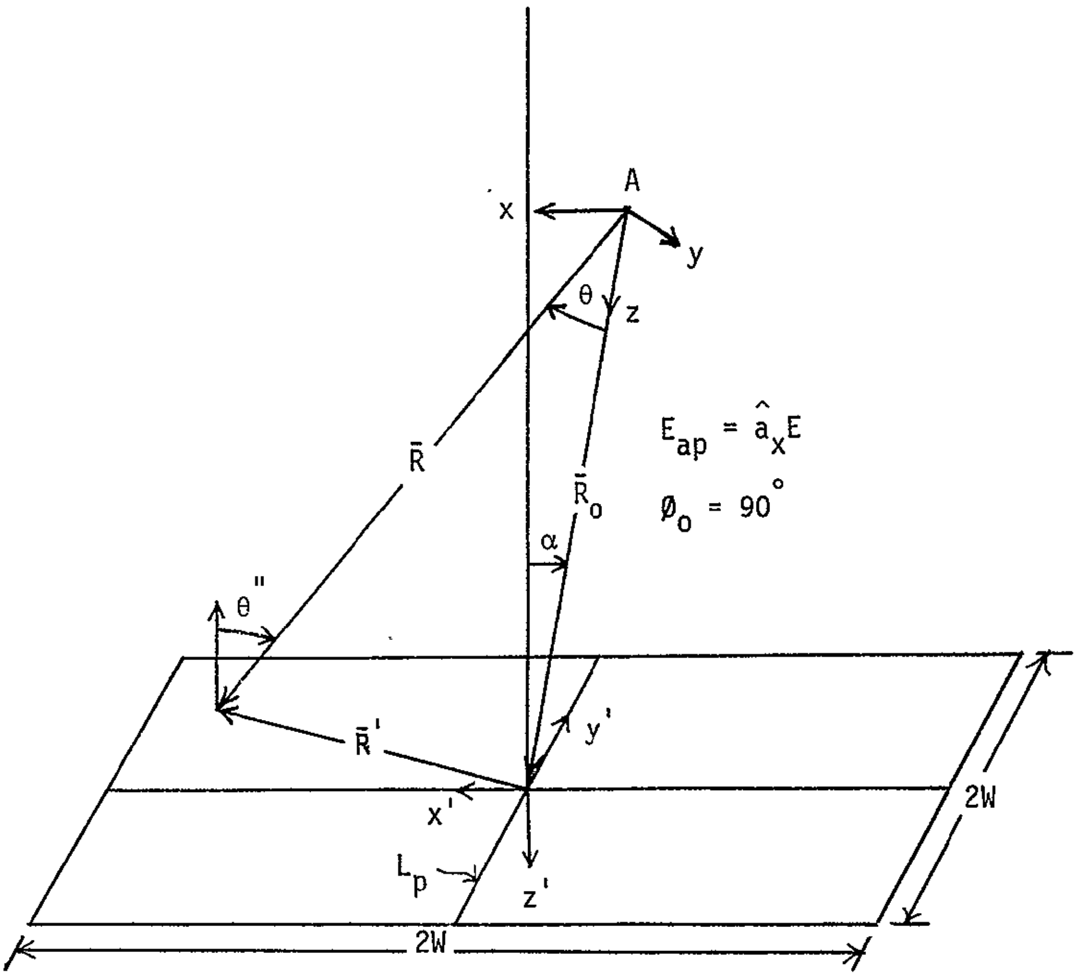

Fig. 4. Z-axis Coordinate System Orientation for Horizontal Polarization.

Figures 3 and 4 which are written as

$$\hat{x} = \hat{x}'(\cos\alpha \cos\phi_0 + \sin\phi_0) + \hat{z}' \sin\alpha \cos\phi_0 \qquad (30a)$$

$$\hat{y} = \hat{y}'(\cos\alpha \sin\phi_0 + \cos\phi_0) + \hat{z}' \sin\alpha \sin\phi_0 \qquad (30b)$$

$$\hat{z} = - \hat{x}' \sin\alpha \cos\phi_0 - \hat{y}' \sin\alpha \sin\phi_0 + \hat{z}' \cos\alpha \qquad (30c)$$

The angle θ'' can be expressed as

$$\cos\theta'' = \bar{R} \cdot \hat{z}' / |\bar{R}| \, |\hat{z}'| \qquad (31)$$

where

$$\bar{R} = R \, \hat{r} = R(\hat{x} \sin\theta \cos\phi + \hat{y} \sin\theta \sin\phi + \hat{z} \cos\theta) \qquad (32)$$

Substituting (30a), (30b), and (30c) into (32), one obtains

$$\bar{R} = R(R_x \hat{x}' + R_y \hat{y}' + R_z \hat{z}')$$

$$\begin{aligned}\bar{R} = R \{&\hat{x}' [\sin\theta \cos\phi (\cos\alpha \cos\phi_0 + \sin\phi_0) - \sin\alpha \cos\phi_0 \cos\theta] \\ &+ \hat{y}' [\sin\theta \sin\phi (\cos\alpha \sin\phi_0 + \cos\phi_0) - \sin\alpha \sin\phi_0 \cos\theta] \\ &+ \hat{z}' [\sin\theta \cos\phi \sin\alpha \cos\phi_0 + \sin\theta \sin\phi \sin\alpha \sin\phi_0 \\ &+ \cos\theta \cos\alpha]\}\end{aligned} \qquad (33)$$

Since the magnitude of the unit vector $\hat{z}'$ is unity and $\bar{R} \cdot \hat{z}'$ is known from (33), $\cos\theta''$ in (31) can now be expressed as

$$\cos\theta'' = \sin\theta \cos\emptyset \sin\alpha \cos\emptyset_0 + \sin\theta \sin\emptyset \sin\alpha \sin\emptyset_0 + \cos\theta \cos\alpha \quad (34)$$

This allows the evaluation of the incidence angle θ'' as a function of θ, $\emptyset$, α, and polarization ($\emptyset_0$).

In order to evaluate $G^h(\theta,\emptyset)$ and $G^v(\theta,\emptyset)$ for the z-axis geometry, $\hat{h}(\theta,\emptyset,\alpha,\emptyset_0)$ and $\hat{v}(\theta,\emptyset,\alpha,\emptyset_0)$ must be found. The vectors $\hat{v}$ and $\hat{h}$ are defined by the vector relationships

$$\hat{h} \cdot \hat{r} = 0 \quad (35)$$

$$\hat{h} \cdot \hat{z} = \hat{h} \cdot \hat{z}' = 0 \quad (36)$$

$$\hat{v} = \hat{h} \times \hat{r} \quad (37)$$

and can be written as

$$\hat{h} = H_x\hat{x}' + H_y\hat{y}' + H_z\hat{z}' \quad (38a)$$

$$\hat{v} = V_x\hat{x}' + V_y\hat{y}' + V_z\hat{z}' \quad (38b)$$

Equation (36) implies that $H_z = 0$ and (35) can then be expanded to yield

$$H_x R_x + H_y R_y = 0 \quad (39)$$

Since $\hat{h}$ is a unit vector,

$$H_x^2 + H_y^2 = 1 \tag{40}$$

Solving (39) and (40) simultaneously, one finds that

$$H_x = -R_y/\sqrt{R_x^2 + R_y^2} \tag{41a}$$

$$H_y = R_x/\sqrt{R_x^2 + R_y^2} \tag{41b}$$

Expanding (37) yields

$$\hat{v} = H_y R_z \hat{x}' - H_x R_z \hat{y}' + [H_x R_y - H_y R_x] \hat{z}' \tag{42}$$

Therefore,

$$V_x = H_y R_z \tag{43a}$$

$$V_y = -H_x R_z \tag{43b}$$

$$V_z = H_x R_y - H_y R_x \tag{43c}$$

The vectors $\hat{v}$ and $\hat{h}$ have now been broken into their primed rectangular coordinate components. The unit vectors $\hat{\phi}$ and $\hat{\theta}$ can also be expressed this way to allow the dot products to be taken. One must begin with the vectors in the unprimed coordinates

$$\hat{\theta} = \hat{x} \cos\theta \cos\phi + \hat{y} \cos\theta \sin\phi - \hat{z} \sin\theta \tag{44a}$$

$$\hat{\phi} = -\hat{x} \sin\phi + \hat{y} \cos\phi \tag{44b}$$

Using (30a), and (30b), and (30c), we can write (44a) and (44b) as

$$\hat{\theta} = T_x \hat{x}' + T_y \hat{y}' + T_z \hat{z}' \tag{45a}$$

$$\hat{\phi} = P_x \hat{x}' + P_y \hat{y}' + P_z \hat{z}' \tag{45b}$$

where

$$T_x = \cos\theta \cos\phi \, (\cos\alpha \cos\phi_o + \sin\phi_o) + \sin\alpha \sin\theta \cos\phi_o \tag{46a}$$

$$T_y = \cos\theta \sin\phi \, (\cos\alpha \sin\phi_o + \cos\phi_o) + \sin\alpha \sin\theta \sin\phi_o \tag{46b}$$

$$T_z = \sin\alpha \cos\theta \, (\cos\phi \cos\phi_o + \sin\phi \sin\phi_o) - \sin\theta \cos\alpha \tag{46c}$$

$$P_x = \sin\phi \, (\cos\alpha \cos\phi_o + \sin\phi_o) \tag{46d}$$

$$P_y = \cos\phi \, (\cos\alpha \sin\phi_o + \cos\phi_o) \tag{46e}$$

$$P_z = -\sin\alpha \sin\phi_o \cos\phi + \sin\alpha \cos\phi_o \sin\phi \tag{46f}$$

The dot products in (23) and (24) can now be evaluated using (45a)-(46f) as

$$\hat{\theta} \cdot \hat{h} = T_x H_x + T_y H_y \tag{47a}$$

$$\hat{\phi} \cdot \hat{h} = P_x H_x + P_y H_y \tag{47b}$$

$$\hat{\theta} \cdot \hat{v} = T_x V_x + T_y V_y + T_z V_z \tag{47c}$$

$$\hat{\phi} \cdot \hat{v} = P_x V_x + P_y V_y + P_z V_z \tag{47d}$$

To evaluate the variables T_{aw}, T_{ae}, and T_{as} using (27), (28), and (29), respectively, the only parameters still not known are the limits of integration and the angle $\theta_s(\theta,\emptyset,\alpha)$ (the angle measured from zenith) needed to evaluate T_{bs} (θ_s).

Since the z-axis always passes through the center of the wave tank, then for any value of $\emptyset$, as θ is varied from 0 to π, we will always be integrating first over the water, the earth, and then the sky. What is needed then are the values of θ as a function of $\emptyset$ at which the water-earth boundary and the horizon (earth-sky boundary) occur. We will define $\theta_{we}(\emptyset,\alpha,\emptyset_0)$ as the water-earth boundary and $\theta_{es}(\emptyset,\alpha,\emptyset_0)$ as the horizon. Due to the symmetry of the problem, the integration limits of $\emptyset$ can be made 0 to π for the vertical polarization case and $\pi/2$ to $3\pi/2$ for the horizontal polarization.

We will first outline the procedure in determining θ_{we}. Referring to Figure 3, we can write that

$$\cos\theta_{we} = \frac{\bar{G} \cdot \bar{R}_0}{|\bar{G}|\ |\bar{R}_0|} \tag{48}$$

where

$$\bar{R}_0 = R_0(-\hat{x}' \sin\alpha \cos\emptyset_0 - \hat{y}' \sin\alpha \sin\emptyset_0 + \hat{z}' \cos\alpha) \tag{49a}$$

$$|\bar{R}_0| = R_0 \tag{49b}$$

The vector $\bar{G}$ is found by defining the position of each end of the vector referenced to the primed coordinate system. The coordinates of the point A are $x' = R_0 \sin\alpha \cos\phi_0$, $y' = R_0 \sin\alpha \sin\phi_0$, and $z' = -R_0 \cos\alpha$. The coordinates of the points along the edge of the tank are shown in Figure 5, which is a view of the wave tank looking straight down, and are given by

$$x' = W, \qquad y' = W \tan\phi' \qquad \frac{\pi}{4} > \phi' \geq -\frac{\pi}{4} \tag{50a}$$

$$x' = W \cot\phi', \qquad y' = W \qquad \frac{3\pi}{4} > \phi' \geq \frac{\pi}{4} \tag{50b}$$

$$x' = -W, \qquad y' = -W \tan\phi' \qquad \frac{5\pi}{4} > \phi' \geq \frac{3\pi}{4} \tag{50c}$$

$$x' = -W \cot\phi', \qquad y' = -W \qquad \frac{7\pi}{4} > \phi' \geq \frac{5\pi}{4} \tag{50d}$$

For all cases $z' = 0$. This gives four difference expressions for $\bar{G}$. To eliminate the redundancy of showing the derivations for all four cases, we will show the details of finding θ_{we} for case 1 when $\frac{\pi}{4} > \phi' > -\frac{\pi}{4}$ and then list θ_{we} for the other values of ϕ'.

For case 1 $(\frac{\pi}{4} > \phi' > -\frac{\pi}{4})$, the vector $\bar{G}$ can be expressed as

$$\bar{G} = (W - R_0 \sin\alpha \cos\phi_0)\,\hat{x}' + (W \tan\phi' - R_0 \sin\alpha \sin\phi_0)\,\hat{y}' + R_0 \cos\alpha\,\hat{z}' \tag{51}$$

By defining W_n as the ratio of W/R_0, we can write the dot product in (48) as

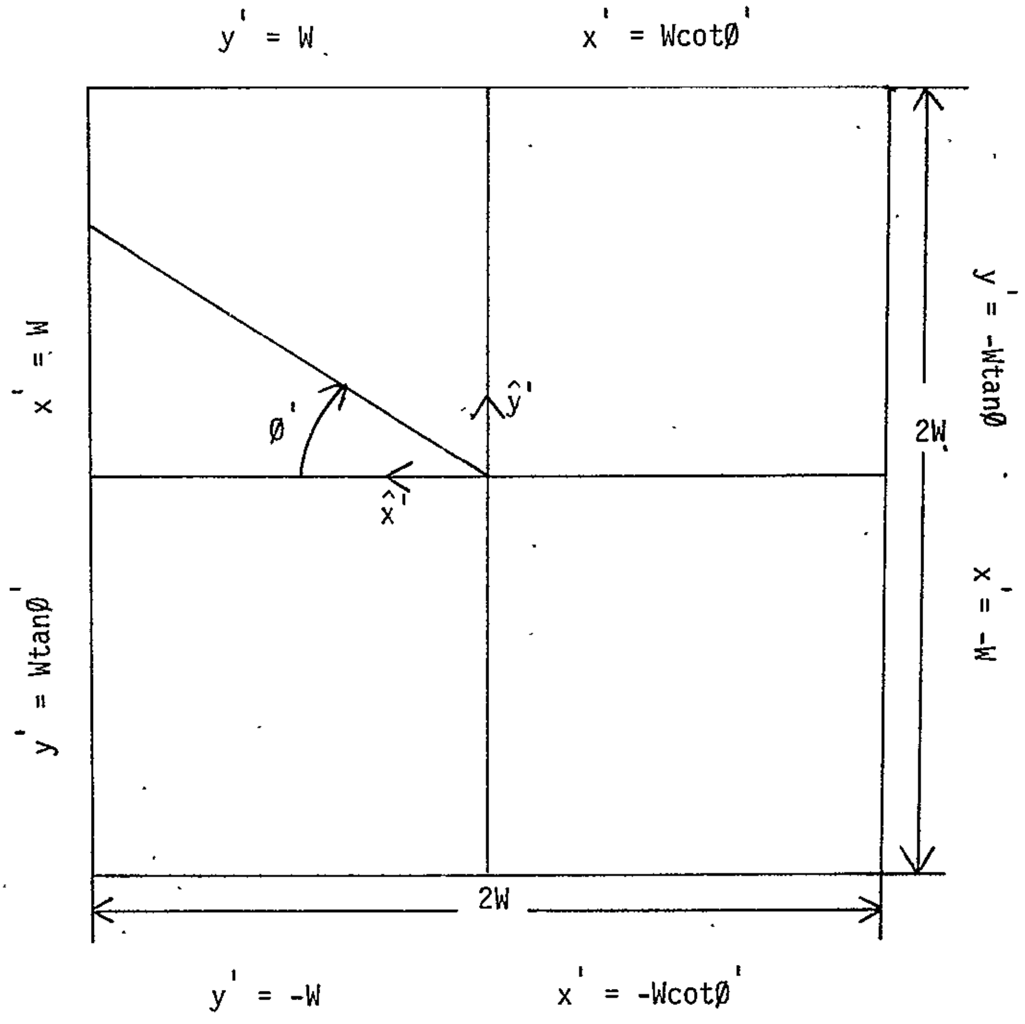

Fig. 5. Overhead View of Wave Tank with Coordinates for the Z-axis Geometry.

$$\bar{G} \cdot \overline{R_o} = [(-\sin\alpha \cos\phi_o)(W_n - \sin\alpha \cos\phi_o)$$
$$+ (-\sin\alpha \sin\phi_o)(W_n \tan\phi' - \sin\alpha \sin\phi_o) + \cos^2\alpha]R_o^2 \quad (52)$$

Equation (52) can be simplified into the form

$$\bar{G} \cdot \overline{R_o} = [1 - W_n \sin\alpha (\cos\phi_o + \sin\phi_o \tan\phi')]R_o^2 \quad (53)$$

The magnitude of the vector $\bar{G}$ is given by

$$|\bar{G}| = R_o[(W_n - \sin\alpha \cos\phi)^2 + (W_n \tan\phi' - \sin\alpha \sin\phi_o)^2$$
$$+ \cos^2\alpha]^{\frac{1}{2}} \quad (54)$$

which can be reduced to

$$|\bar{G}| = R_o[W_n^2 - 2 W_n \sin\alpha \cos\phi_o + 1 + W_n^2 \tan^2\phi' - 2 W_n \tan\phi'$$
$$\sin\alpha \sin\phi_o]^{\frac{1}{2}} \quad (55)$$

Substituting (49b), (53), and (55) into (48) and solving for θ_{we} of case 1 yields

$$\theta_{we} = \cos^{-1}\{[1 - W_n \sin\alpha (\cos\phi_o + \sin\phi_o \tan\phi')]/[W_n^2 - 2W_n \sin\alpha \cos\phi_o$$
$$+ 1 + W_n^2 \tan^2\phi' - 2 W_n \tan\phi' \sin\alpha \sin\phi_o]^{\frac{1}{2}}\} \quad (56)$$

For case 2, $\frac{3\pi}{4} > \phi' \geq \frac{\pi}{4}$, θ_{we} is found by

$$\theta_{we} = \cos^{-1}\{[1 - W_n \sin\alpha\, (\cot\emptyset' \cos\emptyset_o + \sin\emptyset_o)]/[W_n^2 - 2W_n \sin\alpha \sin\emptyset_o + 1 + W_n^2 \cot^2\emptyset' - 2\, W_n \cot\emptyset' \sin\alpha \cos\emptyset_o]^{\frac{1}{2}}\} \quad (57)$$

When $\frac{5\pi}{4} > \emptyset' \geq \frac{3\pi}{4}$, we have case 3 and for this

$$\theta_{we} = \cos^{-1}\{[1 + W_n \sin\alpha\, (\cos\emptyset_o + \sin\emptyset_o \tan\emptyset')]/[W_n^2 + 2W_n \sin\alpha \cos\emptyset_o + 1 + W_n^2 \tan^2\emptyset' + 2\, W_n \tan\emptyset' \sin\alpha \sin\emptyset_o]^{\frac{1}{2}}\} \quad (58)$$

For $\frac{7\pi}{4} > \emptyset' \geq \frac{5\pi}{4}$, θ_{we} is given by

$$\theta_{we} = \cos^{-1}\{[1 + W_n \sin\alpha\, (\cot\emptyset' \cos\emptyset_o + \sin\emptyset_o)]/[W_n^2 + 2W_n \sin\alpha \sin\emptyset_o + 1 + W_n^2 \cot^2 \emptyset + 2\, W_n \cot\emptyset' \sin\alpha \cos\emptyset_o]^{\frac{1}{2}}\} \quad (59)$$

Given α and $\emptyset'$ one can now find θ_{we}. However, the integration will be performed in the unprimed coordinate system, so a relationship between $\emptyset$ and $\emptyset'$ is needed. This can be found from the relationship, referring to Figures 3 and 4, $\bar{R} = \bar{R}_o + \bar{R}'$. The vector $\bar{R}$ has already been expressed in the primed coordinate system by (33), $\bar{R}_o$ by (49a), and $\bar{R}'$ is given by

$$\bar{R}' = R' \,(\hat{x}' \cos\emptyset' + \hat{y}' \sin\emptyset') \quad (60)$$

since $\theta' = \frac{\pi}{2}$ on the water surface. Using (33), (49a), and (60), the three vector components of the equation $\bar{R}' = \bar{R} - \bar{R}_o$ yield

$$R' \cos\phi' = R[\sin\theta \cos\phi \, (\cos\alpha \cos\phi_0 + \sin\phi_0)$$

$$- \sin\alpha \cos\theta \cos\phi_0] + R_0 \sin\alpha \cos\phi_0 \qquad (61)$$

$$R' \sin\phi' = R[\sin\theta \sin\phi \, (\cos\alpha \sin\phi_0 + \cos\phi_0)$$

$$- \sin\alpha \cos\theta \sin\phi_0] + R_0 \sin\alpha \sin\phi_0 \qquad (62)$$

$$0 = R \, [\sin\theta \sin\alpha \, (\sin\phi \sin\phi_0 + \cos\phi \cos\phi_0)$$

$$+ \cos\theta \cos\alpha] - R_0 \cos\alpha \qquad (63)$$

Substituting (63) into (61) and (62), one can write

$$(\frac{R'}{R}) \sin\phi' = \sin\theta \sin\phi \cos^2\alpha \sin\phi_0 + \sin\theta \sin\phi \cos\phi_0 \cos\alpha + \sin^2\alpha \sin\phi_0$$

$$\sin\theta \cos\phi \cos\phi_0 + \sin^2\alpha \sin^2\phi_0 \sin\theta \sin\phi \qquad (64)$$

$$(\frac{R'}{R}) \cos\phi' = \sin\theta \cos\phi \cos^2\alpha \cos\phi_0 + \sin\theta \cos\phi \cos\alpha \sin\phi_0 + \sin\theta \cos\phi$$

$$\sin^2\alpha \cos\phi_0 + \sin\theta \sin\phi \sin^2\alpha \sin\phi_0 \cos\phi_0 \qquad (65)$$

Since ϕ_0 is either 0 or $\frac{\pi}{2}$, $\sin\phi_0 = \sin^2\phi_0$, $\cos\phi_0 = \cos^2\phi_0$, and $\sin\phi_0 \cos\phi_0 = 0$, (64) and (65) can be reduced considerably to

$$(\frac{R'}{R}) \sin\phi' = \sin\phi \sin\theta \, (\cos\phi_0 \cos\alpha + \sin\phi_0) \qquad (66)$$

$$(\frac{R'}{R}) \cos\phi' = \cos\phi \sin\theta \, (\sin\phi_0 \cos\alpha + \cos\phi_0) \qquad (67)$$

Dividing (66) by (67), we get the desired relationship between $\emptyset$ and $\emptyset'$ to be

$$\tan\emptyset' = \frac{\sin\emptyset\ (\cos\emptyset_o \cos\alpha + \sin\emptyset_o)}{\cos\emptyset\ (\sin\emptyset_o \cos\alpha + \cos\emptyset_o} \tag{68}$$

With the above relationship between $\emptyset'$, $\emptyset$, $\emptyset_o$, and α, (56), (57), (58), and (59) can be used to evaluate θ_{we} ($\emptyset$, α, $\emptyset_o$).

Finding an expression for θ_{es} is considerably easier. As the observation point moves farther away from the wave tank, the vectors $\bar{R}$ and $\bar{R}'$ become nearly equal. In the limit, as the observation point approaches infinity, $\bar{R} = \bar{R}'$. With this approximation for the horizon, equating the $\hat{z}'$ components of $\bar{R}$ and $\bar{R}'$ yield

$$\cos\theta' = \sin\alpha \cos\emptyset_o \cos\emptyset \sin\theta + \sin\alpha$$
$$\sin\emptyset_o \sin\emptyset \sin\theta + \cos\alpha \cos\theta \tag{69}$$

Solving (69) for θ_{es}, which occurs when $\theta' = \frac{\pi}{2}$, results in

$$\theta_{es} = \tan^{-1}\left[\frac{\cos\alpha}{-\sin\alpha \cos\emptyset \cos\emptyset_o - \sin\alpha \sin\emptyset \sin\emptyset_o}\right] \tag{70}$$

The angle θ_s, measured from zenith, can also be found from (69), since

$$\theta_s = \pi - \theta' \tag{71}$$

Using (71) and (69) yields

$$\theta_s = \cos^{-1}[-\sin\alpha \cos\phi_o \cos\phi \sin\theta$$

$$- \sin\alpha \sin\phi_o \sin\phi \sin\theta - \cos\alpha \cos\theta \qquad (72)$$

Now, given $T_{bs}(\theta_s)$, T_{be}, $T_{bwh}(\theta'')$, $T_{bwv}(\theta'')$, $E_\theta(\theta,\phi)$, $E_\phi(\theta,\phi)$ and the tank dimensions, we can now find T_{aw}, T_{ae}, and T_{as} as function of α for both polarizations. The scan angle β would be equal to zero in these calculations. To calculate the T_a's as a function of β (for a given α) requires a transformation of variables. Referring to Figures 6a and 6b, the vertical scanning involves coordinate system rotation about the y-axis and for the horizontal scanning an x-axis rotation. It can be seen that the antenna gain functions will be known in the x_1, y_1, z_1 coordinate system or as functions of θ_1 and ϕ_1. To integrate in the unprimed coordinate system, θ_1 and ϕ_1 need to be expressed as functions of θ and ϕ. Appendix I contains a derivation of these transformations. For the vertical scanning, pictured in Figure 6a,

$$\phi_1 = \tan^{-1}\left[\frac{\sin\phi \sin\theta}{\cos\beta \cos\phi \sin\theta + \sin\beta \cos\theta}\right] \qquad (73)$$

$$\theta_1 = \cos^{-1}[-\sin\beta \cos\phi \sin\theta + \cos\beta \cos\theta] \qquad (74)$$

For the horizontal polarization, illustrated in Figure 6b,

$$\phi_1 = \tan^{-1}\left[\frac{\cos\beta \sin\phi \sin\theta + \sin\beta \cos\theta}{\cos\phi \sin\theta}\right] \qquad (75)$$

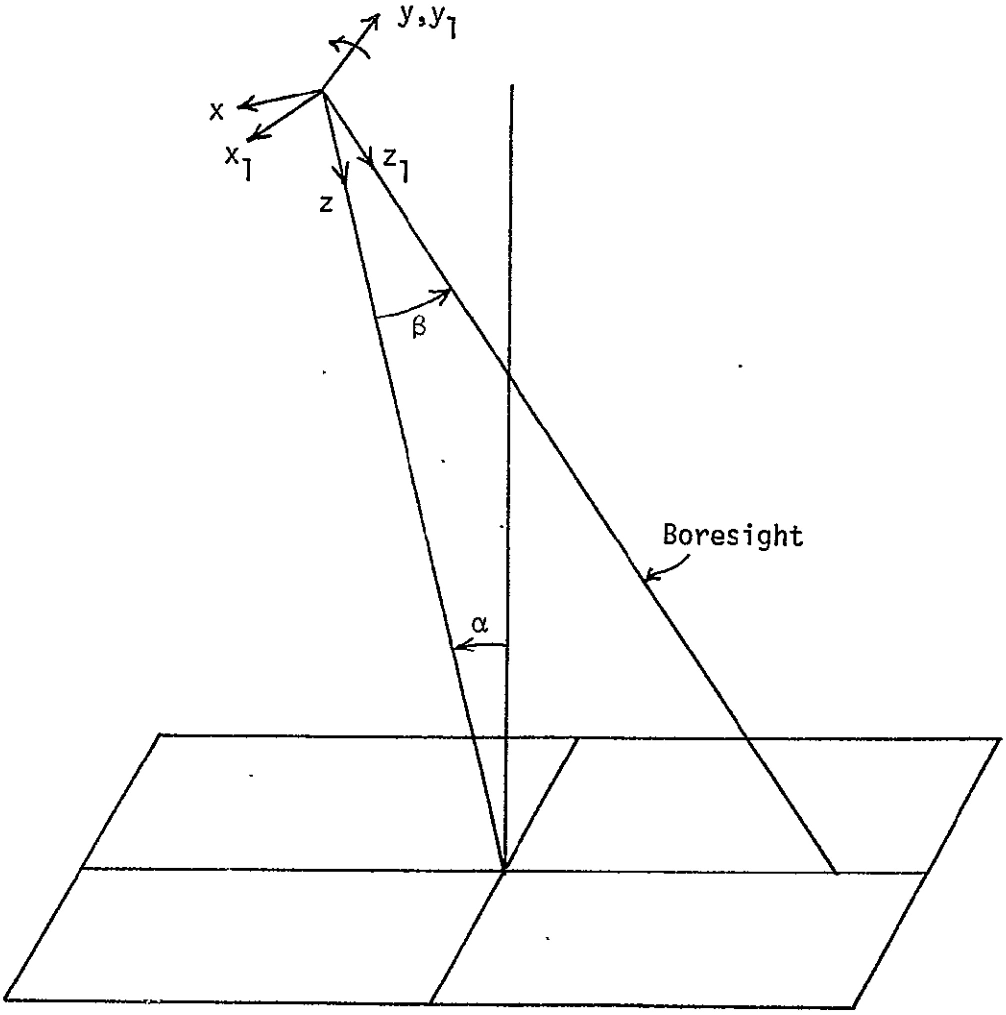

Fig. 6a. Coordinate System Transformation Describing Vertical Scanning (β variations) for the Z-axis Geometry.

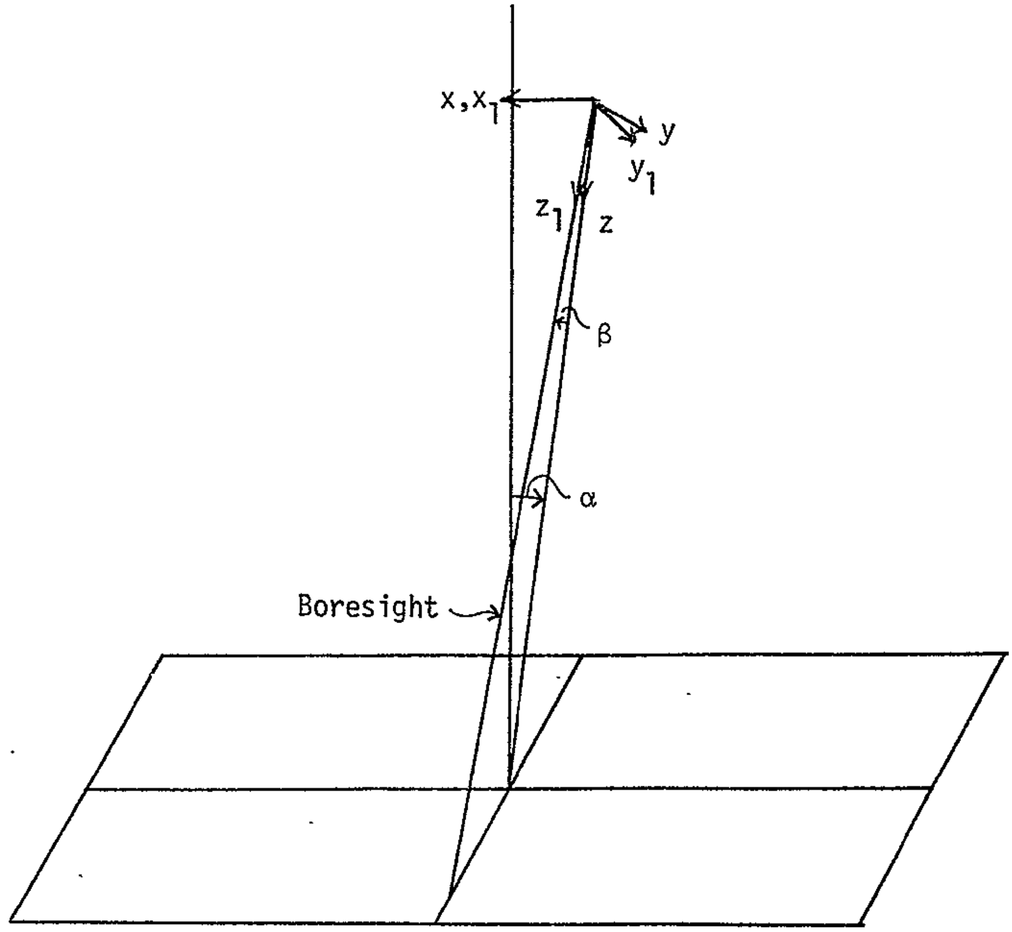

Fig. 6b. Coordinate System Transformation Describing Horizontal Scanning (β variations) for the Z-axis Geometry.

$$\theta_1 = \cos^{-1}[-\sin\beta \sin\phi \sin\theta + \cos\beta \cos\theta] \qquad (76)$$

By using $G^v(\theta_1,\phi_1)$, $G^h(\theta_1,\phi_1)$, and $G(\theta_1,\phi_1)$ in (27), (28), and (29), T_{aw}, T_{ae}, and T_{as} can be found as functions of α and β for both polarizations. However, using this geometry, (27), (28), and (29) must be evaluated by numerical integration for each value of α and β. One would also have to solve the transcendental equations relating θ_1 and ϕ_1 to θ and ϕ at each integration point. This would require considerable computer time and can be avoided if the scanning of the antenna is described by a rotation about the z-axis instead of a rotation about the x- or y- axis as given by (73)-(76).

2. X-Axis Normal to Radiometer Antenna Aperture

An alternate coordinate system that avoids the transcendental equations describing the scanning is illustrated in Figure 7. In this case the x-axis is used as the boresight of the antenna for both horizontal and vertical scans. These scans are now mathematically described by rotations about the z-axis, and the transformations of coordinates during the scan (as shown in Appendix 1) leave the θ variable unaffected and change ϕ by a constant value. The elimination of the transcendental equations is not the only advantage of rotating about the z-axis. It will be shown that by utilizing this geometry, the integration with respect to ϕ and the

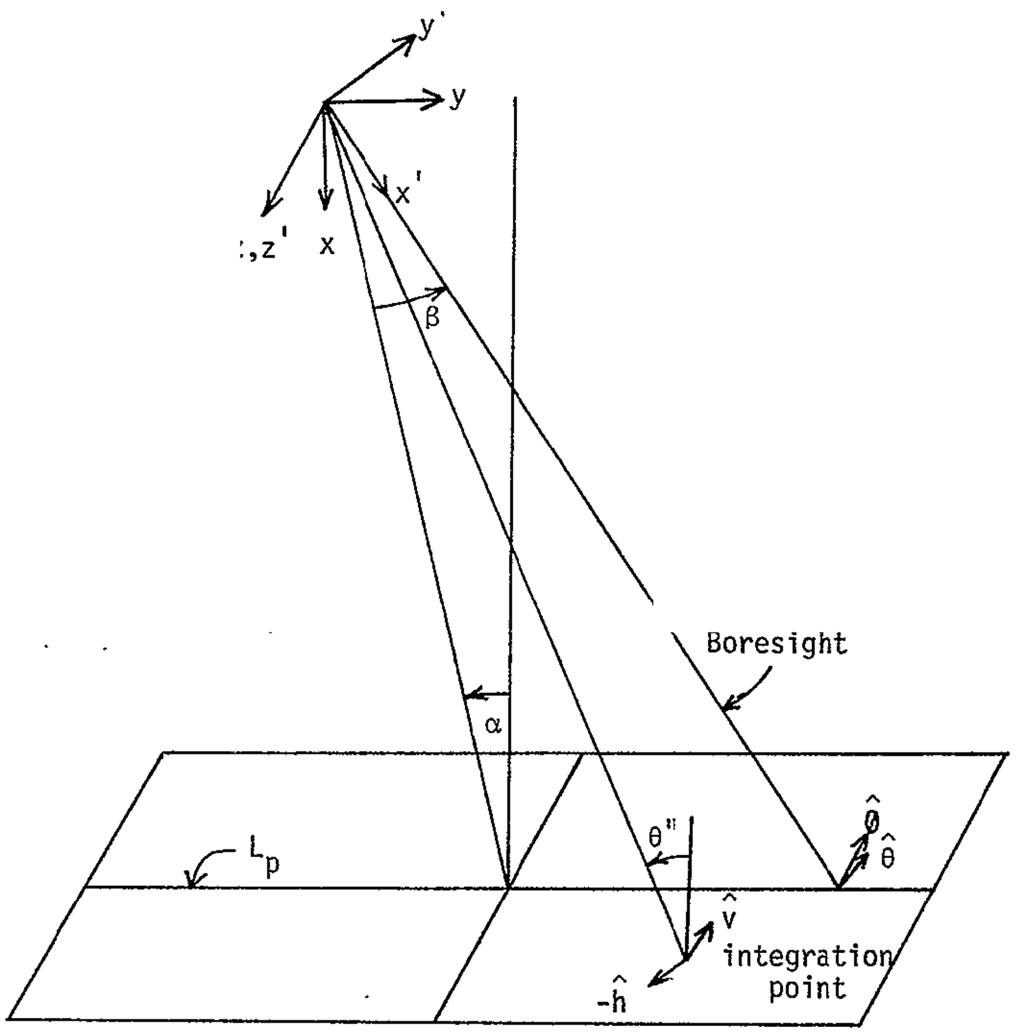

Fig. 7. X-axis Geometry and Vector Alignment on the Wave Tank Surface.

functional variation with respect to β of (27), (28), and (29) can be established in a correlation form and evaluated conveniently and efficiently by Fourier transform techniques. It was for this reason that this system was adopted.

Since the antenna system is now restricted to rotations about the z-axis, it is not going to be scanned in two orthogonal planes to establish the two different polarizations. Instead, the scanning will be restricted in one plane but the antenna orientation (aperture field) will be changed to accomplish this. To receive primarily the vertical polarization, the aperture field is assumed to be oriented in the $\hat{y}'$ direction. If the horizontal polarization is desired, the E_θ and E_ϕ fields are those calculated with the aperture field in the $\hat{z}'$ direction. We shall use the subscript p to denote a function that depends upon polarization. The subscript p will represent h for horizontal or v for vertical polarization.

To evaluate (27), (28), and (29) with the new geometry, we again need to find the dot products that represent the degree of alignment between the $\hat{\theta}'$ and $\hat{\phi}'$ vectors of the antenna's coordinate system and the horizontal and vertical unit vectors. The incidence angle θ'' and the various limits of integration also need to be known. The dot products and incidence angle will be found utilizing the geometry as represented in Figure 8.

The planes defined by constant values of ϕ form on the water surface straight lines N which are parallel to the z-axis.

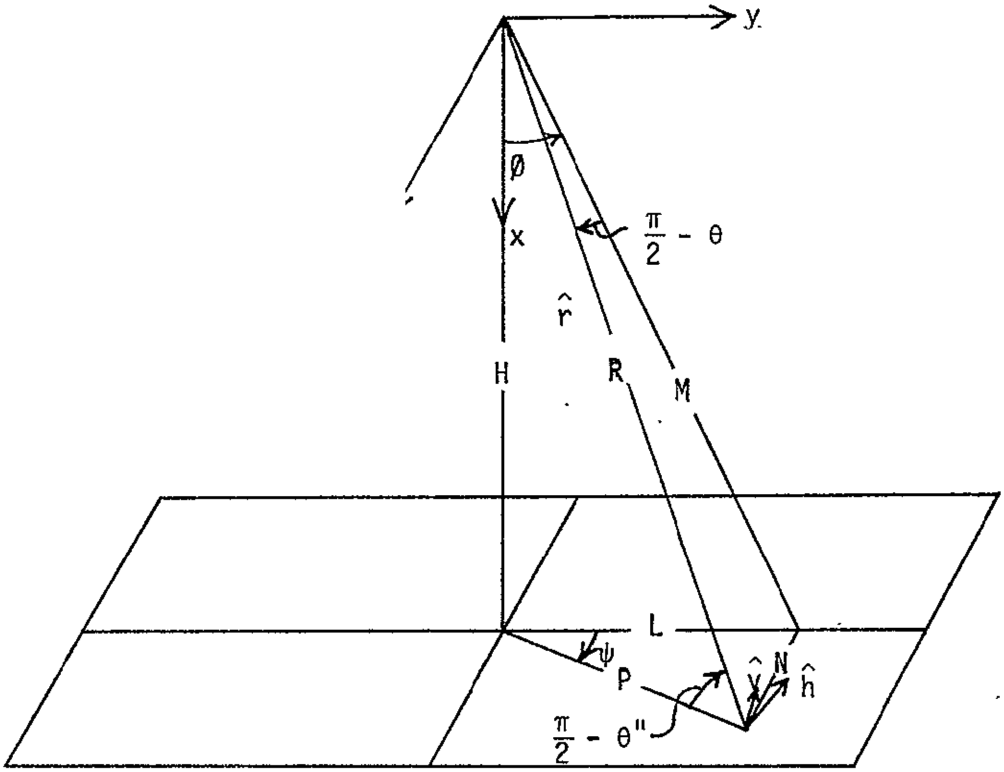

Fig. 8. X-axis Geometry and Parameters Describing the Vector Alignment Dot Products.

Along each one of these lines, $\emptyset$ is defined as the angle between the projection of the radial line into the x-y plane and the x-axis. The radial line is R and its projection into the x-y plane is M. Therefore, $\emptyset$ is the angle between H and M. The angle between the z-axis and R is θ. Since the line N and the z-axis are parallel, the lines R,M,N, and the z-axis all lie in the same plane. The z-axis and M intersect at right angles, so the angle between M and R is $\frac{\pi}{2} - \theta$, defined positive in the direction shown.

The horizontal vector $\hat{h}$ always lies in the plane that th surface of the water defines. Therefore, if one can find ψ as a function of θ and $\emptyset$ then $\hat{h}$ can be found from ψ. The plane the water surface defines is parallel to the y-z plane and $\hat{h}$ is given by

$$\hat{h} = \hat{y}\sin\psi - \hat{z}\cos\psi \qquad (77)$$

Line segment length L is found from

$$L = H\tan\emptyset \qquad (78)$$

and M by

$$M = \sqrt{H^2 + L^2} = H\sec\emptyset \qquad (79)$$

To find N we use the relation

$$\frac{N}{M} = \tan\left(\frac{\pi}{2} - \theta\right) = \cot\theta \qquad (80)$$

Substituting (79) into (80) we can find N to be

$$N = H \sec \phi \cot \theta \tag{81}$$

Using (78) and (81), we find that

$$\psi = \tan^{-1}\left(\frac{N}{L}\right) = \tan^{-1}\left[\frac{\cos\theta}{\sin\phi}\right] \tag{82}$$

The vector $\hat{h}$ is now known from (77) and we can get $\hat{v}$ from the relationship

$$\hat{v} = \hat{r} \times \hat{h} \tag{83}$$

The unit vectors $\hat{\theta}$, $\hat{\phi}$, and $\hat{r}$ are expressed in (44a), (44b) and (32), respectively. Using (32) and (77) in (83) yields

$$\begin{aligned} \hat{v} &= \hat{x}\,(-\cos\psi \sin\phi \sin\theta - \sin\psi \cos\theta) \\ &\quad + \hat{y} \cos\psi \cos\phi \sin\theta + \hat{z} \sin\psi \cos\phi \sin\theta \end{aligned} \tag{84}$$

Knowing the vectors $\hat{h}$, $\hat{v}$, $\hat{\theta}$, and $\hat{\phi}$, the various dot products needed to evaluate (23) and (24) can be expressed as

$$\hat{\theta} \cdot \hat{h} = \sin\phi \cos\theta \sin\psi + \sin\theta \cos\psi \tag{85a}$$

$$\hat{\phi} \cdot \hat{h} = \cos\phi \sin\psi \tag{85b}$$

$$\hat{\theta} \cdot \hat{v} = \cos\phi \cos\theta \, (- \cos\psi \sin\phi \sin\theta - \sin\psi \cos\theta)$$

$$+ \sin\phi \cos\theta \cos\psi \cos\phi \sin\theta - \sin\psi \cos\phi \sin^2\theta \qquad (85c)$$

$$\hat{\phi} \cdot \hat{v} = \sin\phi \, (\cos\psi \sin\phi \sin\theta + \sin\psi \cos\theta)$$

$$+ \cos\psi \cos^2\phi \sin\theta \qquad (85d)$$

Expanding and simplifying (85c) and (85d), we find that

$$\hat{\theta} \cdot \hat{v} = - \hat{\phi} \cdot \hat{h} = -\sin\psi \cos\phi \qquad (86a)$$

$$\hat{\phi} \cdot \hat{v} = \hat{\theta} \cdot \hat{h} = \sin\psi \cos\theta \sin\phi + \cos\psi \sin\theta \qquad (86b)$$

We now have the needed dot products in the unprimed coordinate system.

The incidence angle θ'' is found by the relationship

$$\tan \left(\frac{\pi}{2} - \theta''\right) = H/P \qquad (87)$$

and P from

$$P = \sqrt{L^2 + N^2} = H\sqrt{\cot^2\theta(1 + \sec^2\phi)} \qquad (88)$$

Substituting (88) into (87) yields

$$\theta'' = \tan^{-1}[\sqrt{\cot^2\theta(1 + \sec^2\phi)} \qquad (89)$$

Now that the incidence angle is known, let us next find the relationship between the primed coordinate system of the antenna and the unprimed coordinate system representing the water. Referring to Figure 7, the primed coordinate system is rotated about the z-axis through the angle $\alpha + \beta$. From Appendix I, we know the transformation to be

$$\theta = \theta' \tag{90}$$

$$\phi = \phi' + \alpha + \beta \tag{91}$$

We can now express (27), (28), and (29) as functions of α and β.

$$T_{awp}(\alpha,\beta) = \iint_{\substack{\text{over}\\\text{water}}} [\hat{h}(\theta,\phi) \cdot \hat{\theta}\, E_{\theta p}(\theta,\phi - (\alpha + \beta))$$

$$+ \hat{h}(\theta,\phi) \cdot \hat{\phi}\, E_{\phi p}(\theta,\phi - (\alpha + \beta))]^2 T_{bwh}[\theta''(\theta,\phi)] \sin\theta \, d\theta \, d$$

$$+ \iint_{\substack{\text{over}\\\text{water}}} [\hat{v}(\theta,\phi) \cdot \hat{\theta}\, E_{\theta p}(\theta,\phi - (\alpha + \beta)) + \hat{v}(\theta,\phi) \cdot$$

$$\hat{\phi}\, E_{\phi p}(\theta,\phi - (\alpha + \beta))]^2\, T_{bwv}[\theta''(\theta,\phi)] \sin\theta \, d\theta \, d\phi \tag{92}$$

$$T_{aep}(\alpha,\beta) = \iint_{\substack{\text{over}\\\text{earth}}} T_{be}(\theta,\phi)\, G_p(\theta,\phi - (\alpha + \beta)) \sin\theta \, d\theta \, d\phi \tag{93}$$

$$T_{asp}(\alpha,\beta) = \iint_{\substack{\text{over}\\\text{sky}}} T_{bs}(\theta,\phi)\, G_p(\theta,\phi - (\alpha + \beta)) \sin\theta \, d\theta \, d\phi \tag{94}$$

where G_p has been normalized so that its value over the entire solid angle is unity.

In order to evaluate (92), (93), and (94), we need to find the limits of integration. The edges of the tank which are parallel to the z-axis, as illustrated in Figure 9, lie in constant $\emptyset$ plane. The values of $\emptyset$ which define these edges are indicated in Figure 10 as $\emptyset_1$ and $\emptyset_2$. The boom length is ρ and

$$H = \rho \cos\alpha \tag{95}$$

The distances C and D are known as

$$C = W/2 - \rho \sin\alpha \tag{96a}$$

$$D = W/2 + \rho \sin\alpha \tag{96b}$$

The relationship between $\emptyset_1$, $\emptyset_2$, C, and D are

$$\emptyset_1 = \tan^{-1}(D/H) \tag{97a}$$

$$\emptyset_2 = \tan^{-1}(C/H) \tag{97b}$$

Substituting (95), (96a), and (96b) into (97a) and (97b), we find the limits of integration for $\emptyset$ between the water and earth to be

$$\emptyset_1 = \tan^{-1}[(W/2 + \rho \sin\alpha)/\rho \cos\alpha] \tag{98a}$$

$$\emptyset_2 = \tan^{-1}[(W/2 - \rho \sin\alpha)/\rho \cos\alpha] \tag{98b}$$

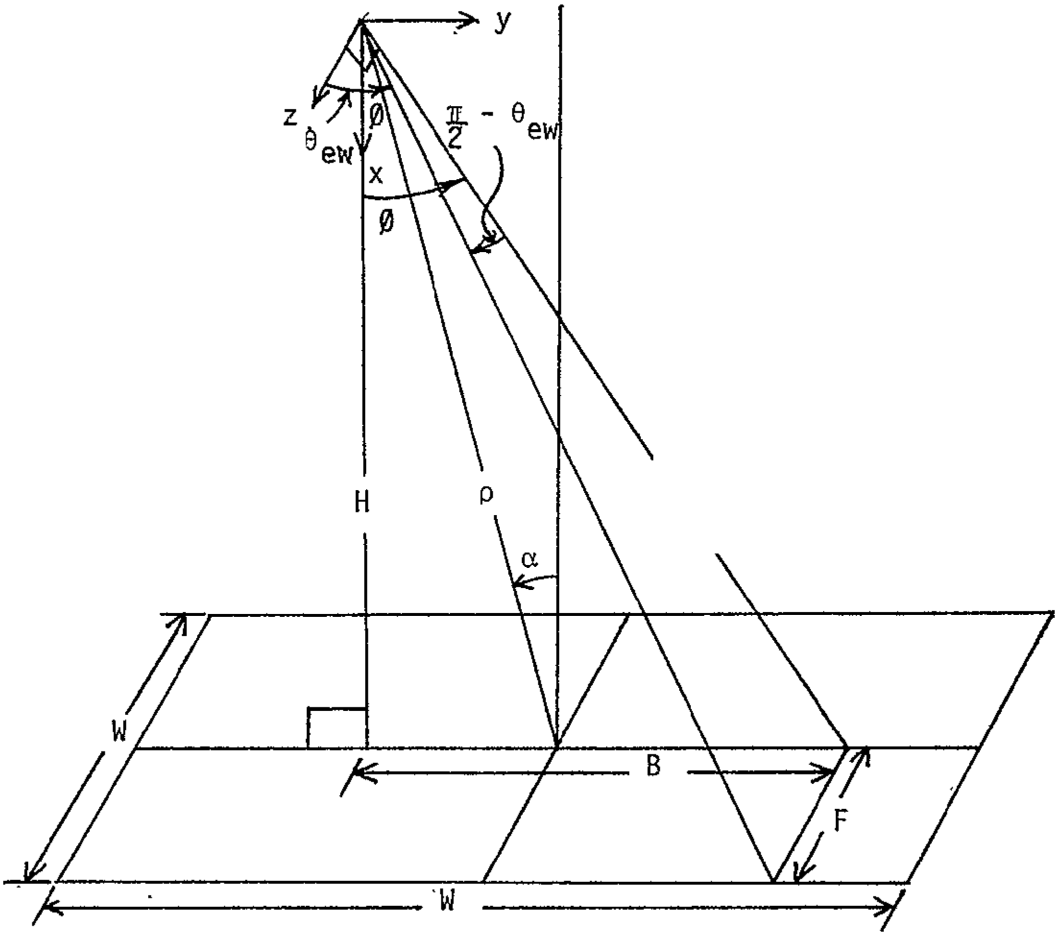

Fig. 9. Wave Tank Configuration to Determine the θ Limits of Integration for the X-axis Geometry.

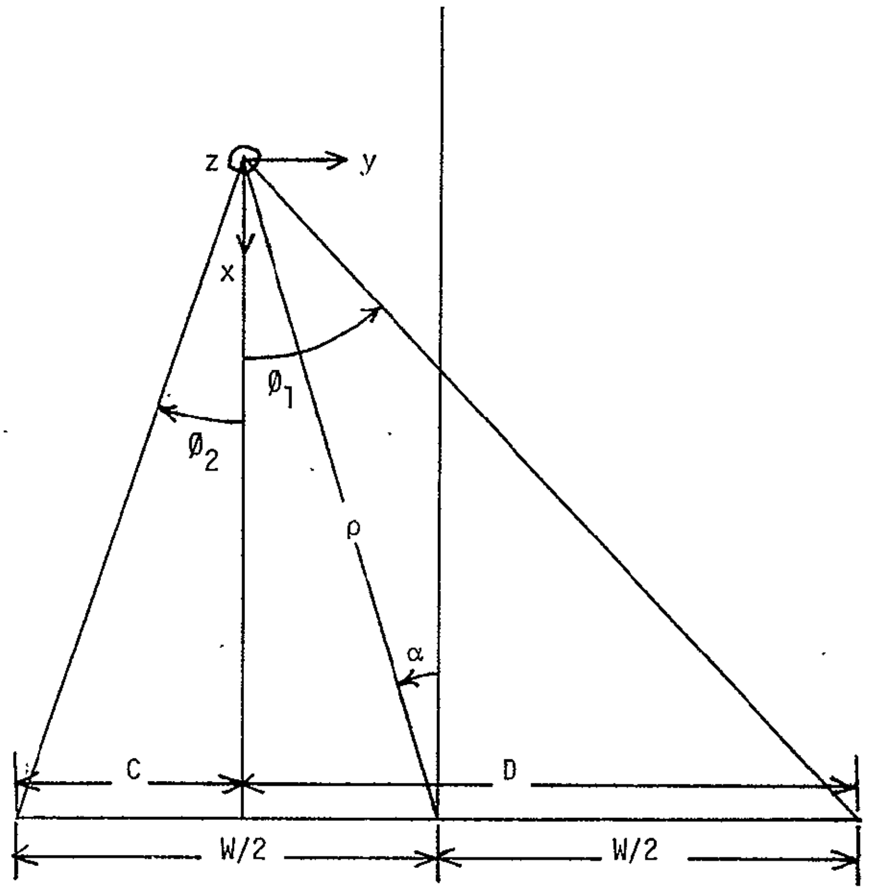

Fig. 10. Wave Tank Scanning Plane to Determine the Ø Limits of Integration for the X-axis Geometry.

Referring to Figure 9, for each value of ϕ between $-\phi_2$ and ϕ_1 we need to find the value of θ_{ew} that defines the other edge of the tank. First, we find B by

$$B = H \tan\phi \tag{99}$$

We express E as

$$E = \sqrt{H^2 + B^2} \tag{100}$$

By combining (95), (99), and (100), we find E as a function of ρ, α, and ϕ as

$$E = p \cos\alpha \sec \phi \tag{101}$$

It can be seen from Figure 9 that

$$\tan\left(\frac{\pi}{2} - \theta_{ew}\right) = F/E = \cot(\theta_{ew}) \tag{102}$$

and for this square tank

$$F = W/2 \tag{103}$$

The angle θ_{ew} is found from (101), (102), and (103) as

$$\theta_{ew} = \cot^{-1}[(W/2)/o \cos\alpha \ \sec \phi] \tag{104}$$

For values of ϕ not between $-\phi_2$ and ϕ_1 we will define θ_{ew} as $\frac{\pi}{2}$. The sky is integrated for values of ϕ between $\frac{\pi}{2}$ and $\frac{3\pi}{2}$ for all values of θ. We can now rewrite (92), (93), and (94), showing the limits of integration, as

$$T_{awp}(\alpha,\beta) = \int_{-\emptyset_2}^{\emptyset_1} \int_{\theta_{ew}(\alpha,\rho,W,\emptyset)}^{\pi/2} [\text{same as in (92)}] \sin\theta \, d\theta \, d\emptyset$$

$$+ \int_{-\emptyset_2}^{\emptyset_1} \int_{\theta_{ew}(\alpha,\rho,W,\emptyset)}^{\pi/2} [\text{same as in (92)}] \sin\theta \, d\theta \, d\emptyset \qquad (105)$$

$$T_{aep}(\alpha,\beta) = \int_{-\pi/2}^{\pi/2} \int_{0}^{\theta_{ew}(\alpha,\rho,W,\emptyset)} [\text{same as in (93)}] \sin\theta \, d\theta \, d\emptyset \qquad (106)$$

$$T_{asp}(\alpha,\beta) = \int_{\pi/2}^{3\pi/2} \int_{0}^{\pi/2} [\text{same as in (94)}] \sin\theta \, d\theta . d\emptyset \qquad (107)$$

where G_p has been normalized so that its value over the entire solid angle is 2.

We need only integrate θ from 0 to π/2 because the geometry is symmetrical about the x-y plane. It should be noted here that the geometry does not have to be symmetrical to obtain a solution to the problem. The tank need not be square but of any shape. We need only to know Γ as a function of B to find θ_{ew} as a function of ∅. If the tank is not symmetrical about the x-y plane, then we need to integrate θ from 0 to π. The value of θ_{ew} that describes the back edge of the tank can be found in the same manner as the θ_{ew} for θ between 0 and $\pi/2$.

By utilizing the rotation about the z-axis to represent the rotation of the support arm through the angle α and the scanning angle β, we obtain a much more powerful representation of the problem than is possible with the earlier geometry which utilized the z-axis perpendicular to the aperture of the antenna. Previously we found θ_{we} from (56), (57), (58), and (59) and θ_{es} from (70). Equations (98a), (98b) and (104) are much simpler. The dot products for the first coordinate system (z-axis normal to antenna aperture) are functions of θ, ϕ, α, and polarization (ϕ_0). By rotating about the z-axis, the dot products are only functions of θ and ϕ because the transformation between θ, ϕ and θ', ϕ' is performed merely by the addition of a constant to ϕ. Figure 11a shows the vectors $\hat{\theta}$ and $\hat{\phi}$ on the surface of the water when the z-axis is directed straight down into the water surface. The vector $\hat{\theta}$ is equal to $\hat{v}$ and $\hat{\phi}$ equal to $\hat{h}$ and all of the dot products are either 1 or 0. When we rotate this coordinate system about either the x or y axis, the $\hat{\phi}'$ vector no longer lies in the plane of the water surface and the dot products become functions of θ', ϕ', and the amount of angular rotation. The dot products would, therefore, need to be calculated for each rotation angle. This is a consequence of the transformation of variables between θ, ϕ and θ', ϕ' shown in transcendental form in Appendix I. Figure 11b shows how the vectors $\hat{\phi}$ and $\hat{\theta}$ align on the surface for the second system (x-axis normal to antenna aperture). If this coordinate system is rotated about the z-axis and the vector $\hat{\theta}'$ and $\hat{\phi}'$ were

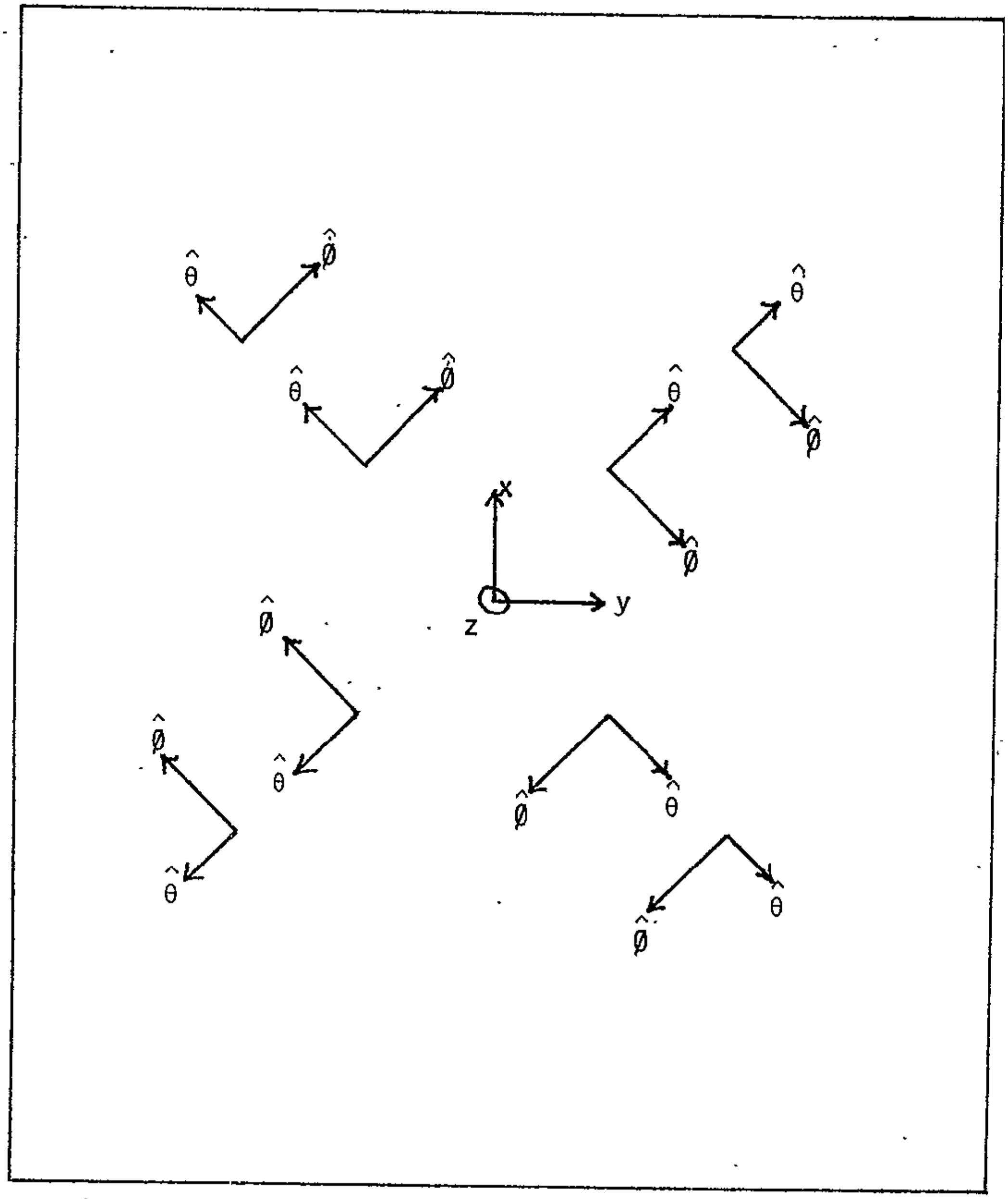

Fig. 11a. Overhead View of the Unit Vector Alignment on the Wave Tank Surface for the Z-axis Geometry.

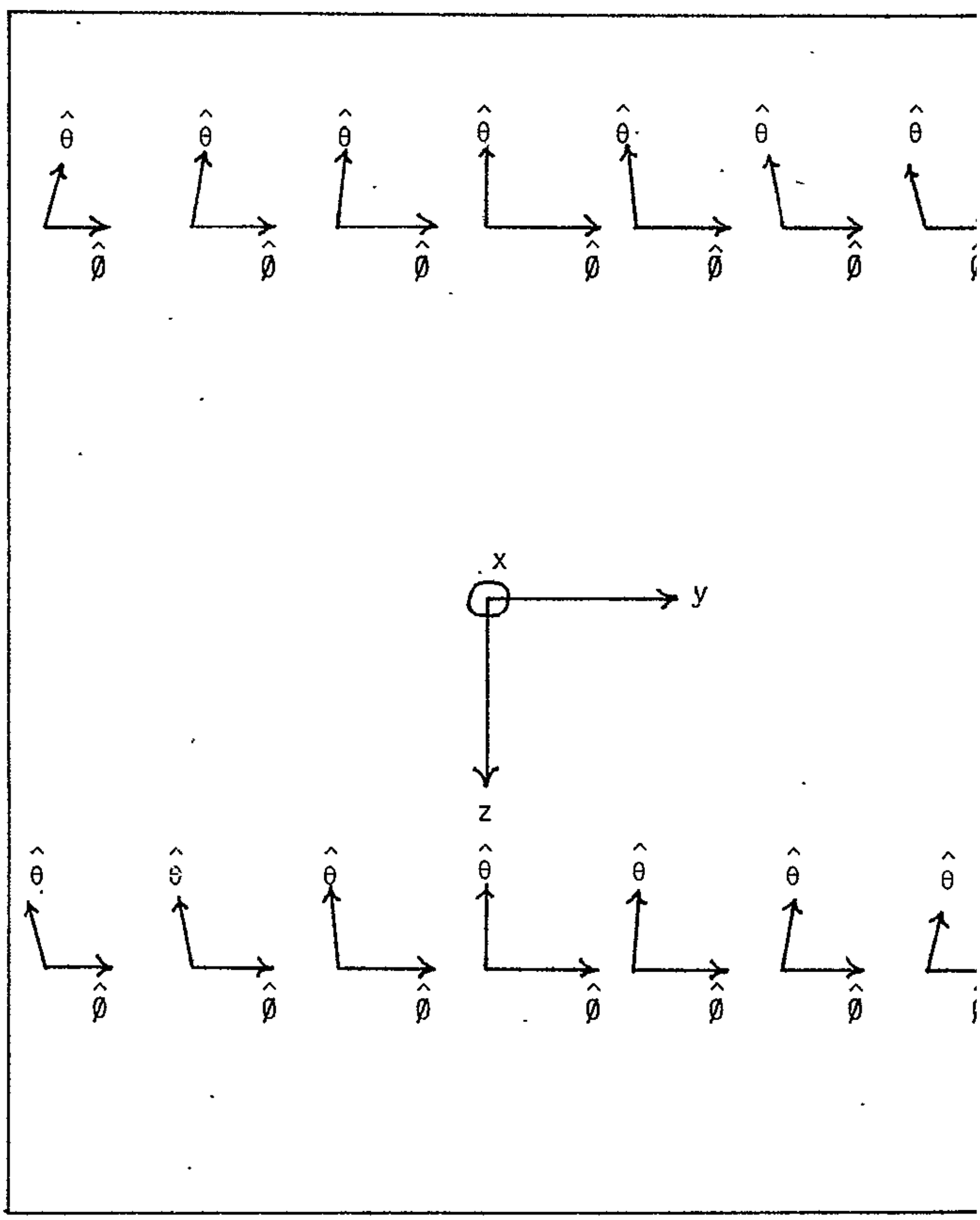

Fig. 11b. Overhead View of the Unit Vector Alignment on the Wave Tank Surface for the X-axis Geometry.

plotted they would look exactly the same all the time. Rotation about the z-axis does not affect the alignment of the vectors on the surface and consequently does not alter the dot products.

In addition to all the above advantages, the rotation about the z-axis has another tremendous advantage. The integration with respect to $\emptyset$ is in the form of a correlation, which can be evaluated by the use of Fourier transform techniques. The integration with respect to θ will be executed by numerical integration.

In order to reduce the computation time, we make the gain functions independent of α. This way the spectrum of the gain need only be found once and used for all values of α. To do this we add α to $\emptyset$ in the integrands of (105), (106), and (107) and then subtract α from the limits of integration creating $\emptyset_o = \emptyset - \alpha$. This yields

$$T_{awp}(\alpha,\beta) = \int_{-\emptyset_2-\alpha}^{\emptyset_1-\alpha} \int_{\theta_{ew}(\alpha,\rho,W,\emptyset_o+\alpha)}^{\pi/2} [\hat{h}(\theta,\emptyset_o+\alpha)\cdot\hat{\theta}\, E_{\theta p}(\theta,\emptyset_o-\beta) + \hat{h}(\theta,\emptyset_o+\alpha)\cdot$$

$$\hat{\emptyset}\, E_{\emptyset p}(\theta,\emptyset_o-\beta)]^2\, T_{bwh}[\theta,\emptyset_o+\alpha)]\sin\theta\, d\theta\, d\emptyset_o$$

$$+ \int_{-\emptyset_2-\alpha}^{\emptyset_1-\alpha} \int_{\theta_{ew}(\alpha,\rho,W,\emptyset_o+\alpha)}^{\pi/2} [\hat{v}(\theta,\emptyset_o+\alpha)\cdot\hat{\theta}\, E_{\theta p}(\theta,\emptyset_o-\beta) + \hat{v}(\theta,\emptyset_o+\alpha)\cdot$$

$$\hat{\emptyset}\, E_{\emptyset p}(\theta,\emptyset_o-\beta)]^2\, T_{bwv}[\theta''(\theta,\emptyset_o+\alpha)]\sin\theta\, d\theta\, d\emptyset_o. \quad (108)$$

$$T_{aep}(\alpha,\beta) = \int_{-\pi/2-\alpha}^{\pi/2-\alpha} \int_{0}^{\theta_{ew}(\alpha,\rho,W,\emptyset_o+\alpha)} T_{be}(\theta,\emptyset_o+\alpha)\ G_p(\theta,\emptyset_o-\beta)\ \sin\theta\ d\theta\ d\emptyset_o \qquad (109)$$

$$T_{asp}(\alpha,\beta) = \int_{\pi/2-\alpha}^{3\pi/2-\alpha} \int_{0}^{\pi/2} T_{bs}(\theta,\emptyset_o+\alpha)\ G_p(\theta,\emptyset_o-\beta)\ \sin\theta\ d\theta\ d\emptyset_o \qquad (110)$$

The following functions will now be defined:

$$T'_{bwh}(\theta,\emptyset_o+\alpha) \equiv \begin{cases} T_{bwh}(\theta'') & \text{for } -\emptyset_2-\alpha \le \emptyset_o \le \emptyset_1-\alpha \\ & \text{and } \theta_{ew} \le \theta \le \pi/2 \\ 0 & \text{elsewhere} \end{cases} \qquad (110a)$$

$$T'_{bwv}(\theta,\emptyset_o+\alpha) \equiv \begin{cases} T_{bwv}(\theta'') & \text{for } -\emptyset_2-\alpha \le \emptyset_o \le \emptyset_1-\alpha \\ & \text{and } \theta_{ew} \le \theta \le \pi/2 \\ 0 & \text{elsewhere} \end{cases} \qquad (110b)$$

$$T'_{be}(\theta,\emptyset_o+\alpha) \equiv \begin{cases} T_{be}(\theta,\emptyset_o+\alpha) & \text{for } -\pi/2-\alpha \le \emptyset_o \le \pi/2-\alpha \\ & \text{and } 0 \le \theta \le \theta_{ew} \\ 0 & \text{elsewhere} \end{cases} \qquad (110c)$$

$$T'_{bs}(\theta,\phi_o+\alpha) \equiv \begin{cases} T_{bs}(\theta,\phi_o+\alpha) & \text{for } \pi/2-\alpha < \phi_o < 3\pi/2-\alpha \text{ and all } \theta \\ 0 & \text{elsewhere} \end{cases} \quad (110d)$$

Using the primed functions we can rewrite (108) - (110) as

$$T_{awp}(\alpha,\beta) = \int_0^{2\pi}\int_0^{\pi/2} \{[\hat{h}(\theta,\phi_o+\alpha)\cdot\hat{\theta}\,E_{\theta p}(\theta,\phi_o-\beta) + \hat{h}(\theta,\phi_o+\alpha)\cdot$$

$$\hat{\phi}\,E_{\phi p}(\theta,\phi_o-\beta)]^2\,T'_{bwh}(\theta,\phi_o+\alpha) + [\hat{v}(\theta,\phi_o+\alpha)\cdot$$

$$\hat{\theta}\,E_{\theta p}(\theta,\phi_o-\beta) + \hat{v}(\theta,\phi_o+\alpha)\cdot\hat{\phi}\,E_{\phi p}(\theta,\phi_o-\beta)]^2$$

$$T'_{bwv}(\theta,\phi_o+\alpha)\}\,\sin\theta\,d\theta\,d\phi_o \quad (111)$$

$$T_{aep}(\alpha,\beta) = \int_0^{2\pi}\int_0^{\pi/2} T'_{be}(\theta,\phi_o+\alpha)\,G_p(\theta,\phi_o-\beta)\,\sin\theta\,d\theta\,d\phi_o \quad (112)$$

$$T_{asp}(\alpha,\beta) = \int_0^{2\pi}\int_0^{\pi/2} T'_{bs}(\theta,\phi_o+\alpha)\,G_p(\theta,\phi_o-\beta)\,\sin\theta\,d\theta\,d\phi_o \quad (113)$$

Expanding (111) and dropping the arguments for convenience, yields

$$T_{awp}(\alpha,\beta) = \int_0^{2\pi}\int_0^{\pi/2} [(\hat{h}\cdot\hat{\theta})^2 E_{\theta p}^{\;2} T'_{bwh} + (\hat{h}\cdot\hat{\emptyset})^2 E_{\emptyset p}^{\;2} T'_{bwh}$$

$$+ 2(\hat{h}\cdot\hat{\theta})(\hat{h}\cdot\hat{\emptyset}) E_{\theta p} E_{\emptyset p} T'_{bwh}$$

$$+ (\hat{v}\cdot\hat{\theta})^2 E_{\theta p}^{\;2} T'_{bwv} + (\hat{v}\cdot\hat{\emptyset})^2 E_{\emptyset p}^{\;2} T'_{bwv}$$

$$+ 2(\hat{v}\cdot\hat{\theta})(\hat{v}\cdot\hat{\emptyset}) E_{\theta p} E_{\emptyset p} T'_{bwv}] \sin\theta \, d\theta \, d\emptyset_o \qquad (114)$$

Equations (112), (113), and (114) are all of the form

$$T_a(\alpha,\beta) = \int_0^{2\pi}\int_0^{\pi/2} T'_b(\theta,\emptyset_o+\alpha)\, G(\theta,\emptyset_o-\beta) \sin\theta \, d\theta \, d\emptyset_o \qquad (115)$$

By performing the integration with respect to θ as a summation, (115) can be written as

$$T_a(\alpha,\beta) = \sum_{i=1}^{N} W_i \sin\theta_1 \int_0^{2\pi} T_b(\theta_i,\emptyset_o+\alpha)\, G(\theta_i,\emptyset_o-\beta)\, d\emptyset_o \qquad (116)$$

The variable θ is sampled N times while $\theta_1 = 0$ and $\theta_N \cong \pi/2$. The function W_i is the weighting factor for the particular numerical integration technique used.

For any constant value of α, (116) can be evaluated as

$$T_a(\alpha_0, -\beta) = \sum_{i=1}^{N} W_i \sin\theta_i \; F^{-1}\{\overline{T_b(f)_i}\; \overline{G(f)_i}^{*}\} \qquad (117)$$

where

$\overline{T_b(f)_i}$ = the periodic Fourier transform of $T_b(\theta_i, \emptyset_o + \alpha_o)$

$\overline{G(f)_i}^*$ = the complex conjugate of the transform of $G(\theta_i, \emptyset_o)$

Since $F^{-1}[\bar{A}] + F^{-1}[\bar{B}]$ is equivalent to $F^{-1}[\bar{A} + \bar{B}]$, computation time can be reduced by evaluating (117) as

$$T_a(\alpha_o, -\beta) = F^{-1}\{\sum_{i=1}^{N} \overline{T_b(f)_i}\ \overline{G(f)_i}^*\ W_i \sin\theta_i\} \tag{118}$$

The antenna temperature contributions can now be found as

$$\begin{aligned} T_{awp}(\alpha_o, -\beta) = F^{-1} \{ & \sum_{i=1}^{N} [\overline{T'_{bwhi}(\hat{\theta} \cdot \hat{h})_i^2}\ \overline{E_{\theta pi}^2}^*\ W_i \sin\theta_i] \\ & + 2\sum_{i=1}^{N} [\overline{T'_{bwhi}(\hat{\theta} \cdot \hat{h})_i (\hat{\emptyset} \cdot \hat{h})_i}\ \overline{E_{\emptyset pi} E_{\emptyset pi}}^*\ W_i \sin\theta_i] \\ & + \sum_{i=1}^{N} [\overline{T'_{bwhi}(\hat{\emptyset} \cdot \hat{h})_i^2}\ \overline{E_{\emptyset pi}^2}^*\ W_i \sin\theta_i] \\ & + \sum_{i=1}^{N} [\overline{T'_{bwvi}(\hat{\theta} \cdot \hat{v})_i^2}\ \overline{E_{\theta pi}^2}^*\ W_i \sin\theta_i] \\ & + 2\sum_{i=1}^{N} [\overline{T'_{bwvi}(\hat{\theta} \cdot \hat{v})_i (\hat{\emptyset} \cdot \hat{v})_i}\ \overline{E_{\theta pi} E_{\emptyset pi}}^*\ W_i \sin\theta_i] \\ & + \sum_{i=1}^{N} [\overline{T'_{bwvi}(\hat{\emptyset} \cdot \hat{v})_i^2}\ \overline{E_{\emptyset pi}^2}^*\ W_i \sin\theta_i] \} \end{aligned} \tag{119}$$

$$T_{aep}(\alpha_o,-\beta) = F^{-1}\{\sum_{i=1}^{N} \overline{T'_{bei}\, G_{pi}}\, \overline{W_i}^{*} \sin\theta_i\} \qquad (120)$$

$$T_{asp}(\alpha_o,-\beta) = F^{-1}\{\sum_{i=1}^{N} \overline{T'_{bsi}\, G_{pi}}\, \overline{W_i}^{*} \sin\theta_i\} \qquad (121)$$

Given α, equations (119), (120), and (121) can be used to find T_{awp}, T_{aep}, and T_{asp}, respectively, for all values of β. The transforms of the gain functions for each polarization, $\overline{E^2_{\theta pi}}^{*}$, $\overline{E^2_{\emptyset pi}}^{*}$, and $\overline{E_{\theta\rho}\, E_{\emptyset pi}}^{*}$, need be computed only once, since the gain functions are never needed in the time domain. The function $\overline{G_{pi}}^{*}$ is equal to $\overline{E^2_{\theta pi}}^{*} + \overline{E^2_{\emptyset pi}}^{*}$ and need not be computed separately.

The problem has now been formulated in two coordinate system configurations. The first used the z-axis as the antenna boresight to conform with the circularity of the antenna's power pattern. The second required the x-axis as the boresight. This allows the use of Fourier transforms to perform the integration and reduce the computation time when the T_a's for all values of β are computed. The necessity of knowing the T_a's for all values of β will become apparent in the inversion process.

D. The Gain Functions

In order to use either the z-axis or x-axis analysis, one must know the radiation characteristics of the antenna. Figure 12a shows the antenna geometry when the z-axis is taken to be perpendicular to the antenna aperture and Figure 12b shows the geometry with the x-axis perpendicular to the aperture. For either

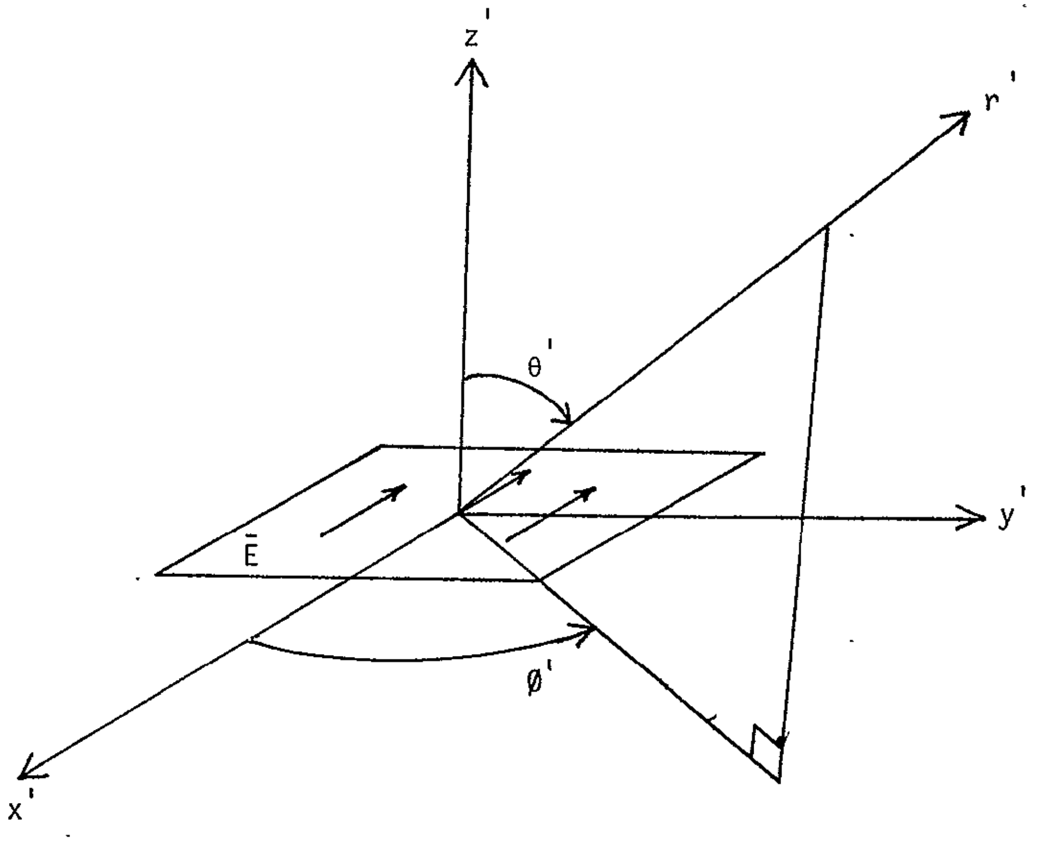

Fig. 12a. Z-axis Antenna Geometry.

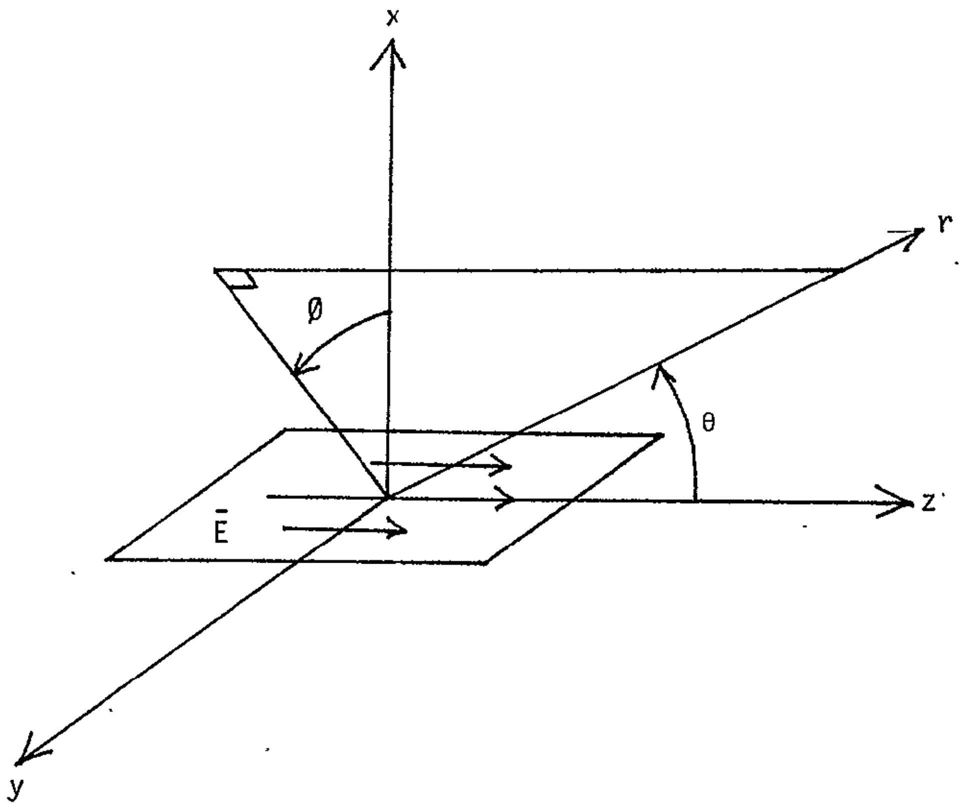

Fig. 12b. X-axis Antenna Geometry.

geometry, the three-dimensional power pattern can be obtained by

$$G(\theta,\phi) = G[\theta'(\theta,\phi), \phi' = 0]\cos^2\phi'(\theta,\phi) + G[\theta'(\theta,\phi), \phi' = \tfrac{\pi}{2}]\sin^2\phi'(\theta,\phi) \quad (122)$$

where

$$\theta' = \cos^{-1}\{\cos\phi \sin\theta\} \quad (123a)$$

$$\phi' = \tan^{-1}\{-\sin\phi \tan\theta\} \quad (123b)$$

Equations (122) and (12a) - (123b) can be used to construc the three-dimensional gain patterns from principal plane measurements whenever they can not be determined analytically.

E. Cross-polarization

Most practical antennas possess what is usually referred to as a cross-polarization pattern. For example, referring to Figure 12a, if there is no cross-polarization pattern, then in the E-plane (ϕ'=0) there would only be an E_θ component and in the H-plane ($\phi' = \frac{\pi}{2}$) only an E_ϕ component. Any radiated component which is orthogonal to the principal polarization is usually referred to as cross-polarization. Having no cross-polarization in the principal planes does not insure no cross-polarization in any other plane, as is demonstrated for a reflector system by

Silver [13]. In this investigation, the cross-polarized pattern will be assumed to have the same shape as the principal pattern. With this assumption, the antenna temperatures with cross-polarization (T'_{av} and T'_{ah}) can be related to the antenna temperatures with no cross-polarization (T_{av} and T_{ah}) by

$$T'_{av} = T_{av}/(1 + CROSS) + T_{ah} \cdot CROSS/(1 + CROSS) \qquad (124a)$$

$$T'_{ah} = T_{ah}/(1 + CROSS) + T_{av} \cdot CROSS/(1 + CROSS) \qquad (124b)$$

where CROSS refers to the fraction of power in the cross-polarized pattern. For example, if there is a -20 db cross-polarized pattern, then CROSS is 0.01. Equations (124a) and (124b) are exact if the shape of the cross-polarized pattern is the same as the principal pattern.

III. Inversion

A. Two-dimensional Approximation

So far, we have only concerned ourselves with the direct problem, that of finding the antenna temperature $T_a(\alpha,\beta)$ from the brightness temperature $T_b(\theta,\emptyset)$. Let us now approach the inverse problem of finding $T_b(\theta,\emptyset)$ from $T_a(\alpha,\beta)$. This inversion problem for the wave tank geometry was first approached by Fisher [7]. Referring to Figure 7, Fisher used a two-dimensional approximation to represent the wave tank system. Assuming that the antenna maximum (boresight) is directed only along the $\theta = \frac{\pi}{2}$ plane, the water is scanned along the line L_p. The two-dimensional approximation assumes that most of the energy of the antenna is within the major lobe and only integration along the $\theta = \frac{\pi}{2}$ plane is necessary. With this approximation (111), (112), and (113) can be reduced considerably. The dot products can be expressed as

$$\hat{\theta} \cdot \hat{h}(\tfrac{\pi}{2},\emptyset_o + \alpha) = \hat{\emptyset} \cdot \hat{v}(\tfrac{\pi}{2},\emptyset_o + \alpha) = 1 \tag{125a}$$

$$\hat{\emptyset} \cdot \hat{h}(\tfrac{\pi}{2},\emptyset_o + \alpha) = \hat{\theta} \cdot \hat{v}(\tfrac{\pi}{2},\emptyset_o + \alpha) = 0 \tag{125b}$$

Renormalizing the gain functions so that

$$\int_0^{2\pi} G_p(\tfrac{\pi}{2},\emptyset)d\emptyset_o = 1 \tag{126}$$

we can write (111), (112), and (113) as

$$T_{awp}(\alpha,\beta) \simeq \int_0^{2\pi} E^2_{\theta p}(\tfrac{\pi}{2},\emptyset_o - \beta)\, T'_{bwh}(\tfrac{\pi}{2},\emptyset_o + \alpha)\, d\emptyset_o$$

$$+ \int_0^{2\pi} E^2_{\emptyset p}(\tfrac{\pi}{2},\emptyset_o - \beta)\, T'_{bwv}(\tfrac{\pi}{2},\emptyset_o + \alpha)\, d\emptyset_o \qquad (127)$$

$$T_{aep}(\alpha,\beta) \simeq \int_0^{2\pi} G_p(\tfrac{\pi}{2},\emptyset_o - \beta)\, T'_{be}(\tfrac{\pi}{2},\emptyset_o + \alpha)\, d\emptyset_o \qquad (128)$$

$$T_{asp}(\alpha,\beta) \simeq \int_0^{2\pi} G_p(\tfrac{\pi}{2},\emptyset_o - \beta)\, T'_{bs}(\tfrac{\pi}{2},\emptyset_o + \alpha)\, d\emptyset_o \qquad (129)$$

The limits of integration can be made 0 to 2π since the primed brightness temperature functions are equal to zero in their respective regions to avoid overlapping. Assuming no cross-polarization in the principal planes, $E^2_{\emptyset p}$ is zero for the horizontal scan and $E^2_{\theta p}$ is zero for the vertical scan. We can then write (127), (128) and (129) as

$$T_{awp}(\alpha,\beta) \simeq \int_0^{2\pi} G_p(\emptyset_o - \beta)\, T'_{bwp}(\tfrac{\pi}{2},\emptyset_o + \alpha)\, d\emptyset_o \qquad (130)$$

$$T_{aep}(\alpha,\beta) \simeq \int_0^{2\pi} G_p(\emptyset_o - \beta)\, T'_{be}(\tfrac{\pi}{2},\emptyset_o + \alpha)\, d\emptyset_o \qquad (131)$$

$$T_{asp}(\alpha,\beta) \simeq \int_0^{2\pi} G_p(\emptyset_o-\beta)\; T'_{bs}(\tfrac{\pi}{2},\emptyset_o+\alpha)\; d\emptyset_o \tag{132}$$

which are of the same form as reported by Fisher [7] and Holmes [8]. With this two-dimensional approximation we can find the total antenna temperature by summing T_{awp}, T_{aep}, and T_{asp}, or T_{ap} can be found from one integral. To calculate T_a directly we use the continuous $T_{bp}(\frac{\pi}{2},\emptyset_o+\alpha)$ which is

$$T_{bp}(\emptyset_o+\alpha) = T'_{bwp}(\tfrac{\pi}{2},\emptyset_o+\alpha) + T'_{be}(\tfrac{\pi}{2},\emptyset_o+\alpha) + T'_{bs}(\tfrac{\pi}{2},\emptyset_o+\alpha) \tag{133}$$

We can therefore find $T_{ap}(\alpha,\beta)$ as

$$T_{ap}(\alpha,\beta) \simeq \int_0^{2\pi} G_p(\emptyset_o-\beta)\; T_{bp}(\emptyset_o+\alpha)\; d\emptyset_o \tag{134}$$

Equations (130), (131), (132), and (134) are all now in correlation form and can be evaluated, using Fourier transforms, as

$$T_{awp}(\alpha_o,-\beta) = F^{-1}\,\{\overline{G_p}^{*}\cdot\overline{T'_{bwp}}\} \tag{135}$$

$$T_{aep}(\alpha_o,-\beta) = F^{-1}\,\{\overline{G_p}^{*}\cdot\overline{T'_{be}}\} \tag{136}$$

$$T_{asp}(\alpha_o,-\beta) = F^{-1}\,\{\overline{G_p}^{*}\cdot\overline{T'_{bs}}\} \tag{137}$$

$$T_{ap}(\alpha_o, -\beta) = F^{-1}\{\overline{G_p}^* \cdot \overline{T_{bp}}\} \tag{138}$$

Using (138) as an example, T_{bp} can be found from T_{ap} by a simple division in the frequency domain followed by an inverse transform, or

$$T_{bp}(\emptyset_o + \alpha_o) = F^{-1}\{\overline{T_{ap}}/\overline{G_p}^*\} \tag{139}$$

Although (139) is a valid expression for the T_{bp} expressed in (134), the inversion technique is extremely sensitive to error in T_{ap}. Small errors in T_{ap} can cause large oscillations in the inverted function for T_{bp}[8]. The instability of the equation can be explained in both the spatial and frequency domains. In the frequency domain, we note that, for the type of functions used for G_p, the high frequency components of its spectrum are small compared to the low frequency components. Due to the division by $\overline{G_p}^*$, relatively small errors in the high frequency components of $\overline{T_{ap}}$ can cause large errors in the corresponding components of $\overline{T_{bp}}$. These errors cause high frequency oscillations in the spatial domain solution of T_{bp} in (139). This instability can also be explained by observing (134). If a high frequency sinusoid is added to T_{bp}, the function T_{ap} will be nearly unaffected [3,4]. Therefore, (134) does not uniquely define T_{bp} for a T_{ap} known with a moderate accuracy.

The inversion of the Fredholm integral equation, of which (134) is one type, has been encountered and studied in the fields of aerosol detection, astronomical measurement interpretation, and spectral analysis where cause and effect situations are of interest. Twomey [3] and Phillips [4] investigated the Fredholm equation of the first kind and were able to stabilize its inversion by employing matrix filtering techniques. Bracewell and Roberts [5] have reported an iterative restoration process which is particularly adaptable to our needs. The process introduced by Bracewell and Roberts and applied to a two-dimensional modelling of the wave tank geometry by Holmes stabilizes the inversion by avoiding the direct division by $\overline{G_p}^*$ in (139). Writing $1/\overline{G_p}^*$ of (139) as $1/[1 - (1-\overline{G_p}^*)]$, and then performing a series expansion [5] results in

$$T_{bp}(\emptyset + \alpha_o) = F^{-1}\{\overline{T_{awp}}\,[1 + (1 - \overline{G_p}^*) + (1 - \overline{G_p}^*)^2 + (1 - \overline{G_p}^*)^3 + ...]\} \tag{140}$$

The infinite series expansion of $1/\overline{G_p}^*$ converges provided that $|1-\overline{G_p}^*| < 1$. For most antennas used in radiometry, their gain patterns are symmetrical, smooth varying functions which insure that $\overline{G_p}^*$ is always real and positive in the dominant frequencies. The maximum values of these $\overline{G_p}^*$'s will be the average value of the spatial domain functions. Since G_p is normalized by (126), the average value is $1 / 2\pi$. The necessary conditions to insure the convergence of the series are therefore met. As the series converges, (140) becomes equal to (139) and the presence of error in T_{awp} will again cause oscillations. Fortunately, these unwanted oscillations mainly arise from the higher order terms in the series expansion of $1/\overline{G}_p^*$. By properly truncating the series we can obtain the smooth principle solution of the inversion. This inversion process can also be performed in the space domain. The first term of the series expansion assumes that T_{ap} is the first approximation of T_{bp} and each addition term represents a new approximation of T_{bp}. This restoring process can be interpreted as letting the values of T_{bp} be equal, respectively, to

$$T_{bpo} = T_{ap} \tag{141a}$$

$$T_{bp1} = T_{bpo} + (T_{ap} - G_p * T_{bpo}) \tag{141b}$$

$$T_{bp2} = T_{bp1} + (T_{ap} - G_p * T_{bp1}) \tag{141c}$$

$$\vdots$$

$$T_{bpn} = T_{bp(n-1)} + [T_{ap} - G_p * T_{bp(n-1)}] \tag{141d}$$

where * implies correlation. The altered inversion procedure reduces to an iterative method, as indicated by (141a) - (141d), and will be referred to as restoration [5]. The second term in (141a)-(141d) is a correction factor which is added to the values of the previous restored brightness temperature to obtain the newly created function.

Holmes [8] has tested the restoration process with the two-dimensional simulation of the wave tank problem. He has calculated $T_{ap}(\alpha_o,\beta)$ from the semi-empirical brightness temperature models, added errors to represent measuring inaccuracies, and restored the data using a truncated series to represent $1/\overline{G}_p^*$ in (140). Errors that caused large oscillation by direct inversion (139) did not create a stability problem in the restoration method.

B. Three-dimensional Inversion

Let us now investigate the problem of inverting the data using the three-dimensional model. As seen in (114), T_{awh} is dependent on both T'_{bwh} and T'_{bwv} and the same is true of T_{awv}. The equations are coupled and inversion is more complicated than in the two-dimensional case. At this point, we should review the goals of our inversion and what we will be given to obtain the necessary information. The desired results will be to obtain $T_{bwh}(\theta'')$ and $T_{bwv}(\theta'')$, where θ'' is the incidence angle, given $T_{ah}(\alpha_o,\beta)$ and $T_{av}(\alpha_o,\beta)$. To accomplish this, we will first need to make estimates of $T'_{be}(\theta,\emptyset)$ and $T'_{bs}(\theta,\emptyset)$ to calculate $T_{aep}(\alpha_o,\beta)$ and $T_{asp}(\alpha_o,\beta)$ The estimated T_{aep} and T_{asp} will then be subtracted from the total antenna temperature to find $T_{awh}(\alpha_o,\beta)$ and $T_{awv}(\alpha_o,\beta)$. In turn,the $T_{awh}(\alpha_o,\beta)$ and $T_{awv}(\alpha_o,\beta)$ functions will be inverted to restore $T_{bwh}(\theta'')$ and $T_{bwv}(\theta'')$.

At this point, we must make some assumptions about either the environment or the antenna in order to estimate T'_{bs} and T'_{be}. The sky brightness temperature (T'_{bs}) is not extremely critical. In the calculations the brightness temperature of the sky was assumed to be only a function of $\emptyset$. The functional variation of T'_{bs} along the $\theta = \frac{\pi}{2}$ plane as a function of $\emptyset$ can be approximated by either the empirical sky model or by the T_{ap} measured through the sky. Using these approximations of $T'_{bs}(\emptyset)$ for all values of θ is a good representation of the hemispherical brightness temperature profile except for the values of θ near 0 and π. Since these areas are only seen by the sidelobes of the antenna, this error causes negligible error in T'_{asp}.

The brightness temperature of the earth is a little more critical since it borders the water. Since, for the earth, there is no functional relationship between the brightness temperature in the $\theta = \frac{\pi}{2}$ plane and the other θ planes, we assume that T'_{be} is only a function of $\emptyset$. T_{ap} can be used as an approximation of T'_{be} except for the values of β which put the boresight near the wave tank. Referring to Figure 10, we define a new function $T''_b(\emptyset)$ as

$$T''_b(\emptyset) = T_{ap}(\beta = \emptyset_1 - \alpha + \tfrac{\pi}{90}) \qquad \emptyset_1 + \tfrac{\pi}{90} > \emptyset > 0 \tag{142a}$$

$$T''_b(\emptyset) = T_{ap}(\beta = \emptyset - \alpha) \qquad \tfrac{\pi}{2} > \emptyset > \emptyset_1 + \tfrac{\pi}{90} \tag{142b}$$

$$T''_b(\emptyset) = 0 \qquad \tfrac{3\pi}{2} > \emptyset > \tfrac{\pi}{2} \tag{142c}$$

$$T''_b(\emptyset) = T_{ap}(\beta = \emptyset - \alpha) \qquad 2\pi - \emptyset_2 - \tfrac{\pi}{90} > \emptyset > \tfrac{3\pi}{2} \tag{142d}$$

$$T''_b(\emptyset) = T_{ap}(\beta = -\emptyset_2 - \alpha - \tfrac{\pi}{90}) \quad 2\pi > \emptyset > 2\pi - \emptyset_2 - \tfrac{\pi}{90} \tag{142e}$$

Using θ_{ew} as expressed in (104) and $T_b''(\emptyset)$, we can form $T_{be}'(\theta,\emptyset)$ as

$$T_{be}'(\theta,\emptyset) = T_b''(\emptyset) \qquad \text{if } \theta < \theta_{ew} \tag{143a}$$

$$T_{be}'(\theta,\emptyset) = 0 \qquad \text{if } \theta > \theta_{ew} \tag{143b}$$

Equation (120) can now be used to find $T_{aep}(\alpha_o,\beta)$.

Referring to Figures 8 and 10, the x'-axis (antenna boresight) intersects the plane of the water surface at incidence angles between 0 and $\emptyset_1$ if $\emptyset_2$ is positive or between $-\emptyset_2$ and $\emptyset_1$ if $\emptyset_2$ is negative. Knowing the T_{bwp}'s for these incidence angles is sufficient to compute the T_{bwp}'s over nearly the entire water surface of the tank, since the incidence angle can be computed exactly over the entire water surface with the use of (89). The only points which have incidence angles not in these ranges are the corners of the tank that are the farthest from the antenna. The brightness temperature functions of the water can be interpolated for these points. Given $T_{bwv}'(\frac{\pi}{2},\emptyset)$ and $T_{bwh}'(\frac{\pi}{2},\emptyset)$, the brightness temperature all over the water surface can be found and, from (119), $T_{awh}(\alpha_o,\beta)$ and $T_{awv}(\alpha_o,\beta)$ can be calculated.

The restoration process used by Holmes [8] will now be applied to the three-dimensional problem. The first approximation of $T_{bwh}'(\frac{\pi}{2},\emptyset_o)$ and $T_{bwv}'(\frac{\pi}{2},\emptyset_o)$, for the particular range of incidence angles needed, will be $T_{awh}(\beta)$ and $T_{awv}(\beta)$, respectively. These first approximations will be called $T_{bwh1}(\emptyset_o)$ and $T_{bwv1}(\emptyset_o)$, and from them we can find $T_{awh1}(\beta)$ and $T_{awv1}(\beta)$ through (119). The difference between $T_{awh1}(\beta)$ and $T_{awh}(\beta)$ will be defined as $ER_{h1}(\beta)$.

Similarly, the difference between $T_{awv1}(\beta)$ and $T_{awv}(\beta)$ will be called $ER_{v1}(\beta)$.

A second approximation of T_{bwv} and T_{bwh}(T_{bwv2} and T_{bwh2}, respectively) needs to be found from T_{bwv1}, T_{bwh1}, ER_{h1}, and ER_{h2}. Since the brightness temperatures and antenna temperatures are coupled, the following algorithm will be used to restore T_{bwh} and T_{bwv}:

$$T_{bwh2} = T_{bwh1} + WF_1 \cdot ER_{h1} + WF_2 \cdot ER_{v1} \tag{144a}$$

$$T_{bwv2} = T_{bwv1} + WF_3 \cdot ER_{h1} + WF_4 \cdot ER_{v1} \tag{144b}$$

or in general

$$T_{bwh(n+1)} = T_{bwh(n)} + WF_1 \cdot ER_{h(n)} + WF_2 \cdot ER_{v(n)} \tag{145a}$$

$$T_{bwv(n+1)} = T_{bwv(n)} + WF_3 \cdot ER_{h(n)} + WF_4 \cdot ER_{v(n)} \tag{145b}$$

The terms WF_1, WF_2, WF_3, and WF_4 are weighting functions.

To determine the weighting functions for any value of β, we find what percentage of the power of the antenna incident on the water surface aligns with the horizontal vectors and what percentage aligns with the vertical vectors. If x% of the antenna's power picks up T_{bwh} while measuring $T_{awh}(\beta_o)$, then x% of the error in the approximation of T_{bwh} at that particular incidence angle can be corrected by $ER_{h1}(\beta_o)$. The functions WF_1, WF_2, WF_3, and WF_4 are defined to be the percentage alignment of G_h, G_h, G_v, and G_v in the h, v, h, and v directions, respectively, for each value of β. For example, the weighting function WF_1 would be found as

$$WF_1(\beta) = \frac{\iint\limits_{\substack{\text{over}\\\text{water}}} [\hat{h} \cdot \hat{\theta}\, E_{\theta h} + \hat{h} \cdot \hat{\emptyset}\, E_{\emptyset h}]^2 \sin\theta \, d\theta \, d\emptyset.}{\iint\limits_{\substack{\text{over}\\\text{water}}} G_h \sin\theta \, d\theta \, d\emptyset.} \tag{146}$$

All the functions in (145a and b) have now been defined and the restoration can be performed.

The three-dimensional restoration acknowledges the influence of the following:
1. the vector misalignment off the principal axes of the antenna, 2. any cross-polarization in the antenna pattern, 3. the entire three dimensional environment, and 4. the true two variable power pattern of the antenna. The previously mentioned stability characteristics of the restoration procedure are also retained.

IV. Computations and Results

A. Finite Wave Tank

The modeling of the interaction between the wave tank environment and the radiometer antenna has now been described in several different ways. In order to establish the validity of the various methods, computations were made with each of the methods while viewing identical environments with the same antenna. The results of these computations will establish the accuracy of the three-dimensional vector formulations and also the shortcomings of the two-dimensional scalar method.

Given the brightness temperature characteristics of the wave tank environment, the antenna temperature for the horizontal scan T_{ah} and the vertical scan T_{av} can now be predicted with four different computer programs developed during the course of this investigation. The first of these is a computer program based on the three-dimensional analysis when the z-axis is normal to the radiometer antenna aperture, similar to the one developed by Beck [9], of the wave tank system. The integration with respect to the spherical coordinates θ and $\emptyset$ is numerically performed with the trapezoidal rule. This program is designed to make direct calculations of $T_{ah}(\alpha,\beta=0)$ and $T_{av}(\alpha,\beta=0)$ given the brightness temperature profiles of the water, $T_{bwh}(\theta,\emptyset)$ and $T_{bwv}(\theta,\emptyset)$, of the earth $T_{be}(\theta,\emptyset)$, and of the sky $T_{bs}(\theta,\emptyset)$. Since $\beta=0$ (no scanning) for all cases with this program, the antenna is always assumed to be viewing the center of the tank at the incidence angle α. Secondly, another three-dimensional computer program has been developed that takes the x-axis perpendicular to the radiometer antenna aperture and performs the calculations again with numerical integration. The integration with respect to Ø is done using a 256 point midpoint rule and with respect to θ using a 32 point Gaussian quadrature method. This program was written to yield T_{ah} and T_{av} for various α's and $\beta=0$, as was the first program. The third and most important program uses the same coordinate system alignment as the second program (x-axis perpendicular to the aperture) but has the capability to handle scanning in the Ø direction. It uses a 32-point Gaussian quadrature method to integrate with respect to θ. However, the scanning of the antenna through the entire 360° range of the angle β and the integration with respect to Ø is handled simultaneously in the transform domain via the correlation form and a 256 sample point fast Fourier transform technique. The results of this program can be compared with those of the two previous programs for $\beta=0$. It is the use of this program that enables the inversion (restoration) of the data. The last program that predicts the radiometer response is the two-dimensional approximation used by Fisher [7] and Holmes [8]. This formulation also uses fast Fourier transform techniques to carry out the integration for the scanning of the radiometer.

Computed data of the same geometry using these four programs will be used to verify the analyses and computer programming of the equations. Several different comparisons between them will be made to validate the techniques. If the results from the z-axis and x-axis programs agree, the validity of both formulations as well as the accuracy of the programming and integration techniques will be established. When the results of the x-axis numerical integration program match the output of the x-axis fast Fourier transform program, they insure that the transform techniques is accurately performing the necessary integration. Finally, comparisons of the two-dimensional approximation with the three-dimensional data provides criteria as to when it is mandatory to use the three-dimensional program to obtain the desired accuracy.

To test these various methods, the radiation characteristics of two different radiometer antennas will be used. Both of the antennas are pyramidal, corrugated horns with square apertures. The first horn has an aperture width of 12λ and a total flare angle of 13°. The half-power beamwidth of this horn is approximately 6°. This is the antenna that is being used by NASA to take measurements in the wave tank system. In addition to the 12λ aperture antenna, the response of the system using an 8λ corrugated horn with a half-power beamwidth of 10° and a total flare angle of 19° will also be examined. The flare angles of these horns were designed so there would be a 120° phase lag in the wave at the edges of the aperture as compared to the wave at the center. This particular phase taper in the aperture field creates a far-field pattern with no appreciable sidelobes or backlobes, which is desirable for radiometric measurements. Shown in Figures 13 and 14 are the principal plane patterns

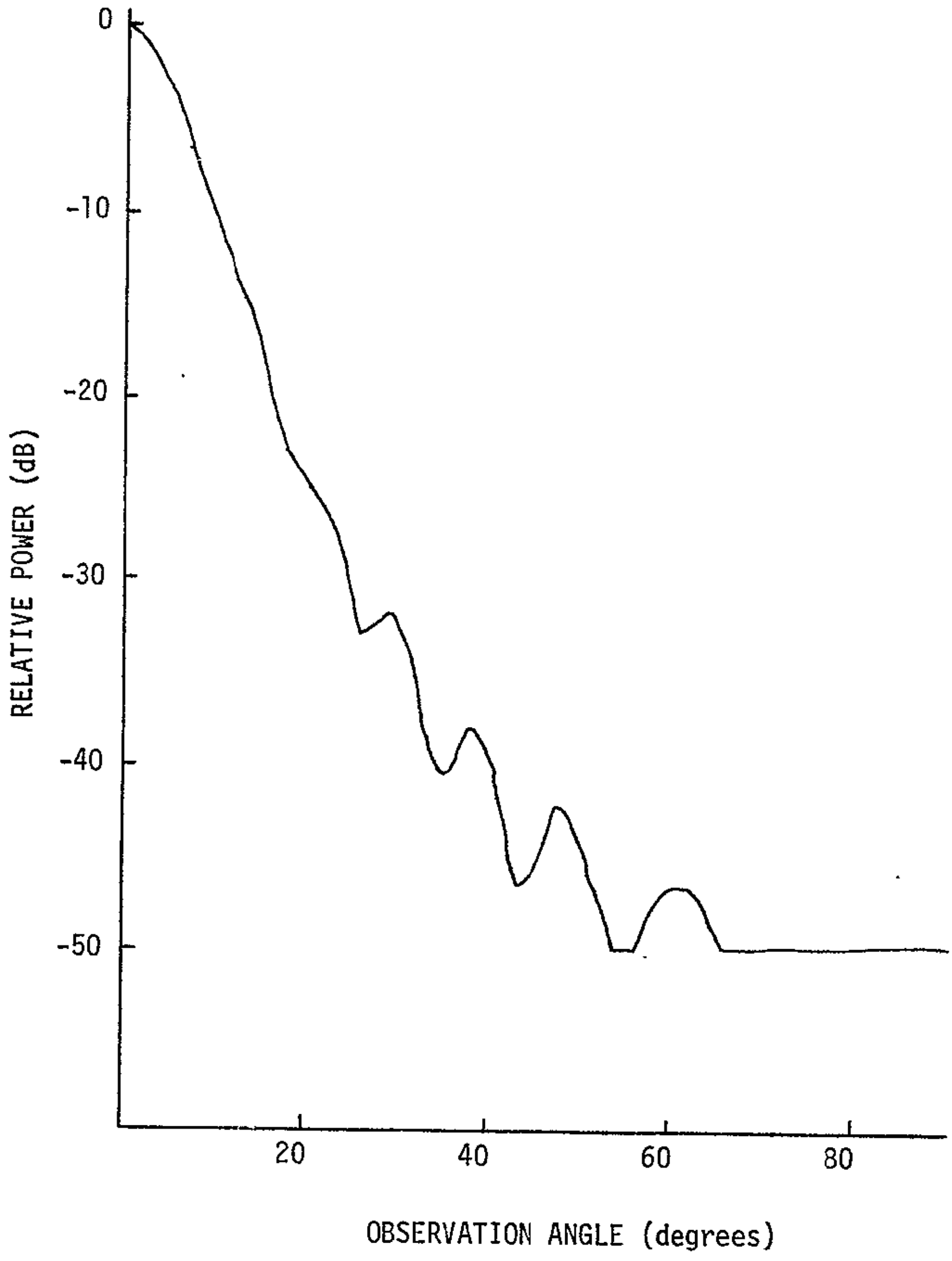

Fig. 13. Principal Plane Power Pattern of the 8λ Corrugated Horn Antenna.

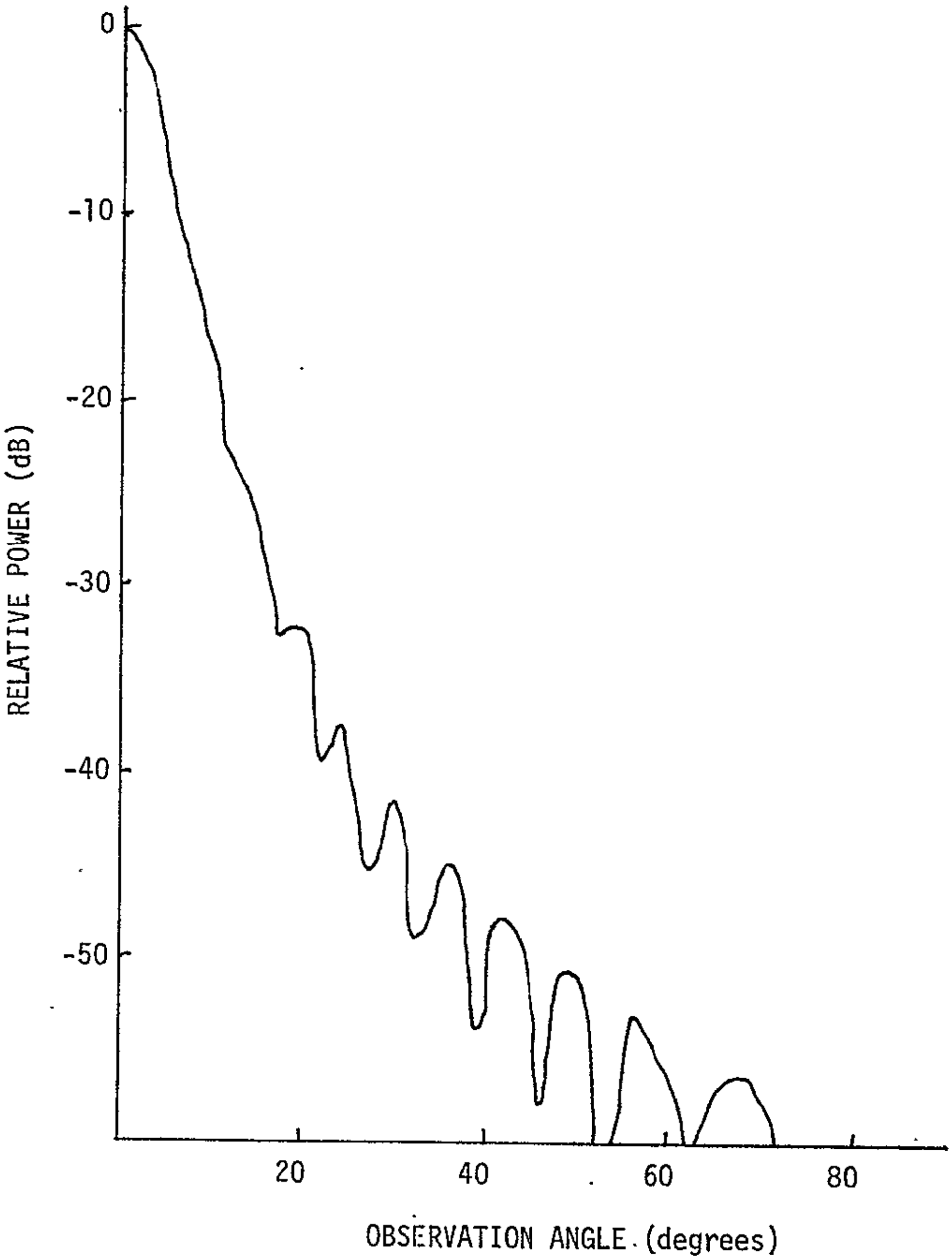

Fig. 14. Principal Plane Power Pattern of the 12λ Corrugated Horn Antenna.

of the 8λ and 12λ horns, respectively. These will be used to carry out the necessary computations of the finite wave tank system.

Before attempting any inversions, it will be desirable to perform some direct computations, calculating the antenna temperatures given the brightness temperatures, to validate the analyses and computer programming. Upon a successful evaluation of the formulation and programming, inversion (restoration) of data will then be examined.

1. Direct Computations of Antenna Temperatures

Physically, the wave tank is 14 feet square and the length of the boom that supports the antenna can be either 13 feet or 26 feet. In Table I, the predicted results for the 12λ horn and the 13 foot boom are shown. The variables T_{awh} and T_{awv} are the horizontal and vertical antenna temperature contributions from the water's surface, and T_{aes} is the combined antenna temperature from the earth and sky. All three of the three-dimensional programs yield nearly identical results. With this antenna and boom length combination, the two-dimensional formulation also yields fairly accurate results.

In Table II, the predicted results for the 8λ horn and the 13 foot boom are shown. It is quite evident that the data from the two x-axis programs are almost identical and agreement with the z-axis results is very good. With the wider 8λ horn, agreement

TABLE I

Computed Antenna Temperatures for Finite Wave Tank System

(ρ = 13 feet, Antenna = 12λ horn)

(f = 10.69 GHz, T_m = 284°K, S = 0 $^0/oo$)

		$\alpha=0^\circ$	$\alpha=20^\circ$	$\alpha=40^\circ$	$\alpha=60^\circ$	$\alpha=80^\circ$
3-D Z-AXIS N.I.	T_{awh}	109.07	104.12	89.17	64.47	34.31
	T_{awv}	109.07	114.48	133.37	176.71	231.84
	T_{aes}	0.08	0.09	0.19	1.28	36.34
3-D X-AXIS FFT	T_{awh}	109.07	104.13	89.18	64.48	34.46
	T_{awv}	109.07	114.46	133.37	176.77	232.91
	T_{aes}	0.08	0.10	0.18	1.20	35.08
3-D X-AXIS N.I.	T_{awh}	109.07	104.12	89.18	64.48	34.46
	T_{awv}	109.07	114.46	133.37	176.77	232.91
	T_{aes}	0.08	0.09	0.18	1.20	35.06
2-D FFT	T_{awh}	108.95	104.00	89.05	64.46	34.24
	T_{awv}	109.23	114.59	133.40	176.74	233.14
	T_{aes}	0.03	0.05	0.14	1.15	34.79

TABLE II

Computed Antenna Temperatures for Finite Wave Tank System

(ρ = 13 feet, Antenna = 8λ horn)

(f = 10.69 GHz, T_m = 284°K, S = 0 ^{o}/oo)

		α=0°	α=20°	α=40°	α=60°	α=80°
3-D Z-AXIS N.I.	T_{awh}	108.96	103.98	88.90	63.52	30.84
	T_{awv}	108.96	114.40	133.17	173.03	201.28
	T_{aes}	0.41	0.46	1.12	7.19	63.18
3-D X-AXIS FFT	T_{awh}	108.97	104.01	88.96	63.58	31.14
	T_{awv}	108.97	114.38	133.22	173.23	202.79
	T_{aes}	0.38	0.46	1.00	6.90	61.06
3-D X-AXIS N.I.	T_{awh}	108.96	104.00	88.95	63.58	31.14
	T_{awv}	108.97	114.37	133.21	173.22	202.79
	T_{aes}	0.38	0.46	1.00	6.90	60.98
2-D FFT	T_{awh}	108.74	103.77	88.74	63.54	31.16
	T_{awv}	109.35	114.72	133.41	173.30	204.12
	T_{aes}	.16	.12	.79	6.61	59.42

between the three- and two-dimensional computations is not as good.

The results obtained using the 12λ horn and the 26 foot boom are shown in Table III. Again the three-dimensional modelings yiel(results in agreement; however, the two-dimensional programming is not as accurate even though the more efficient 12λ horn was used. With the 26 foot boom, the angular limits of the wave tank are appreciably smaller and some of the main beam power spills over intc the earth. Since the earth is very warm, as compared to the water, an accurate modeling is needed at directions off the antenna boresight. The two-dimensional modeling can not provide this accuracy.

To demonstrate how the greater accuracy of the three-dimensional formulation becomes imperative for antennas with wider main beams, the computed responses of the wave tank system with the 8λ horn antenna and the 26 foot boom are shown in Table IV. By examining the data it is clear that, although all of the three-dimensional modelings agree well, the two-dimensional approximation is no longer an accurate method for predicting the radiometer response. Having now established the accuracy and necessity of the three-dimensional formulation, an examination of the inversion (restoration) procedure, as applied to the wave tank system, will be undertaken.

2. Inversion (Restoration) Techniques for Antenna Brightness Temperature

With the 26 foot boom and the 14 foot wave tank, the

TABLE III

Computed Antenna Temperatures for Finite Wave Tank System

(ρ = 26 feet, Antenna = 12λ horn)

(f = 10.69 GHz, T_m = 284°K, S = 0 $^o/oo$)

		$\alpha=0^\circ$	$\alpha=20^\circ$	$\alpha=40^\circ$	$\alpha=60^\circ$	$\alpha=80^\circ$
3-D Z-AXIS N.I.	T_{awh}	108.76	103.76	88.58	64.40	25.09
	T_{awv}	108.76	114.06	132.32	169.73	173.30
	T_{aes}	.94	1.16	2.34	11.95	104.03
3-D X-AXIS FFT	T_{awh}	108.76	103.81	88.66	62.65	25.04
	T_{awv}	108.77	114.10	132.49	170.37	173.31
	T_{aes}	.93	1.03	2.02	10.85	104.12
3-D X-AXIS N.I.	T_{awh}	108.77	103.81	88.66	62.65	25.04
	T_{awv}	108.76	114.10	132.49	170.37	173.31
	T_{aes}	0.93	1.03	2.02	10.85	104.10
2-D FFT	T_{awh}	108.82	103.83	88.71	62.83	27.30
	T_{awv}	109.09	114.38	132.78	170.84	188.43
	T_{aes}	.41	.58	1.39	9.90	85.90

TABLE IV

Computed Antenna Temperatures for Finite Wave Tank System

(ρ = 26 feet, Antenna = 8λ horn)

(f = 10.69 GHz, T_m = 284°K, S = 0 $^0/_{oo}$)

		$\alpha=0^\circ$	$\alpha=20^\circ$	$\alpha=40^\circ$	$\alpha=60^\circ$	$\alpha=80^\circ$
3-D Z-AXIS N.I.	T_{awh}	106.94	101.72	85.60	57.48	18.66
	T_{awv}	106.94	111.78	127.53	154.66	128.18
	T_{aes}	5.94	7.12	12.90	36.46	150.02
3-D X-AXIS FFT	T_{awh}	106.93	101.96	85.82	58.04	18.42
	T_{awv}	106.92	112.03	128.00	156.01	126.85
	T_{aes}	5.99	6.45	12.03	34.07	151.43
3-D X-AXIS N.I.	T_{awh}	106.93	101.96	85.82	58.04	18.42
	T_{awv}	106.92	112.03	128.00	156.01	126.85
	T_{aes}	5.98	6.44	12.03	34.05	151.36
2-D FFT	T_{awh}	107.88	102.78	86.76	59.23	21.58
	T_{awv}	108.42	113.44	129.77	158.99	147.34
	T_{aes}	2.61	3.33	8.15	28.60	127.10

boresight of the antenna will intersect the edges of the wave tank when $\beta = \pm 15^\circ$ for $\alpha=0^\circ$. With the 13 foot boom, the angular limits of the wave tank are $\beta = \pm 28.3^\circ$ for $\alpha=0^\circ$. For all other values of α, the angular space for viewing the wave tank is reduced. Since the antenna only possesses finite resolution, the range of incidence angles from which the brightness temperatures can be restored will be less than the angular limits of the wave tank. Therefore, in order to get continuous restored brightness temperature profiles, it will be necessary to combine the data from several values of α. The values of α that were chosen are 5°, 10°, 20°, 30°, 40°, 50°, 55°, 60°, 65°, 70°, 75°, and 80°.

In Figure 15, the results of a restoration process are shown. For the above mentioned values of α, antenna temperature profiles were calculated, using the 12λ horn antenna and the 13 foot antenna supporting boom, from the semi-empirical brightness temperature models of Stogryn [11]. Each α value only yields a limited range of incidence angles. The resulting antenna temperature profiles T_a, the original brightness temperature profiles T_b, and the restored brightness temperatures T_{bres}, using three iterations, are shown in the figure for vertical and horizontal polarizations. By combining the profiles for the different α's, nearly continuous curves have been formed. To improve the accuracy of the resulting curves, one could draw smooth curves through the $\beta=0^\circ$ points of the data. These points yield fairly accurate results since they represent the system while the boresight is viewing the center of the wave tank. This has been done and the antenna, the restored

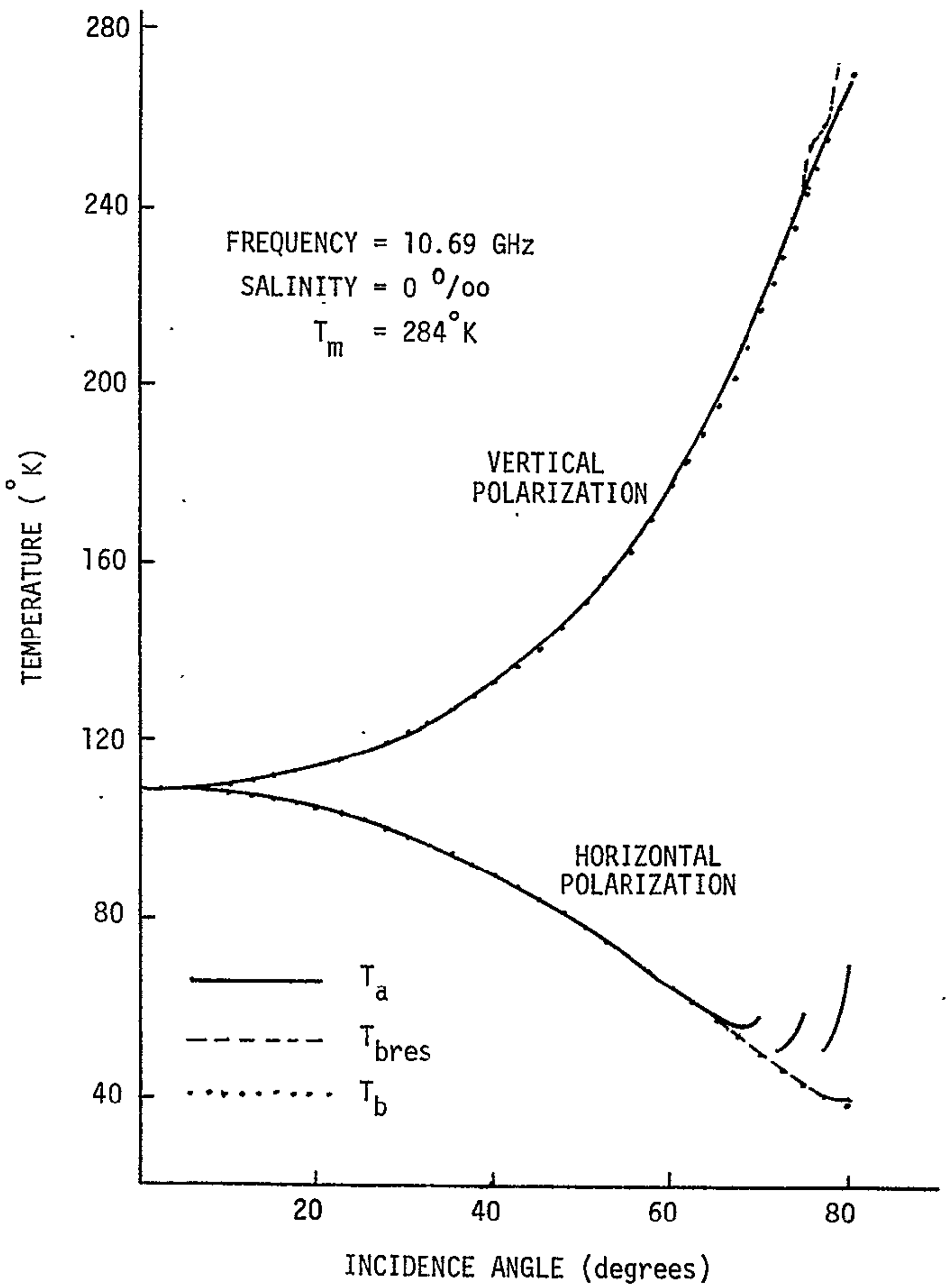

Fig. 15. Continuous Incidence Angle Restoration Results for the Finite Wave Tank (Antenna = 12λ horn, ρ = 13 feet, three iterations).

brightness and the empirical brightness temperatures for the 12λ horn, 13 foot boom, and $\beta=0^\circ$ data are shown in Figure 16. It can be seen from the plotted data in Figures 15 and 16 that the horizontal polarization results are improved by the restoration process for incidence angles greater than 60°, and the vertical polarization inversion results are less accurate than the antenna temperatures for the larger angles. However, little can be inferred about the accuracy of the results for the incidence angles less than 60° for both polarizations.

In order to get a more detailed look at the accuracy of the restoration process, some of the data from Figures 15 and 16 is listed in Table V. This table includes the total antenna temperature T_a, the restored brightness temperature T_{bres}, the difference between T_a and the original brightness temperature T_b, and the difference between T_{bres} and T_b. As can be seen, the restored brightness temperatures are always a better approximation of the true brightness temperature than the antenna temperatures for the horizontal polarization. Improvement is obtained in the vertical polarization case for all incidence angles up to and including 60°. Although the differences between the antenna temperatures and the brightness temperatures were very small, the restoration process was still able to improve the results.

Any instability in the solution will become evident as more restorations are taken. To show that the computations with three iterations are indeed convergent and are an improvement from those

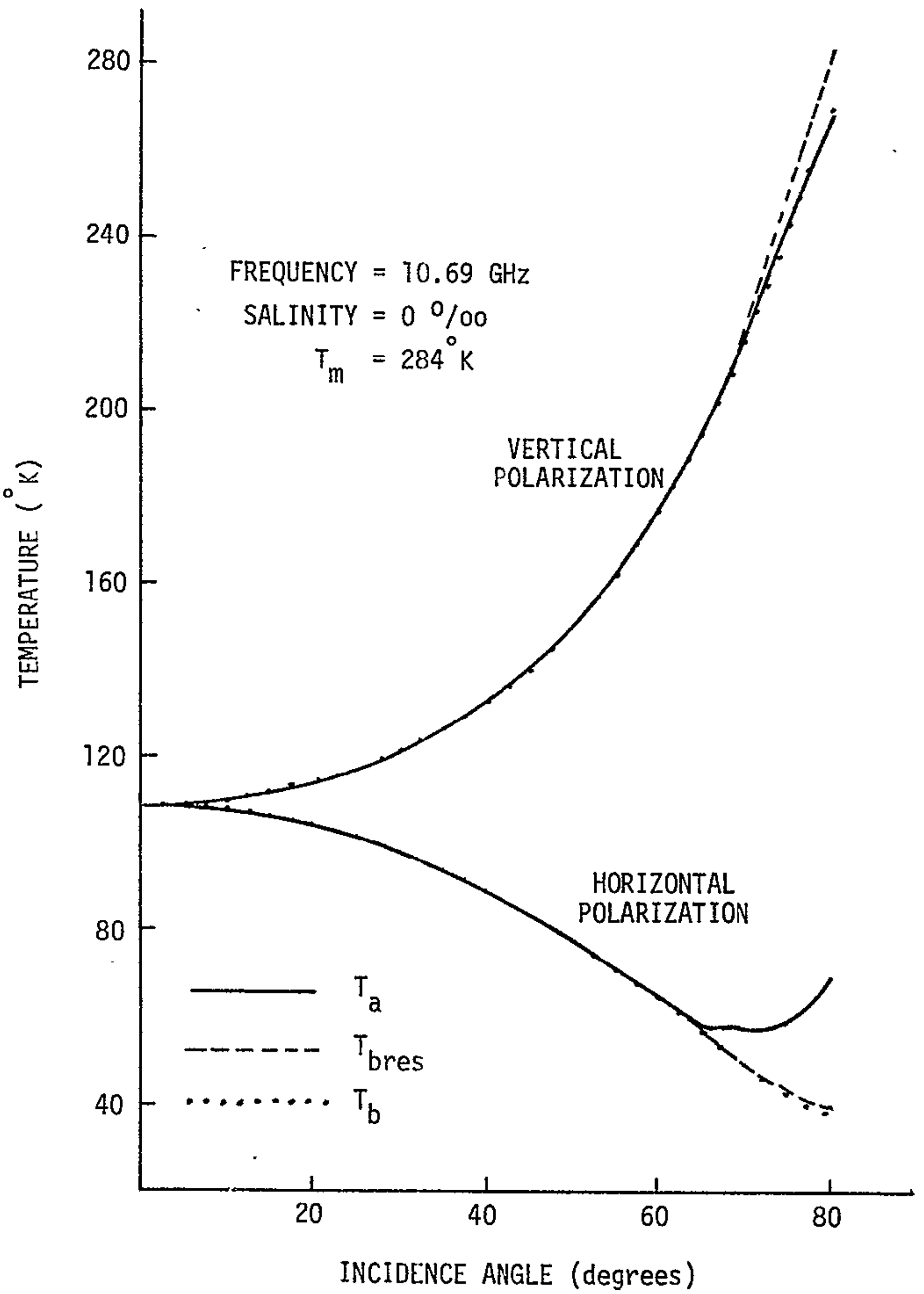

Fig. 16. Smoothed β=0 Restoration Results for the Finite Wave Tank (Antenna = 12λ horn, ρ = 13 feet, three iterations).

TABLE V

Restored Antenna Temperatures for Finite Wave Tank with Three Restorations

(Antenna = 12λ horn, ρ = 13 feet, f = 10.69 GHz, T_m = 284°K, S = 0 ‰)

HORIZONTAL POLARIZATION

Incidence Angle	T_a	T_{bres}	$T_a - T_b$	$T_{bres} - T_b$
0°	109.14	109.08	0.04	- 0.02
10°	107.92	107.88	0.06	0.01
20°	104.22	104.17	0.06	0.01
30°	98.02	97.98	0.06	0.01
40°	89.36	89.25	0.10	- 0.01
50°	78.44	77.97	0.34	- 0.13
60°	65.69	64.56	0.98	- 0.14
70°	58.15	50.42	8.20	0.48
80°	69.54	39.90	31.57	1.93

VERTICAL POLARIZATION

Incidence Angle	T_a	T_{bres}	$T_a - T_b$	$T_{bres} - T_b$
0°	109.18	109.12	0.08	0.02
10°	110.46	110.41	0.07	0.01
20°	114.56	114.46	0.12	0.01
30°	121.92	121.75	0.19	0.02
40°	133.55	133.17	0.36	- 0.02
50°	151.25	150.12	0.68	- .45
60°	177.97	176.15	1.10	- .73
70°	219.07	220.28	2.11	3.32
80°	267.99	283.05	- 1.71	13.35

obtained with fewer restorations, the results of the inversion process for the 12λ horn and the 13 foot boom with one restoration are listed in Table VI. By comparing Table V with Table VI, one can see that, with the exception of the 80° incidence angle, more accurate results are obtained with the three-restoration process. When $\alpha=80^\circ$, the angular limits of the wave tank (see Figure 7) are at $\beta = +3.5^\circ$ and $\beta = -11.3^\circ$. This is too small of an angular sector to expect accurate results. The restoration process is shown to be convergent and to yield improved results.

In Figure 17, the computed antenna, the restored brightness (three restorations), and the empirical brightness temperatures for the continous incidence angle data, utilizing the 8λ horn and the 13 foot boom, are shown. In Figure 18, the smoothed $\beta=0^\circ$ curves for the same case are shown. As with the 12λ horn and 13 foot data, an improvement can be seen in the horizontal polarization with a slight instability for the vertical polarization at incidence angles greater than 60°. For a more accurate analysis of the data, Table VII has been included. From the table, one can see that the restored data yields a more accurate approximation than the antenna temperatures for all angles listed, except 70° for the vertical polarization. Table VIII lists the one restoration results for the 8λ horn and the 13 foot boom. Again one can conclude that the restoration process has proven to be convergent and utilitarian.

The restoration process has also been applied to computed antenna temperatures for the 12λ horn and the 26 foot boom. For

TABLE VI

Restored Antenna Temperatures for Finite Wave Tank
with One Restoration

(Antenna = 12λ horn, ρ = 13 feet, f = 10.69 GHz, T_m = 284°K, S = 0 °/oo)

HORIZONTAL POLARIZATION

Incidence Angle	T_a	T_{bres}	$T_a - T_b$	$T_{bres} - T_b$
0°	109.14	109.08	0.04	- 0.02
10°	107.92	107.87	0.06	0.01
20°	104.22	104.17	0.06	0.01
30°	98.02	97.98	0.06	0.02
40°	89.36	89.30	0.10	0.04
50°	78.44	78.27	0.34	0.17
60°	65.69	65.16	0.98	0.46
70°	58.15	51.08	8.20	1.14
80°	69.54	38.90	31.57	0.93

VERTICAL POLARIZATION

Incidence Angle	T_a	T_{bres}	$T_a - T_b$	$T_{bres} - T_b$
0°	109.18	109.12	0.08	0.02
10°	110.46	110.41	0.07	0.01
20°	114.56	114.46	0.12	0.01
30°	121.92	121.77	0.19	0.04
40°	133.55	133.30	0.36	0.11
50°	151.25	151.17	0.68	0.60
60°	177.97	179.15	1.10	2.28
70°	219.07	224.60	2.11	7.63
80°	267.99	271.27	- 1.71	1.56

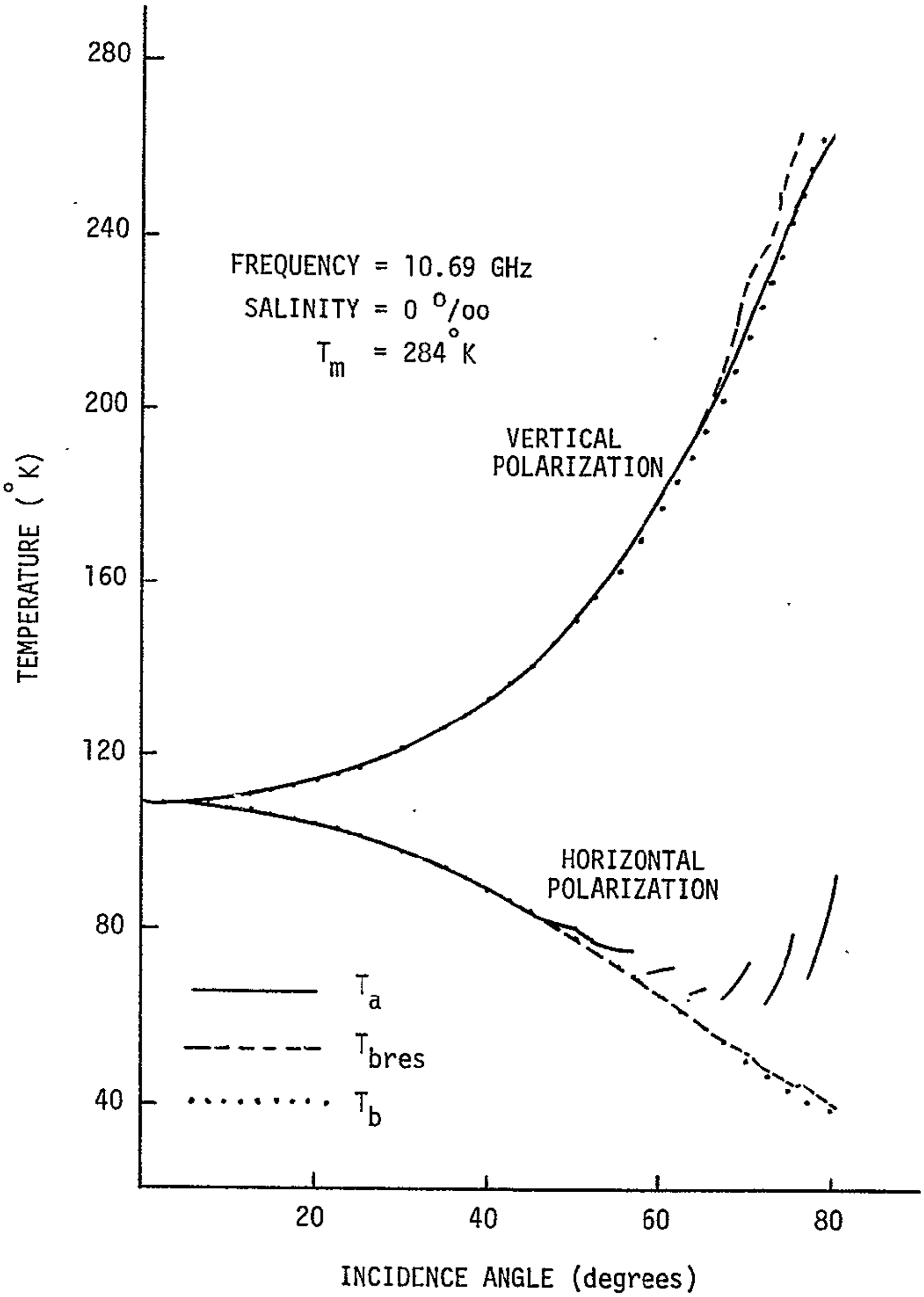

Fig. 17. Continuous Incidence Angle Restoration Results for the Finite Wave Tank (Antenna = 8λ horn, ρ = 13 feet, three iterations).

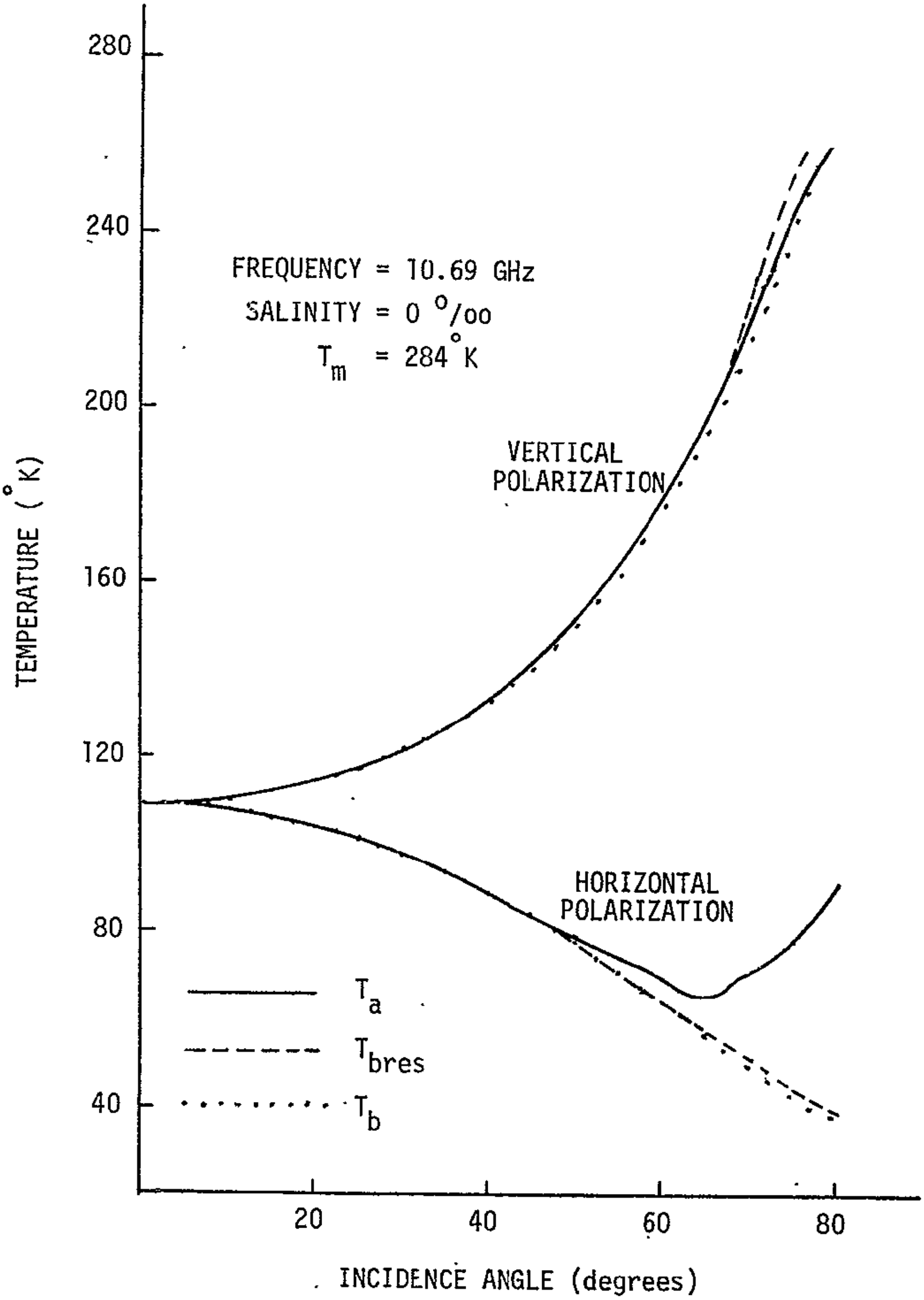

Fig. 18. Smoothed β=0 Restoration Results for the Finite Wave Tank (Antenna = 8λ horn, ρ = 13 feet, three iterations)

TABLE VII

Restored Antenna Temperatures for Finite Wave Tank
with Three Restorations

(Antenna = 8λ horn, ρ = 13 feet, f = 10.69 GHz, T_m = 284°K, S = 0 ‰)

HORIZONTAL POLARIZATION.

Incidence Angle	T_a	T_{bres}	$T_a - T_b$	$T_{bres} - T_b$
0°	109.34	109.12	0.24	0.03
10°	108.14	107.87	0.27	0.01
20°	104.47	104.12	0.31	- 0.40
30°	98.41	97.80	0.44	- 0.16
40°	89.96	89.03	0.70	- 0.23
50°	80.31	77.90	2.22	- 0.19
60°	70.48	64.84	5.78	0.13
70°	71.81	51.62	21.86	1.68
80°	92.20	38.86	54.23	0.89

VERTICAL POLARIZATION

Incidence Angle	T_a	T_{bres}	$T_a - T_b$	$T_{bres} - T_b$
0°	109.39	109.17	0.29	0.07
10°	110.68	110.40	0.28	0.00
20°	114.84	114.37	0.39	- 0.08
30°	122.36	121.39	0.64	- 0.34
40°	134.22	132.57	1.02	- 0.62
50°	152.63	149.97	2.06	- 0.60
60°	180.13	177.74	3.25	0.87
70°	221.39	229.98	4.43	13.02
80°	263.84	272.49	- 5.86	2.79

TABLE VIII

Restored Antenna Temperatures for Finite Wave Tank
with One Restoration

(Antenna = 8λ horn, ρ = 13 feet, f = 10.69 GHz, T_m = 284°K, S=0 ⁰/oo)

HORIZONTAL POLARIZATION

Incidence Angle	T_a	T_{bres}	$T_a - T_b$	$T_{bres} - T_b$
0°	109.34	109.12	0.24	0.02
10°	108.14	107.96	0.27	0.10
20°	104.47	104.31	0.31	0.15
30°	98.41	98.19	0.44	0.23
40°	89.96	89.68	0.70	0.42
50°	80.31	79.02	2.22	0.92
60°	70.48	65.87	5.78	1.16
70°	71.81	51.22	21.86	1.28
80°	92.20	37.38	54.23	- 0.59

VERTICAL POLARIZATION

Incidence Angle	T_a	T_{bres}	$T_a - T_b$	$T_{bres} - T_b$
0°	109.39	109.16	0.29	0.06
10°	110.68	110.51	0.28	0.11
20°	114.84	114.68	0.39	0.24
30°	122.36	122.19	0.64	0.46
40°	134.22	134.30	1.02	1.11
50°	152.63	153.83	2.06	3.26
60°	180.13	182.87	3.25	6.00
70°	221.39	224.71	4.43	7.75
80°	263.84	252.18	- 5.86	- 17.52

three restorations, the continuous incidence angle data is shown in Figure 19 and the smoothed $\beta=0$ data is shown in Figure 20. The x's in Figure 20 indicate antenna temperatures that did not fit on the smooth curve. Improvement can be seen in the results except at the larger incidence angles for the vertical polarization. Table IX lists some of the data used in Figure 19 and 20. An improvement with the restored data can be seen at all angles for the horizontal polarization and up to 60° incidence for the vertical. It should be noted that with the 26 foot boom the angular limits of the wave tank are $\beta = +4.2^\circ$ and $\beta = -17.0^\circ$ for $\alpha=70^\circ$, and $\beta = +2.1^\circ$ and $\beta = -3.6^\circ$ for $\alpha=80^\circ$. To again demonstrate the convergence of the restoration process, the one-restoration computations are listed in Table X. Comparing the data in Tables IX and X again verifies the convergence and the need for the restoration process.

The fourth and final antenna and boom combination is the 8λ horn with the 26 foot boom. For three restorations, the continuous incidence angle data is shown in Figure 21 and the smoothed $\beta = 0$ data is shown in Figure 22. For this case, the largest difference between the antenna and brightness temperatures is realized and the restoration process is needed the most. As can be seen in the figures, the restoration process works very well and yields an improved result for both polarizations at all incidence angles. Tabulating the data shown in Figures 21 and 22, one obtains Table XI and can see that the inversion process does recover the original water brightness temperatures T_{bwh} and T_{bwv} with good accuracy up to an incidence angle of about 60°. To again check

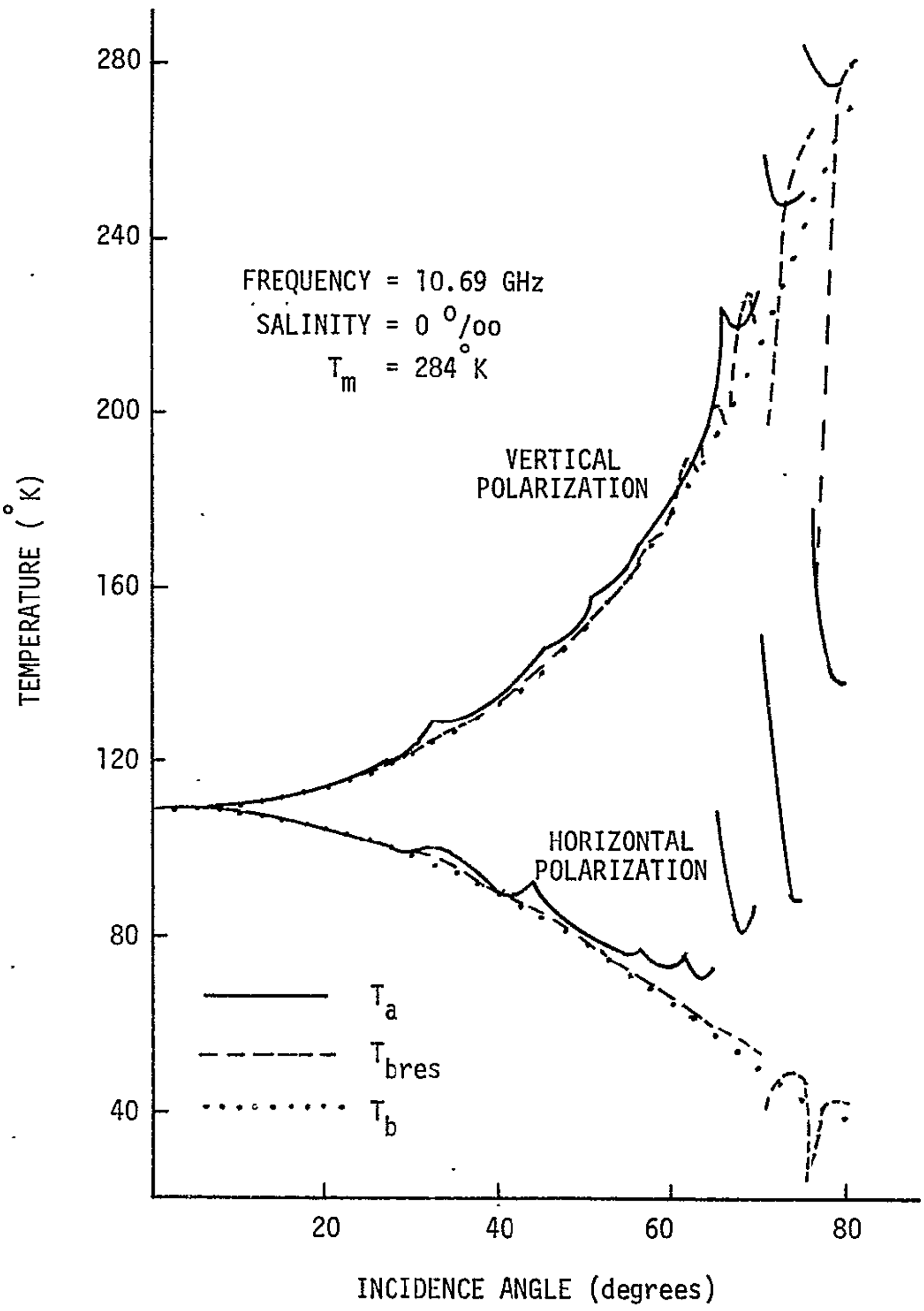

Fig. 19. Continuous Incidence Angle Restoration Results for the Finite Wave Tank (Antenna = 12λ horn, ρ = 26 feet, three iterations).

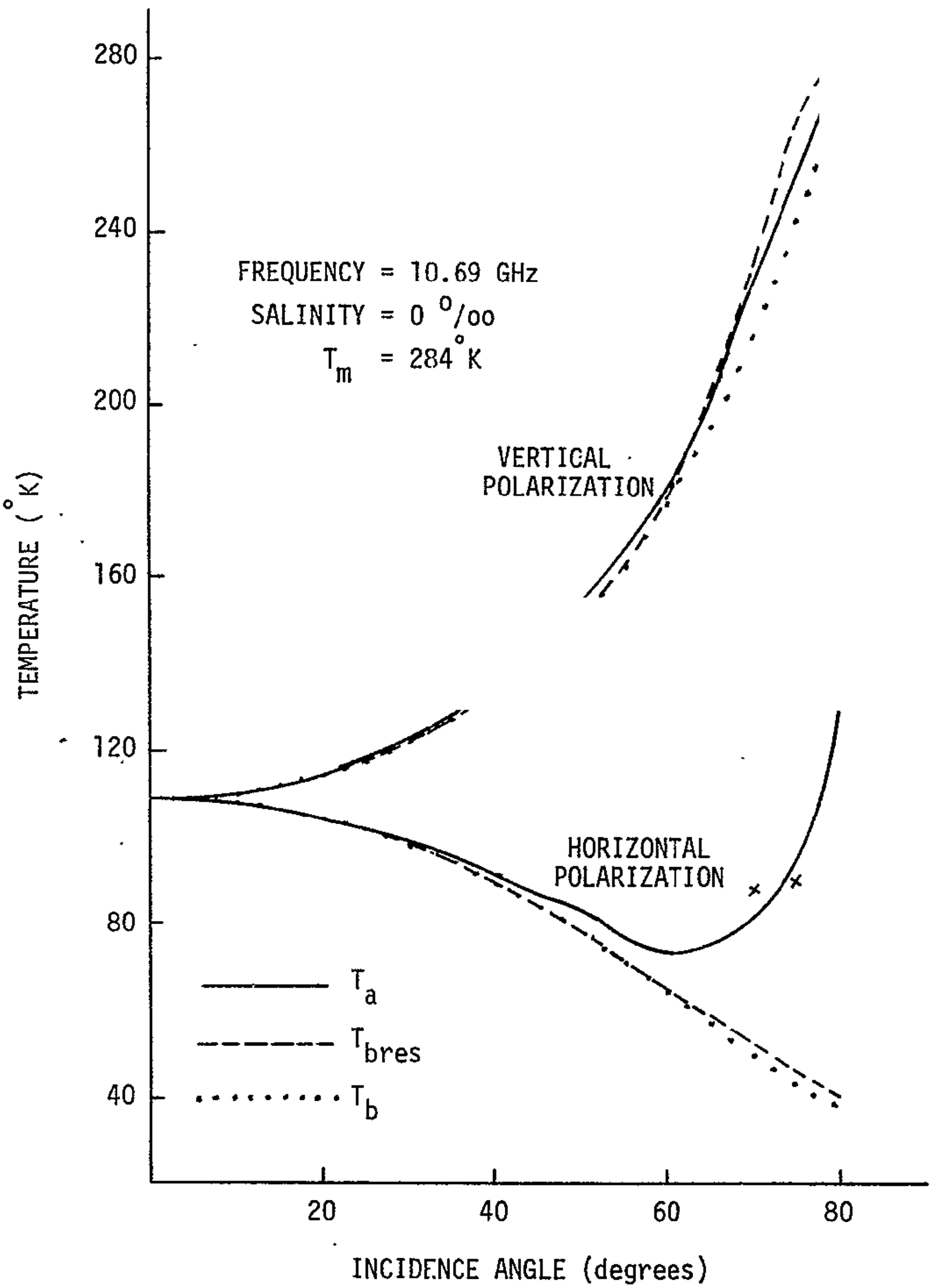

Fig. 20. Smoothed β=0 Restoration Results for the Finite Wave Tank (Antenna = 12λ horn, ρ = 26 feet, three iterations).

TABLE IX

Restored Antenna Temperatures for Finite Wave Tank
with Three Restorations

(Antenna = 12λ horn, ρ = 26 feet, f = 10.69 GHz, T_m = 284°K, S= 0 ‰)

HORIZONTAL POLARIZATION

Incidence Angle	T_a	T_{bres}	$T_a - T_b$	$T_{bres} - T_b$
0°	110.14	109.04	1.04	- .06
10°	108.41	107.74	.54	- .13
20°	104.84	103.88	.68	- .28
30°	98.90	97.56	.94	- .40
40°	90.68	88.80	1.42	- .46
50°	82.69	77.83	4.60	- .27
60°	73.50	65.17	8.79	.46
70°	88.07	52.86	38.12	2.92
80°	129.16	40.39	91.19	2.42

VERTICAL POLARIZATION

Incidence Angle	T_a	T_{bres}	$T_a - T_b$	$T_{bres} - T_b$
0°	110.18	109.08	1.08	- .02
10°	110.94	110.25	.54	- .15
20°	115.13	114.08	.68	- .37
30°	122.65	121.12	.93	- .60
40°	134.52	132.42	1.33	- .77
50°	153.70	150.24	3.13	- .33
60°	181.23	179.19	4.35	2.32
70°	227.85	231.94	10.89	14.98
80°	277.43	281.69	7.73	11.99

TABLE X

Restored Antenna Temperatures for Finite Wave Tank with One Restoration

(Antenna = 12λ horn, ρ = 26 feet, f = 10.69 GHz, T_m = 284°K, S = 0 °/oo)

HORIZONTAL POLARIZATION

Incidence Angle	T_a	T_{bres}	$T_a - T_b$	$T_{bres} - T_b$
0°	110.14	108.98	1.04	- 0.12
10°	108.41	108.16	0.54	0.29
20°	104.84	104.58	0.68	0.42
30°	98.90	98.64	0.94	0.68
40°	90.68	90.30	1.42	1.04
50°	82.69	79.97	4.60	1.87
60°	73.50	66.96	8.79	2.26
70°	88.07	51.88	38.12	1.94
80°	129.16	34.99	91.19	- 2.98

VERTICAL POLARIZATION

Incidence Angle	T_a	T_{bres}	$T_a - T_b$	$T_{bres} - T_b$
0°	110.18	109.02	1.08	- 0.08
10°	110.94	110.72	0.54	0.32
20°	115.13	114.97	0.68	0.52
30°	122.65	122.71	0.93	0.99
40°	134.52	135.09	1.33	1.90
50°	153.70	155.02	3.13	4.45
60°	181.23	184.29	4.35	7.42
70°	227.85	223.46	10.89	6.50
80°	277.43	242.77	7.73	- 26.92

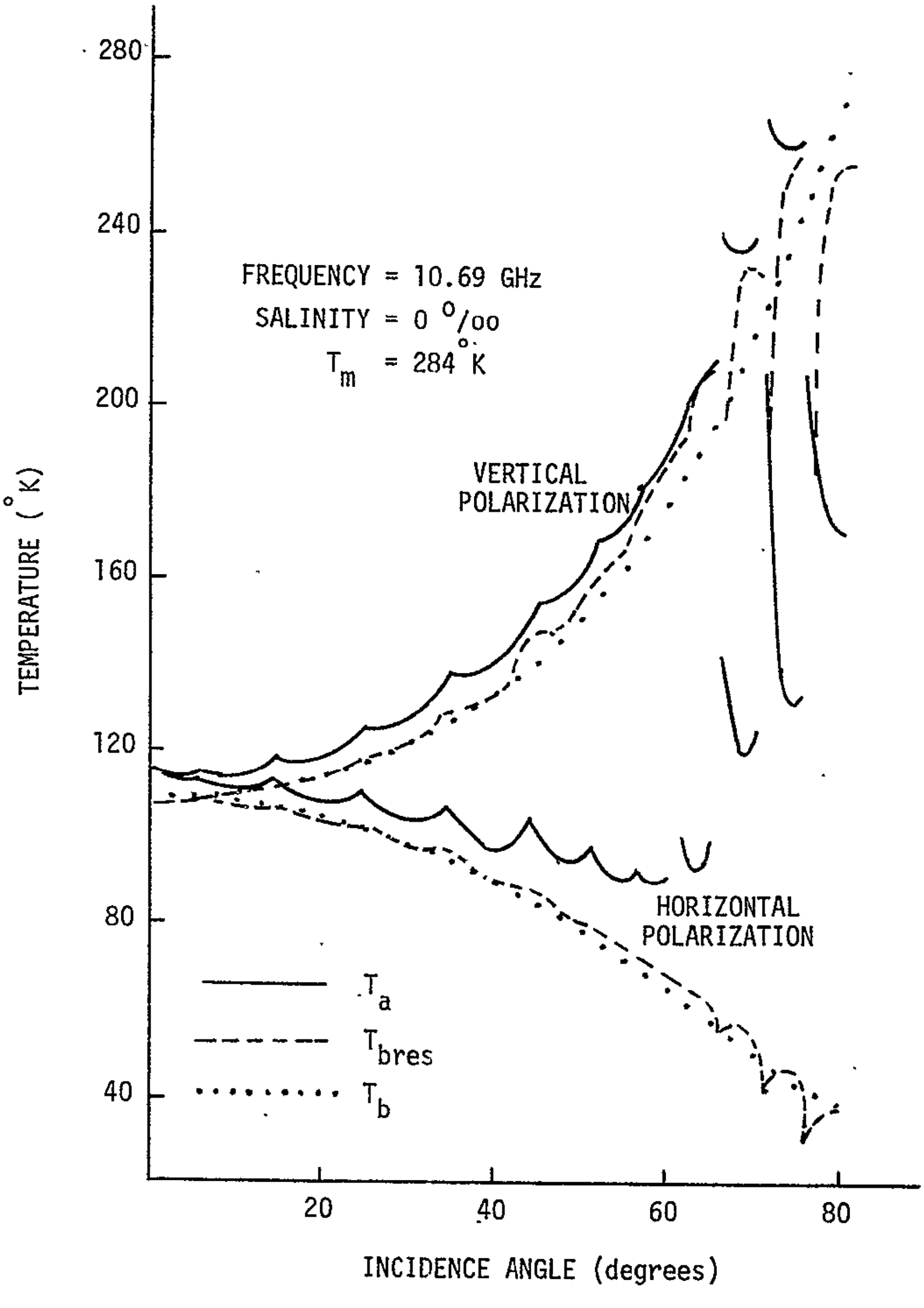

Fig. 21. Continuous Incidence Angle Restoration Results for the Finite Wave Tank (Antenna = 8λ horn, ρ = 26 feet, three iterations).

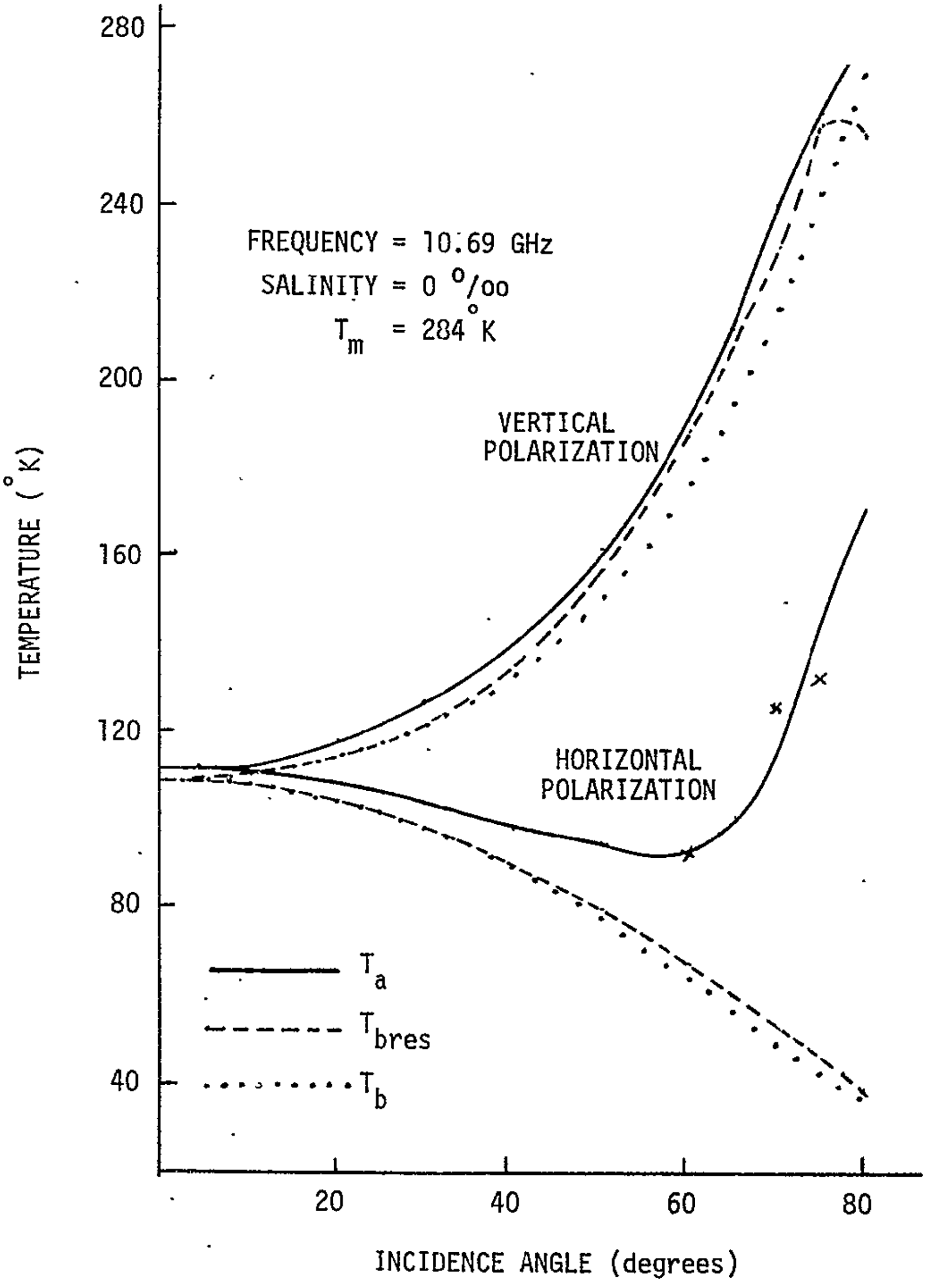

Fig. 22. Smoothed β=0 Restoration Results for the Finite Wave Tank (Antenna = 8λ horn, ρ = 26 feet, three iterations).

TABLE XI

Restored Antenna Temperatures for Finite Wave Tank with Three Restorations

(Antenna = 8λ horn, ρ= 26 feet, f = 10.69 GHz, T_m = 284°K, S = 0 ^{o}/oo)

HORIZONTAL POLARIZATION

Incidence Angle	T_a	T_{bres}	$T_a - T_b$	$T_{bres} - T_b$
0°	115.43	106.80	6.33	- 2.30
10°	111.36	107.24	3.49	- .63
20°	108.41	103.60	4.25	- .57
30°	103.90	97.67	5.94	- .29
40°	97.85	89.47	8.60	.21
50°	95.52	80.30	17.43	2.21
60°	92.11	67.61	27.40	2.90
70°	124.80	53.63	74.85	3.68
80°	169.85	36.87	131.88	- 1.08

VERTICAL POLARIZATION

Incidence Angle	T_a	T_{bres}	$T_a - T_b$	$T_{bres} - T_b$
0°	115.45	106.82	6.35	- 2.28
10°	113.85	109.80	3.45	- .59
20°	118.48	113.84	4.03	- .61
30°	126.98	121.43	5.26	- .30
40°	140.03	133.84	6.84	.64
50°	161.81	156.76	11.25	6.19
60°	190.08	188.16	13.20	11.29
70°	238.86	229.40	21.89	12.44
80°	278.28	254.82	8.58	- 14.88

the convergence of the restoration process, the single restoration data for the 8λ horn and the 26 foot boom is listed in Table XII. Comparing Tables XI and XII, the data shows that the process is convergent with the exception of the larger incidence angles.

Now that the restoration process has been investigated with error-free data, antenna temperatures with added errors will be examined to determine their effect on the inversion. To include error in the data, the antenna temperature functions will be sampled every 5.6° and then interpolated between these points to obtain the 256 needed data points (sampling every 1.4°). The first interpolation method to be used is a routine called SPLINE which was provided by Squire [14]. The SPLINE program uses a polynomial to represent the function between the sample points. The polynomials are formed so that the derivative of the interpolated curve is continuous at the sample points. In addition to the SPLINE interpolation method, linear interpolation was also used. The results obtained using these two interpolation methods are listed in Tables XIII through XXVIII. These tables show the data obtained with (a) 12λ antenna, 13 foot boom; (b) 8λ antenna, 13 foot boom; (c) 12λ antenna, 26 foot boom; and (d) 8λ antenna and 26 foot boom. For each antenna and boom combination and particular interpolation method used, a graph is included of the results obtained with the optimum number of restorations using the β=0 data. These graphs comprise Figures 23 through 30.

For the 12λ horn and the 13 foot boom, examination of the

TABLE XII

Restored Antenna Temperatures for Finite Wave Tank with One Restoration

(Antenna = 8λ horn, ρ = 26 feet, f = 10.69 GHz, T_m = 284°K, S = 0 ‰)

HORIZONTAL POLARIZATION

Incidence Angle	T_a	T_{bres}	$T_a - T_b$	$T_{bres} - T_b$
0°	115.43	108.69	6.33	- 0.41
10°	111.36	109.81	3.49	1.94
20°	108.41	106.56	4.25	2.40
30°	103.90	100.86	5.94	2.90
40°	97.85	92.55	8.60	3.29
50°	95.52	81.88	17.43	3.79
60°	92.11	67.88	27.40	3.17
70°	124.80	48.69	74.85	- 1.25
80°	169.85	28.66	131.88	- 9.31

VERTICAL POLARIZATION

Incidence Angle	T_a	T_{bres}	$T_a - T_b$	$T_{bres} - T_b$
0°	115.45	108.71	6.35	- 0.39
10°	113.85	112.48	3.45	2.08
20°	118.48	117.35	4.03	2.91
30°	126.98	125.76	5.26	4.03
40°	140.03	138.75	6.84	5.56
50°	161.81	158.61	11.25	8.04
60°	190.08	185.40	13.20	8.52
70°	238.86	203.71	21.89	- 13.25
80°	278.28	196.29	8.58	- 73.41

TABLE XIII

Restored SPLINE Interpolated Antenna Temperatures

for Finite Wave Tank with One Restoration

(Antenna = 12λ horn, ρ = 13 feet, f = 10.69 GHz, T_m = 284 °K, S = 0 ‰)

HORIZONTAL POLARIZATION

Incidence Angle	T_a	T_{bres}	$T_a - T_b$	$T_{bres} - T_b$
0°	109.18	109.14	0.08	0.04
10°	107.92	107.86	0.06	- 0.01
20°	104.22	104.20	0.06	0.04
30°	98.02	98.05	0.06	0.08
40°	89.36	89.18	0.10	- 0.08
50°	78.44	78.23	0.34	0.13
60°	65.69	66.19	0.98	1.48
70°	58.15	48.87	8.20	- 1.08
80°	69.54	38.34	31.57	0.37

VERTICAL POLARIZATION

Incidence Angle	T_a	T_{bres}	$T_a - T_b$	$T_{bres} - T_b$
0°	109.21	109.17	0.12	0.08
10°	110.46	110.40	0.07	0.00
20°	114.56	114.48	0.12	0.04
30°	121.92	121.81	0.20	0.08
40°	133.55	133.23	0.36	0.04
50°	151.25	151.16	0.68	0.59
60°	177.97	179.46	1.10	2.58
70°	219.07	224.09	2.11	7.13
80°	267.99	270.61	- 1.71	0.91

TABLE XIV

Restored SPLINE Interpolated Antenna Temperatures for
Finite Wave Tank with Three Restorations

(Antenna = 12λ horn, ρ = 13 feet, f = 10.69 GHz, $T_m = 284^\circ K$, S = 0 ‰)

HORIZONTAL POLARIZATION

Incidence Angle	T_a	T_{bres}	$T_a - T_b$	$T_{bres} - T_b$
0°	109.18	109.17	0.08	0.07
10°	107.92	107.80	0.06	- 0.06
20°	104.22	104.32	0.06	0.15
30°	98.02	98.26	0.06	0.29
40°	89.36	88.72	0.10	- 0.54
50°	78.44	77.88	0.34	- 0.21
60°	65.69	68.83	0.98	4.12
70°	58.15	43.76	8.20	- 6.19
80°	69.54	37.77	31.57	- 0.20

VERTICAL POLARIZATION

Incidence Angle	T_a	T_{bres}	$T_a - T_b$	$T_{bres} - T_b$
0°	109.21	109.21	0.12	0.11
10°	110.46	110.35	0.07	- 0.05
20°	114.56	114.57	0.12	0.13
30°	121.92	121.94	0.20	0.21
40°	133.55	132.87	0.36	- 0.32
50°	151.25	150.14	0.68	- 0.43
60°	177.97	177.44	1.10	0.56
70°	219.07	218.79	2.11	1.83
80°	267.99	280.72	- 1.71	11.02

TABLE XV

Restored Linearly Interpolated Antenna Temperatures

for Finite Wave Tank with One Restoration

(Antenna = 12λ horn, ρ = 13 feet, f = 10.69 GHz, T_m = 284°K, S = 0 ⁰/oo)

HORIZONTAL POLARIZATION

Incidence Angle	T_a	T_{bres}	$T_a - T_b$	$T_{bres} - T_b$
0°	109.08	109.02	- 0.02	- 0.08
10°	107.92	107.91	0.06	0.04
20°	104.22	104.21	0.06	0.04
30°	98.02	98.01	0.06	0.04
40°	89.36	89.23	0.10	- 0.03
50°	78.44	77.62	0.35	- 0.48
60°	65.69	63.48	0.98	- 1.23
70°	58.15	43.21	8.20	- 6.73
80°	69.54	32.39	31.57	- 5.58

VERTICAL POLARIZATION

Incidence Angle	T_a	T_{bres}	$T_a - T_b$	$T_{bres} - T_b$
0°	109.25	109.19	0.15	0.09
10°	110.46	110.36	0.07	- 0.04
20°	114.56	114.37	0.12	- 0.07
30°	121.92	121.64	0.20	- 0.08
40°	133.55	133.09	0.36	- 0.10
50°	151.25	150.65	0.68	0.08
60°	177.97	178.38	1.10	1.50
70°	219.07	223.20	2.11	6.24
80°	267.99	272.14	- 1.71	2.44

TABLE XVI

Restored Linearly Interpolated Antenna Temperatures for Finite Wave Tank with Three Restorations

(Antenna = 12λ horn, ρ = 13 feet, f = 10.69 GHz, T_m = 284°K, S = 0 ‰)

HORIZONTAL POLARIZATION

Incidence Angle	T_a	T_{bres}	$T_a - T_b$	$T_{bres} - T_b$
0°	109.08	109.02	- 0.02	- 0.08
10°	107.92	108.00	0.06	0.13
20°	104.22	104.32	0.06	0.15
30°	98.02	98.14	0.06	0.18
40°	89.36	89.35	0.10	0.09
50°	78.44	77.09	0.35	- 1.01
60°	65.69	61.16	0.98	- 3.55
70°	58.15	25.12	8.20	- 24.83
80°	69.54	19.15	31.57	- 18.82

VERTICAL POLARIZATION

Incidence Angle	T_a	T_{bres}	$T_a - T_b$	$T_{bres} - T_b$
0°	109.25	109.20	0.15	0.10
10°	110.46	110.26	0.07	- 0.14
20°	114.56	114.22	0.12	- 0.23
30°	121.92	121.44	0.20	- 0.28
40°	133.55	132.70	0.36	- 0.49
50°	151.25	149.02	0.68	- 1.55
60°	177.97	174.21	1.10	- 2.67
70°	219.07	215.87	2.11	- 1.09
80°	267.99	287.06	- 1.71	17.36

TABLE XVII

Restored SPLINE Interpolated Antenna Temperatures for

Finite Wave Tank with One Restoration

(Antenna = 8λ horn, ρ = 13 feet, f = 10.69 GHz, T_m = 284°K, S = 0°/oo).

HORIZONTAL POLARIZATION

Incidence Angle	T_a	T_{bres}	$T_a - T_b$	$T_{bres} - T_b$
0°	109.38	109.17	0.28	0.07
10°	108.14	107.96	0.27	0.09
20°	104.47	104.33	0.31	0.17
30°	98.41	98.20	0.44	0.24
40°	89.96	89.63	0.70	0.37
50°	80.31	79.15	2.22	1.05
60°	70.48	65.99	5.78	1.28
70°	71.81	50.74	21.86	0.80
80°	92.20	37.11	54.23	- 0.86

VERTICAL POLARIZATION

Incidence Angle	T_a	T_{bres}	$T_a - T_b$	$T_{bres} - T_b$
0°	109.42	109.21	0.32	0.11
10°	110.68	110.51	0.28	0.11
20°	114.84	114.70	0.39	0.25
30°	122.36	122.19	0.64	0.47
40°	134.22	134.28	1.02	1.08
50°	152.63	153.89	2.06	3.32
60°	180.13	182.90	3.25	6.02
70°	221.39	224.61	4.43	7.65
80°	263.84	252.07	- 5.86	- 17.63

TABLE XVIII

Restored SPLINE Interpolated Antenna Temperatures

for Finite Wave Tank with Three Restorations

(Antenna = 8λ horn, ρ = 13 feet, f = 10.69 GHz, T_m = 284°K, S = 0 °/oo)

HORIZONTAL POLARIZATION

Incidence Angle	T_a	T_{bres}	$T_a - T_b$	$T_{bres} - T_b$
0°	109.38	109.20	0.28	0.10
10°	108.14	107.85	0.27	- 0.02
20°	104.47	104.23	0.31	0.06
30°	98.41	97.83	0.44	- 0.14
40°	89.96	88.73	0.70	- 0.53
50°	80.31	78.60	2.22	0.50
60°	70.48	65.70	5.78	0.99
70°	71.81	49.96	21.86	0.02
80°	92.20	38.06	54.23	0.09

VERTICAL POLARIZATION

Incidence Angle	T_a	T_{bres}	$T_a - T_b$	$T_{bres} - T_b$
0°	109.42	109.24	0.32	0.14
10°	110.68	110.38	0.28	- 0.02
20°	114.84	114.45	0.39	0.01
30°	122.36	121.40	0.64	- 0.32
40°	134.22	132.40	1.02	- 0.79
50°	152.63	150.30	2.06	- 0.27
60°	180.13	177.95	3.25	1.08
70°	221.39	229.62	4.43	12.66
80°	263.84	272.15	- 5.86	2.45

TABLE XIX

Restored Linearly Interpolated Antenna Temperatures

for Finite Wave Tank with One Restoration

(Antenna = 8λ horn, ρ = 13 feet f = 10.69 GHz, T_m = 284°K, S = 0 ‰)

HORIZONTAL POLARIZATION

Incidence Angle	T_a	T_{bres}	$T_a - T_b$	$T_{bres} - T_b$
0°	109.30	109.06	0.20	- 0.04
10°	108.14	107.93	0.27	0.06
20°	104.47	104.25	0.31	0.09
30°	98.41	98.02	0.44	0.06
40°	89.96	89.24	0.70	- 0.01
50°	80.31	77.82	2.22	- 0.28
60°	70.48	63.45	5.78	- 1.26
70°	71.81	46.68	21.86	- 3.26
80°	92.19	33.41	54.22	- 4.56

VERTICAL POLARIZATION

Incidence Angle	T_a	T_{bres}	$T_a - T_b$	$T_{bres} - T_b$
0°	109.47	109.24	0.38	0.14
10°	110.68	110.43	0.28	0.03
20°	114.84	114.54	0.39	0.09
30°	122.36	121.94	0.64	0.22
40°	134.22	133.90	1.02	0.71
50°	152.63	153.11	2.06	2.54
60°	180.13	181.97	3.25	5.09
70°	221.39	223.95	4.43	6.99
80°	263.84	253.20	- 5.86	- 16.50

TABLE XX

Restored Linearly Interpolated Antenna Temperatures for Finite Wave Tank with Three Restorations

(Antenna = 8λ horn, ρ = 13 feet, f = 10.69 GHz, T_m = 284°K, S = 0 ‰)

HORIZONTAL POLARIZATION

Incidence Angle	T_a	T_{bres}	$T_a - T_b$	$T_{bres} - T_b$
0°	109.30	109.11	0.20	0.02
10°	108.14	107.93	0.27	0.06
20°	104.47	104.25	0.31	0.09
30°	98.41	97.76	0.44	- 0.20
40°	89.96	88.44	0.70	- 0.82
50°	80.31	75.28	2.22	- 2.82
60°	70.48	57.69	5.78	- 7.02
70°	71.81	35.77	21.87	- 14.18
80°	92.19	26.16	54.23	- 11.81

VERTICAL POLARIZATION

Incidence Angle	T_a	T_{bres}	$T_a - T_b$	$T_{bres} - T_b$
0°	109.47	109.30	0.38	0.20
10°	110.68	110.28	0.28	- 0.12
20°	114.84	114.14	0.39	- 0.30
30°	122.36	120.96	0.64	- 0.77
40°	134.22	131.74	1.02	- 1.46
50°	152.63	148.18	2.06	- 2.38
60°	180.13	174.95	3.25	- 1.93
70°	221.39	227.67	4.43	10.71
80°	263.84	277.49	- 5.86	7.79

TABLE XXI

Restored SPLINE Interpolated Antenna Temperatures for Finite Wave Tank with One Restoration

(Antenna = 12λ horn, ρ = 26 feet, f = 10.69 GHz, T_m = 284°K, S = 0 ‰)

HORIZONTAL POLARIZATION

Incidence Angle	T_a	T_{bres}	$T_a - T_b$	$T_{bres} - T_b$
0°	111.33	110.76	2.23	1.66
10°	108.41	107.86	0.54	- 0.01
20°	104.84	104.42	0.68	0.26
30°	98.90	98.88	0.94	0.92
40°	90.68	91.22	1.42	1.96
50°	82.69	80.11	4.60	2.01
60°	73.50	65.73	8.79	1.02
70°	88.07	49.69	38.13	- 0.26
80°	129.16	34.05	91.19	- 3.92

VERTICAL POLARIZATION

Incidence Angle	T_a	T_{bres}	$T_a - T_b$	$T_{bres} - T_b$
0°	111.36	110.79	2.26	1.69
10°	110.94	110.43	0.54	0.03
20°	115.13	114.82	0.68	0.38
30°	122.65	122.88	0.93	1.16
40°	134.52	135.69	1.33	2.50
50°	153.70	155.12	3.14	4.56
60°	181.23	183.98	4.35	7.11
70°	227.85	222.52	10.89	5.55
80°	277.43	242.35	7.73	- 27.35

TABLE XXII

Restored SPLINE Interpolated Antenna Temperatures

for Finite Wave Tank with Three Restorations

(Antenna = 12λ horn, ρ = 26 feet, f = 10.69 GHz, T_m = 284°K, S = 0 $^o/oo$)

HORIZONTAL POLARIZATION

Incidence Angle	T_a	T_{bres}	$T_a - T_b$	$T_{bres} - T_b$
0°	111.33	111.58	2.23	2.49
10°	108.41	106.20	0.54	- 1.66
20°	104.84	103.22	0.68	- 0.94
30°	98.90	98.81	0.94	0.84
40°	90.68	92.72	1.42	3.46
50°	82.69	78.75	4.60	0.65
60°	73.50	62.30	8.79	- 2.40
70°	88.07	45.60	38.13	- 4.35
80°	129.16	37.28	91.19	- 0.69

VERTICAL POLARIZATION

Incidence Angle	T_a	T_{bres}	$T_a - T_b$	$T_{bres} - T_b$
0°	111.36	111.61	2.26	2.51
10°	110.94	108.79	0.54	- 1.61
20°	115.13	113.44	0.68	- 1.00
30°	122.65	121.98	0.93	0.26
40°	134.52	135.00	1.33	1.81
50°	153.70	150.96	3.13	0.40
60°	181.23	178.88	4.35	2.00
70°	227.85	228.98	10.89	12.02
80°	277.43	280.02	7.73	10.32

TABLE XXIII

Restored Linearly Interpolated Antenna Temperatures

for Finite Wave Tank with One Restoration

(Antenna = 12λ horn, ρ = 26 feet, f = 10.69 GHz, T_m = 284°K, S = 0 ⁰/oo

HORIZONTAL POLARIZATION

Incidence Angle	T_a	T_{bres}	$T_a - T_b$	$T_{bres} - T_b$
0°	110.51	109.46	1.41	0.36
10°	108.41	107.80	0.54	- 0.07
20°	104.84	103.89	0.68	- 0.27
30°	98.90	97.40	0.94	- 0.56
40°	90.68	88.27	1.42	- 0.98
50°	82.69	74.52	4.60	- 3.58
60°	73.50	58.18	8.79	- 6.53
70°	88.07	38.92	38.13	- 11.02
80°	129.16	26.52	91.19	- 11.45

VERTICAL POLARIZATION

Incidence Angle	T_a	T_{bres}	$T_a - T_b$	$T_{bres} - T_b$
0°	110.67	109.63	1.57	0.53
10°	110.94	110.30	0.54	- 0.10
20°	115.13	114.25	0.68	- 0.20
30°	122.65	121.58	0.93	- 0.14
40°	134.52	133.48	1.33	0.29
50°	153.70	151.64	3.13	1.08
60°	181.23	180.33	4.35	3.46
70°	227.85	218.98	10.89	2.02
80°	277.43	241.96	7.73	- 27.74

TABLE XXIV

Restored Linearly Interpolated Antenna Temperatures for Finite Wave Tank with Three Restorations

(Antenna = 12λ horn, ρ = 26 feet, f = 10.69 GHz, T_m = 284°K, S = 0 ‰)

HORIZONTAL POLARIZATION

Incidence Angle	T_a	T_{bres}	$T_a - T_b$	$T_{bres} - T_b$
0°	110.51	109.94	1.41	0.84
10°	108.41	107.49	0.54	- 0.38
20°	104.84	103.10	0.68	- 1.07
30°	98.90	95.77	0.94	- 2.19
40°	90.68	84.98	1.42	- 4.28
50°	82.69	61.76	4.60	- 16.33
60°	73.50	38.34	8.79	- 26.37
70°	88.07	8.88	38.13	- 41.07
80°	129.16	8.35	91.19	- 29.62

VERTICAL POLARIZATION

Incidence Angle	T_a	T_{bres}	$T_a - T_b$	$T_{bres} - T_b$
0°	110.67	110.11	1.57	1.01
10°	110.94	109.76	0.54	- 0.64
20°	115.13	113.04	0.68	- 1.41
30°	122.65	119.28	0.93	- 2.44
40°	134.52	129.22	1.33	- 3.97
50°	153.70	140.55	3.13	- 10.02
60°	181.23	167.55	4.35	- 9.33
70°	227.85	217.12	10.89	0.16
80°	277.43	278.83	7.73	9.12

TABLE XXV

Restored SPLINE Interpolated Antenna Temperatures for Finite Wave Tank with One Restoration

(Antenna = 8λ horn, ρ = 26 feet, f = 10.69 GHz, T_m = 284°K, S = 0 °/oo)

HORIZONTAL POLARIZATION

Incidence Angle	T_a	T_{bres}	$T_a - T_b$	$T_{bres} - T_b$
0°	115.30	108.51	6.20	- 0.59
10°	111.36	109.83	3.49	1.96
20°	108.41	106.66	4.25	2.50
30°	103.90	101.04	5.94	3.07
40°	97.85	92.75	8.60	3.49
50°	95.52	81.81	17.43	3.72
60°	92.11	67.52	27.40	2.81
70°	124.80	47.96	74.85	- 1.98
80°	169.85	28.07	131.88	- 9.907

VERTICAL POLARIZATION

Incidence Angle	T_a	T_{bres}	$T_a - T_b$	$T_{bres} - T_b$
0°	115.32	108.53	6.23	- 0.56
10°	113.85	112.49	3.45	2.10
20°	118.48	117.43	4.03	2.99
30°	126.98	125.90	5.26	4.17
40°	140.03	138.90	6.84	5.71
50°	161.81	158.59	11.25	8.02
60°	190.08	185.27	13.20	8.40
70°	238.86	203.44	21.90	- 13.52
80°	278.28	196.18	8.58	- 73.52

TABLE XXVI

Restored SPLINE Interpolated Antenna Temperatures

for Finite Wave Tank with Three Restorations

(Antenna = 8λ horn, ρ = 26 feet, f = 10.69 GHz, T_m = 284°K, S = 0 ^{0}/oo)

HORIZONTAL POLARIZATION

Incidence Angle	T_a	T_{bres}	$T_a - T_b$	$T_{bres} - T_b$
0°	115.30	106.66	6.20	- 2.43
10°	111.36	107.30	3.49	- 0.56
20°	108.41	104.10	4.25	- 0.06
30°	103.90	98.72	5.94	0.76
40°	97.85	90.76	8.60	1.50
50°	95.52	80.46	17.43	2.36
60°	92.11	66.87	27.40	2.16
70°	124.80	51.28	74.86	1.34
80°	169.85	34.62	131.88	- 3.35

VERTICAL POLARIZATION

Incidence Angle	T_a	T_{bres}	$T_a - T_b$	$T_{bres} - T_b$
0°	115.32	106.69	6.23	- 2.41
10°	113.85	109.86	3.45	- 0.54
20°	118.48	114.27	4.03	- 0.18
30°	126.98	122.26	5.26	0.53
40°	140.03	134.78	6.84	1.59
50°	161.81	156.99	11.25	6.42
60°	190.08	188.03	13.20	11.15
70°	238.86	228.58	21.90	11.62
80°	278.28	254.42	8.58	- 15.28

TABLE XXVII

Restored Linearly Interpolated Antenna Temperatures

for Finite Wave Tank with One Restoration

(Antenna = 8λ horn, ρ = 26 feet, f = 10.69 GHz, T_m = 284°K, S = 0 °/oo)

HORIZONTAL POLARIZATION

Incidence Angle	T_a	T_{bres}	$T_a - T_b$	$T_{bres} - T_b$
0°	116.30	109.53	7.20	0.44
10°	111.36	108.64	3.49	0.78
20°	108.41	105.08	4.25	0.91
30°	103.90	98.74	5.94	0.77
40°	97.85	89.55	8.60	0.29
50°	95.52	77.21	17.43	- 0.89
60°	92.11	61.88	27.40	- 2.83
70°	124.80	41.61	74.86	- 8.34
80°	169.85	25.03	131.88	- 12.94

VERTICAL POLARIZATION

Incidence Angle	T_a	T_{bres}	$T_a - T_b$	$T_{bres} - T_b$
0°	116.44	109.67	7.34	0.57
10°	113.85	111.30	3.45	0.91
20°	118.48	115.92	4.03	1.48
30°	126.98	123.89	5.26	2.17
40°	140.03	136.44	6.84	3.24
50°	161.81	155.61	11.25	5.04
60°	190.08	182.42	13.20	5.54
70°	238.86	201.28	21.90	- 15.68
80°	278.38	196.41	8.58	- 73.29

TABLE XXVIII

Restored Linearly Interpolated Antenna Temperatures for Finite Wave Tank with Three Restorations

(Antenna = 8λ horn, ρ = 26 feet, f = 10.69 GHz, T_m = 284°K, S = 0 °/oo)

HORIZONTAL POLARIZATION

Incidence Angle	T_a	T_{bres}	$T_a - T_b$	$T_{bres} - T_b$
0°	116.30	108.70	7.20	- 0.40
10°	111.36	104.85	3.49	- 3.02
20°	108.41	100.40	4.25	- 3.76
30°	103.90	92.46	5.94	- 5.50
40°	97.85	81.06	8.60	- 8.20
50°	95.52	64.89	17.43	- 13.21
60°	92.11	47.16	27.40	- 17.55
70°	124.80	27.05	74.86	- 22.90
80°	169.85	21.46	131.88	- 16.51

VERTICAL POLARIZATION

Incidence Angle	T_a	T_{bres}	$T_a - T_b$	$T_{bres} - T_b$
0°	116.44	108.83	7.34	- 0.27
10°	113.85	107.35	3.45	- 3.04
20°	118.48	110.68	4.03	- 3.77
30°	126.98	116.81	5.26	- 4.92
40°	140.03	127.37	6.84	- 5.82
50°	161.81	147.13	11.25	- 3.44
60°	190.08	178.35	13.20	1.47
70°	238.86	220.41	21.90	3.45
80°	278.28	255.46	8.58	- 15.24

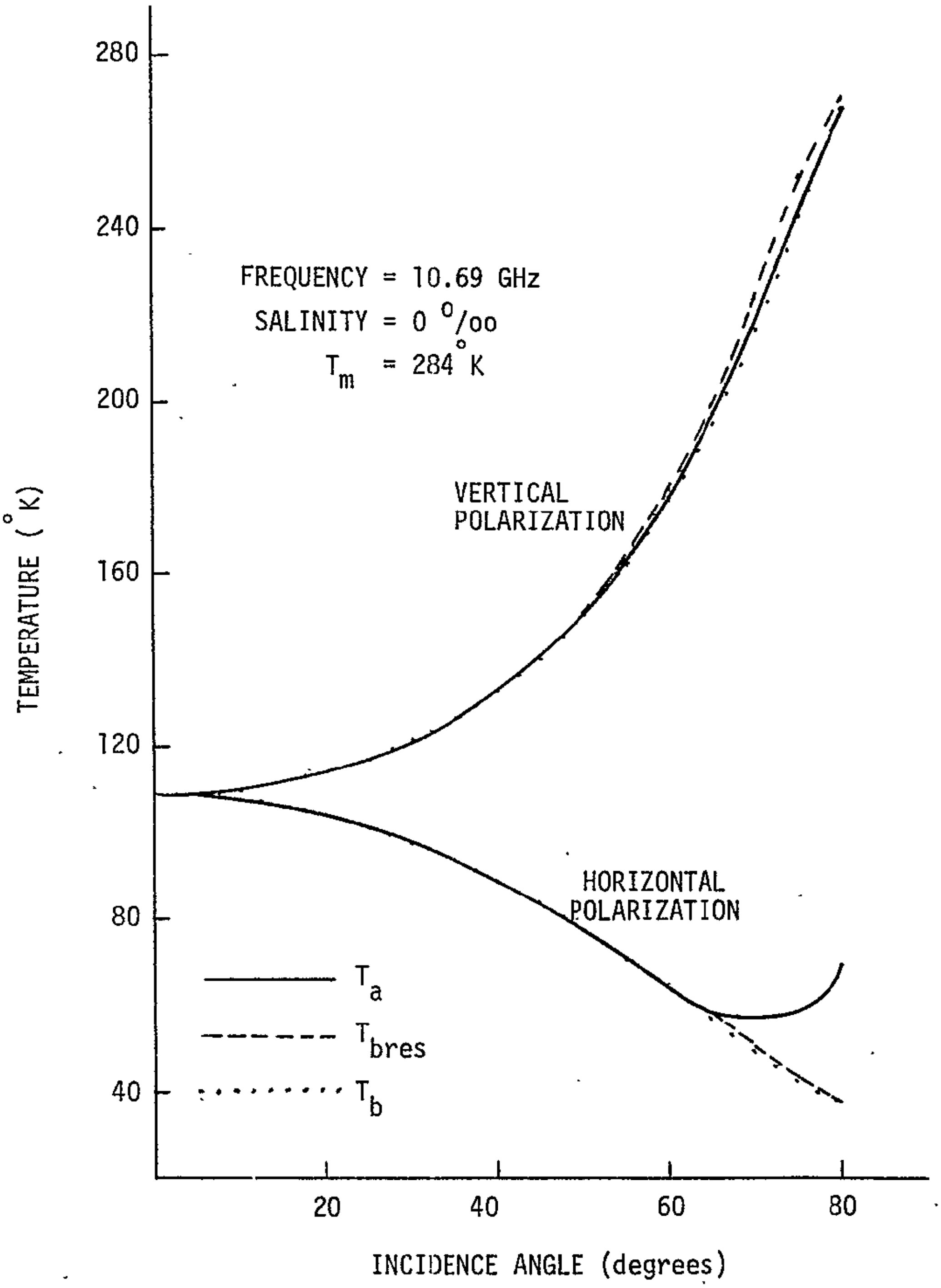

Fig. 23. Restoration of SPLINE Interpolated Data for the Finite Wave Tank (Antenna = 12λ horn, ρ = 13 feet, one iteration).

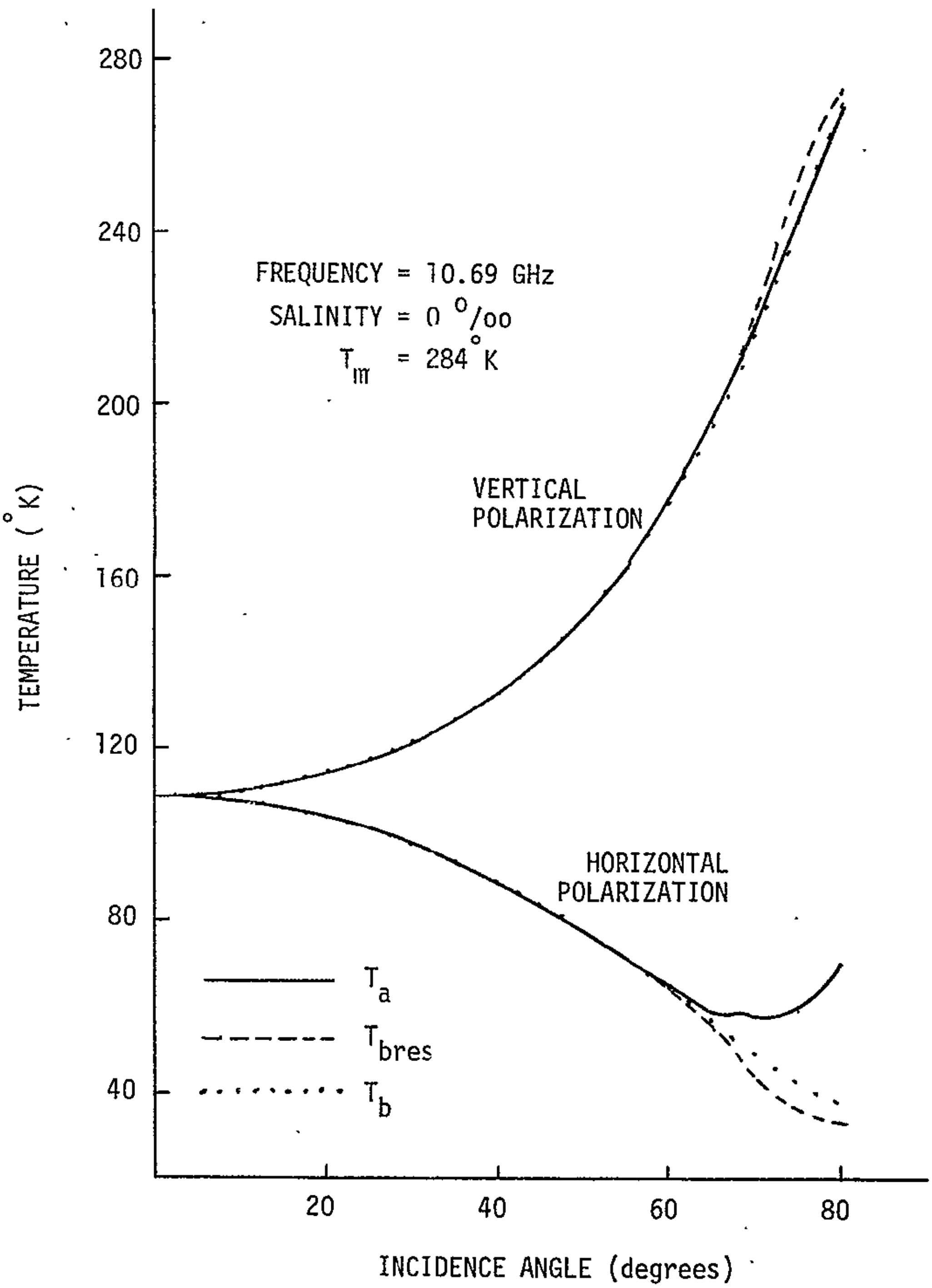

Fig. 24. Restoration of Linearly Interpolated Data for the Finite Wave Tank (Antenna = 12λ horn, ρ = 13 feet, one iteration).

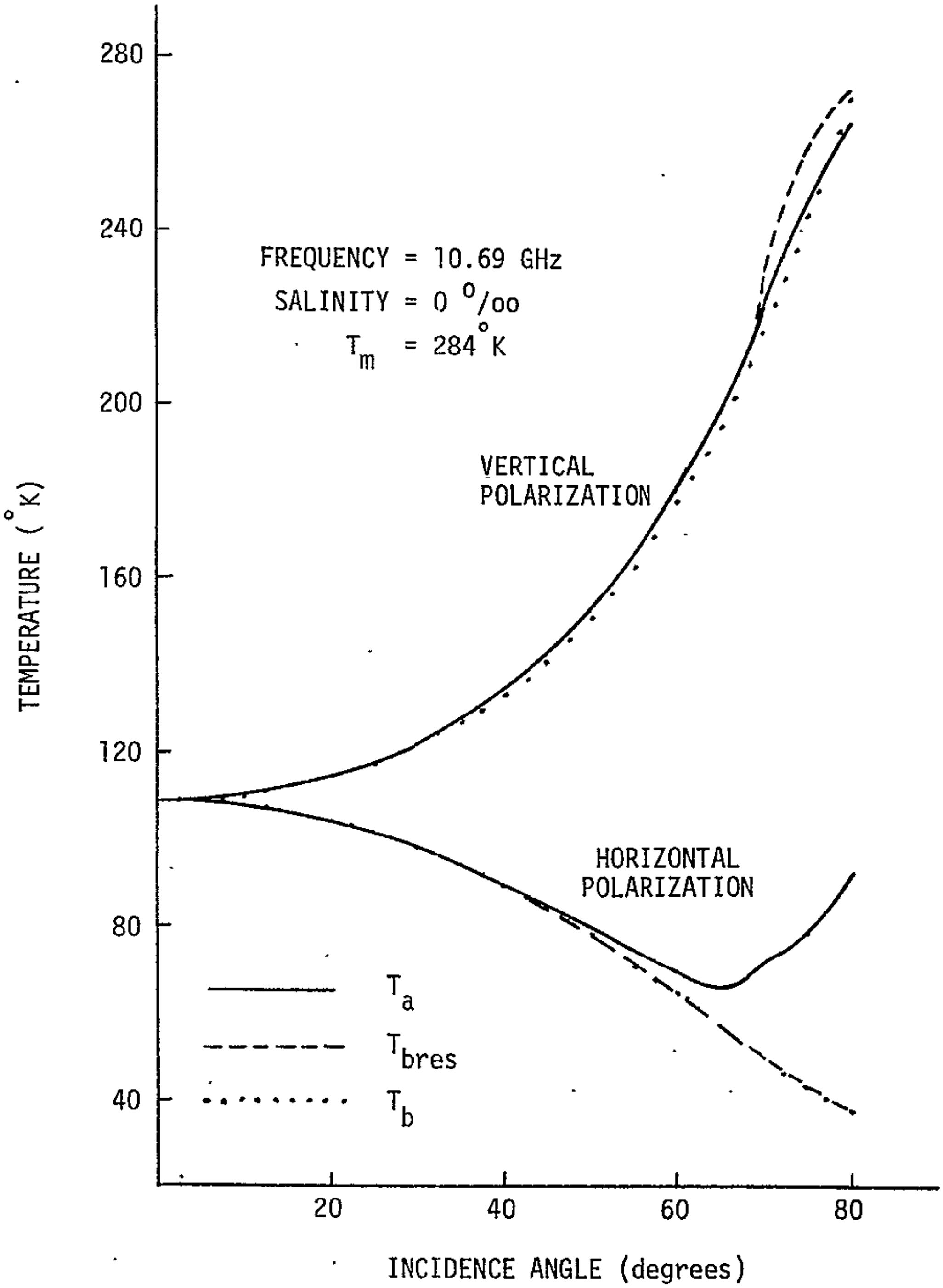

Fig. 25. Restoration of SPLINE Interpolated Data for the Finite Wave Tank (Antenna = 8λ horn, ρ = 13 feet, three iterations).

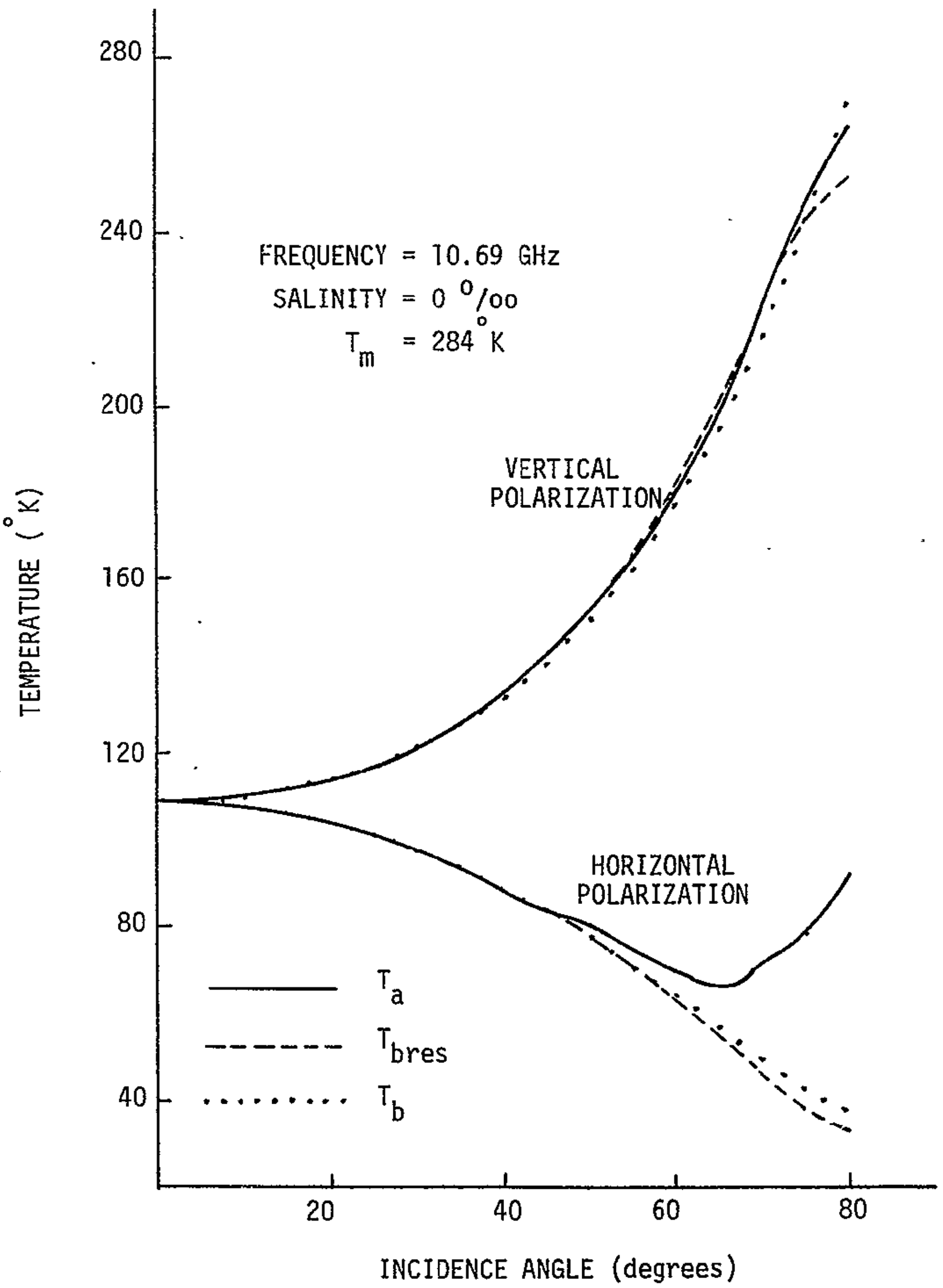

Fig. 26. Restoration of Linearly Interpolated Data for the Finite Wave Tank (Antenna = 8λ horn, ρ = 13 feet, one iteration).

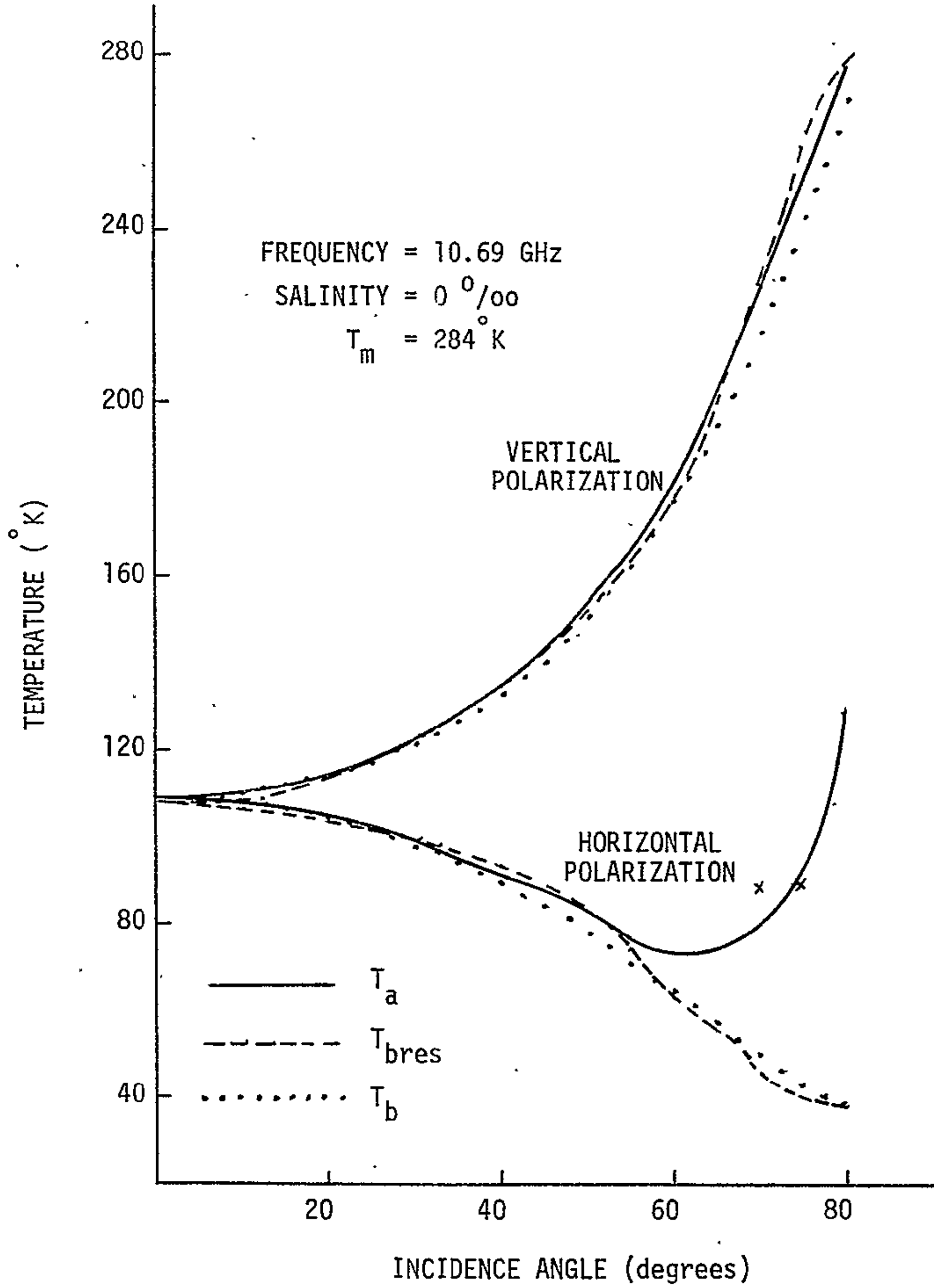

Fig. 27. Restoration of SPLINE Interpolated Data for the Finite Wave Tank (Antenna = 12λ horn, ρ = 26 feet, three iterations).

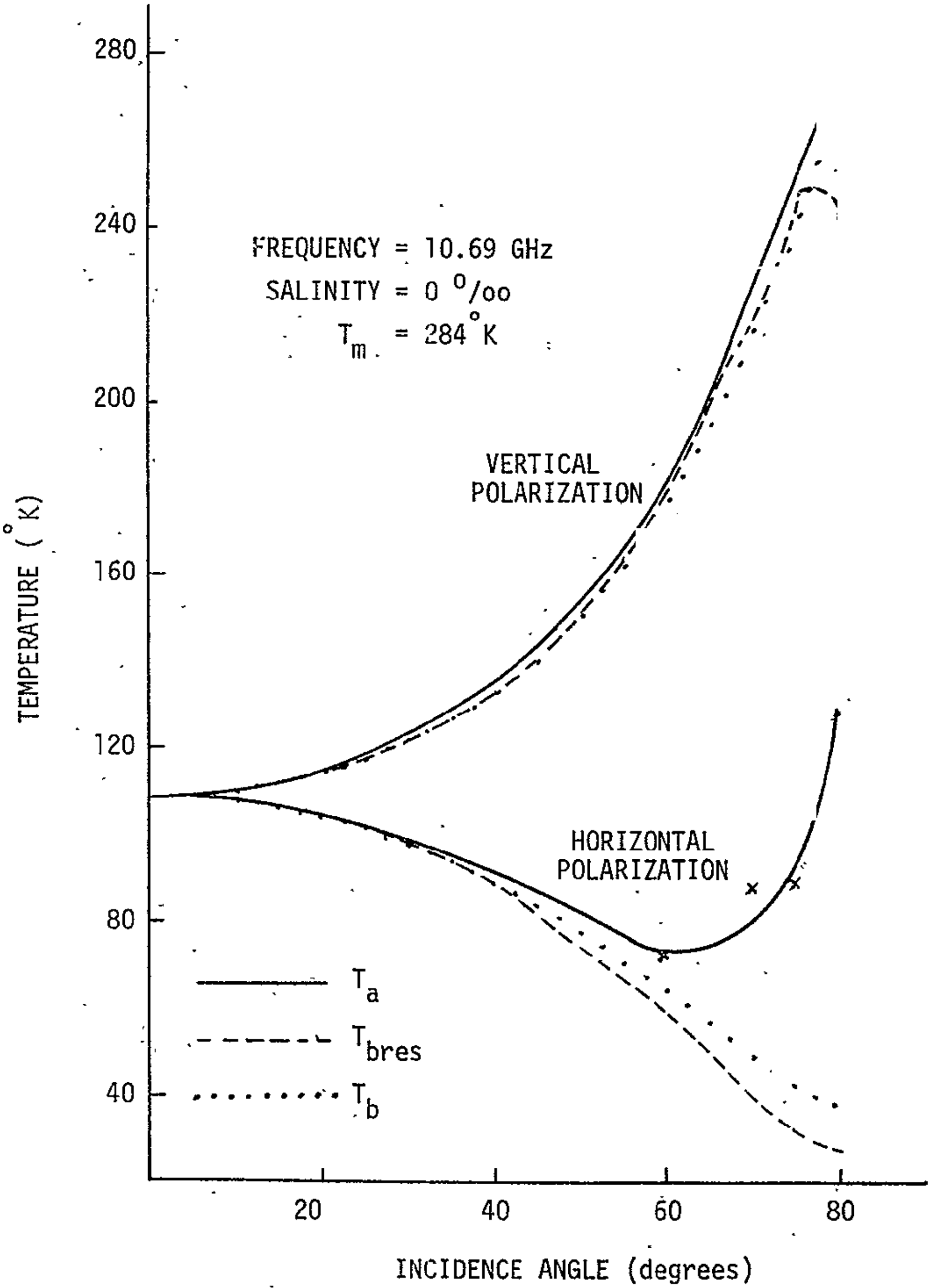

Fig. 28. Restoration of Linearly Interpolated Data for the Finite Wave Tank (Antenna = 12λ horn, ρ = 26 feet, one iteration).

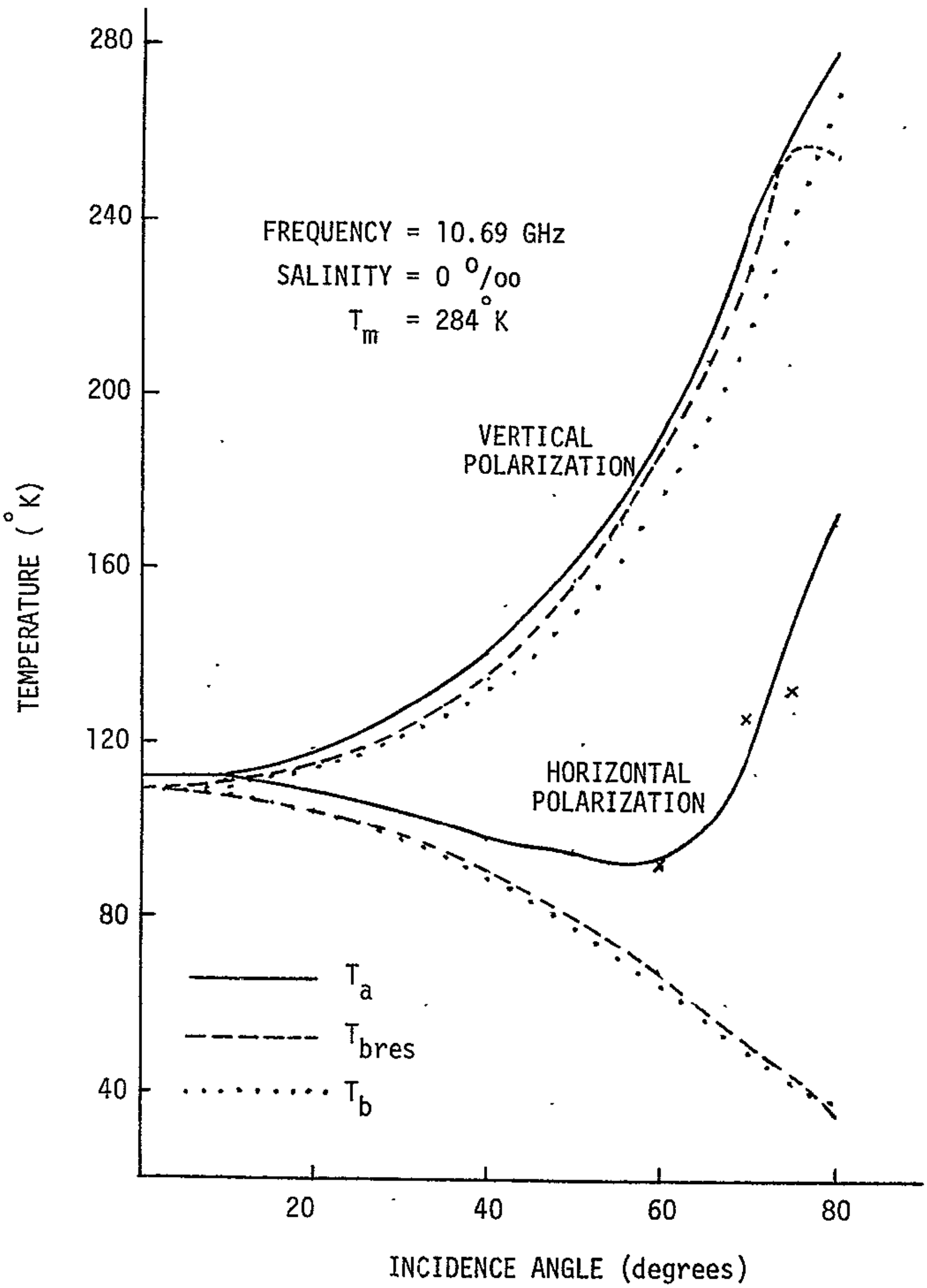

Fig. 29. Restoration of SPLINE Interpolated Data for the Finite Wave Tank (Antenna = 8λ horn, ρ = 26 feet, three iterations).

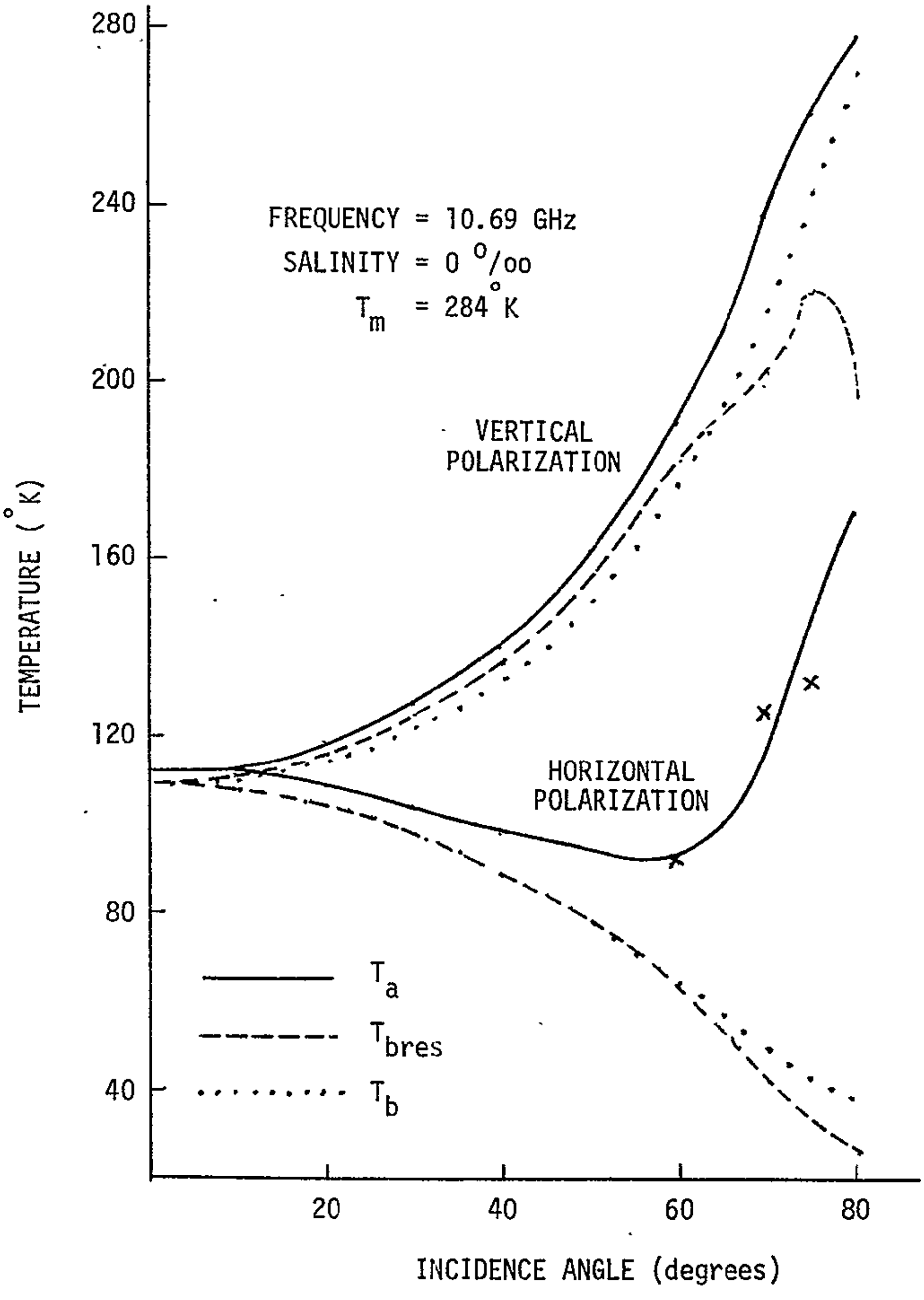

Fig. 30. Restoration of Linearly Interpolated Data for the Finite Wave Tank (Antenna = 8λ horn, ρ = 26 feet, one iteration).

SPLINE interpolated data shows that the single iteration results are more accurate than those obtained with three restorations. With the interpolation error, three restorations can no longer be taken and still achieve accurate results. With one restoration, improvement is achieved up to an incidence angle of about 60°. With linear interpolation, again the single iteration data is better than with three restorations and it is an improvement over the antenna temperatures. Due to the high frequency error in the spectrum of the linearly interpolated antenna temperatures, the inversion results, using three restorations, are less accurate than for the SPLINE routine. The accuracy of the results yielded with one restoration is about the same with either interpolation method.

With the 8λ horn antenna and the 13 foot support boom, the tabulation of the SPLINE interpolated data shows that three restorations yield more accurate results than one iteration, and the recovered brightness temperatures are almost always better approximations than the interpolated antenna temperatures. Examination of the linearly interpolated data shows that additional restorations are not useful due to the previously mentioned high frequency error in the spectrum of the antenna temperatures. However, the single iteration case does yield improved results over the original antenna temperatures at the lower incidence angles for vertical polarization and at all incidence angles for horizontal polarization. Comparing the best case data for the two different interpolation techniques, one can see that with the 8λ horn and 13 foot boom combination, SPLINE interpolation is superior.

Next, the effect of interpolation will be examined for the 12λ horn and 26 foot boom computations. With SPLINE interpolation, the accuracy of the one- and three-iteration results appears to be very nearly the same but with a slight overall superiority for the three restorations. With this antenna and boom combination, the tank looks very narrow and the antenna, having a very narrow beam, creates a rapidly varying function as the tank is scanned. The 5.6° sampling is not rapid enough in this case to let the SPLINE routine fit an accurate curve. With the rapidly varying functions involved with this antenna-boom combination, the high frequency error in the linear interpolation is most pronounced making the three restoration results much inferior than those of one iteration. The one restoration case does, however, yield improved results over the antenna temperatures. Due to the rapidly varying functions, the linear interpolation yields better results than does the SPLINE routine.

Finally, the antenna temperatures for the 8λ horn and the 26 foot boom vary less rapidly than those yielded with the narrow 12λ horn and 26 foot support boom. Consequently, the restoration of the SPLINE interpolated data is more convergent and the three-iteration case does yield better results than the single restoration. With three restorations, results are yielded that are a considerable improvement over the interpolated antenna temperatures. With the linear interpolation, multiple iterations are not desirable and the best results are obtained with one restoration where the recovery process definitely yields improved results and should be used. For the 8λ horn and the 26 foot boom, a slightly more accurate approximation of the water brightness temperature can be obtained with linear rather than SPLINE interpolation.

The restoration process has up to now been investigated using error-free and interpolated antenna temperatures. The process will now be examined with a random error added to the antenna temperatures. A Gaussian error with a mean of 0° and a standard deviation of 1° was added to the antenna temperature profiles for each value of α. The maximum error that was added to the antenna temperatures was approximately ± 2.8°. These profiles were then smoothed through the use of a Fortran subroutine named ICSSMU of the IBM IMSL library. The function with error and the standard deviation of the error is supplied to the subroutine which places a smooth cubic spline along the given set of data points. The subroutine can also interpolate between the data points. In this investigation, the subroutine was used to smooth the antenna temperatures that were known every 1.4°, after the random error had been added. Also, to show the combined effect of both the random error and interpolation, data with the random error was supplied to the subroutine at 5.6° intervals and the program was used to both smooth the antenna temperatures and interpolate to provide the needed 1.4° sampling. Tables XXIX through XXXVI show the results obtained by smoothing the antenna temperatures with added random error and not interpolating. All four combinations of the 12λ,

TABLE XXIX

Restored Antenna Temperatures for Finite Wave Tank with Random Error, No Interpolation, and One Restoration

(Antenna = 12λ horn, ρ = 13 feet, f = 10.69 GHz, T_m = 284°K, S = 0 ‰)

HORIZONTAL POLARIZATION

Incidence Angle	T_a	T_{bres}	$T_a - T_b$	$T_{bres} - T_b$
0°	108.94	108.63	- 0.16	- 0.47
10°	108.48	108.81	0.61	0.95
20°	104.78	105.12	0.62	0.96
30°	98.59	98.96	0.63	0.99
40°	89.92	90.26	0.66	1.00
50°	78.98	79.25	0.88	1.15
60°	66.15	66.11	1.44	1.40
70°	57.66	49.73	7.71	- 0.21
80°	72.66	43.72	34.69	5.75

VERTICAL POLARIZATION

Incidence Angle	T_a	T_{bres}	$T_a - T_b$	$T_{bres} - T_b$
0°	108.98	108.67	- 0.12	- 0.43
10°	111.01	111.33	0.61	0.93
20°	115.11	115.39	0.66	0.94
30°	122.47	122.70	0.75	0.98
40°	134.09	134.22	0.90	1.03
50°	151.77	152.09	1.20	1.52
60°	178.44	180.00	1.57	3.12
70°	219.46	225.10	2.50	8.14
80°	268.90	272.60	- 0.80	2.90

TABLE XXX

Restored Antenna Temperatures for Finite Wave Tank with Random Error, No Interpolation, and Three Restorations

(Antenna = 12λ horn, ρ = 13 feet, f = 10.69 GHz, T_m = 284°K, S = 0 ⁰/oo)

HORIZONTAL POLARIZATION

Incidence Angle	T_a	T_{bres}	$T_a - T_b$	$T_{bres} - T_b$
0°	108.94	108.33	- 0.16	- 0.76
10°	108.48	109.38	0.61	1.52
20°	104.78	105.69	0.62	1.52
30°	98.59	99.52	0.63	1.56
40°	89.92	90.76	0.66	1.50
50°	78.98	79.58	0.88	1.48
60°	66.15	66.58	1.44	1.88
70°	57.66	47.60	7.71	- 2.34
80°	72.66	46.79	34.69	8.82

VERTICAL POLARIZATION

Incidence Angle	T_a	T_{bres}	$T_a - T_b$	$T_{bres} - T_b$
0°	108.98	108.37	- 0.12	- 0.72
10°	111.01	111.88	0.61	1.48
20°	115.11	115.93	0.66	1.48
30°	122.47	123.23	0.75	1.51
40°	134.09	134.62	0.90	1.43
50°	151.77	151.62	1.20	1.05
60°	178.44	177.66	1.57	0.78
70°	219.46	220.85	2.50	3.88
80°	268.90	284.78	- 0.80	15.07

TABLE XXXI

Restored Antenna Temperatures for Finite Wave Tank with Random Error, No Interpolation, and One Restoration

(Antenna = 8λ horn, ρ = 13 feet, f = 10.69 GHz, T_m = 284°K, S = 0 ⁰/oo)

HORIZONTAL POLARIZATION

Incidence Angle	T_a	T_{bres}	$T_a - T_b$	$T_{bres} - T_b$
0°	109.21	108.74	0.11	- 0.35
10°	108.51	108.62	0.64	0.75
20°	104.85	105.01	0.69	0.85
30°	98.76	98.86	0.80	0.89
40°	90.30	90.37	1.04	1.11
50°	80.46	79.40	2.37	1.30
60°	70.04	64.92	5.33	0.21
70°	73.17	53.15	23.23	3.21
80°	95.16	42.20	57.19	4.24

VERTICAL POLARIZATION

Incidence Angle	T_a	T_{bres}	$T_a - T_b$	$T_{bres} - T_b$
0°	109.26	108.79	0.16	- 0.31
10°	111.04	111.15	0.65	0.75
20°	115.21	115.36	0.76	0.91
30°	122.71	122.83	0.99	1.11
40°	134.56	134.96	1.37	1.77
50°	152.86	154.28	2.29	3.71
60°	180.22	182.95	3.34	6.07
70°	222.10	225.88	5.14	8.92
80°	264.92	253.94	- 4.78	- 15.76

TABLE XXXII

Restored Antenna Temperatures for Finite Wave Tank with

Random Error, No Interpolation, and Three Restorations

(Antenna = 8λ horn, ρ = 13 feet, f = 10.69 GHz, T_m = 284°K, S = 0 ⁰/oo)

HORIZONTAL POLARIZATION

Incidence Angle	T_a	T_{bres}	$T_a - T_b$	$T_{bres} - T_b$
0°	109.21	108.28	0.11	- 0.82
10°	108.51	109.03	0.64	1.16
20°	104.85	105.36	0.69	1.20
30°	98.76	98.99	0.80	1.03
40°	90.30	90.38	1.04	1.12
50°	80.46	79.07	2.37	0.97
60°	70.04	63.29	5.33	- 1.42
70°	73.17	54.00	23.23	4.06
80°	95.16	46.49	57.19	8.52

VERTICAL POLARIZATION

Incidence Angle	T_a	T_{bres}	$T_a - T_b$	$T_{bres} - T_b$
0°	109.26	108.32	0.16	- 0.78
10°	111.04	111.53	0.65	1.13
20°	115.21	115.56	0.76	1.11
30°	122.71	122.54	0.99	0.81
40°	134.56	133.81	1.37	0.62
50°	152.86	150.99	2.29	0.42
60°	180.22	177.83	3.34	0.95
70°	222.10	231.74	5.14	14.77
80°	264.92	275.36	- 4.78	5.66

TABLE XXXII

Restored Antenna Temperatures for Finite Wave Tank with Random Error, No Interpolation, and One Restoration

(Antenna = 12λ horn, ρ = 26 feet, f = 10.69 GHz, T_m = 284°K, S = 0 ‰)

HORIZONTAL POLARIZATION

Incidence Angle	T_a	T_{bres}	$T_a - T_b$	$T_{bres} - T_b$
0°	109.86	108.42	0.76	- 0.68
10°	108.97	109.18	1.10	1.31
20°	105.37	105.56	1.21	1.40
30°	99.40	99.63	1.44	1.67
40°	91.13	91.25	1.87	1.99
50°	82.36	79.33	4.26	1.24
60°	72.97	65.68	8.26	0.97
70°	90.45	54.91	40.51	4.97
80°	135.40	44.67	97.43	6.70

VERTICAL POLARIZATION

Incidence Angle	T_a	T_{bres}	$T_a - T_b$	$T_{bres} - T_b$
0°	109.89	108.45	0.79	- 0.65
10°	111.50	111.73	1.10	1.33
20°	115.65	115.94	1.21	1.49
30°	123.16	123.68	1.43	1.96
40°	134.96	135.99	1.77	2.80
50°	153.65	154.88	3.08	4.32
60°	181.24	184.15	4.36	7.27
70°	228.78	224.54	11.82	7.58
80°	279.24	245.46	9.54	- 24.24

TABLE XXXIV

Restored Antenna Temperatures for Finite Wave Tank with Random Error, No Interpolation, and Three Restorations

(Antenna = 12λ horn, ρ = 26 feet, f = 10.69 GHz, T_m = 284°K, S = 0 °/oo)

HORIZONTAL POLARIZATION

Incidence Angle	T_a	T_{bres}	$T_a - T_b$	$T_{bres} - T_b$
0°	109.86	108.10	0.76	- 0.99
10°	108.97	109.39	1.10	1.52
20°	105.37	105.51	1.21	1.34
30°	99.40	99.36	1.44	1.40
40°	91.13	90.82	1.87	1.56
50°	82.36	77.12	4.26	- 0.98
60°	72.97	62.85	8.26	- 1.86
70°	90.45	56.27	40.51	6.33
80°	135.40	54.16	97.43	16.19

VERTICAL POLARIZATION

Incidence Angle	T_a	T_{bres}	$T_a - T_b$	$T_{bres} - T_b$
0°	109.89	108.14	0.79	- 0.96
10°	111.50	111.89	1.10	1.49
20°	115.65	115.68	1.21	1.23
30°	123.16	122.86	1.43	1.13
40°	134.96	134.23	1.77	1.04
50°	153.65	150.22	3.08	- 0.35
60°	181.24	178.93	4.36	2.05
70°	228.78	233.05	11.82	16.09
80°	279.24	285.24	9.54	15.54

TABLE XXXV

Restored Antenna Temperatures for Finite Wave Tank with Random Error, No Interpolation, and One Restoration

(Antenna = 8λ horn, ρ = 26 feet, f = 10.69 GHz, T_m = 284°K, S = 0 ‰)

HORIZONTAL POLARIZATION

Incidence Angle	T_a	T_{bres}	$T_a - T_b$	$T_{bres} - T_b$
0°	114.58	107.20	5.48	- 1.90
10°	111.64	110.51	3.77	2.64
20°	108.52	106.92	4.36	2.76
30°	103.74	100.66	5.78	2.70
40°	97.33	91.56	8.07	2.30
50°	95.30	81.09	17.20	2.99
60°	92.65	68.25	27.94	3.54
70°	128.57	54.50	78.63	4.56
80°	174.54	36.31	136.57	- 1.66

VERTICAL POLARIZATION

Incidence Angle	T_a	T_{bres}	$T_a - T_b$	$T_{bres} - T_b$
0°	114.61	107.22	5.51	- 1.88
10°	114.13	113.17	3.73	2.78
20°	118.61	117.73	4.16	3.29
30°	126.90	125.68	5.18	3.96
40°	139.70	138.12	6.51	4.93
50°	161.73	158.21	11.17	7.64
60°	190.37	185.58	13.49	8.70
70°	240.58	206.28	23.62	- 10.68
80°	280.25	199.50	10.54	- 70.20

TABLE XXXVI

Restored Antenna Temperatures for Finite Wave Tank with

Random Error, No Interpolation, and Three Restorations

(Antenna = 8λ horn, ρ = 26 feet, f = 10.69 GHz, T_m = 284°K, S = 0 °/oo)

HORIZONTAL POLARIZATION

Incidence Angle	T_a	T_{bres}	$T_a - T_b$	$T_{bres} - T_b$
0°	114.58	104.42	5.48	- 4.68
10°	111.64	109.11	3.77	1.24
20°	108.52	104.91	4.36	0.75
30°	103.74	97.96	5.78	0.00
40°	97.33	88.17	8.07	- 1.09
50°	95.30	78.67	17.20	0.57
60°	92.65	67.62	27.94	2.91
70°	128.57	62.23	78.63	12.28
80°	174.54	48.27	136.57	10.30

VERTICAL POLARIZATION

Incidence Angle	T_a	T_{bres}	$T_a - T_b$	$T_{bres} - T_b$
0°	114.61	104.44	5.51	- 4.65
10°	114.13	111.64	3.73	1.25
20°	118.61	115.13	4.16	0.68
30°	126.90	121.86	5.18	0.14
40°	139.70	133.10	6.51	- 0.09
50°	161.73	155.95	11.17	5.38
60°	190.37	188.17	13.49	11.29
70°	240.58	233.06	23.62	16.10
80°	280.25	259.57	10.54	- 10.13

8λ horn antennas and 13 foot, 26 foot supporting booms are listed with one and three restorations. Figures 31 through 34 are graphs using the $\beta=0$ points for each of the four cases and the optimum number of restorations. Tables XXXVII through XLIV and Figures 35 through 38 show data analogous to Tables XXIX through XXXVI and Figures 31 through 34, respectively, but with interpolation and smoothing provided by the subroutine ICSSMU.

With the 12λ horn and the 13 foot boom, the error that has been added is greater than the difference between the antenna temperatures and the brightness temperatures. Consequently, the restored brightness temperatures are not as good an approximation of the brightness temperatures as are the smoothed antenna temperatures. Multiple restoration makes the restored results inferior. For this antenna and boom length, these observations are valid for both the interpolated and uninterpolated data.

For the 8λ horn and the 13 foot boom data that contains the random error, multiple restorations are not desirable either with or without interpolation. When the antenna temperatures are not interpolated, some improvement at the larger incidence angles for horizontal polarization is achieved with one iteration. With interpolation, the smoothed antenna temperatures are more accurate than the restored results.

Using the 12λ horn 26 foot boom, and no interpolation, the three-restoration results are better than those for one interation. With this antenna and boom combination, and no interpolation,

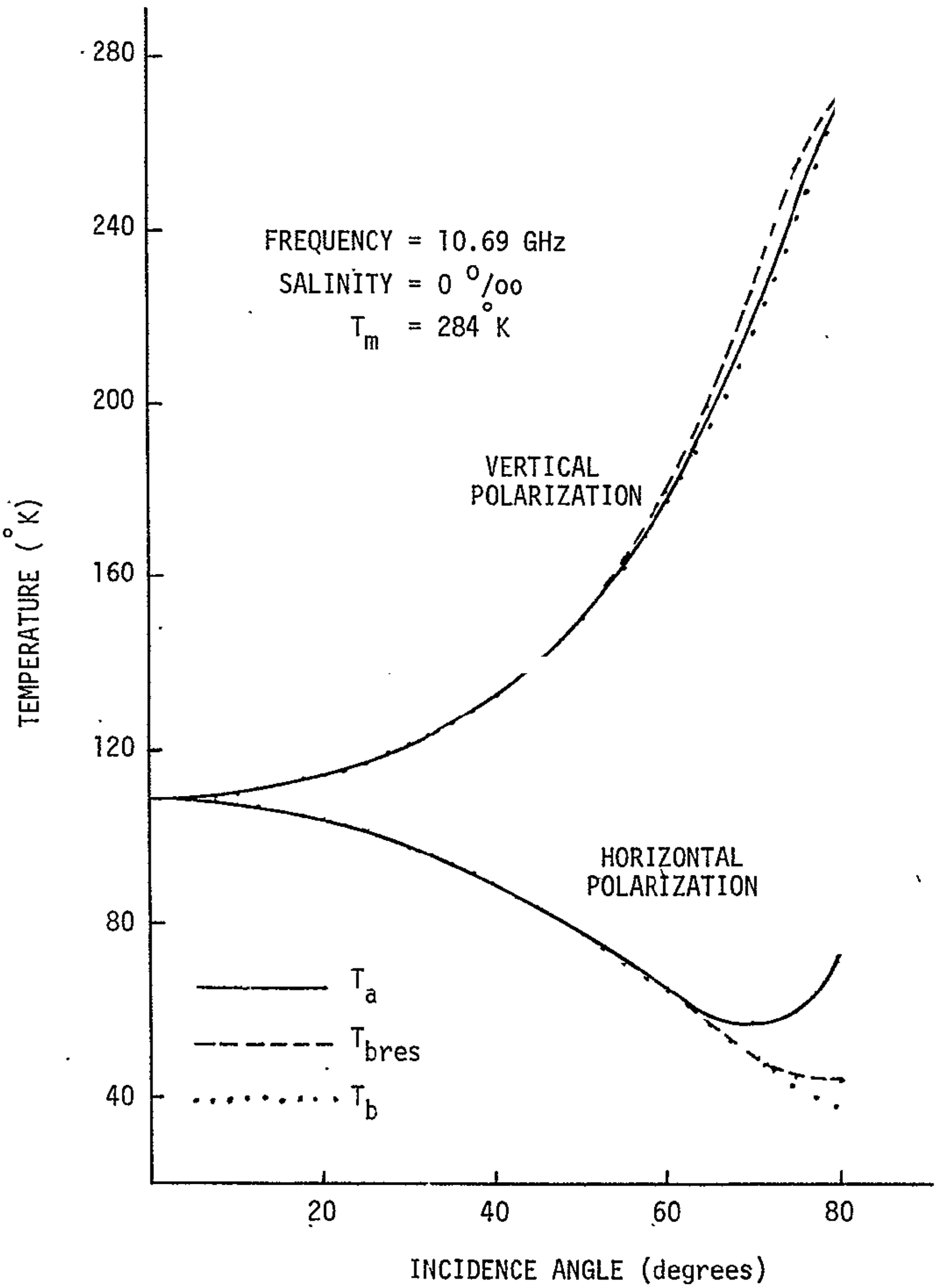

Fig. 31. Restoration of the Finite Wave Tank Data with Random Error and No Interpolation (Antenna = 12λ horn, ρ = 13 feet, one iteration).

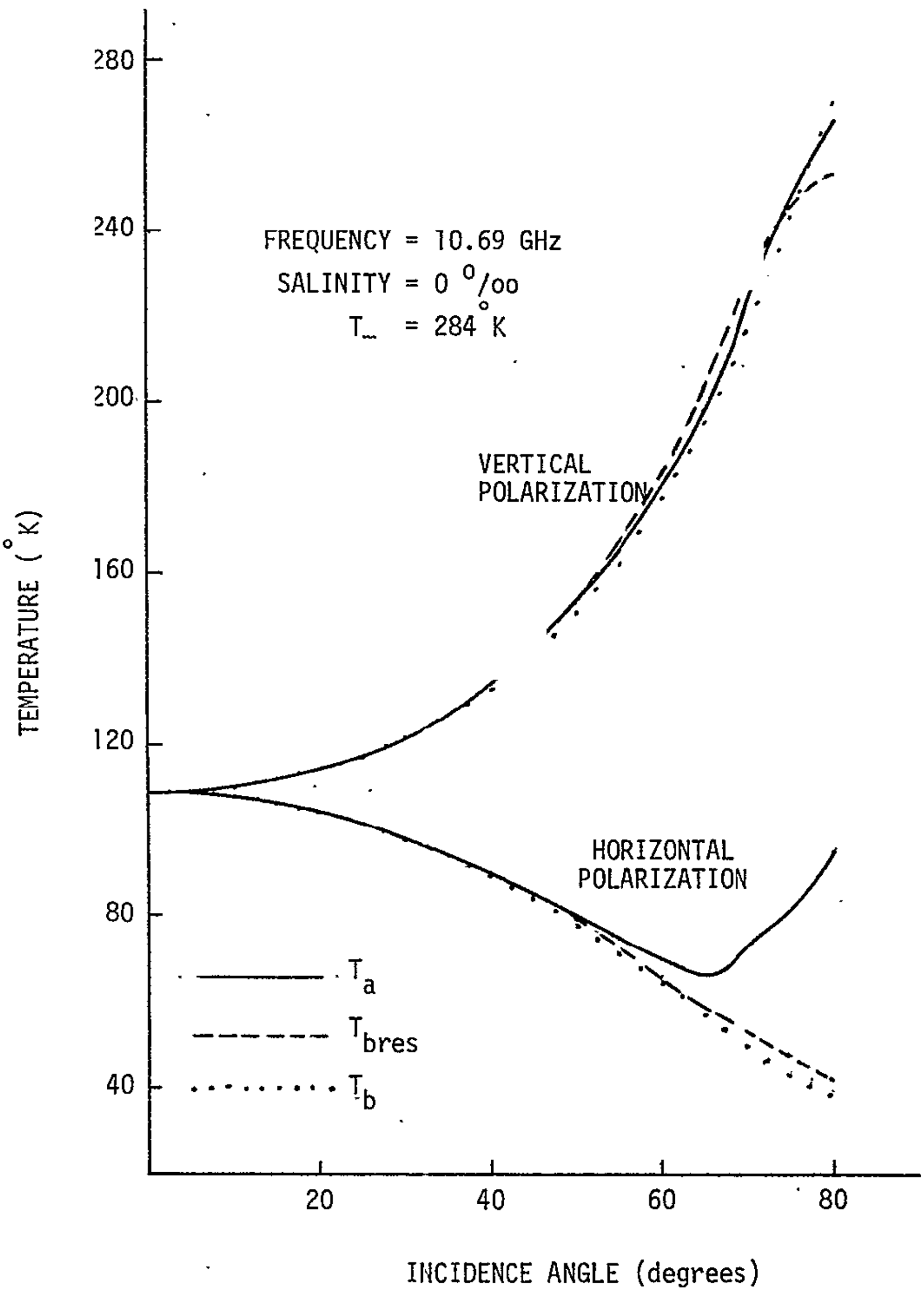

Fig. 32. Restoration of the Finite Wave Tank Data with Random Error and No Interpolation (Antenna = 8λ horn, ρ = 13 feet, one iteration).

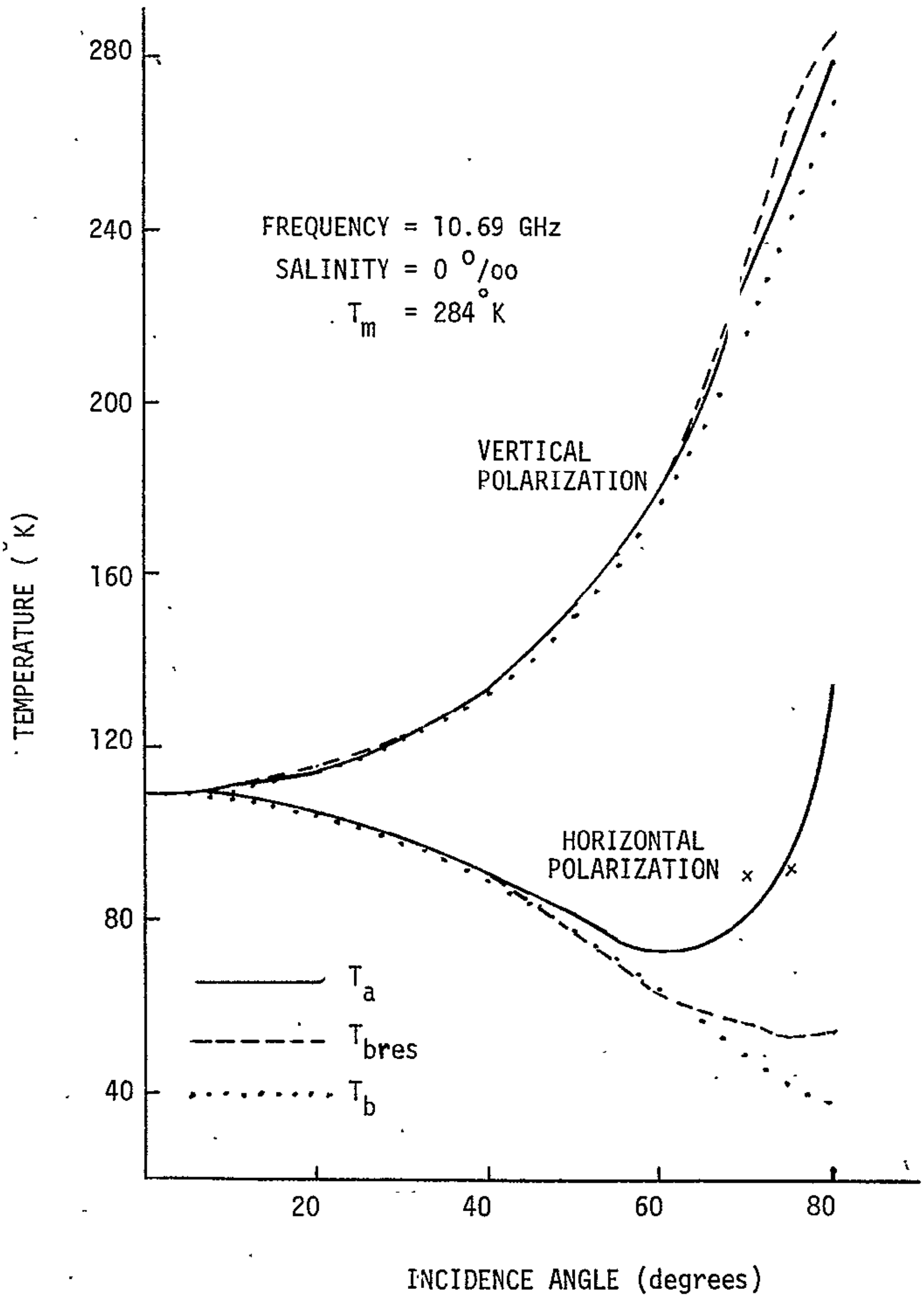

Fig. 33. Restoration of the Finite Wave Tank Data with Random Error and No Interpolation (Antenna = 12λ horn, ρ = 26 feet, three iterations).

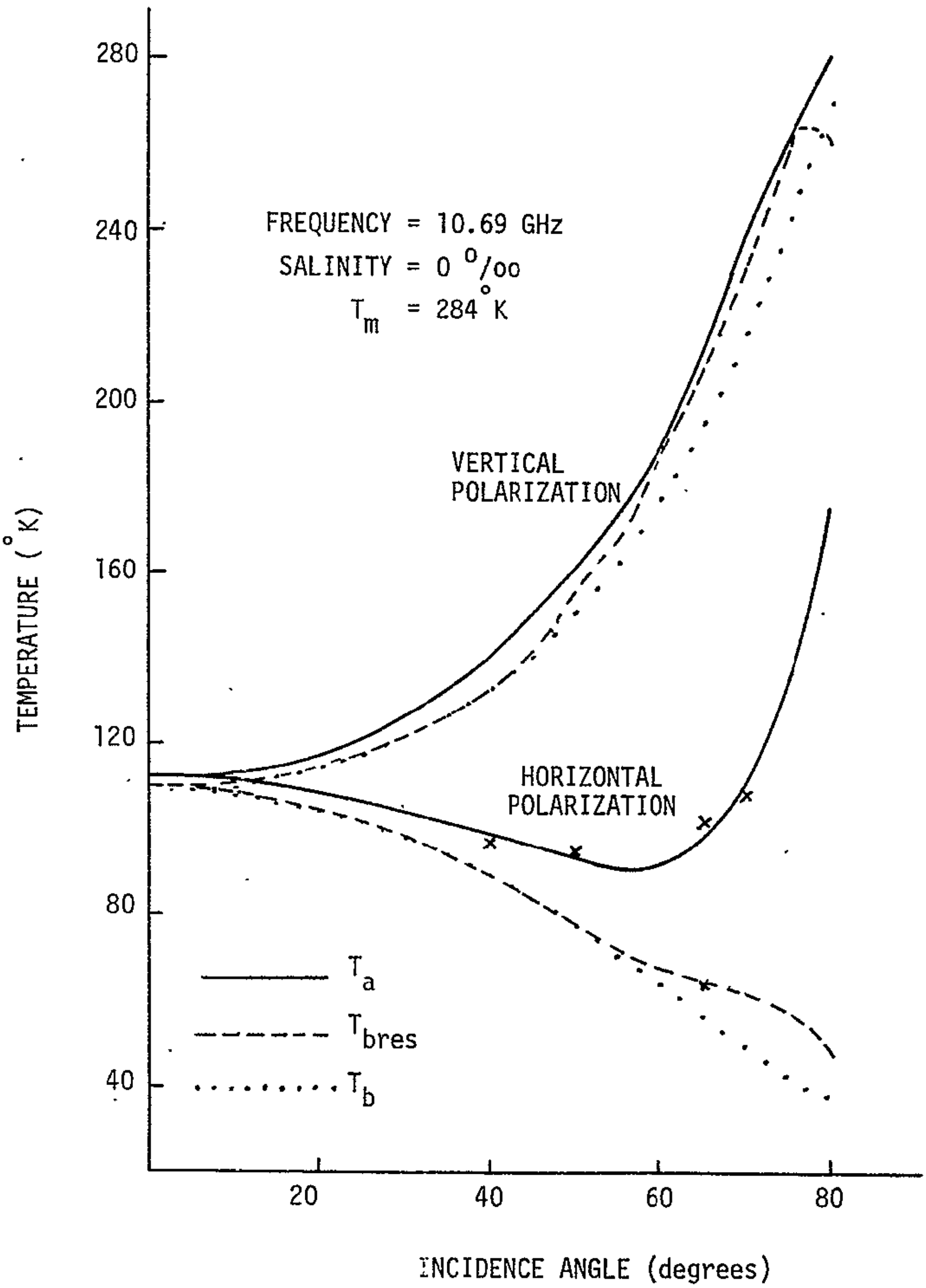

Fig. 34. Restoration of the Finite Wave Tank Data with Random Error and No Interpolation (Antenna = 8λ horn, ρ = 26 feet, three iterations).

TABLE XXXVII

Restored Antenna Temperatures for Finite Wave Tank with Random Error, Interpolation, and One Restoration

(Antenna = 12λ horn, ρ = 13 feet, f = 10.69 GHz, T_m = 284°K, S = 0 $^o/oo$)

HORIZONTAL POLARIZATION

Incidence Angle	T_a	T_{bres}	$T_a - T_b$	$T_{bres} - T_b$
0°	109.42	109.28	0.32	0.18
10°	108.50	108.90	0.63	1.04
20°	104.81	105.18	0.64	1.01
30°	98.65	99.07	0.68	1.11
40°	89.99	90.57	0.73	1.31
50°	78.26	78.46	0.17	0.37
60°	63.50	62.34	- 1.21	- 2.37
70°	61.06	52.70	11.12	2.75
80°	77.78	50.57	39.81	12.60

VERTICAL POLARIZATION

Incidence Angle	T_a	T_{bres}	$T_a - T_b$	$T_{bres} - T_b$
0°	109.44	109.30	0.34	0.20
10°	111.03	111.42	0.63	1.02
20°	115.13	115.45	0.69	1.01
30°	122.51	122.80	0.79	1.08
40°	134.10	134.38	0.91	1.18
50°	151.30	151.52	0.73	0.95
60°	177.67	178.80	0.79	1.92
70°	220.44	226.19	3.48	9.22
80°	270.94	275.13	1.24	5.43

TABLE XXXVIII

Restored Antenna Temperatures for Finite Wave Tank with Random Error, Interpolation, and Three Restorations

(Antenna = 12λ horn, ρ = 13 feet, f = 10.69 GHz, T_m = 284°K, S = 0 ⁰/oo)

HORIZONTAL POLARIZATION

Incidence Angle	T_a	T_{bres}	$T_a - T_b$	$T_{bres} - T_b$
0°	109.42	108.73	0.32	- 0.36
10°	108.50	109.44	0.63	1.58
20°	104.81	105.56	0.64	1.40
30°	98.65	99.41	0.68	1.45
40°	89.99	91.03	0.73	1.77
50°	78.26	79.13	0.17	1.03
60°	63.50	63.12	- 1.21	- 1.59
70°	61.06	47.93	11.12	- 2.01
80°	77.78	54.91	39.81	16.94

VERTICAL POLARIZATION

Incidence Angle	T_a	T_{bres}	$T_a - T_b$	$T_{bres} - T_b$
0°	109.44	108.76	0.34	- 0.34
10°	111.03	111.94	0.63	1.54
20°	115.13	115.84	0.69	1.40
30°	122.51	123.14	0.79	1.42
40°	134.10	134.72	0.91	1.53
50°	151.30	151.10	0.73	0.53
60°	177.67	176.30	0.79	- 0.58
70°	220.44	221.48	3.48	4.52
80°	270.94	287.72	1.24	18.02

TABLE XXXIX

Restored Antenna Temperatures for Finite Wave Tank with Random Error, Interpolation, and One Restoration

(Antenna = 8λ horn, ρ = 13 feet, f = 10.69 GHz, T_m = 284°K, S = 0 °/oo)

HORIZONTAL POLARIZATION

Incidence Angle	T_a	T_{bres}	$T_a - T_b$	$T_{bres} - T_b$
0°	109.52	109.33	0.42	0.23
10°	108.55	108.85	0.68	0.98
20°	104.85	105.25	0.68	1.09
30°	98.65	99.01	0.69	1.05
40°	89.84	89.99	0.58	0.73
50°	79.00	76.96	0.90	- 1.14
60°	69.13	62.87	4.42	- 1.84
70°	76.63	58.06	26.69	8.12
80°	98.74	46.98	60.77	9.01

VERTICAL POLARIZATION

Incidence Angle	T_a	T_{bres}	$T_a - T_b$	$T_{bres} - T_b$
0°	109.54	109.36	0.44	0.26
10°	111.07	111.36	0.67	0.96
20°	115.19	115.55	0.74	1.10
30°	122.60	122.91	0.87	1.18
40°	134.22	134.65	1.03	1.46
50°	152.18	153.11	1.61	2.55
60°	180.20	182.76	3.33	5.88
70°	223.11	227.37	6.15	10.40
80°	265.05	253.82	- 4.65	- 15.88

TABLE XL

Restored Antenna Temperatures for Finite Wave Tank with Random Error, Interpolation, and Three Restorations

(Antenna = 8λ horn, ρ = 13 feet, f = 10.69 GHz, T_m = 284°K, S = 0 °/oo)

HORIZONTAL POLARIZATION

Incidence Angle	T_a	T_{bres}	$T_a - T_b$	$T_{bres} - T_b$
0°	109.52	108.98	0.42	- 0.12
10°	108.55	109.52	0.68	1.65
20°	104.85	105.91	0.68	1.74
30°	98.65	99.68	0.69	1.71
40°	89.84	90.60	0.58	1.34
50°	79.00	75.89	0.90	- 2.20
60°	69.13	59.59	4.42	- 5.12
70°	76.63	60.00	26.69	10.05
80°	98.74	52.49	60.77	14.52

VERTICAL POLARIZATION

Incidence Angle	T_a	T_{bres}	$T_a - T_b$	$T_{bres} - T_b$
0°	109.54	109.00	0.44	- 0.10
10°	111.07	111.99	0.67	1.60
20°	115.19	116.03	0.74	1.58
30°	122.60	123.02	0.87	1.29
40°	134.22	133.84	1.03	0.65
50°	152.18	149.37	1.61	- 1.20
60°	180.20	177.19	3.33	0.32
70°	223.11	233.63	6.15	16.67
80°	265.05	275.29	- 4.65	5.59

TABLE XLI

Restored Antenna Temperatures for Finite Wave Tank with Random Error, Interpolation, and One Restoration

(Antenna = 12λ horn, ρ = 26 feet, f = 10.69 GHz, T_m = 284°K, S = 0 °/oo)

HORIZONTAL POLARIZATION

Incidence Angle	T_a	T_{bres}	$T_a - T_b$	$T_{bres} - T_b$
0°	109.08	107.33	- 0.02	- 1.77
10°	108.81	109.54	0.94	1.68
20°	104.80	105.18	0.64	1.01
30°	97.80	97.67	- 0.17	- 0.29
40°	88.18	87.22	- 1.08	- 2.04
50°	80.84	76.34	2.74	- 1.75
60°	74.02	65.29	9.32	0.58
70°	97.44	62.98	47.49	13.04
80°	140.57	51.02	102.60	13.05

VERTICAL POLARIZATION

Incidence Angle	T_a	T_{bres}	$T_a - T_b$	$T_{bres} - T_b$
0°	109.09	107.34	- 0.01	- 1.76
10°	111.32	112.06	0.92	1.66
20°	115.12	115.58	0.68	1.13
30°	121.84	122.08	0.11	0.36
40°	132.72	132.90	- 0.47	- 0.29
50°	152.44	152.57	1.87	2.01
60°	181.29	183.41	4.41	6.53
70°	231.74	227.89	14.77	10.92
80°	283.17	250.76	13.47	- 18.94

TABLE XLII

Restored Antenna Temperatures for Finite Wave Tank with
Random Error, Interpolation, and Three Restorations
(Antenna = 12λ horn, ρ = 26 feet, f = 10.69 GHz, T_m = 284°K, S = 0 ‰)

HORIZONTAL POLARIZATION

Incidence Angle	T_a	T_{bres}	$T_a - T_b$	$T_{bres} - T_b$
0°	109.08	105.87	- 0.02	- 3.23
10°	108.81	110.29	0.94	2.42
20°	104.80	105.70	0.64	1.54
30°	97.80	98.19	- 0.17	0.23
40°	88.18	87.47	- 1.08	- 1.79
50°	80.84	72.69	2.74	- 5.40
60°	74.02	60.26	9.32	- 4.45
70°	97.44	63.26	47.49	13.31
80°	140.57	59.61	102.60	21.64

VERTICAL POLARIZATION

Incidence Angle	T_a	T_{bres}	$T_a - T_b$	$T_{bres} - T_b$
0°	109.09	105.88	- 0.01	- 3.22
10°	111.32	112.72	0.92	2.32
20°	115.12	115.85	0.68	1.40
30°	121.84	121.86	0.11	0.14
40°	132.72	131.49	- 0.47	- 1.70
50°	152.44	146.93	1.87	- 3.63
60°	181.29	177.35	4.41	0.47
70°	231..74	236.06	14.77	19.10
80°	283.17	290.88	13.47	21.17

TABLE XLIII

Restored Antenna Temperatures for Finite Wave Tank with Random Error, Interpolation, and One Restoration

(Antenna = 8λ horn, ρ = 26 feet, f = 10.69 GHz, T_m = 284°K, S = 0 °/oo)

HORIZONTAL POLARIZATION

Incidence Angle	T_a	T_{bres}	$T_a - T_b$	$T_{bres} - T_b$
0°	113.88	107.11	4.78	- 1.99
10°	110.04	108.22	2.17	0.36
20°	106.61	103.86	2.44	- 0.30
30°	101.66	97.04	3.70	- 0.92
40°	95.44	87.88	6.18	- 1.38
50°	95.99	81.16	17.89	3.06
60°	95.64	71.76	30.93	7.05
70°	135.46	64.13	85.52	14.18
80°	180.96	45.97	142.99	8.00

VERTICAL POLARIZATION

Incidence Angle	T_a	T_{bres}	$T_a - T_b$	$T_{bres} - T_b$
0°	113.94	107.16	4.84	- 1.94
10°	112.58	110.96	2.19	0.57
20°	116.84	114.91	2.39	0.46
30°	125.10	122.56	3.37	0.84
40°	138.18	135.18	4.98	1.98
50°	162.06	158.00	11.49	7.44
60°	191.71	187.00	14.83	10.12
70°	243.91	210.83	26.95	- 6.13
80°	282.27	202.52	12.57	- 67.19

TABLE XLIV

Restored Antenna Temperatures for Finite Wave Tank with Random Error, Interpolation, and Three Restorations

(Antenna = 8λ horn, ρ = 26 feet, f = 10.69 GHz, T_m = 284°K, S = 0 ⁰/oo)

HORIZONTAL POLARIZATION

Incidence Angle	T_a	T_{bres}	$T_a - T_b$	$T_{bres} - T_b$
0°	113.88	106.67	4.78	- 2.43
10°	110.04	106.82	2.17	- 1.04
20°	106.61	101.23	2.44	- 2.93
30°	101.66	93.00	3.70	- 4.97
40°	95.44	82.45	6.18	- 6.81
50°	95.99	77.42	17.89	- 0.67
60°	95.64	71.00	30.93	6.29
70°	135.46	73.84	85.52	23.90
80°	180.96	60.11	142.99	22.14

VERTICAL POLARIZATION

Incidence Angle	T_a	T_{bres}	$T_a - T_b$	$T_{bres} - T_b$
0°	113.94	106.72	4.84	- 2.38
10°	112.58	109.45	2.19	- 0.95
20°	116.84	111.74	2.39	- 2.71
30°	125.10	117.59	3.37	- 4.13
40°	138.18	128.54	4.98	4.65
50°	162.06	154.77	11.49	4.21
60°	191.71	189.37	14.83	12.49
70°	243.91	238.35	26.95	21.39
80°	282.27	263.17	12.57	- 6.54

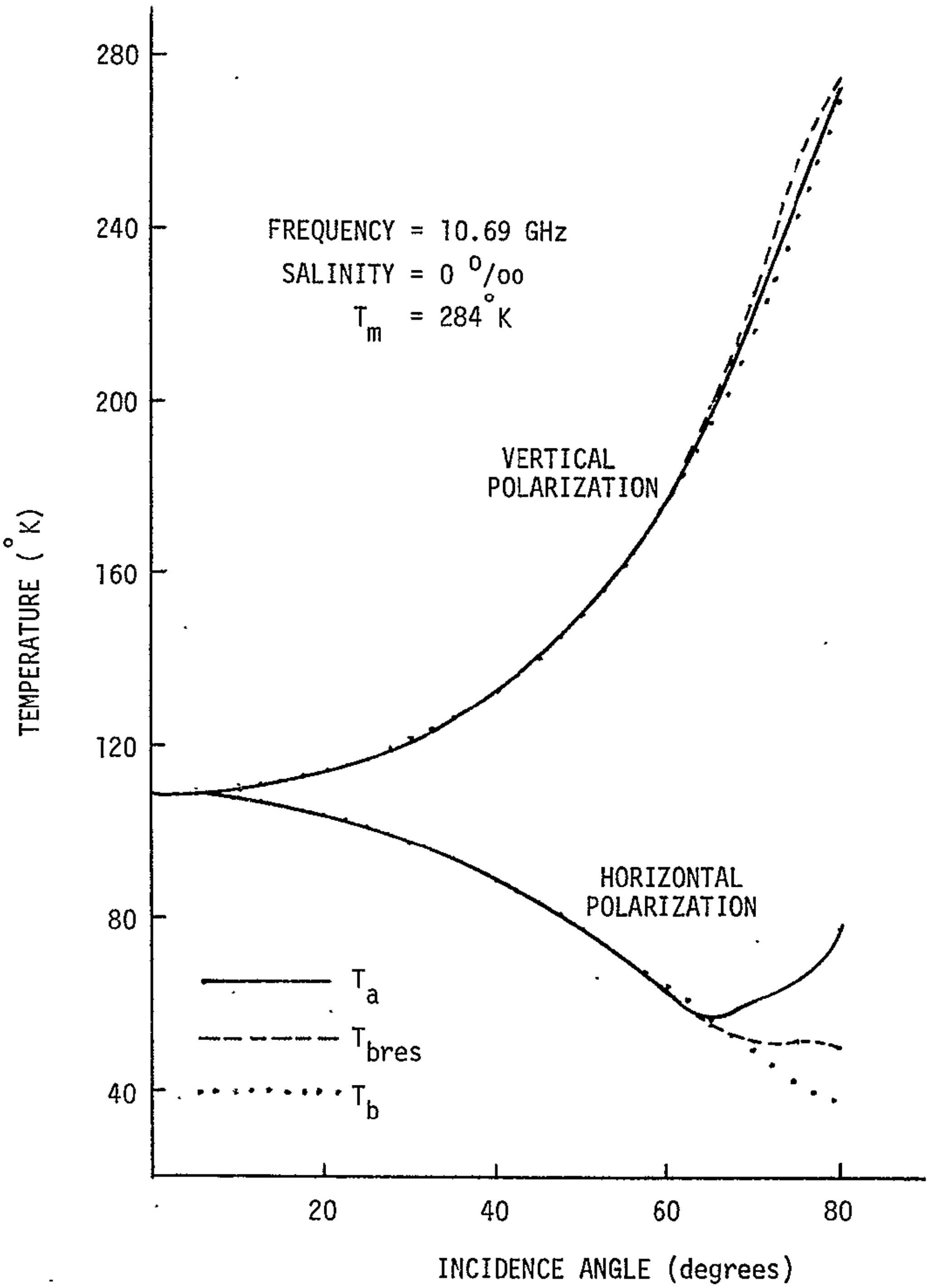

Fig. 35. Restoration of the Finite Wave Tank Data with Random Error and Interpolation (Antenna = 12λ horn, ρ = 13 feet, one iteration).

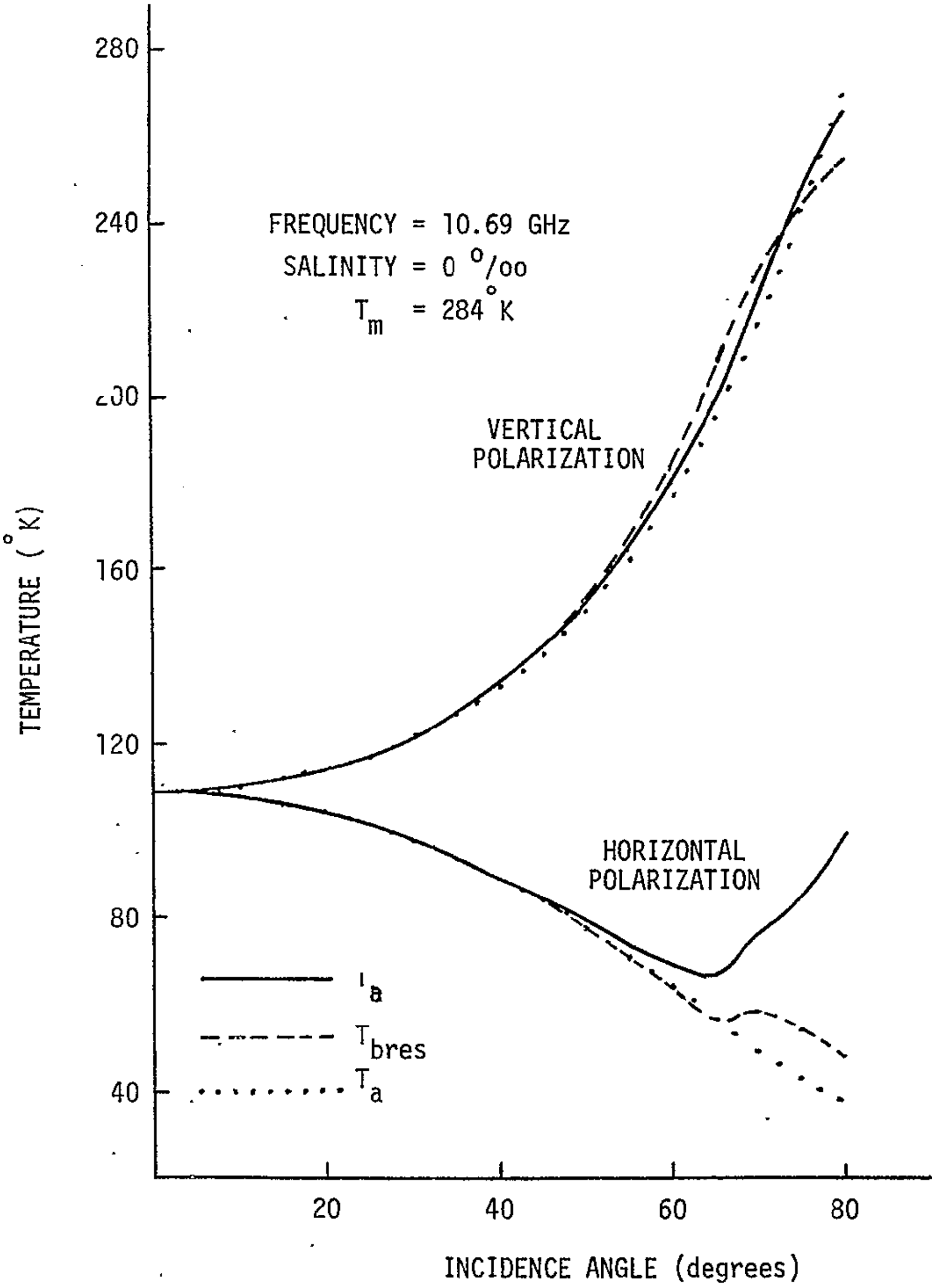

Fig. 36. Restoration of the Finite Wave Tank Data with Random Error and Interpolation (Antenna = 8λ horn, ρ = 13 feet, one iteration).

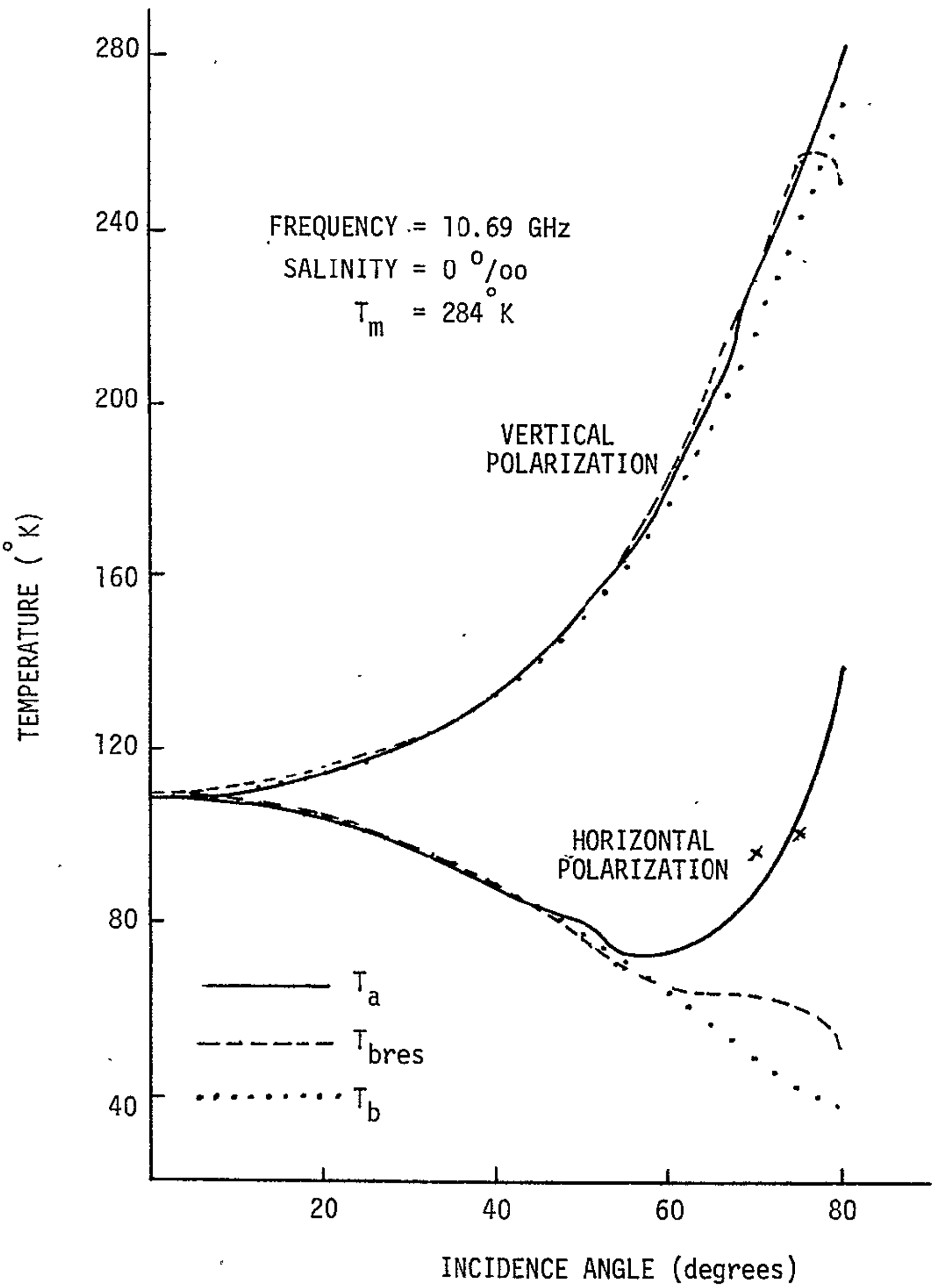

Fig. 37. Restoration of the Finite Wave Tank Data with Random Error and Interpolation (Antenna = 12λ horn, ρ = 26 feet, one iteration).

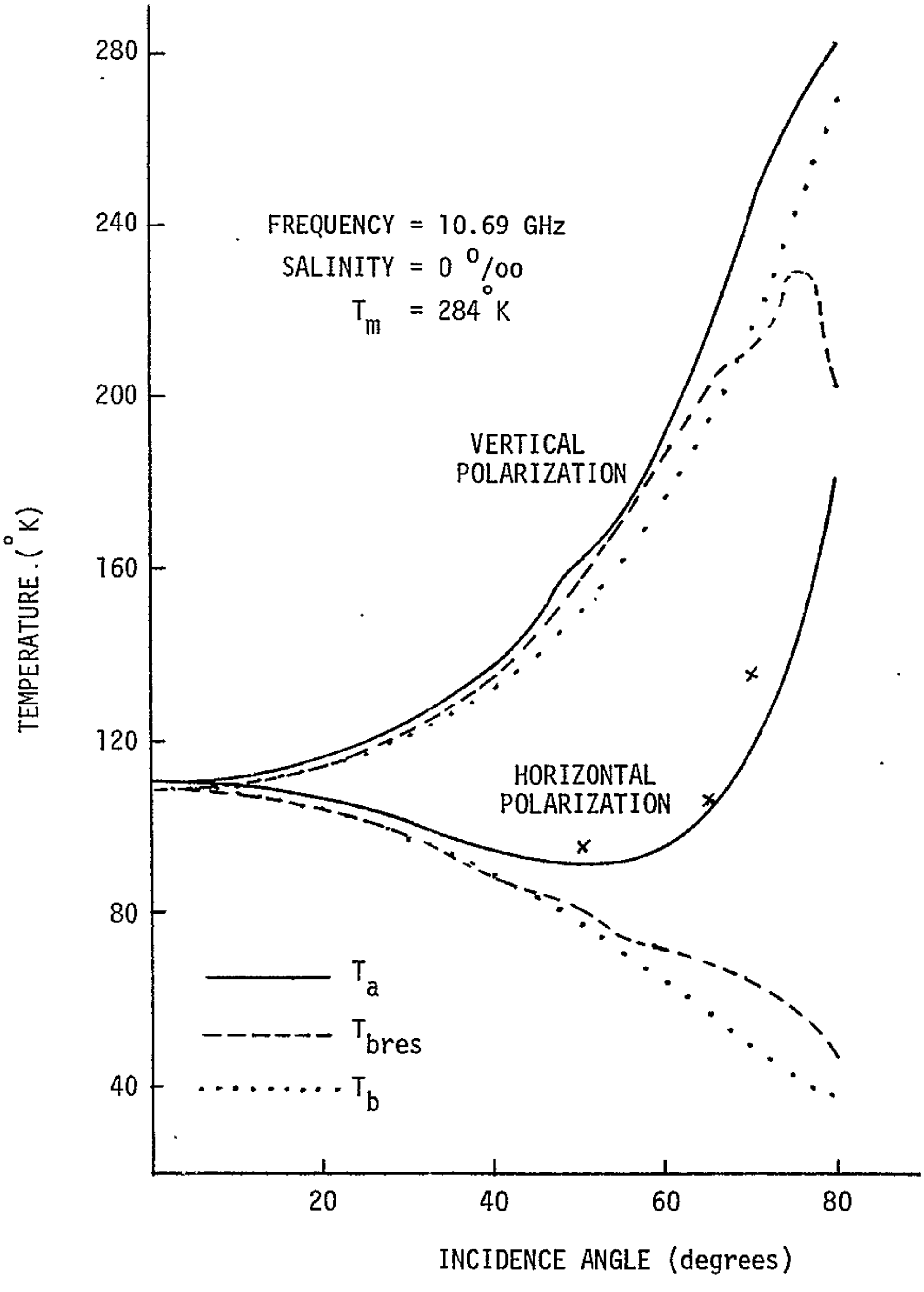

Fig. 38. Restoration of the Finite Wave Tank Data with Random Error and Interpolation (Antenna = 8λ horn, ρ = 26 feet, one iteration).

there is enough difference between the antenna and brightness temperatures to prevent the error from dominating the process. Even at the incidence angles where the smoothed antenna temperatures are more accurate than the restored brightness temperatures, the restoration process does not yield results that indicate instability. When interpolation is used, there is some improvement in the horizontal polarization data but none in the vertical polarization with one restoration. Multiple iterations yield less accurate results. In addition to the random error, there is considerable interpolation error with the rapidly varying functions involved in the 12λ horn and 26 foot boom case.

For the 8λ horn and the 26 foot boom, improved results are obtained by restoring the smoothed antenna temperatures with and without interpolation. With no interpolation, the results with three restorations are much superior than those with one restoration. The inversion is stable even with the added error and the results are improved significantly through the restoration process. With interpolation, the three-restoration results are inferior to those with one iteration. The results obtained with one restoration are, however, a definite improvement over the smoothed and interpolated antenna temperatures. This is true for both polarizations and nearly all incidence angles.

To partially summarize the parametric studies for the NASA finite wave tank, four tables will now be presented to show the recommended number of restorations for the various antenna, boom length, and data sampling combinations. Tables XLV, XLVI, XLVII, and XLVII summarize the 12λ horn and 13 foot boom, 8λ horn and 13 foot boom, 12λ horn and 26 foot boom, and 8λ horn and 26 foot boom cases. An "X", "V", or "H" indicate the recommended number of restorations for vertical-horizontal, vertical, or horizontal polarizations, respectively. Recommending no restorations indicates that the antenna temperature is a more accurate estimation of the true brightness temperature than the restored brightness temperature. These tables were based on the accuracy of the data from 0° to 60° incidence angle, since the data above 60° is of little practical concern. With these tables, one should be able to use the most effective number of restorations for the system under investigation.

It should be noted that the two-restoration data was investigated, but at no time did it yield the best results.

Appendix II contains a listing of the Fortran program that performs the three-dimensional inversion.

In addition to accounting for the non ideal pencil beam characteristics of the antennas, there is another major factor that needs to be compensated for in the restoration of measurements. This is the cross-polarization in the radiation characteristics of the antenna which was discussed in Section E of the theory. In practice, horns as well as other aperture antennas are not perfectly polarized even in the principal planes, but do possess a smaller orthogonal component to the principal field. Since the cross-polarized term is orthogonal to the principal component, it responds

TABLE XLV

Optimum Restoration for the Finite Wave Tank

with the 12λ Horn Antenna and the 13 Foot Boom

Type of Data Sampling	Recommended Number of Restorations			
	0	1	2	3
No Error				X
SPLINE Interpolation		X		
Linear Interpolation		X		
Random Error - No Interpolation	X			
Random Error - Interpolation	X			

TABLE XLVI

Optimum Restoration for the Finite Wave Tank

with the 8λ Horn Antenna and the 13 Foot Boom

Type of Data Sampling	Recommended Number of Restorations			
	C	1	2	3
No Error				X
SPLINE Interpolation				X
Linear Interpolation		X		
Random Error - No Interpolation	V	H		
Random Error - Interpolation	X			

TABLE XLVII

Optimum Restoration for the Finite Wave Tank

with the 12λ Horn Antenna and the 26 Foot Boom

Type of Data Sampling	Recommended Number of Restorations			
	0	1	2	3
No Error				X
SPLINE Interpolation				X
Linear Interpolation		X		
Random Error - No Interpolation				X
Random Error - Interpolation	V	H		

TABLE XLVIII

Optimum Restoration for the Finite Wave Tank

with the 8λ Horn Antenna and the 26 Foot Boom

Type of Data Sampling	Recommended Number of Restorations			
	0	1	2	3
No Error				X
SPLINE Interpolation				X
Linear Interpolation		X		
Random Error - No Interpolation				X
Random Error - Interpolation		X		

to the polarization which is orthogonal to the principal wave for a given scan. As the incidence angle becomes larger and the difference between the horizontal and vertical emissions of the water get larger, the effect of this cross-polarization becomes more pronounced. To show the effect of cross-polarization on the measurements, antenna temperatures have been calculated for different assumed values of cross-polarization. The data listed in Table XLIX shows the effect of the different cross-polarizations for the 12λ horn antenna and the 13 foot boom. Similar results are shown in Table L for the 8λ corrugated horn and the 13 foot boom. Table LI shows the effect of cross-polarization for the 12λ horn and the 26 foot boom and Table LII lists the results for the 8λ horn and the 26 foot boom. From these tables, one can immediately conclude that cross-polarization becomes a very significant factor no matter how narrow the antenna pattern is or which boom is used. This is to be expected since the effect of cross-polarization is mainly a function of the difference between the orthogonal radiation characteristics of the environment.

To show how well this cross-polarization phenomenon can be compensated for in the restoration process, antenna temperature profiles have been calculated, for various α's, assuming -20 dB cross-polarization and then restored to examine its importance. For the 12λ antenna and the 13 foot boom, the results, with three restorations, are listed in Table LIII. By comparing these results with those in Table V, it becomes clear how well the restoration process compensates for the cross-polarization. The antenna temperatures are

TABLE XLIX

Antenna Temperatures for the Finite Wave Tank with Cross-Polarization

(Antenna = 12λ horn, ρ = 13 feet)

(f = 10.69 GHz, T_m = 284°K, S = 0 ^{o}/oo)

	T_{ah}	T_{ah}	T_{ah}	T_{ah}	T_{av}	T_{av}	T_{av}	T_{av}
	none	-25 dB	-20 dB	-15 dB	none	-25 dB	-20 dB	-15 dB
$\alpha = 0^\circ$	109.15	109.15	109.15	109.15	109.15	109.15	109.15	109.15
$\alpha = 20^\circ$	104.22	104.25	104.32	104.54	114.56	114.53	114.46	114.24
$\alpha = 40^\circ$	89.36	89.50	89.80	90.71	133.55	133.41	133.11	132.20
$\alpha = 60^\circ$	65.69	66.04	66.80	69.13	177.97	177.62	176.86	174.53
$\alpha = 80^\circ$	69.54	70.17	71.50	75.62	267.99	267.36	266.03	261.91

TABLE L

Antenna Temperatures for the Finite Wave Tank with Cross-Polarization

(Antenna = 8λ horn, ρ = 13 feet)

(f = 10.69 GHz, T_m = 284°K, S = 0 °/oo)

	T_{ah}	T_{ah}	T_{ah}	T_{ah}	T_{av}	T_{av}	T_{av}	T_{av}
	none	-25 dB	-20 dB	-15 dB	none	-25 dB	-20 dB	-15 dB
α = 0°	109.37	109.37	109.37	109.37	109.37	109.37	109.37	109.37
α = 20°	104.47	104.50	104.57	104.79	114.84	114.81	114.74	114.52
α = 40°	89.96	90.10	90.40	91.32	134.22	134.08	133.78	132.86
α = 60°	70.48	70.83	71.57	73.84	180.13	179.78	179.04	176.77
α = 80°	92.20	92.74	93.90	97.46	263.84	263.30	262.14	258.58

TABLE LI

Antenna Temperatures for the Finite Wave Tank with Cross-Polarization (Antenna = 12λ horn, ρ = 26 feet)

(f = 10.69 GHz, T_m = 284°K, S = 0 ^{o}/oo)

	T_{ah}	T_{ah}	T_{ah}	T_{ah}	T_{av}	T_{av}	T_{av}	T_{av}
CROSS-POLARIZATION	none	-25 dB	-20 dB	-15 dB	none	-25 dB	-20 dB	-15 dB
$\alpha = 0^\circ$	109.70	109.70	109.70	109.70	109.69	109.69	109.69	109.69
$\alpha = 20^\circ$	104.84	104.87	104.94	105.16	115.13	115.10	115.03	114.81
$\alpha = 40^\circ$	90.68	90.82	91.12	92.03	134.52	134.38	134.08	133.18
$\alpha = 60^\circ$	73.50	73.84	74.57	76.80	181.23	180.89	180.16	177.93
$\alpha = 80^\circ$	129.16	129.63	130.63	133.71	277.43	276.97	275.97	272.89

TABLE LII

Antenna Temperatures for the Finite Wave Tank with Cross-Polarization (Antenna = 8λ horn, ρ = 26 feet)

(f = 10.69 GHz, T_m = 284°K, S = 0 °/oo)

	T_{ah}	T_{ah}	T_{ah}	T_{ah}	T_{av}	T_{av}	T_{av}	T_{av}
CROSS - POLARIZATION	none	-25 dB	-20 dB	-15 dB	none	-25 dB	-20 dB	-15 dB
α = 0°	112.92	112.92	112.92	112.92	112.91	112.91	112.91	112.91
α = 20°	108.41	108.44	108.51	108.72	118.48	118.45	118.38	118.17
α = 40°	97.85	97.99	98.27	99.15	140.03	139.90	139.61	138.74
α = 60°	92.11	92.42	93.08	95.11	190.08	189.77	189.11	187.08
α = 80°	169.85	170.19	170.92	173.17	278.28	277.94	277.21	274.96

TABLE LIII

Restored Antenna Temperatures for Finite Wave Tank with -20 dB Cross-Polarization and Three Restorations

(Antenna = 12λ horn, ρ = 13 feet, f = 10.69 GHz, T_m = 284°K, S = 0 ‰)

HORIZONTAL POLARIZATION

Incidence Angle	T_a	T_{bres}	$T_a - T_b$	$T_{bres} - T_b$
0°	109.14	109.08	0.04	- 0.02
10°	107.95	107.88	0.08	0.01
20°	104.32	104.17	0.16	0.01
30°	98.26	97.98	0.30	0.02
40°	89.80	89.26	0.54	0.00
50°	79.16	77.96	1.06	- 0.14
60°	66.80	64.52	2.09	- 0.19
70°	59.74	50.26	9.80	0.32
80°	71.50	40.10	33.53	2.13

VERTICAL POLARIZATION

Incidence Angle	T_a	T_{bres}	$T_a - T_b$	$T_{bres} - T_b$
0°	109.18	109.12	0.08	0.02
10°	110.44	110.41	0.04	0.01
20°	114.46	114.46	0.02	0.02
30°	121.69	121.75	- 0.03	0.03
40°	133.11	133.17	- 0.08	- 0.02
50°	150.52	150.12	- 0.05	- 0.45
60°	176.86	176.20	- 0.02	- 0.68
70°	217.48	220.45	0.52	3.49
80°	266.02	282.85	- 3.68	13.15

different for the two cases, but the restored brightness temperatures are almost identical. The effect of the cross-polarization is therefore accurately compensated. In Table LIV, similar results are shown for the 8λ antenna and 13 foot boom which can be compared with those shown in Table VII. Table LV shows the results of the restoration process of antenna temperatures with -20 dB cross-polarization for the 12λ horn and the 26 foot boom. Comparing Table LV with Table IX, one can see that again the inversion process is able to remove the effect of the cross-polarization. The results of the inversion of the antenna temperatures with cross- polarization for the 8λ horn and the 26 foot boom are shown in Table LVI. Comparing Table LVI with Table XI yields the same conclusion that the effect of the cross-polarization has been removed. It is concluded that the restoration process removes the effect of the cross-polarization for any antenna and boom length combination.

Recently, some preliminary measurements have been made on the wave tank system at NASA Langley Research Center, Hampton, Virginia. It would then be fruitful to examine the restoration of the data even though it may not be very accurate but it is representative of the response of the system. The measurements were taken at a frequency of 10.69 GHz using a 12λ corrugated horn and the 26 foot boom. The values of α that were used were 0°, 10°, 20°, 30°, 40°, and 50°. For the first three values of α, the measurement had to be adjusted to remove a contribution attributed mainly to the standing wave pattern produced between the antenna

TABLE LIV

Restored Antenna Temperatures for Finite Wave Tank with -20 dB

Cross-Polarization and Three Restorations

(Antenna = 8λ horn, ρ = 13 feet, f = 10.69 GHz, T_m = 284°K, S = 0 °/oo)

HORIZONTAL POLARIZATION

Incidence Angle	T_a	T_{bres}	$T_a - T_b$	$T_{bres} - T_b$
0°	109.34	109.13	0.24	0.03
10°	108.17	107.88	0.30	0.01
20°	104.57	104.12	0.41	- 0.04
30°	98.64	97.80	0.68	- 0.16
40°	90.39	89.01	1.13	- 0.25
50°	81.03	77.83	2.93	- 0.27
60°	71.60	64.69	6.89	- 0.02
70°	73.29	51.66	23.35	1.72
80°	93.89	39.27	55.92	1.30

VERTICAL POLARIZATION

Incidence Angle	T_a	T_{bres}	$T_a - T_b$	$T_{bres} - T_b$
0°	109.39	109.17	0.29	0.07
10°	110.66	110.39	0.26	- 0.01
20°	114.73	114.37	0.29	- 0.08
30°	122.13	121.39	0.41	- 0.33
40°	133.78	132.58	0.59	- 0.61
50°	151.91	150.04	1.34	- 0.53
60°	179.04	177.90	2.16	1.02
70°	219.91	229.94	2.95	12.98
80°	262.14	272.08	- 7.56	2.38

TABLE LV

Restored Antenna Temperatures for Finite Wave Tank with -20 dB Cross - Polarization and Three Restorations

(Antenna = 12λ horn, ρ = 26 feet, f = 10.69 GHz, T_m = 284 °K, S = 0 ‰)

HORIZONTAL POLARIZATION

Incidence Angle	T_a	T_{bres}	$T_a - T_b$	$T_{bres} - T_b$
0°	110.14	109.04	1.04	- .06
10°	108.43	107.74	.57	- .13
20°	104.94	103.88	.78	- .29
30°	99.13	97.55	1.17	- .41
40°	91.12	88.77	1.86	- .48
50°	83.39	77.74	5.30	- .35
60°	74.57	65.03	9.86	.32
70°	89.46	52.94	39.51	2.99
80°	130.63	41.10	92.66	3.13

VERTICAL POLARIZATION

Incidence Angle	T_a	T_{bres}	$T_a - T_b$	$T_{bres} - T_b$
0°	110.18	109.08	1.08	- .02
10°	110.92	110.25	.52	- .15
20°	115.03	114.08	.58	- .37
30°	122.42	121.13	.70	- .59
40°	134.08	132.45	.89	- .74
50°	153.00	150.32	2.43	- .25
60°	180.16	179.33	3.28	2.45
70°	226.47	231.86	9.50	14.90
80°	275.97	280.98	6.26	11.27

TABLE LVI

Restored Antenna Temperatures for Finite Wave Tank with - 20 dB Cross - Polarization and Three Restorations

(Antenna = 8λ horn, ρ = 26 feet, f = 10.69 GHz, T_m = 284°K, S = 0 ^{0}/oo)

HORIZONTAL POLARIZATION

Incidence Angle	T_a	T_{bres}	$T_a - T_b$	$T_{bres} - T_b$
0°	115.43	106.80	6.33	- 2.30
10°	111.38	107.24	3.52	- .63
20°	108.51	103.58	4.35	- .59
30°	104.13	97.63	6.16	- .33
40°	98.27	89.39	9.01	.13
50°	96.18	80.24	10.08	2.14
60°	93.08	67.60	28.37	2.89
70°	125.92	54.05	75.98	4.10
80°	170.92	38.14	132.95	.17

VERTICAL POLARIZATION

Incidence Angle	T_a	T_{bres}	$T_a - T_b$	$T_{bres} - T_b$
0°	115.45	106.82	6.35	- 2.23
10°	113.82	109.81	3.42	- .59
20°	118.38	113.85	3.93	- .59
30°	126.75	121.47	5.03	- .26
40°	139.61	133.91	6.42	.72
50°	161.16	156.82	10.59	6.25
60°	189.11	188.17	12.23	11.30
70°	237.73	228.98	20.76	12.02
80°	277.21	253.54	7.50	-16.16

and observed surface. The inverted data, using one restoration, is shown in Figure 39. Since the $\beta=0^{\circ}$ points are the more accurate values on the restored brightness temperature profiles, curves were drawn through these points and are shown in the figure. For the larger incidence angles, the restoration process shows a significant difference between the restored brightness temperatures and the measured antenna temperatures.

B. Infinite Tank(Ocean) Data

The developed programs can be used to predict and/or restore data from observations made at oceans or other large bodies of water. In these cases, the dimensions of the finite wave tank can be adjusted to fit the particular need. In Table LVII and LVIII are lists of data obtained by calculating the antenna temperature profiles from the empirical brightness temperatures and then restoring them to recover the original brightness temperatures using the 12λ and 8λ horns, respectively. The restored brightness temperatures are almost exactly equal to the original profiles in these cases. The restoration process works better for the infinite tank case than in the finite tank case because the functions involved are smoother. All the finite tank cases involve a discontinuity in the water brightness temperature profile at the edge of the wave tank which causes high frequency content to be included in its spectrum. Since practical antennas can not detect this discontinuity (because of limited spectral resolution), the

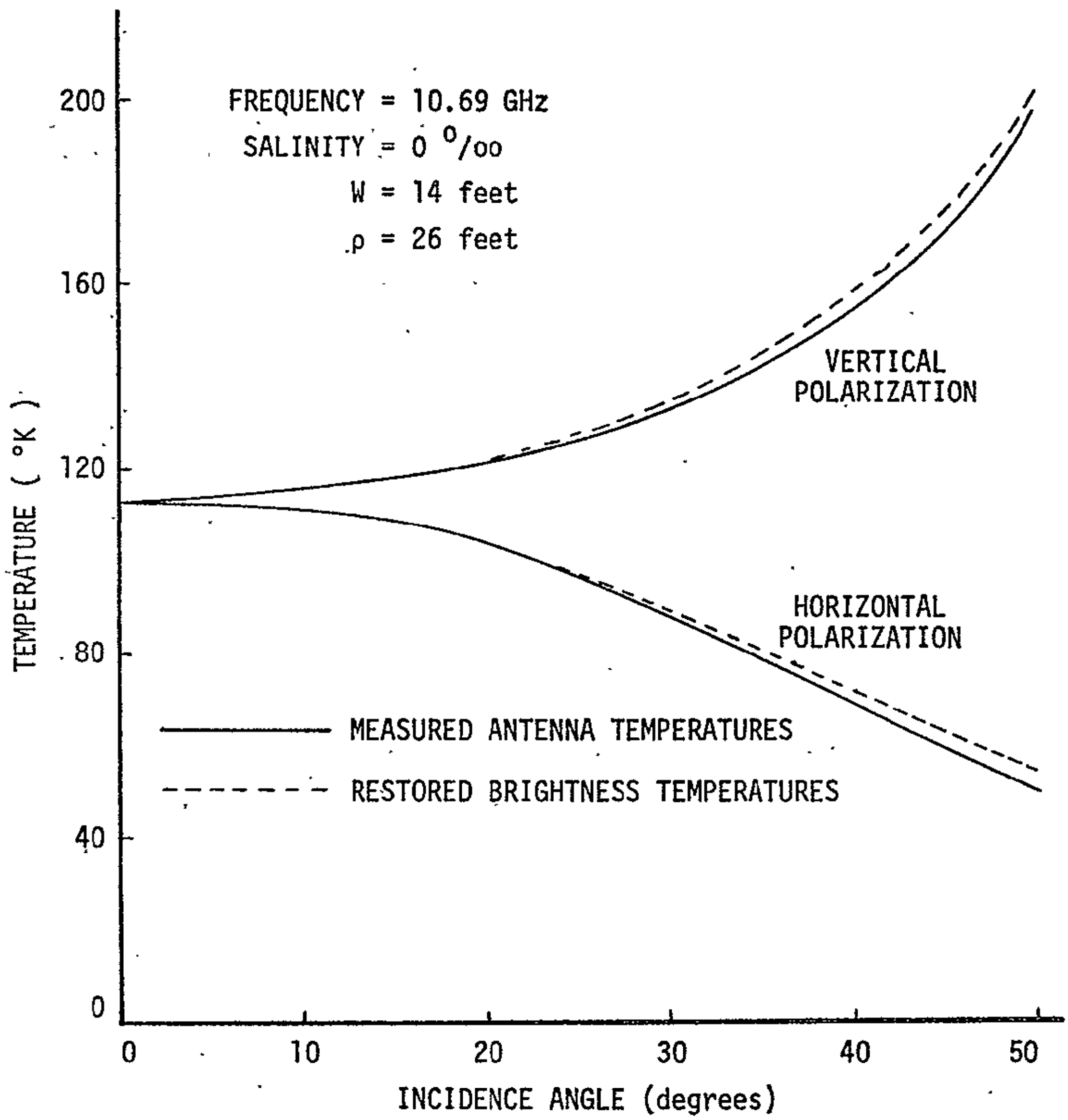

Fig. 39. Measured Total Antenna Temperatures and Restored Water Brightness Temperatures for the NASA LaRC Wave Tank.

TABLE LVII

Restoration of Error-Free Infinite Tank

Data (Antenna = 12λ horn)

(f = 10.69 GHz, T_m = 284°K, S = 0 °/oo)

β	T_{ah}	T_{bh}	T_{bresh}	T_{av}	T_{bv}	T_{bresv}
0	109.105	109.099	109.101	109.105	109.099	109.097
5	108.712	108.710	108.701	109.520	109.508	109.516
10	107.905	107.905	107.902	110.380	110.358	110.362
15	106.145	106.149	106.149	112.292	112.249	112.251
20	104.306	104.316	104.315	114.338	114.273	114.274
25	101.164	101.182	101.182	117.967	117.862	117.864
30	98.286	98.311	98.311	121.442	121.299	121.299
35	93.754	93.788	93.789	127.237	127.028	127.029
40	89.836	89.876	89.879	132.597	132.324	132.326
45	83.929	83.977	83.979	141.369	140.991	140.990
50	77.269	77.320	77.320	152.425	151.909	151.908
55	71.812	71.861	71.859	162.580	161.938	161.940
60	64.009	64.037	64.033	179.234	178.405	178.407
65	57.876	57.856	57.867	194.561	193.613	193.620
70	49.671	49.485	49.556	219.304	218.492	218.451
75	44.174	43.540	43.839	240.448	240.648	240.552
80	41.688	37.871	36.234	263.427	270.379	270.476

TABLE LVIII

Restoration of Error-Free Infinite

Tank Data (Antenna = 8λ horn)

(f = 10.69 GHz, T_m = 284°K, S = 0 ⁰/oo)

β	T_{ah}	T_{bh}	T_{bresh}	T_{av}	T_{bv}	T_{bresv}
0	109.112	109.099	109.101	109.112	109.099	109.099
5	108.719	108.710	108.701	109.531	109.508	109.519
10	107.910	107.905	107.898	110.401	110.358	110.367
15	106.145	106.149	106.146	112.336	112.249	112.253
20	104.303	104.316	104.315	114.408	114.273	114.276
25	101.154	101.182	101.184	118.083	117.862	117.864
30	98.269	98.311	98.312	121.603	121.299	121.300
35	93.728	93.788	93.787	127.476	127.028	127.029
40	89.805	89.876	89.880	132.910	132.324	132.329
45	83.890	83.977	83.975	141.804	140.991	140.997
50	77.234	77.320	77.330	153.013	151.909	151.926
55	71.784	71.861	71.856	163.296	161.938	161.949
60	64.028	64.037	64.087	180.098	178.405	178.370
65	57.981	57.856	57.951	195.427	193.613	193.444
70	50.069	49.485	49.231	219.419	218.492	217.892
75	45.496	43.540	42.715	238.464	240.648	240.690
80	44.689	37.871	33.979	252.473	270.379	272.900

exact brightness temperature profile can not be restored. With the smooth functions involved in the infinite tank case, one can obtain a very good approximation of the T_b's.

At Cape Cod Canal, Massachusetts, measurements were made by Swift [15] over a body of water which can be modeled as an infinite tank in one direction and finite in the other. The antenna used was a horn operating at 7.55 GHz and whose principal plane power patterns are shown in Figures 40 and 41. These two patterns were combined to construct the total three-dimensional pattern by using (122) and (123). In Figure 42 the measured antenna temperatures have been plotted along with the restored (two- and three-dimensional) and the empirical brightness temperature profiles. As can be seen, the restored three-dimensional and the empirical curves are very similar and different from the measurements. The three-dimensional restoration works very well and it is more accurate than the two-dimensional, especially for larger incidence angles.

As has been previously stated, a two-dimensional approximation of the wave tank system [7,8] has been used that takes advantage of the vector alignment in the $\theta = \frac{\pi}{2}$ plane. In this plane $\hat{\theta}$ and $\hat{h}$ are aligned together as are $\hat{\phi}$ and $\hat{v}$. This means that for the vertical scan only the vertical brightness temperature is received by the antenna and similarly the horizontal brightness temperature for the horizontal scan. However, the vector alignment in the other planes is not perfect and the opposite brightness temperature will

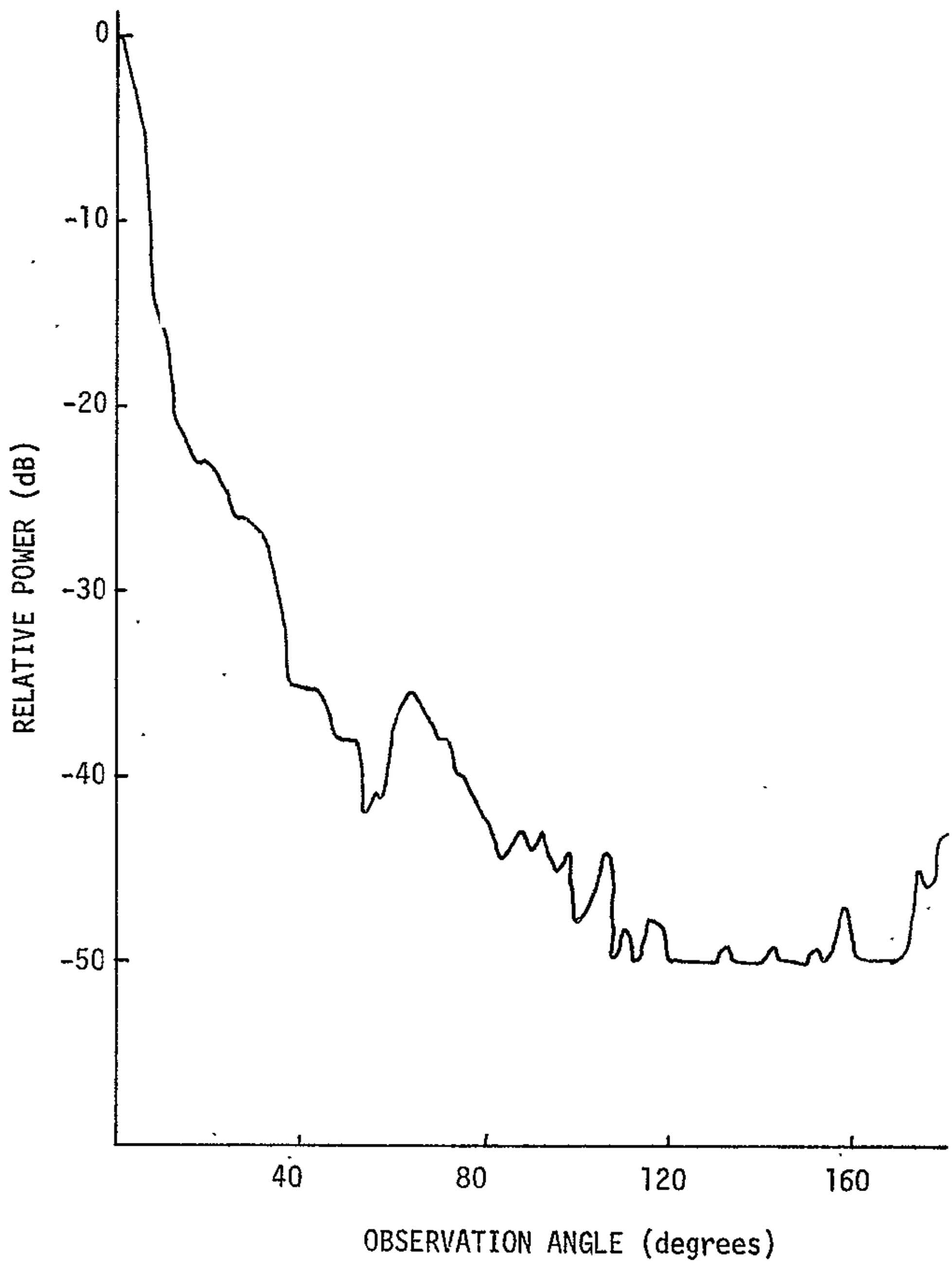

Fig. 40 . E-plane Power Pattern of the 7.55 GHz
Cape Cod Canal Antenna.

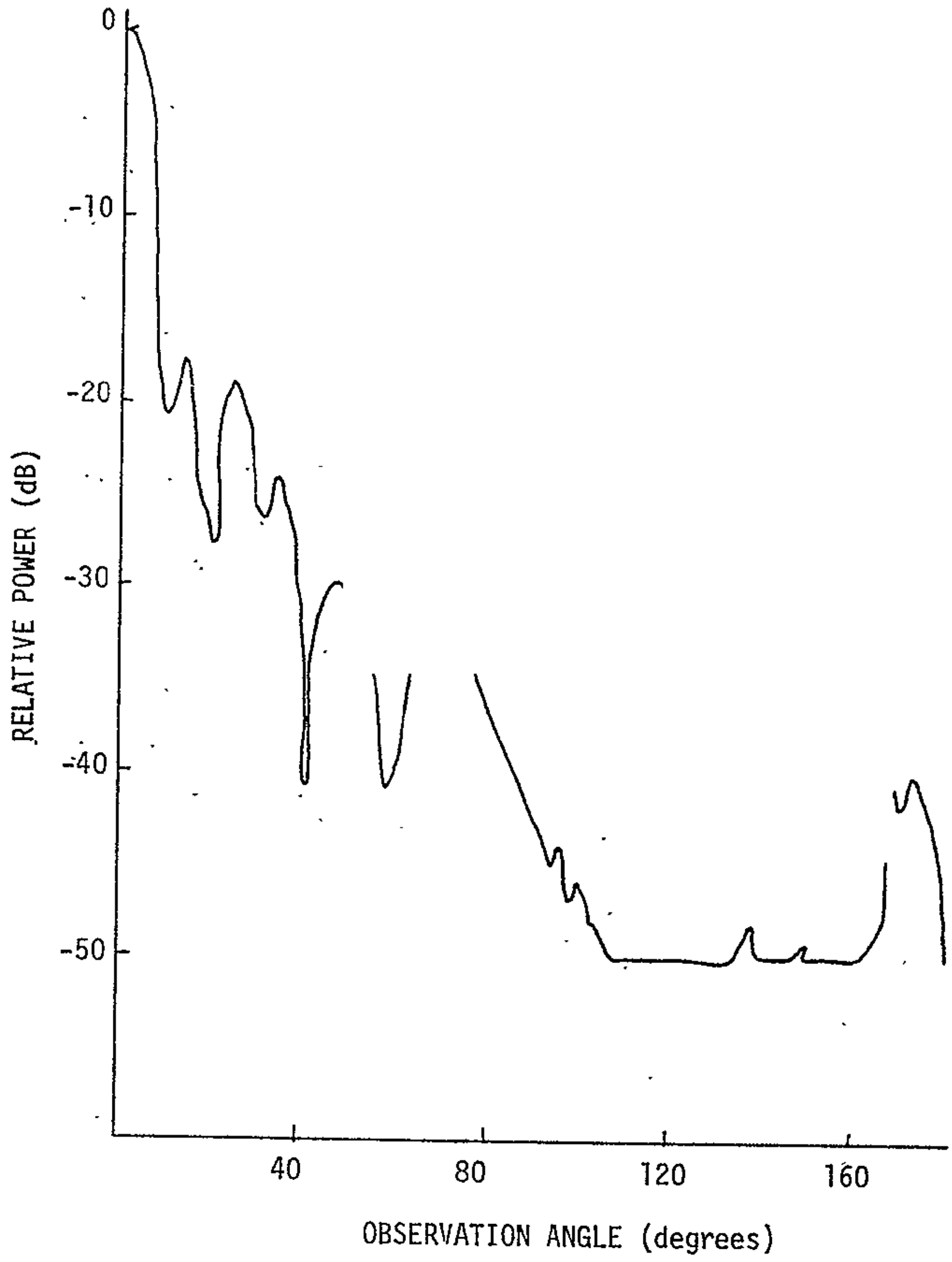

Fig. 41. H-plane Power Pattern of the 7.55 GHz Cape Cod Canal Antenna.

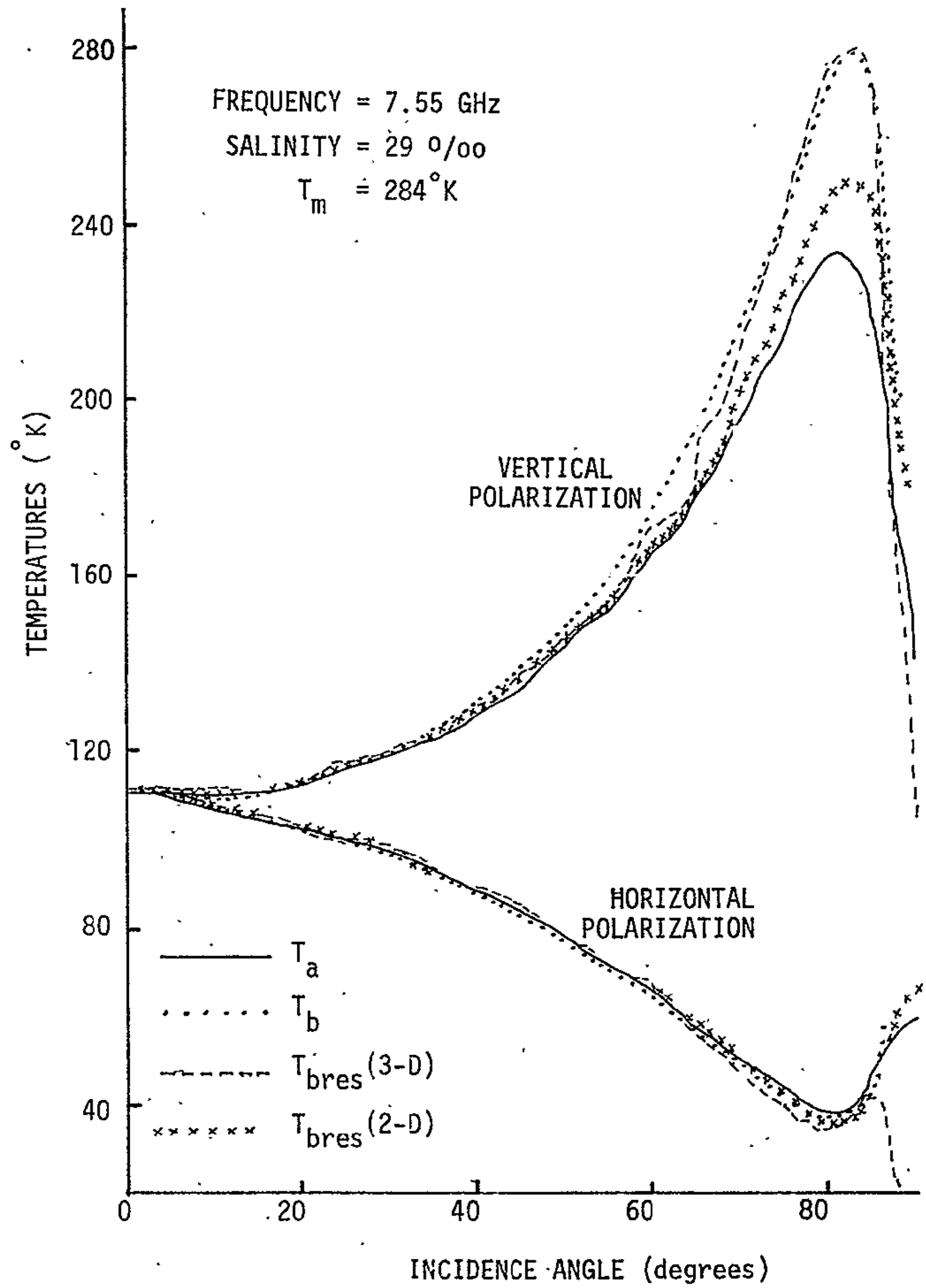

Fig. 42. Measured Total Antenna Temperatures, Restored and Empirical Water Brightness Temperatures for Cape Cod Canal Experiment.

also contribute. The effect of this cross-coupling can only be accounted for by the three-dimensional modeling which calculates the vector alignment and integrates over all values of θ.

The strength of the cross-coupling has been taken into account in the restoration process by the functions WF_1, WF_2, WF_3, and WF_4 in (144a)-(145b). In Figure 43 these functions have been plotted for the finite wave tank system and the 8λ horn antenna and for the Cape Cod canal and the 7.55 GHz parabolic dish. From the data shown in these two figures, it is clear that cross-coupling is significant and the three-dimensional inversion is essential.

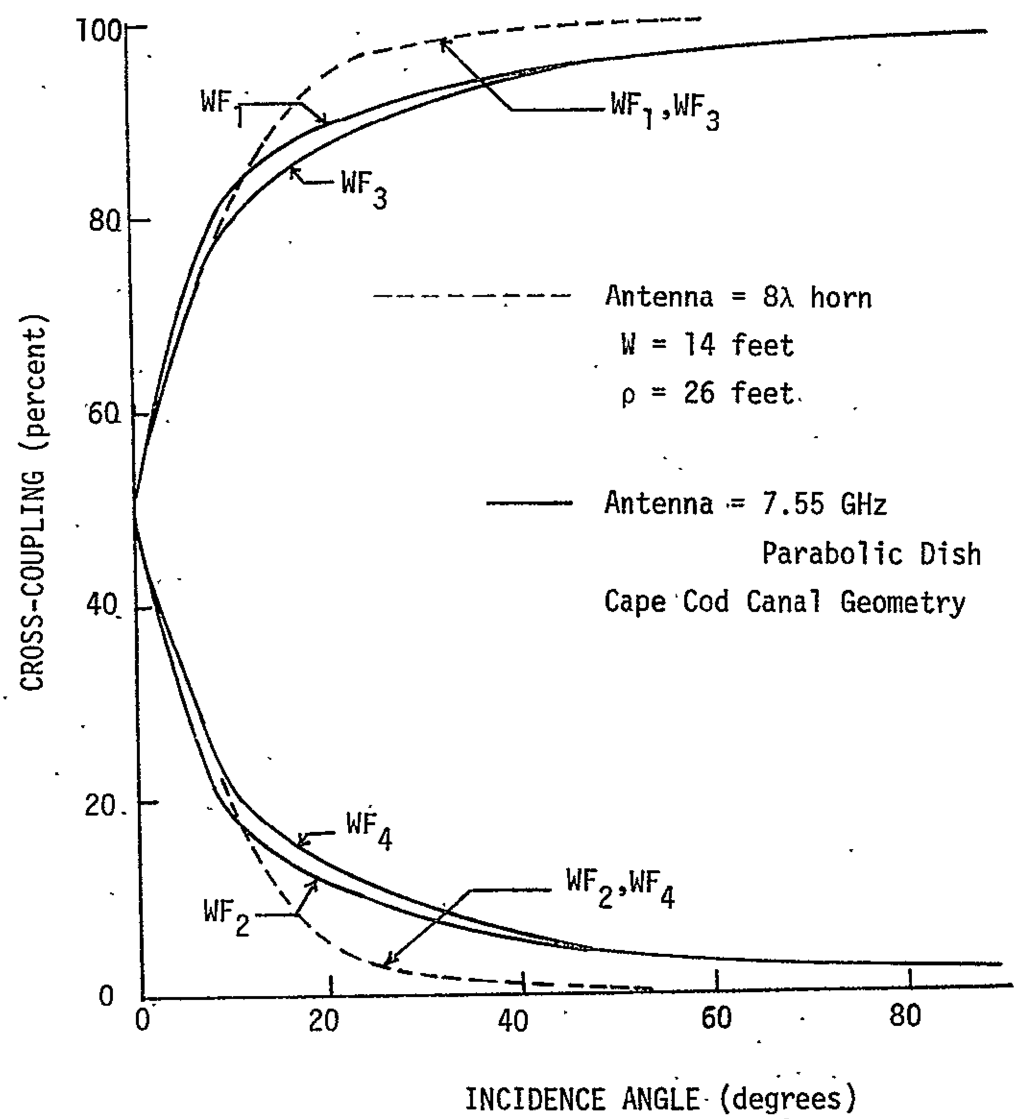

Fig. 43. Cross-Coupling Functions in the Three - Dimensional Analysis.

V. Conclusions

In the course of this investigation, the three-dimensional vector interaction between a microwave radiometer and a wave tank environment was modeled. With the computer programs developed one is able to predict the response of the radiometer to the known brightness temperature characteristics of the surroundings. More importantly, however, a computer program was developed that can invert (restore) the radiometer measurements. In other words, one can use this computer program to estimate the brightness temperatur profiles of a water surface from the radiometer response.

The three-dimensional modeling of the problem was accomplished using two different coordinate system geometries. In one formulation, the z-axis was taken perpendicular to the radiometer antenna aperture and in the other formulation the x-axis was perpendicular to the aperture. Computations were made to predict the radiometer response to the wave tank environment with both formulations and it was established that they both were accurate models of the three-dimensional vector interaction. The three-dimensional models were also compared to a previously used two-dimensional scalar approximation of the problem. From this comparison, it was established that, unless the antenna used has a high main beam efficiency, the three-dimensional vector formulation is necessary to achieve an accurate result.

With the x-axis formulation, it was shown that inversion (restoration) of the data was possible. Antenna temperature profiles for the wave tank system were computed and brightness temperatures were restored with a very good approximation. Errors were added to the computed antenna temperature profiles and the restoration process proved to be fairly stable. The effect of cross-polarization on the radiometer response was demonstrated as well as the capability of the restoration process to account for its presence.

In addition to inverting (restoring) data for the wave tank system, it has been shown that the computer programs can be used to simulate the viewing of large bodies of water. In this situation the restoration process is extremely accurate with the smooth functions involved.

Preliminary measured data for the wave tank system, made available by NASA personnel, was restored taking into account the contributions from the surrounding earth and sky. Data taken at Cape Cod Canal, Massachusetts, by NASA was also considered and resulted in a very successful restoration.

With the restoration process and the future improved accuracy of the wave tank system, investigators should be able to experimentally verify the semi-empirical brightness temperature equations for various frequencies, salinities, incidence angles, and temperatures. The effect of surface roughness could then be experimentally measured with the controlled wave tank system. This knowledge could then be applied to analyze multiple frequency radiometer measurements received from satellites monitoring the ocean, in order to determine wind speed (surface roughness), water temperature, atmospheric conditions, and salinity.

BIBLIOGRAPHY

[1] G.M. Hindy, et. al., "Development of a Satellite Microwave Radiometer to Sense the Surface Temperature of the World Oceans," NASA Contractor Report, Report CR-1960, North American Rockwell Corporation, Downey, California.

[2] D.H. Staelin, K.F. Kunzi, P.W. Rosenkranz, J.W. Waters, "Environmental Sensing with Nimbus Satellite Passive Microwave Spectrometers," California Institute of Technology (Contract 952568), Quarterly Progress Report No. 112, January 15, 1974, Massachusetts Institute of Technology, Research Laboratory of Electronics, Cambridge, Massachusetts.

[3] S. Twomey, "The Application of Numerical Filtering to the Solution of Integral Equations Encountered in Indirect Sensing Measurements," J. Franklin Inst., vol. 279, Feb. 1965.

[4] D.L. Phillips, "A Technique for the Numerical Solution of Certain Integral Equations of the First Kind," J. Ass. Comput. Mach., pp. 84-97, 1962.

[5] R.N. Bracewell and J.A. Roberts, "Aerial Smoothing in Radio Astronomy," Aust. J. Phys., vol. 7, pp. 615-640, Dec. 1954.

[6] J.P. Claassen and A.F. Fung, "The Recovery of Polarized Apparent Temperature Distribution of Flat Scenes from Antenna Temperature Measurements," IEEE Trans. Antennas Propagat., vol. AP-22, pp. 433-442, May 1974.

[7] V.L. Fisher, "Fourier Transform Techniques for the Inversion of Radiometric Measurements," MSEE Thesis, West Virginia University, Morgantown, West Virginia, 1973.

[8] J.J. Holmes, "Application and Sensitivity Investigation of Fourier Transforms for Microwave Radiometric Inversions," M.S.E.E. Thesis, West Virginia Univ., Morgantown, West Virginia, 1974.

[9] J.R. Fisher, "Fortran Program for Fast Fourier Transform," NRL Report 7041, April, 1970.

[10] F. Beck, "Antenna Pattern Corrections to Microwave Radiometer Temperature Calculations," Radio Science, vol. 10, No. 10, pp. 839-845, Oct. 1975.

[11] A. Stogryn, "Equations for Calculating the Dielectric Constant of Saline Water," IEEE Trans. Microwave Theory and Techniques, pp. 733-736, 1971.

[12] W.H. Peake, "The Microwave Radiometer as a Remote Sensing Instrument," Technical Report 1903-8, Jan., 1969, Electro-Sciences Laboratory, The Ohio State University, Columbus, Ohio.

[13] S. Silver, Microwave Antenna Theory and Design, New York: McGraw-Hill, 1949.

[14] W. Squire, private communication, West Virginia University, Morgantown, West Virginia.

[15] C.T. Swift, "Microwave Radiometer Measurements of the Cape Cod Canal," Radio Science, pp. 641-653, July, 1974.

Appendix I

Transformation of Coordinates

A right-handed orthogonal coordinate system x, y, z can be transformed into any new right-handed orthogonal coordinate system x''', y''', z''', with the same origin, by three rotations about at least two different axes. An example of this type of transformation is shown in Figure I-1. This particular transform uses rotations about all three axes. The transformation of rectangular unit vectors for each rotation is described by the simultaneous equations shown below in matrix form. For the rotation about the x-axis (Figure I-1)

$$\begin{bmatrix} \hat{x}' \\ \hat{y}' \\ \hat{z}' \end{bmatrix} = \begin{bmatrix} 1 & 0 & 0 \\ 0 & \cos\lambda & \sin\lambda \\ 0 & -\sin\lambda & \cos\lambda \end{bmatrix} \begin{bmatrix} \hat{x} \\ \hat{y} \\ \hat{z} \end{bmatrix} = [A] \begin{bmatrix} \hat{x} \\ \hat{y} \\ \hat{z} \end{bmatrix} \qquad \text{(I-1)}$$

about the y - axis (Figure I-1)

$$\begin{bmatrix} \hat{x}'' \\ \hat{y}'' \\ \hat{z}'' \end{bmatrix} = \begin{bmatrix} \cos\mu & 0 & -\sin\mu \\ 0 & 1 & 0 \\ \sin\mu & 0 & \cos\mu \end{bmatrix} \begin{bmatrix} \hat{x}' \\ \hat{y}' \\ \hat{z}' \end{bmatrix} = [B] \begin{bmatrix} \hat{x}' \\ \hat{y}' \\ \hat{z}' \end{bmatrix} \qquad \text{(I-2)}$$

and about the z-axis (Figure I-1)

$$\begin{bmatrix} \hat{x}''' \\ \hat{y}''' \\ \hat{z}''' \end{bmatrix} = \begin{bmatrix} \cos\nu & \sin\nu & 0 \\ -\sin\nu & \cos\nu & 0 \\ 0 & 0 & 1 \end{bmatrix} \begin{bmatrix} \hat{x}'' \\ \hat{y}'' \\ \hat{z}'' \end{bmatrix} = [C] \begin{bmatrix} \hat{x}'' \\ \hat{y}'' \\ \hat{z}'' \end{bmatrix} \qquad \text{(I-3)}$$

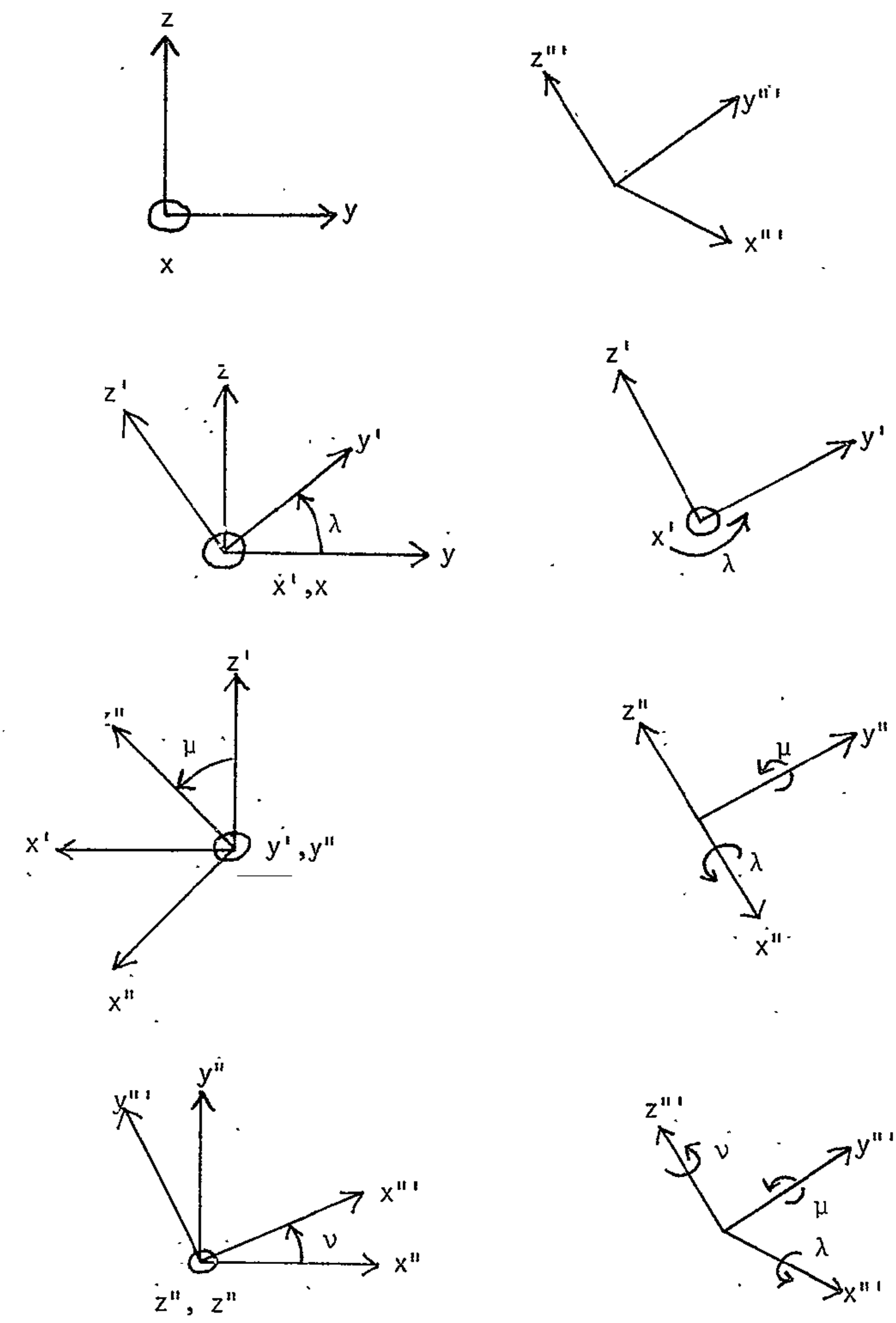

Fig. I-1. General three-dimensional rotation.

The unit vectors $\hat{x}'''$, $\hat{y}'''$, and $\hat{z}'''$ can be found directly in terms of the original unit vectors $(\hat{x},\hat{y},\hat{z})$ by combining (I-1), (I-2), and (I-3) leading to

$$\begin{bmatrix} \hat{x}''' \\ \hat{y}''' \\ \hat{z}''' \end{bmatrix} = [C]\,[B]\,[A] \begin{bmatrix} \hat{x} \\ \hat{y} \\ \hat{z} \end{bmatrix} \tag{I-4}$$

Although θ''' and $\emptyset'''$ can be found directly from θ and $\emptyset$ by equating $\hat{r}$ to $\hat{r}'''$, it will be more illustrative to show the transformation for each rotation.

For the rotation about the x-axis we can solve (I-1) as

$$\begin{bmatrix} \hat{x} \\ \hat{y} \\ \hat{z} \end{bmatrix} = [A]^{-1} \begin{bmatrix} \hat{x}' \\ \hat{y}' \\ \hat{z}' \end{bmatrix} = \begin{bmatrix} 1 & o & o \\ o & \cos\lambda & -\sin\lambda \\ o & \sin\lambda & \cos\lambda \end{bmatrix} \begin{bmatrix} \hat{x}' \\ \hat{y}' \\ \hat{z}' \end{bmatrix} \tag{I-5}$$

The radial vectors $\hat{r}$ and $\hat{r}'$ are

$$\hat{r} = \hat{x}\cos\emptyset\sin\theta + \hat{y}\sin\emptyset\sin\theta + \hat{z}\cos\theta \tag{I-6}$$

$$\hat{r}' = \hat{x}\cos\emptyset'\sin\theta' + \hat{y}\sin\emptyset'\sin\theta' + \hat{z}'\cos\theta' \tag{I-7}$$

Using (I-5), (I-6) can be written as

$$\begin{aligned} \hat{r} = {} & \hat{x}'\cos\emptyset\sin\theta \\ & + \hat{y}'(\cos\lambda\sin\emptyset\sin\theta + \sin\lambda\cos\theta) \\ & + \hat{z}'(-\sin\lambda\sin\emptyset\sin\theta + \cos\lambda\cos\theta) \end{aligned} \tag{I-8}$$

Equating (II-8) and (II-7) yields

$$\cos\emptyset'\sin\theta' = \cos\emptyset\sin\theta \tag{I-9}$$

$$\sin\emptyset'\sin\theta' = \cos\lambda\sin\emptyset\sin\theta + \sin\lambda\cos\theta \tag{I-10}$$

$$\cos\theta' = -\sin\lambda\sin\emptyset\sin\theta + \cos\lambda\cos\theta \qquad \text{(I-11)}$$

From (I-9), (I-10), and (I-11), we can find θ' and $\emptyset'$ in terms of $\theta, \emptyset$, and λ as

$$\emptyset' = \tan^{-1}\left\{ \frac{\cos\lambda\sin\emptyset\sin\theta + \sin\lambda\cos\theta}{\cos\emptyset\sin\theta} \right\} \qquad \text{(I-12)}$$

$$\theta' = \cos^{-1}\{-\sin\lambda\sin\emptyset\sin\theta + \cos\lambda\cos\theta\} \qquad \text{(I-13)}$$

For the rotation about the y-axis, (I-2) can be written as

$$\begin{bmatrix} \hat{x}' \\ \hat{y}' \\ \hat{z}' \end{bmatrix} = [B]^{-1} \begin{bmatrix} \hat{x}'' \\ \hat{y}'' \\ \hat{z}'' \end{bmatrix} = \begin{bmatrix} \cos\mu & o & \sin\mu \\ o & 1 & o \\ -\sin\mu & o & \cos\mu \end{bmatrix} \begin{bmatrix} \hat{x}'' \\ \hat{y}'' \\ \hat{z}'' \end{bmatrix} \qquad \text{(I-14)}$$

We can express the radial vectors as

$$\hat{r}'' = \hat{x}''\cos\emptyset''\sin\theta'' + \hat{y}''\sin\emptyset''\sin\theta'' + \hat{z}''\cos\theta'' \qquad \text{(I-15)}$$

$$\hat{r}' = \hat{x}''(\cos\mu\cos\emptyset'\sin\theta' - \sin\mu\cos\theta')$$
$$+ \hat{y}''\sin\emptyset'\sin\theta'$$
$$+ \hat{z}''(\sin\mu\cos\emptyset'\sin\theta' + \cos\mu\cos\theta') \qquad \text{(I-16)}$$

Equating (I-15) and (I-16) yields

$$\cos\emptyset''\sin\theta'' = \cos\mu\cos\emptyset'\sin\theta' - \sin\mu\cos\theta' \qquad \text{(I-17)}$$

$$\sin\emptyset''\sin\theta'' = \sin\emptyset'\sin\theta' \qquad \text{(I-18)}$$

$$\cos\theta'' = \sin\mu\cos\emptyset'\sin\theta' + \cos\mu\cos\theta' \qquad \text{(I-19)}$$

From (I-17), (I-18), and (I-19), we can find the relationships between θ'' and $\emptyset''$ and θ', $\emptyset'$, and μ as

$$\emptyset'' = \tan^{-1}\left\{ \frac{\sin\emptyset' \sin\theta'}{\cos\mu\cos\emptyset' \sin\theta' - \sin\mu\cos\theta'} \right\} \tag{I-20}$$

$$\theta'' = \cos^{-1}\{\sin\mu\cos\emptyset' \sin\theta' + \cos\mu\cos\theta'\} \tag{I-21}$$

For the rotation about the z-axis, (I-3) can be rewritten as

$$\begin{bmatrix} \hat{x}'' \\ \hat{y}'' \\ \hat{z}'' \end{bmatrix} = [C]^{-1} \begin{bmatrix} \hat{x}''' \\ \hat{y}''' \\ \hat{z}''' \end{bmatrix} = \begin{bmatrix} \cos\nu & -\sin\nu & 0 \\ \sin\nu & \cos\nu & 0 \\ 0 & 0 & 1 \end{bmatrix} \begin{bmatrix} \hat{x} \\ \hat{y} \\ \hat{z} \end{bmatrix} \tag{I-22}$$

The radial vectors are given by

$$\hat{r}''' = \hat{x}''' \cos\emptyset''' \sin\theta''' + \hat{y}\sin\emptyset''' \sin\theta''' + \hat{z}''' \cos\theta''' \tag{I-23}$$

$$\begin{aligned} \hat{r}'' = {} & \hat{x}''' (\cos\nu\cos\emptyset'' \sin\theta'' + \sin\nu\sin\emptyset'' \sin\theta'') \\ & + \hat{y}''' (-\sin\nu\cos\emptyset'' \sin\theta'' + \cos\nu\sin\emptyset'' \sin\theta'') \\ & + \hat{z}''' \cos\theta'' \end{aligned} \tag{I-24}$$

If we set $\hat{r}'' = \hat{r}'''$, we find

$$\cos\emptyset''' \sin\theta''' = \cos\nu\cos\emptyset'' \sin\theta'' + \sin\nu\sin\emptyset'' \sin\theta'' \tag{I-25}$$

$$\sin\emptyset''' \sin\theta''' = -\sin\nu\cos\emptyset'' \sin\theta'' + \cos\nu\sin\emptyset'' \sin\theta'' \tag{I-26}$$

$$\cos\theta''' = \cos\theta'' \tag{I-27}$$

If we multiply (I-25) by $\sin\nu$, (I-26) by $\cos\nu$, and then add we find that

$$\sin\nu\cos\emptyset''' + \cos\nu\sin\theta''' = \sin\emptyset'' = \sin(\emptyset''' + \nu) \tag{I-28}$$

from (I-27) and (I-28) we find

$$\theta''' = \theta'' \qquad \text{(I-29)}$$

$$\emptyset''' = \emptyset'' - \nu \qquad \text{(I-30)}$$

As can be seen, unless the rotation is only about the z-axis, the transformation of the spherical variables θ and ∅ involve transcendental equations. If the new coordinate system has a different z-axis, these transcendental equations cannot be avoided.

Appendix II

Restoration Computer Program

```
C
C     PROGRAM TO INVERT WAVE TANK MEASUREMENTS FROM THE NASA LANGLEY WAVE TANK.
C
      DIMENSION TAH(256),TAV(256),TBH(256),TBV(256),ANGA(256),ALPA(17)
C     CALLING THE SUBROUTINE VALUES RESTORES THE MEASUREMENTS FOR THE VARIOUS
C     ALPHA'S AND THEN COMBINES THEM TO FORM CONTINUOUS ARRAYS THAT VARY WITH
C     INCIDENCE ANGLE. IT YIELDS THE FOLLOWING:
C           TAH=HORIZONTAL MEASURED ANTENNA TEMPERATURES.
C           TAV=VERTICAL MEASURED ANTENNA TEMPERATURES.
C           TBH=HORIZONTAL RESTORED BRIGHTNESS TEMPERATURE.
C           TBV=VERTICAL RESTORED BRIGHTNESS TEMPERATURES.
C          ANGA=THE CORRESPONDING INCIDENCE ANGLES.
C        ICOUNT=AN INTEGER WHICH GIVES THE LENGTH OF THE ARRAYS.
C
      NREST=1
      NUMALP=12
      LSTATE=5
C
C     THE SUBROUTINE VALUES MUST BE SUPPLIED WITH THE FOLLOWING DATA THROUGH
C     THE CALL LIST:
C        NREST=AN INTEGER SPECIFYING THE NUMBER OF RESTORATIONS DESIRED.
C       NUMALP=AN INTEGER SPECIFYING THE NUMBER OF ALPHA'S TO BE USED.
C       LSTATE=AN INTEGER SPECIFYING THE TYPE OF EARTH AND SKY BRIGHTNESS
C              TEMPERATURE MODELING TO BE USED.IF LSTATE=5 ,THE EMPIRICAL MODEL
C              OF PEAK IS USED FOR THE SKY AND THE EARTH IS MODELED WITH A
C              CONSTAINT BRIGHTNESS TEMPERATURE TE. IF LSTATE=6 ,THE MEASURED
C              ANTENNA TEMPERATURES ARE USED AS THE BRIGHTNESS TEMPERATURES OF
C              THE EARTH AND SKY.IF LSTATE=7 ,THE MEASURED ANTENNA TEMPERATURES
C              ARE RESTORED FOUR TIMES AND THEN USED AS THE BRIGHTNESS
C              TEMPERATURES FOR THE EARTH AND SKY.
C         FEFF=THE PERPENDICULAR DISTANCE FROM THE LINE FORMED BY THE INTER-
C              SECTION OF THE SCANNING PLANE AND THE WATER SURFACE TO THE
C              LATERAL EDGE OF THE WATER-EARTH BOUNDARY.
C            W=THE WIDTH OF THE WATER TANK IN THE SCANNING PLANE.
C          RHO=THE LENGTH OF THE BOOM.
C       DBCROS=THE AMOUNT OF CROSS-POLARIZATION PRESENT IN DB.
C           TK=THE AMBIENT TEMPERATURE OF THE SYSTEM IN DEGREES KELVIN.
C           TE=THE CONSTANT VALUE FOR THE BRIGHTNESS TEMPERATURE OF THE EARTH.
C         ALPA=AN ARRAY WHICH CONTAINS THE ALPHA VALUES IN DEGREES. THE ALPHA'S
C              MUST BE READ IN ASCENDING ORDER AND BE MULTIPLES OF FIVE DEGREES
    4 CONTINUE
C       INDATA=AN INTEGER SPECIFYING THE TYPE OF DATA PROSSESSING TO BE USED.
C              IF INDATA = 1 , THE 256 DATA POINTS THAT ARE READ INTO THE
C              PROGRAM ARE USED AS THEY ARE. IF INDATA = 2 , SPLINE INTEPOLATION
C              IS USED TO FIT 5.6 DEGREE SAMPLING TO THE NEEDED 1.4 DEGREE
C              SAMPLING. 256 DATA POINTS STILL MUST BE READ INTO THE PROGRAM
C              EVEN WHEN INTERPOLATION IS USED, SO THREE ZERO'S CAN BE READ IN
C              AFTER EACH DATA POINT. IF INDATA = 3 , LINEAR INTERPOLATION
C              IS USED. IF INDATA = 4 , THE 256 SAMPLE POINTS WILL BE SMOOTHED
C              ASSUMING THEY CONTAIN RANDOM ERROR. IF INDATA = 5 , THE 64 SAMPLE
C              POINTS WILL BE INTERPOLATED AND SMOOTHED ASSUMING THEY CONTAIN
C              RANDOM ERROR. AGAIN, AS WITH ALL INTERPOLATION MODES , 256 DATA
C              POINTS MUST BE READ IN WITH THREE DUMMY SAMPLE POINTS AFTER EACH
C              REAL DATA POINT.
C
      FEFF=7.
      DBCROS=-100.
      RHO=13.
      W=14.
      TE=300.
      INDATA=1
C
C     THE MEASURED ANTENNA TEMPERATURES ARE READ FROM SUBROUTINE INVERT. THE
C     MEASUREMENTS ARE READ IN FOR THE ENTIRE 360 DEGREE SCAN STARTING WITH
C     BETA=-180 DEGREES AND SCANNING IN THE DIRECTION THAT IS FIRST TOWARD
C     THE EARTH. THE DATA CARDS SHOULD BE PLACED IN THE ORDER THAT CONFORMS TO
C     THE READ STATEMENTS SHOWN BELOW. TAMV IS THE VERTICAL SET OF MEASUREMENTS
C     AND TAMH IS THE HORIZONTAL SET.
C
C     DO 1 I=1,NUMALP
C     READ(5,100) (TAMV(J),J=1,256)
C     READ(5,100) (TAMH(J),J=1,256)
C     RESTORATION PROCESS FOR EACH ALPHA
C   1 CONTINUE
C 100 FORMAT(8F10.3)
C
```

```
C     SUBROUTINE VALUES ALSO USES THE FOURIER TRANSFORM OF THE GAIN FUNCTIONS
C     FROM A DISK OR TAPE. THESE TRANSFORMS MUST BE READ ON TO THE DISK OR TAPE
C     WITH A SUPPLEMENTARY PROGRAM
C
      READ(5,300) (ALPA(I),I=1,NUMALP)
 300. FORMAT(8F10.3)
      CALL VALUES (TAH,TAV,TBH,TBV,ANGA,ICOUNT,NRFST,NUMALP,FFFF,
     1 LSTATE,DBCPOS,ALPA,RHO,W,TK,TE,INDATA)
      DO 8 I=1,ICOUNT
      WRITE(6,500) TAH(I),TAV(I),TBH(I),TBV(I),ANGA(I)
 500  FORMAT (' ',5F20.4)
    8 CONTINUE
      STOP
      END
```

```
      SUBROUTINE VALUES (TAH,TAV,TBH,TBV,ANGA,ICOUNT,NREST,NUMALP,
     1 FFFF,LSTATE,DBCROS,ALPA,RHO,W,TK,TE,INDATA)
      DIMENSION TAH(256),TAV(256),ANGA(256),
     1 ALPA(17),NSTART(2,17),NSTOP(2,17)
      DIMENSION TBH(256),TBV(256),TAAWH(256),TAAWV(256),TAAESH(256),
     1 TAAESV(256),TBRESH(256),TBRESV(256)
C
C     THIS SUBROUTINE EXTRACTS THE NEEDED DATA FOR EACH VALUE OF ALPHA FROM THE
C     RESULTS IT RECEIVES FROM SUBROUTINE INVERT AND ASSEMBLES THE DATA INTO THE
C     ARRAYS TAH,TAV,TBH,TBV,.
C
C     THE INTEGER ARRAYS NSTART AND NSTOP DEFINE THE CUTOFF LIMITS OF THE
C     RESTORED TB'S FOR THE 17 POSSIBLE ALPHA VALUES.
C
      DATA NSTOP/130,131,129,131,129,131,128,131,128,131,128,131,129,
     1 131,128,132,128,132,128,131,129,131,130,131,130,132,129,132,129,
     1 132,129,131,130,130/
      DATA NSTART/129,129,127,126,126,124,126,124,125,124,125,124,125,  WVU9900
     1 124,125,124,125,124,125,125,125,125,126,125,127,125,127,125,126,
     1 126,126,126,126,127/
      NDP=256
      NDP21=NDP/2.+1.001
      NRRR=1
      ICOUNT=1
      DEL=360./FLOAT(NDP)
      DO 6 IA=1,NUMALP
      ALP=ALPA(IA)
      CALL INVERT (TAAWH,TAAWV,TAAESH,TAAESV,TBRESH,TBRESV,NREST
     1 ,NRRR,FFFF,LSTATE,DBCROS,RHO,W,TK,ALP,TE,INDATA)
      WRITE(6,200) ALP
      DO 2 J=100,200
      ANG=(J-NDP21)*DEL
      WRITE(6,100) TAAWH(J),TAAESH(J),TBRESH(J),J,TAAWV(J),TAAESV(J),
     1 TBRESV(J),ANG
    2 CONTINUE
  100 FORMAT (' ',3F10.3,I10,4F10.3)
  200 FORMAT ('1',6X,'TAWH',5X,'TAESH',4X,'TBRESH',5X,'INDEX',6X,
     1 'TAWV',5X,'TAESV',4X,'TBRESV',6X,'BETA',5X,'ALPHA=',F5.1)
      IALP=.2*ALP+1.001
      IF(IA.EQ.1) GO TO 3
      IF(IA.EQ.NUMALP) GO TO
      ALP1L=ALPA(IA-1)
      ALP1M=ALPA(IA+1)
      GO TO 5
      ALP1L=-5.0
      ALP1M=ALPA(IA+1)
      GO TO 5
      ALP1L=ALPA(IA-1)
      ALP1M=85.0
      CONTINUE
      ISTART=1
      ISTOP=1
      IF(ALP-ALP1L.GT.7.5) ISTART=2
      IF(ALP1M-ALP.GT.7.5) ISTOP=2
      N1=NSTART(ISTART,IALP)
      N2=NSTOP(ISTOP,IALP)
      DO 7 I=N1,N2
      TAH(ICOUNT)=TAAWH(I)+TAAESH(I)
      TAV(ICOUNT)=TAAWV(I)+TAAESV(I)
      TBH(ICOUNT)=TBRESH(I)
      TBV(ICOUNT)=TBRESV(I)
      ANGA(ICOUNT)=ALP+(I-NDP21)*DEL
      ICOUNT=ICOUNT+1
      CONTINUE
      CONTINUE
      ICOUNT=ICOUNT-1
      RETURN
      END
```

```
      SUBROUTINE INVERT  (TAMH,TAMV,TAESH,TAESV,TBRESH,TBRESV,
     1 NREST,NRRR,FFFF,LSTATE,DBCROS,RHC,W,TK,ALPC,TE,INDATA)
C
C     THIS SUBPCUTIME PERFORMS THE ACTUAL INVERSION OF THE MEASUREMENTS BY
C     CALLING THE OTHER SUBROUTINES TO EXECUTE THE NECESSARY INTEGRATIONS.
C     THESE ARRAYS ARE COMBINED TO FIND THE RESTORED BRIGHTNESS TEMPERATURE
C     PROFILES FOR A GIVEN ALPHA.
C
      COMMON/B1/TAPPV,TAPPH,STHE,NDT,NDP,DEL,DELTHE,ALP
     1   ,PRINCF,CROSSF,THEDIS,WF
      COMMON/BLOC1/AAAA
      COMMON/BLOC2/S,M,INV
      COMMON/B6/GTHEH,GPHIH,GTHEV,GPHIV,GCROH,GCROV
      COMPLEX GTHEH(256),GPHIH(256),GTHEV(256),GPHIV(256)
      COMPLEX GCROH(256),GCROV(256)
      COMPLEX AAAA(8,256)
      DIMENSION PERHP(256),PERHC(256),PERVP(256),PERVC(256)
      DIMENSION TAMH(256),TAMV(256),TAPPH(256),TAPPV(256),STHE(65)
      DIMENSION TAWV(256),TAWH(256),TAESV(256),TAESH(256),ERRV(256),
     1   ERRH(256)
      DIMENSION TAAWH(256),TAAWV(256),TAAESH(256),
     1 TAAESV(256),TBRESH(256),TBRESV(256)
      DIMENSION TBRV(256),TBRH(256)
      DIMENSION INV(128),S(128),M(3)
      DIMENSION TAV(256),TAH(256)
      DIMENSION THEDIS(32),WF(32)
      DIMENSION THEXXX(32),WX(32)
      DIMENSION TINTEV(65),TINTEH(65),ANG(256)
      DIMENSION RANDOM(256)
      DIMENSION A(257),B(257),C(257),D(257),DY(256),WK(250
      DIMENSION C17(257,3)
C
C     THROUGHOUT ALL OF THE INTEGRATING SUBROUTINES THE INTEGRATION WITH RESPECT
C     TO THETA IS PERFORMED WITH GAUSSIAN QUADRATURE NUMERICAL INTEGRATION.THIS
C     IS DONE WITH THE TWO ARRAYS THEXXX AND WX. THEXXX CONTAINS THE VALUES OF
C     THETA AT WHICH THE FUNCTIONS ARE TO BE SAMPLED AND WX CONTAINS THE
C     WEIGHTING FACTOR FOR EACH THETA
C
      DATA THEXXX/1.5680,1.5562,1.5356,1.5067,1.4707,1.4289,1.3827,
     1 1.3338,1.2841,1.2352,1.1890,1.1472,1.1112,1.0923,1.0617,1.0499
     2 ,1.0416,1.0181,.97694,.91912,.84711,.76341,.67104,.57334,.47385,
     3  .37615,.28378,.20007,.12805,.07035,.02902,.000549/
      DATA WX/0.007108467,0.016297929,0.024912439,0.032627787,
     1 0.039164137,0.044285066,0.047805458,0.049598049,0.049598049,
     2 0.047805458,0.044285066,0.039164137,0.032627787,0.024912439,
     3 0.016297929,0.007108487,0.014216989,0.032595869,0.049824879,
     4 0.065255523,0.078329252,0.088570118,0.095616460,0.099196076,
     5 0.099196076,0.095616460,0.088570118,0.078329252,0.065255523,
     6 0.049824879,0.032595869,0.014216989/
      IF(NRRR.NE.1) GO TO 717
C
C           NDP=THE NUMBER OF SAMPLE POINTS FOR PHI AND BETA
C           NDT=THE NUMBER OF SAMPLE POINTS FOR THETA
C     THE ARRAYS M,S, AND INV ARE USED BY HARM THE FAST FOURIER TRANSFORM
C     SUBROUTINE. S AND INV ARE USED AS WORK SPACES.
C          M(1)=BASE 2 LOG OF NDP
C          M(2)=0
C          M(3)=0
      NDP=256
      NDT=32
      M(1)=8
      M(2)=0
      M(3)=0
      ALP1L=-5.0
      DBCROS=10.**(DBCROS/10.)
      PRINCF=1./(1.+DBCROS)
      CROSSF=DBCROS/(1.+DBCROS)
      DEGCOV=90.
      NDP2=NDP/2+.001
      NDP4=NDP/4+.001
      NDP21=NDP2+1
      NDP41=NDP4+1
      DO 8 I=1,NDT
      THEDIS(I)=THEXXX(I)
      WF(I)=WX(I)
```

```
      PI=3.14159
    8 CONTINUE
      DEL=2.*PI/FLOAT(NDP)
      RAD=PI/180.
      DELTHE=DEGCOV*RAD/FLOAT(N
      READ(5,100) (RANDOM(J),J=
  100 FORMAT (8F10.4)
  717 CONTINUE
      ALP=ALPD*RAD
      PHI1=ATAN2(W/2.+RHO*SIN(ALP),RHO*COS(ALP))-ALP
      PHI2=ATAN2(W/2.-RHO*SIN(ALP),RHO*COS(ALP))+ALP
C
C     THE VARIABLES NPHI1 AND NPHI2 DEFINE THE WATER-EARTH BOUNDARIES IN THE
C     SCANNING PLANE
C
      NPHI2=PHI2/DEL
      NPHI1=PHI1/DEL
      DELTHE=DEGCOV*RAD/FLOAT(NDT)
      DO 6 I=1,NDT
      STHE(I)=SIN(THEDIS(I))*WF(I)
    6 CONTINUE
      CALL PEPCEN (NPHI1,NPHI2,FFEF,PEPHP,PEPHC,PERVP,PEPVC,LSTATE,RHO)
  131 FORMAT (7F10.3)
C
C     THE MEASURED ANTENNA TEMPERATURES ARE READ HERE. TAPPV CONTAINS THE
C     VERTICAL MEASUREMENTS AND TAPPH THE HORIZONTAL.
C
      NREAD=.2*(ALPD-ALP1L)+.001
 9876 FORMAT(8F10.3)
      READ(5,9876) (TAPPV(J),J=1,NDP)
      READ(5,9876) (TAPPH(J),J=1,NDP)
      IF (INDATA.EQ.1) GO TO 1333
      IF (INDATA.EQ.2) GO TO 1301
      GO TO 1302
 1301 CONTINUE
      I=1
      DO 319 J=1,NDP,4
      TINTRV(I)=TAPPV(J)
      TINTRH(I)=TAPPH(J)
      I=I+1
  319 CONTINUE
      TINTRV(I)=TAPPV(1)
      TINTRH(I)=TAPPH(1)
      DO 110 J=1,65
      ANG(J)=4.*DEL*(J-1)
  110 CONTINUE
      CALL SPLINA (ANG,TINTRV,65)
      DO 111 J=1,NDP
      ANGLE=DEL*(J-1)
      CALL TERPA (ANGLE,YY)
      TAPPV(J)=YY
  111 CONTINUE
      CALL SPLINA (ANG,TINTRH,65)
      DO 112 J=1,NDP
      ANGLE=DEL*(J-1)
      CALL TERPA (ANGLE,YY)
      TAPPH(J)=YY
  112 CONTINUE
      GO TO 1333
 1302 CONTINUE
      IF (INDATA.EQ.3) GO TO 1303
      GO TO 1304
 1303 CONTINUE
      I=1
      DO 9 J=1,NDP,4
      TINTRV(I)=TAPPV(J)
      TINTRH(I)=TAPPH(J)
      I=I+1
    9 CONTINUE
      TINTRV(I)=TAPPV(1)
      TINTRH(I)=TAPPH(1)
      DO 14 J=1,64
      II=(J-1)*4.+1.001
      TAPPV(II)=TINTRV(J)
      TAPPH(II)=TINTRH(J)
      II=II+1
```

```
      TAPPV(II)=.75*TINTRV(J)+.25*TINTRV(J+1)
      TAPPH(II)=.75*TINTRH(J)+.25*TINTRH(J+1)
      II=II+1
      TAPPV(II)=.50*TINTRV(J)+.50*TINTRV(J+1)
      TAPPH(II)=.50*TINTRH(J)+.50*TINTRH(J+1)
      II=II+1
      TAPPV(II)=.25*TINTRV(J)+.75*TINTRV(J+1)
      TAPPH(II)=.25*TINTRH(J)+.75*TINTRH(J+1)
   14 CONTINUE
      GO TO 1333
 1304 CONTINUE
      IF (INDATA.EQ.4) GO TO 1305
      GO TO 1306
 1305 CONTINUE
       SSSSS=278.
      DO 10 J=1,NDP
      ANG(J)=DEL*(J-1)
      DY(J)=1.
   10 CONTINUE
      CALL ICSSGU (ANG,TAPPV,DY,SSSSS,NDP,A,B,C,D,WK)
      DO 11 J=1,NDP
      TAPPV(J)=A(J+1)
   11 CONTINUE
      CALL ICSSGU(ANG,TAPPH,DY,SSSSS,NDP,A,B,C,D,WK)
      DO 12 J=1,NDP
      TAPPH(J)=A(J+1)
   12 CONTINUE
      GO TO 1333
 1306 CONTINUE
      IF (INDATA.EQ.5) GO TO 1307
      GO TO 1333
 1307 CONTINUE
      SSSSS=278.
      I=1
      DO 209 J=1,NDP,4
      TINTRV(I)=TAPPV(J)
      TINTRH(I)=TAPPH(J)
      I=I+1
  209 CONTINUE
      TINTRV(I)=TAPPV(1)
      TINTRH(I)=TAPPH(1)
      DO 210 J=1,NDP
      ANG(J)=4.*DEL*(J-1)
      DY(J)=1.
  210 CONTINUE
      CALL ICSSGU (ANG,TINTRV,DY,SSSSS,65,A,B,C,D,WK)
      DO 211 I=1,64
      DO 211 II=1,4
      III=4*(I-1)+II
      H=(II-1)*DEL
      TAPPV(III)=((D(I+1)*H+C(I+1))*H+B(I+1))*H+A(I+1)
  211 CONTINUE
      CALL ICSSGU (ANG,TINTRH,DY,SSSSS,65,A,B,C,D,WK)
      DO 212 I=1,64
      DO 212 II=1,4
      III=4*(I-1)+II
      H=(II-1)*DEL
      TAPPH(III)=((D(I+1)*H+C(I+1))*H+B(I+1))*H+A(I+1)
  212 CONTINUE
 1333 CONTINUE
      IF(LSTATE.EQ.5)
     1 CALL NEWSKY (NPHI1,NPHI2,TAESV,TAESH,TK,TE,RHO,FFF..
      IF (LSTATE.EQ.6)
     1 CALL EARSKY (NPHI1,NPHI2,TAESV,TAESH,TBBV,TBBH,LSTATE,FFFF,RHO)
      IF (LSTATE.EQ.7)
     1 CALL TBEART (TBBV,TBBH,PERHP,PERHC,PERVP,PERVC)
      IF (LSTATE.EQ.7)
     1 CALL EARSKY (NPHI1,NPHI2,TAESV,TAESH,TBBV,TBBH,LSTATE,FFFF,RHO)
C
C     THIS LOOP SUBTRACTS THE EARTH AND SKY CONTRIBUTIONS FROM THE MEASUREMENTS.
C
      DO 134 J=1,NDP
      TAPPV(J)=TAPPV(J)-TAESV(J)
      TAPPH(J)=TAPPH(J)-TAESH(J)
      TAMV(J)=TAPPV(J)
      TAMH(J)=TAPPH(J)
```

```
  134 CONTINUE
      DO 109 N=1,NREST
      CALL WATER (NPHI1,NPHI2,TAWV,TAWH,LSTATE,FFFF,RHC)
C
C     THIS LOOP RESTORES THE WATER CONTRIBUTION OF THE ANTENNA TEMPERATURES TO
C     YIELD THE HORIZONTAL AND VERTICAL WATER BRIGHTNESS TEMPERATURES TBRESH
C     AND TBRESV.
C
      DO 7 J=1,NDP
      TAV(J)=TAWV(J)
      TAH(J)=TAWH(J)
      ERRV(J)=TAMV(J)-TAV(J)
      ERRH(J)=TAMH(J)-TAH(J)
C     TAPPV(J)=TAPPV(J)+ERRV(J)
C     TAPPH(J)=TAPPH(J)+ERRH(J)
C     TAPPH(J)=TAPPH(J)+ERRH(J)*PERHP(J)+ERRV(J)*PERHC(J)
C     TAPPV(J)=TAPPV(J)+ERRV(J)*PERVP(J)+ERRH(J)*PERVC(J)
      TAPPH(J)=TAPPH(J)+ERRH(J)*PERHP(J)+ERRV(J)*PERHC(J)
      TAPPV(J)=TAPPV(J)+ERRV(J)*PERVP(J)+ERRH(J)*PERVC(J)
      TBRESH(J)=TAPPH(J)
      TBRESV(J)=TAPPV(J)
    7 CONTINUE
  109 CONTINUE
      ALPOL=ALPD
      NRRP=NRRP+1
      RETURN
      END
```

```
      SUBROUTINE PERCEN (NPHI1,NPHI2,FFFF,PERHP,PERHC,PERVP,PERVC,
     1 LSTATE,RHO)
C
C     THE ANTENNA TEMPERATURE FOR ANY ALPHA AND BETA WILL BE COMPOSED OF
C     CONTRIBUTIONS FROM BOTH THE HORIZONTAL AND THE VERTICAL BRIGHTNESS
C     TEMPERATURES. IN ORDER TO INVERT THE MEASUREMENTS ONE MUST KNOW WHAT
C     PERCENTAGE OF THE ANTENNA TEMPERATURE OF THE WATER CAME FROM THE HORIZONTAL
C     POLARIZATION AND WHAT PERCENTAGE FROM THE VERTICAL. THESE PERCENTAGES FOR
C     ALL SCAN ANGLES (BETA) AND FOR THE ALPHA REQUESTED ARE THE RESULTS OF THIS
C     SUBROUTINE.
C         PERHP=FRACTIONAL CONTRIBUTION OF TBH TO TAWH
C         PERHC=FRACTIONAL CONTRIBUTION OF TBV TO TAWH
C         PERVP-FRACTIONAL CONTRIBUTION OF TBV TO TAWV
C         PERVC=FRACTIONAL CONTRIBUTION OF TBH TO TAWV
C
      COMMON/B1/TAPPV,TAPPH,STHE,NDT,NDP,DEL,DELTHE,ALP
     1   ,PRINCF,CROSSF,THEDIS,WF
      COMMON/BLOC1/T1HP,T1HC,T1VP,T1VC,ST1HP,ST1HC,T1VCRO,T1HCRO
      COMMON/BLOC2/S,M,INV
      COMMON/B6/GTHEH,GPHIH,GTHEV,GPHIV,GCROH,GCROV
      COMPLEX T1VCRO(256),T1HCRO(256)
      COMPLEX ST1HP(256),ST1HC(256),ST1VP(256),ST1VC(256),CMPLX,CP
      COMPLEX T1HP(256),T1HC(256),T1VP(256),T1VC(256)
      COMPLEX GTHEH(256),GPHIH(256),GTHEV(256);GPHIV(256)
      COMPLEX GCROH(256),GCROV(256)
      DIMENSION PERHP(256),PERHC(256),PERVP(256),PERVC
      DIMENSION T1H(256),T1V(256)
      DIMENSION INV(128),S(128),M(3)
      DIMENSION TAPPV(256),TAPPH(256),STHE(65)
      DIMENSION THEDIS(32),WF(32)
      PI=3.14159
      RAD=PI/180.
      NALP=ALP/DEL+.5
      NDP2=NDP/2+.001
      NDP4=NDP/4+.001
      NDP21=NDP2+1
      NDP41=NDP4+1
      N1=NDP21+NPHI1
      N2=NDP21-NPHI2
      CP=CMPLX(1.,0.)
      CALP=COS(ALP)
      DO 3 J=1,NDP
      T1H(J)=1.0
      T1V(J)=1.0
      ST1HP(J)=CMPLX(0.,0.)
      ST1HC(J)=CMPLX(0.,0.)
      ST1VP(J)=CMPLX(0.,0.)
      ST1VC(J)=CMPLX(0.,0.)
      CONTINUE
      DO 10 I=1,NDT
      READ(1) (GTHEH(J),J=1,NDP)
      READ(1) (GPHIH(J),J=1,NDP)
      READ(1) (GTHEV(J),J=1,NDP)
      READ(1) (GPHIV(J),J=1,NDP)
      READ(1) (GCROH(J),J=1,NDP)
      READ(1) (GCROV(J),J=1,NDP)
      DO 13 J=1,NDP
      T1HP(J)=CMPLX(0.,0.)
      T1HC(J)=CMPLX(0.,0.)
      T1VP(J)=CMPLX(0.,0.)
      T1VC(J)=CMPLX(0.,0.)
      T1VCRO(J)=CMPLX(0.,0.)
      T1HCRO(J)=CMPLX(0.,0.)
   13 CONTINUE
      DO 4 J=N2,N1
      PHI=FLOAT(IABS(J-NDP21+NALP))*DEL+.0001
      THE=PI-THEDIS(I)
      TPHI=TAN(PHI)
      THEEW=ATAN(FFFF/(RHO*CALP*SQRT(1.+TPHI*TPHI)))
      THEEW=THEEW+PI/2.
      STHI=SIN(THE)
      CTHE=COS(THE)
      SPHI=SIN(PHI)
      FNOW=SPHI*SPHI/(STHI*STHI*SPHI*SPHI+CTHE*CTHE)
      GAMMA=ARSIN((SIN(PHI)*SIN(PHI)*SIN(THE)+COS(THE)*
     1   /SQRT(SIN(PHI)*SIN(PHI)+COTAN(THE)*COTAN(THE)))
```

```
      NGAMMA=GAMMA/DEL+.5
      NGAMMA=NDP21-NALP+NGAMMA
      IF(THE.GT.THEFW) GO TO 5
      T1HP(J)=T1H(NGAMMA)*FNOW*CR
      T1HC(J)=T1H(NGAMMA)*(1.-FNOW)*CR
      T1VP(J)=T1V(NGAMMA)*FNOW*CR
      T1VC(J)=T1V(NGAMMA)*(1.-FNOW)*CR
      T1VCRO(J)=2.*T1V(NGAMMA)*SQRT(FNOW*(1.-FNOW))*CR
      T1HCRO(J)=2.*T1H(NGAMMA)*SQRT(FNOW*(1.-FNOW))*CR
    5 CONTINUE
    4 CONTINUE
      CALL HARM (T1HP,M,INV,S,1,IFERR)
      CALL HARM (T1HC,M,INV,S,1,IFERR)
      CALL HARM (T1VP,M,INV,S,1,IFERR)
      CALL HARM (T1VC,M,INV,S,1,IFERR)
      CALL HARM(T1HCRO,M,INV,S,2,IFERR)
      CALL HARM(T1VCRO,M,INV,S,2,IFERR)
      DO 12 J=1,NDP
      ST1HP(J)=ST1HP(J)+(T1HP(J)*GTHEH(J)   +T1HC(J)*GPHIH(J)
     1 -T1HCRO(J)*GCROH(J)    )
     1 *STHE(I)
      ST1HC(J)=ST1HC(J)+(T1VP(J)*GPHIH(J)   +T1VC(J)*GTHEH(J)
     1 +T1VCRO(J)*GCROH(J)    )
     1 *STHE(I)
      ST1VP(J)=ST1VP(J)+(T1VP(J)*GPHIV(J)   +T1VC(J)*GTHEV(J)
     1 -T1VCRO(J)*GCROV(J)    )
     1 *STHE(I)
      ST1VC(J)=ST1VC(J)+(T1HP(J)*GTHEV(J)   +T1HC(J)*GPHIV(J)
     1 +T1HCRO(J)*GCROV(J)    )
     1 *STHE(I)
   12 CONTINUE
   10 CONTINUE
      REWIND 1
      CALL HARM (ST1HP,M,INV,S,-2,IFERR)
      CALL HARM (ST1HC,M,INV,S,-2,IFERR)
      CALL HARM (ST1VP,M,INV,S,-2,IFERR)
      CALL HARM (ST1VC,M,INV,S,-2,IFERR)
      WRITE(6,100)
  100 FORMAT(' ','PERHP,PERHC,PERVP,PERVC,INDEX')
  200 FORMAT(' ',4F13.6,I5)
      DO 11 J=1,NDP
      DENHOR=REAL(ST1HP(J)+ST1HC(J))
      DENVER=REAL(ST1VP(J)+ST1VC(J))
      PERHP(J)=(REAL(ST1HP(J)))/DENHOR
      PERHC(J)=(REAL(ST1HC(J)))/DENHOR
      PERVP(J)=(REAL(ST1VP(J)))/DENVER
      PERVC(J)=(REAL(ST1VC(J)))/DENVER
      PX1=PERHP(J)
      PX2=PERHC(J)
      PX3=PERVP(J)
      PX4=PERVC(J)
      PERHP(J)=PX1*PRINCF+PX2*CROSSF
      PERHC(J)=PX2*PRINCF+PX1*CROSSF
      PERVP(J)=PX3*PRINCF+PX4*CROSSF
      PERVC(J)=PX4*PRINCF+PX3*CROSSF
   11 CONTINUE
C     DO 6 J=1,256
C     WRITE(6,200) PERHP(J),PERHC(J),PERVP(J),PERVC(J),J
C   6 CONTINUE
      RETURN
      END
```

```
      SUBROUTINE WATER(NPHI1,NPHI2,TAWV,TAWH,LSTATE,FFFF,RHO)
C
C     THIS SUBROUTINE CALCULATES THE ANTENNA TEMPERATURE CONTRIBUTION FROM THE
C     WATER AS A FUNCTION OF BETA FOR EACH POLARIZATION USING AN ESTIMATE OF
C     THE BRIGHTNESS TEMPERATURE.
C         TAWV=VERTICAL WATER ANTENNA TEMPERATURE CONTRIBUTION
C         TAWH=HORIZONTAL WATER ANTENNA TEMPERATURE CONTRIBUTION
C
      COMMON/B1/TAPPV,TAPPH,STHE,NDT,NDP,DEL,DELTHE,ALP
     1  ,PRINCF,CROSSF,THEDIS,WF
      COMMON/BLOC1/TBHP,TBHC,TBVP,TBVC,STAWH,STAWV,T1VCPO,T1HCRO
      COMMON/BLOC2/S,M,INV
      COMMON/B6/GTHEH,GPHIH,GTHEV,GPHIV,GCROH,GCPOV
      COMPLEX T1VCPO(256),T1HCPO(256)
      COMPLEX GTHEH(256),GPHIH(256),GTHEV(256),GPHIV(256)
      COMPLEX GCPOH(256),GCPOV(256)
      COMPLEX TBHP(256),TBHC(256),TBVP(256),TBVC(256)
      COMPLEX STAWH(256),STAWV(256),CMPLX,CR
      DIMENSION TBWH(256),TBWV(256),TAWV(256),TAWH(256)
      DIMENSION INV(128),S(128),M(3)
      DIMENSION TAPPV(256),TAPPH(256),STHE(65)
      DIMENSION THEDIS(32),WF(32)
      PI=3.14159
      RAD=PI/180.
      NALP=ALP/DEL+.5
      NDP2=NDP/2+.001
      NDP4=NDP/4+.001
      NDP21=NDP2+1
      NDP41=NDP4+1
      N1=NDP21+NPHI1
      N2=NDP21-NPHI2
      CR=CMPLX(1.,0.)
      CALP=COS(ALP)
      DO 3 J=1,NDP
      TBWH(J)=TAPPH(J)
      TBWV(J)=TAPPV(J)
      IF((J.LT.NDP21 -NPHI2).OR.(J.GT.NDP21+NPHI1)) GO TO 1
      GO TO 2
    1 TBWH(J)=0.0
      TBWV(J)=0.0
    2 CONTINUE
      STAWH(J) =CMPLX(0.,0.)
      STAWV(J) =CMPLX(0.,0.)
    3 CONTINUE
      DO 10 I=1,NDT
      READ(1) (GTHEH(J),J=1,NDP)
      READ(1) (GPHIH(J),J=1,NDP)
      READ(1) (GTHEV(J),J=1,NDP)
      READ(1) (GPHIV(J),J=1,NDP)
      READ(1) (GCPOH(J),J=1,NDP)
      READ(1) (GCPOV(J),J=1,NDP)
      DO 13 J=1,NDP
      TBHP(J)  =CMPLX(0.,0.)
      TBHC(J)  =CMPLX(0.,0.)
      TBVP(J)  =CMPLX(0.,0.)
      TBVC(J)  =CMPLX(0.,0.)
      T1VCPO(J)=CMPLX(0.,0.)
      T1HCPO(J)=CMPLX(0.,0.)
   13 CONTINUE
      DO 4 J=N2,N1
      THE=PI-THEDIS(I)
      PHI=FLOAT(IABS(J-NDP21+NALP))*DEL+.0001
      TPHI=TAN(PHI)
      THEFW=ATAN(FFFF/(RHO*CALP*SQRT(1.+TPHI*TPHI)))
      THEFW=THEFW+PI/2.
      STHI=SIN(THE)
      CTHE=COS(THE)
      SPHI=SIN(PHI)
      ENOW=SPHI*SPHI/(STHI*STHI*SPHI*SPHI+CTHE*CTHE)
      T2PHI=TAN(PHI)*TAN(PHI)
      CT2THE=1./(TAN(THE)*TAN(THE) )
      GAMMA=ATAN(SQRT(T2PHI+CT2THE+CT2THE*T2PHI))
      GAMMA=GAMMA/DEL
      NGAMMA=GAMMA
      DELGAM=GAMMA-NGAMMA
      NGAMMA=NDP21-NALP+NGAMMA
```

```
      TBH=TBWH(NGAMMA)+DELGAM*(TBWH(NGAMMA+1)-TBWH(NGAMMA))
      TBV=TBWV(NGAMMA)+DELGAM*(TBWV(NGAMMA+1)-TBWV(NGAMMA))
      IF(NGAMMA.GE.N1) TBH=TBWH(N1)
      IF(NGAMMA.GE.N1) TBV=TBWV(N1)
      IF(THE.GT.THEEW) TBH=0.0
      IF(THE.GT.THEEW) TBV=0.0
      TBHP(J)=TBH*FNOW*CR
      TBHC(J)=TBH*(1.-FNOW)*CR
      TBVP(J)=TBV*FNOW*CR
      TBVC(J)=TBV*(1.-FNOW) *CR
      T1HCRO(J)=2.*TBH*SQRT(FNOW*(1.-FNOW))*CR
      T1VCRO(J)=2.*TBV*SORT(FNOW*(1.-FNOW))*CR
    5 CONTINUE
    4 CONTINUE
      CALL HARM (TBHP,M,INV,S,1,IFERR)
      CALL HARM (TBHC,M,INV,S,2,IFERR)
      CALL HARM (TBVP,M,INV,S,2,IFERR)
      CALL HARM (TBVC,M,INV,S,2,IFERR)
      CALL HARM(T1VCRO,M,INV,S,2,IFERR)
      CALL HARM(T1HCRO,M,INV,S,2,IFERR)
      DO 12 J=1,NDP
      STAWH(J)=STAWH(J)+(TBHP(J)*GTHEH(J)+TBHC(J)*GPHIH(J)+TBVC(J)
     1 *GTHEH(J)+TBVP(J)*GPHIH(J)-T1HCRO(J)*GCROH(J)+T1VCRO(J)*GCROH(J))
     1 *STHE(I)
      STAWV(J)=STAWV(J)+(TBVC(J)*GTHEV(J)+TBVP(J)*GPHIV(J)+TBHP(J)
     1 *GTHEV(J)+TBHC(J)*GPHIV(J)+T1HCRO(J)*GCROV(J)-T1VCRO(J)*GCROV(J))
     1 *STHE(I)
   12 CONTINUE
   10 CONTINUE
      REWIND 1
      CALL HARM (STAWH,M,INV,S,-2,IFERR)
      CALL HARM (STAWV,M,INV,S,-2,IFERR)
      DO 11 J=1,NDP
      TAWV(J)=REAL(STAWV(J))
      TAWH(J)=REAL(STAWH(J))
      TX1=TAWV(J)
      TX2=TAWH(J)
      TAWV(J)=TX1*PPINCF+TX2*CROSSF
      TAWH(J)=TX2*PPINCF+TX1*CROSSF
   11 CONTINUE
      RETURN
      END
```

```
      SUBROUTINE NEWSKY (NPHI1,NPHI2,TAESV,TAESH,TK,TE,RHO,EFFF)
C
C     THIS SUBROUTINE CALCULATES THE ANTENNA TEMPERATURE CONTRIBUTIONS FROM THE
C     EARTH AND SKY USING PEAKE'S MODEL FOR THE SKY BRIGHTNESS TEMPERATURE
C     AND TE AS THE EARTH BRIGHTNESS TEMPERATURE.
C          TAESV=THE VERTICAL ANTENNA TEMPERATURE CONTRIBUTION FROM THE EARTH
C                AND SKY
C          TAESH=THE HORIZONTAL ANTENNA TEMPERATURE CONTRIBUTION FROM THE EARTH
C                AND SKY
C
      COMMON/B1/TAPPV,TAPPH,STHE,NDT,NDP,DEL,DELTHE,ALP
     1 ,PRINCF,CROSSF,THEDIS,WF
      COMMON/BLOC1/TBES,TB,STAESH,STAESV,AAA1
      COMMON/BLOC2/S,M,INV
      COMMON/B6/GTHEH,GPHIH,GTHEV,GPHIV,GCROH,GCROV
      COMPLEX GTHEH(256),GPHIH(256),GTHEV(256),GPHIV(256)
      COMPLEX GCROH(256),GCROV(256),TBEXT(256)
      COMPLEX TBES(256),CMPLX,CR,TB(256),STAESH(256),STAESV(256),
     1 AAA1(4,256)
      DIMENSION INV(128),S(128),M(3)
      DIMENSION TAESV(256),TAESH(256)
      DIMENSION TAPPV(256),TAPPH(256),STHE(65)
      DIMENSION THEDIS(32),WF(32)
      PI=3.14159
      NALP=ALP/DEL+.5
      CALP=COS(ALP)
      NDP4=NDP/4.+.001
      NDPM4=NDP-NDP4+1
      NDP21=NDP/2+1.001
      NDP41=NDP/4.+1.001
      N1=NDP21+NPHI1
      N2=NDP21-NPHI2
      CR=CMPLX(1.,0.)
      DO 3 J=1,NDP
      TB(J)=CMPLX(TE,0.0)
      TBES(J)=CMPLX(0.,0.)
      STAESV(J)=CMPLX(0.,0.)
      STAESH(J)=CMPLX(0.,0.)
    3 CONTINUE
C
C     TG IS THE GALACTIC BRIGHTNESS TEMPERATURE.
C
      TG=3.
      TEFF=1.12*TK-50.
      PTO=3./TEFF
      TAUO=-ALOG(1.-PTO)
      DO 4 J=1,NDP41
      CTI=COS(DEL*(J-1))
      IF (CTI.LT.0.000001) GO TO 22
      IF(J.EQ.NDP41) GO TO 22
      GO TO 33
   22 TB(J)=TEFF*CP
      GO TO 44
   33 CONTINUE
      SECTHP=1./CTI
      TB(J)=(TEFF*(1.-EXP(-TAUO*SECTHP))+TG*EXP(-TAUO*SECTHP))*CP
   44 CONTINUE
      IF(J.EQ.1) GO TO 55
      TB(NDP+2-J)=TB(J)
   55 CONTINUE
    4 CONTINUE
      IF(NALP.EQ.0) GO TO 21
      DO 13 J=1,NDP
      TBEXT(J)=TB(J)
   13 CONTINUE
      NALP1=NALP+1
      DO 14 J=NALP1,NDP
      TB(J-NALP)=TBEXT(J)
   14 CONTINUE
      DO 15 J=1,NALP
      TB(NDP-NALP+J)=TBEXT(J)
   15 CONTINUE
   21 CONTINUE
      DO 10 I=1,NDT
      THE=PI-THEDIS(I)
      READ(1) (GTHEH(J),J=1,NDP)
```

```
      READ(1) (GPHIH(J),J=1,NDP)
      READ(1) (GTHEV(J),J=1,NDP)
      READ(1) (GPHIV(J),J=1,NDP)
      READ(1) (GCROH(J),J=1,NDP)
      READ(1) (GCROV(J),J=1,NDP)
      DO 12 J=1,NDP
      PHI=FLOAT(IABS(J-NDP2I+NALP))*DEL+.0001
      TPHI=TAN(PHI)
      THEEW=ATAN(FEFF/(RHO*CALP*SQRT(1.+TPHI*TPHI)))
      THEFW=THEFW+PI/2.
      TBES(J)=TB(J)
      IF((J.GE.N2).AND.(J.LE.N1).AND.(THE.LT.THEEW))
     1   TBES(J)=CMPLX(0.,0.)
   12 CONTINUE
      CALL HARM(TBES,M,INV,S,2,IFERR)
      DO 10 J=1,NDP
      STAESH(J)=STAFSH(J)+(TBES(J) *(GTHEH(J)+GPHIH(J)))*STHE(I)
      STAESV(J)=STAFSV(J)+(TBES(J) *(GTHEV(J)+GPHIV(J)))*STHE(I)
   10 CONTINUE
      REWIND 1
      CALL HARM (STAESH,M,INV,S,-2,IFERR)
      CALL HARM (STAESV,M,INV,S,-2,IFERR)
      DO 11 J=1,NDP
      TAESH(J)=REAL(STAESH(J))
      TAESV(J)=REAL(STAESV(J))
      TX1=TAESH(J)
      TX2=TAFSV(J)
      TAESH(J)=TX1*PRINCF+TX2*CROSSF
      TAESV(J)=TX2*PRINCF+TX1*CROSSF
   11 CONTINUE
      RETURN
      END
```

```
      SUBROUTINE TBEART(TBBV,TBBH,PERHP,PERHC,PERVP,PERVC)
C
C     THIS SUBROUTINE TAKES THE MEASURED ANTENNA TEMPERATURES AND RESTORES THEM
C     FOUR TIMES. THIS IS DONE TO OBTAIN A BETTER APPROXIMATION OF THE BRIGHTNESS
C     TEMPERATURES OF THE EARTH AND SKY TO BE USED IN SUBROUTINE EARSKY.
C          TBBV=THE RESTORED VERTICAL MEASUREMENTS
C          TBBH=THE RESTORED HORIZONTAL MEASUREMENTS
C
      COMMON/B1/TAPPV,TAPPH,STHE,NDT,NDP,DEL,DELTHE,ALP
     1 ,PRINCF,CROSSF,THEDIS,WF
      COMMON/BLOC1/TBESH,TBESV,STAESH,STAESV,AAA1,ERRV,ERRH
      COMMON/BLOC2/S,M,INV
      COMMON/B6/GTHEH,GPHIH,GTHEV,GPHIV,GCROH,GCROV
      DIMENSION TBBV(256),TBBH(256),PERHP(256),PERHC(256),PERVP(256)
     1 ,PERVC(256)
      COMPLEX GTHEH(256),GPHIH(256),GTHEV(256),GPHIV(256)
      COMPLEX GCROH(256),GCROV(256)
      COMPLEX TBESH(256),CMPLX,CR,TBESV(256),STAESH(256),STAESV(256),
     1 AAA1(4,256)
      DIMENSION INV(128),S(128),M(3)
      DIMENSION TAESV(256),TAESH(256),ERRV(256),ERRH(256)
      DIMENSION TAPPV(256),TAPPH(256),STHE(65)
      DIMENSION THEDIS(32),WF(32)
      DO 3 J=1,NDP
      TBBV(J)=TAPPV(J)
      TBBH(J)=TAPPH(J)
      TBESH(J)=CMPLX(TAPPH(J),0.0)
      TBESV(J)=CMPLX(TAPPV(J),0.0)
      STAESH(J)=CMPLX(0.0,0.0)
      STAESV(J)=CMPLX(0.0,0.0)
    3 CONTINUE
      DO 12 II=1,4
      CALL HARM (TBESH,M,INV,S,2,IFERR)
      CALL HARM (TBESV,M,INV,S,2,IFERR)
      DO 10 I=1,NDT
      READ(1) (GTHEH(J),J=1,NDP)
      READ(1) (GPHIH(J),J=1,NDP)
      READ(1) (GTHEV(J),J=1,NDP)
      READ(1) (GPHIV(J),J=1,NDP)
      READ(1) (GCROH(J),J=1,NDP)
      READ(1) (GCROV(J),J=1,NDP)
      DO 10 J=1,NDP
      STAESH(J)=STAESH(J)+(TBESH(J)*(GTHEH(J)+GPHIH(J)))*STHE(I)
      STAESV(J)=STAESV(J)+(TBESV(J)*(GTHEV(J)+GPHIV(J)))*STHE(I)
   10 CONTINUE
      REWIND 1
      CALL HARM (STAESH,M,INV,S,-2,IFERR)
      CALL HARM (STAESV,M,INV,S,-2,IFERR)
      DO 11 J=1,NDP
      TAESH(J)=REAL(STAESH(J))
      TAESV(J)=REAL(STAESV(J))
      TX1=TAESH(J)
      TX2=TAESV(J)
      TAESH(J)=TX1*PRINCF+TX2*CROSSF
      TAESV(J)=TX2*PRINCF+TX1*CROSSF
      ERRV(J)=TAPPV(J)-TAESV(J)
      ERRH(J)=TAPPH(J)-TAESH(J)
      TBBH(J)=TBBH(J)+ERRH(J)*PERHP(J)+ERRV(J)*PERHC(J)
      TBBV(J)=TBBV(J)+ERRV(J)*PERVP(J)+ERRH(J)*PERVC(J)
      TBESH(J)=CMPLX(TBBH(J),0.0)
      TBESV(J)=CMPLX(TBBV(J),0.0)
   11 CONTINUE
   12 CONTINUE
      RETURN
      END
```

```
      SUBROUTINE EARSKY (NPHI1,NPHI2,TAESV,TAESH,TBBV,TBBH,LSTATE,FFFF,
     1 RHO)
C
C     THIS SUBROUTINE CALCULATES THE ANTENNA TEMPERATURE CONTRIBUTION DUE TO THE
C     EARTH AND SKY FOR BOTH POLARIZATIONS. IF LSTATE=6, THE MEARURED ANTENNA
C     TEMPERATURES ARE USED AS THE BRIGHTNESS TEMPERATURES OF THE EARTH AND SKY.
C     IF LSTATE=7, THE RESULTS OF SUBROUTINE TBEART ARE USED AS THE BRIGHTNESS
C     TEMPERATURES.
C
C         TAESV=THE VERTICAL ANTENNA TEMPERATURE CONTRIBUTION FROM THE EARTH
C               AND SKY
C         TAESH=THE HORIZONTAL ANTENNA TEMPERATURE CONTRIBUTION FROM THE EARTH
C               AND SKY
C
      COMMON/B1/TAPPV,TAPPH,STHE,NDT,NDP,DEL,DELTHE,ALP
     1 ,PRINCE,CROSSE,THEDIS,WF
      COMMON/BLOC1/TBESH,TBESV,STAESH,STAESV,AAA1
      COMMON/BLOC2/S,M,INV
      COMMON/B6/GTHEH,GPHIH,GTHEV,GPHIV,GCROH,GCROV
      COMPLEX GTHEH(256),GPHIH(256),GTHEV(256),GPHIV(256)
      COMPLEX GCROH(256),GCROV(256)
      COMPLEX TBESH(256),CMPLX,CR,TBESV(256),STAESH(256),STAESV(256),
     1 AAA1(4,256)
      DIMENSION TBBH(256),TBBV(256),TBBBH(256),TBBBV(256)
      DIMENSION INV(128),S(128),M(3)
      DIMENSION TAESV(256),TAESH(256)
      DIMENSION TAPPV(256),TAPPH(256),STHE(65)
      DIMENSION THEDIS(32),WF(32)
      NALP=ALP/DEL+.5
      NDP21=NDP/2+1.001
      N1=NDP21+NPHI1
      N2=NDP21-NPHI2
      CALP=COS(ALP)
      PI=3.14159
      CR=CMPLX(1.,0.)
      IF (LSTATE.EQ.7) GO TO 1
      DO 2 J=1,NDP
      TBBBH(J)=TAPPH(J)
      TBBBV(J)=TAPPV(J)
      CONTINUE
      GO TO 4
      CONTINUE
      DO 5 J=1,NDP
      TBBBH(J)=TBBH(J)
      TBBBV(J)=TBBV(J)
      CONTINUE
      CONTINUE
      DO 3 J=1,NDP
      STAESH(J)=CMPLX(0.,0.)
      STAESV(J)=CMPLX(0.,0.)
      CONTINUE
      DO 10 I=1,NDT
      READ(1) (GTHEH(J),J=1,NDP)
      READ(1) (GPHIH(J),J=1,NDP)
      READ(1) (GTHEV(J),J=1,NDP)
      READ(1) (GPHIV(J),J=1,NDP)
      READ(1) (GCROH(J),J=1,NDP)
      READ(1) (GCROV(J),J=1,NDP)
      THE=PI-THEDIS(I)
      DO 20 J=1,NDP
      PHI=FLOAT(IABS(J-NDP21+NALP))*DEL+.0001
      TPHI=TAN(PHI)
      THEEW=ATAN(FFFF/(RHO*CALP*SQRT(1.+TPHI*TPHI)))
      THEEW=THEEW+PI/2.
      TBESH(J)=CMPLX(TBBBH(J),0.0)
      TBESV(J)=CMPLX(TBBBV(J),0.0)
      IF((J.LE.NDP21).AND.(J.GT.N2-3)) GO TO 31
      GO TO 32
   31 TBESH(J)=CMPLX(TBBBH(N2-3),0.0)
      TBESV(J)=CMPLX(TBBBV(N2-3),0.0)
   32 CONTINUE
      IF((J.GT.NDP21).AND.(J.LT.N1+3)) GO TO 33
      GO TO 34
   33 TBESH(J)=CMPLX(TBBBH(N1+3),0.0)
      TBESV(J)=CMPLX(TBBBV(N1+3),0.0)
   34 CONTINUE
```

```
      IF((J.GE.N2).AND.(J.LE.N1).AND.(THE.LT.THEEW)) GO TO 35
      GO TO 36
 35   TBESH(J)=CMPLX(0.,0.)
      TBESV(J)=CMPLX(0.,0.)
 36   CONTINUE
 20   CONTINUE
      CALL  HARM (TBESH,M,INV,S,2,IFERR)
      CALL  HARM (TBESV,M,INV,S,2,IFERR)
      DO 30 J=1,NDP
      STAESH(J)=STAESH(J)+(TBESH(J)*(GTHEH(J)+GPHIH(J)))*STHE(I)
      STAESV(J)=STAESV(J)+(TBESV(J)*(GTHEV(J)+GPHIV(J)))*STHE(I)
 30   CONTINUE
 10   CONTINUE
      REWIND 1
      CALL HARM (STAESH,M,INV,S,-2,IFERR)
      CALL HARM (STAESV,M,INV,S,-2,IFERR)
      DO 11 J=1,NDP
      TAESH(J)=REAL(STAESH(J))
      TAESV(J)=REAL(STAESV(J))
      TX1=TAESH(J)
      TX2=TAESV(J)
      TAESH(J)=TX1*PRINCF+TX2*CROSSF
      TAESV(J)=TX2*PRINCF+TX1*CROSSF
 11   CONTINUE
      RETURN
      END
```

```
      SUBROUTINE SPLINA(XI,YI,N)
CSUBROUTINE FOR INTERPOLATING ,DIFFERENTIATING AND
CINTEGRATING A SET OF DATA POINTS
CXI= INDEPENDENT VARIABLE OF INPUT DATA, IT MUST BE IN
CASCENDING ORDER
CYI=DEPENDENT VARIABLE OF INPUT DATA
CN=NUMBERS OF INPUT DATA
      DIMENSION W(300),Q(300),B(300),A(300),C(300),S(300),Z(300)
      DIMENSION XI(N),YI(N),X(300),Y(300)
       DATA A(1),C(1),Z(1)/-1.,0.0,C.0/
      DO 11 I=1,N
      X(I)=XI(I)
      Y(I)=YI(I)
   11 CONTINUE
      DO 1 J=2,N
       W(J)=X(J)-X(J-1)
1       CONTINUE
         NM=N-1
       DO 2 J=2,NM
       WJ=W(J)
       WP=W(              J+1),
       WS=WJ+WP
       QJ=WJ/WS
      Q(J)=QJ
       QA=1.-.5*QJ*A(J-1)
       A(J)=.5*(1.-QJ)/QA
       B(J)=3.*(WP*Y(J-1)-WS*Y(J)+WJ*Y(J+1))/WP/WJ/W
       C(J)=(B(J)-.5*QJ*C(J-1))/QA
2       CONTINUE
      S(N)=C(NM)/(1.+A(NM))
       S(NM)=S(N)
       NMM=N-2
       DO 3 JJ=1,NMM
      J=NMM-JJ+1
       S(J)=C(J)-A(J)*S(J+1)
3       CONTINUE
         DO 4 J=2,N
       Z(J)=Z(J-1)+.5*W(J)*(Y(J)+Y(J-1)-.0825*W(J)**2*(S(J)+S(J-1)))
4       CONTINUE
       RETURN
      ENTRY TERPA(XV,YV)
CINTERPOLATION-HUNT FOR SUBINTERVAL
      DO 7 JJ=2,N
      J=JJ
      IF (XV.GT.X(J)) GO TO7
      GO TO 8
    7 CONTINUE
CCALCULATE FUNCTION
    8 WJ=W(J)
      D1=(XV-X(J-1))/WJ
      D2=(X(J)-XV)/WJ
      D3=WJ*WJ/6.
       YV=D1*(Y(J)+D3*(D1*D1-1.)*S(J))
       YV=    YV+D2*(Y(J-1)+D3*(D2*D2-1.)*S(J-1)
       RETURN
       ENTRY DERIVA(XV,YV)
CDIFFERENTIATION-HUNT FOR SUBINTERVAL
      DO 5 JJ=2,N
      J=JJ
       IF(XV.GT.X(J)) GO TO 5
       GO TO 6
5       CONTINUE
CCALCULATE DERIVATIVE
6        WJ=W(J)
      D1=(XV-X(J-1))/WJ
       D2=(X(J)-XV)/WJ
       YV=(Y(J)-Y(J-1))/WJ+.5*WJ*((D1*D1-.3333333)*S(J)
     1-(D2*D2-.3333333)*S(J-1))
       RETURN
      ENTRY GEFATA(XV,YV)
CINTEGRATION-HUNT FOR SUBINTERVAL
      DO 9 JJ=2,N
      J=JJ
      IF (XV.GT.X(J)) GO TO 9
      GO TO 10
    9 CONTINUE
```

```
      CCALCULATE INOFFINITE INTERGRAL
   10 WJ=W(J)
        D1=((XV-X(J-1))/WJ)**2
        D2=((X(J)-XV)/WJ)**2
      D3=.0825*WJ*WJ
      YV=Z(J-1)+0.5*WJ*(D1*(Y(J)+D3*(D1-2.)*S(J))+(1.-D2)*(Y(J-1)
     1+D3*(D2-1.)*S(J-1)))
      RETURN
      END
```

```
      SUBROUTINE HARM (A,M,INV,S,IFSET,IFERR)
C
C     THIS PROGRAM CALCULATES THE FOURIER TRANSFORM OF THE SAMPLED FUNCTION A.
C
      DIMENSION A(512),INV(128),S(128),N(3),M(3),NP(3),W(2),W2(2),W3(2)
      EQUIVALENCE (N1,N(1)),(N2,N(2)),(N3,N(3))
   10 IF( IABS(IFSET) - 1) 900,900,12
   12 MTT=MAXO(M(1),M(2),M(3)) -2
      ROOT2=SQRT(2.0E0)
      IF (MTT-MT ) 14,14,13
   13 IFERR=1
      RETURN
   14 IFERR=0
      M1=M(1)
      M2=M(2)
      M3=M(3)
      N1=2**M1
      N2=2**M2
      N3=2**M3
   16 IF(IFSET) 18,18,20
   18 NX= N1*N2*N3
      FN = NX
      DO 19 I = 1,NX
      A(2*I-1) = A(2*I-1)/FN
   19 A(2*I) = -A(2*I)/FN
   20 NP(1)=N1*2
      NP(2)= NP(1)*N2
      NP(3)=NP(2)*N3
      DO 250 ID=1,3
      IL = NP(3)-NP(ID)
      IL1 = IL+1
      MI = M(ID)
      IF (MI)250,250,30
   30 IDIF=NP(ID)
      KBIT=NP(ID)
      MEV = 2*(MI/2)
      IF (MI - MEV )60,60,40
C
C     M IS ODD. DO L=1 CASE
   40 KBIT=KBIT/2
      KL=KBIT-2
      DO 50 I=1,IL1,IDIF
      KLAST=KL+I
      DO 50 K=I,KLAST,2
      KD=K+KBIT
C
C     DO ONE STEP WITH L=1,J=0
C     A(K)=A(K)+A(KD)
C     A(KD)=A(K)-A(KD)
C
      T=A(KD)
      A(KD)=A(K)-T
      A(K)=A(K)+T
      T=A(KD+1)
      A(KD+1)=A(K+1)-T
   50 A(K+1)=A(K+1)+T
      IF (MI - 1)250,250,52
C
   52 LFIRST =3
C     DEF - JLAST = 2**(L-2) -1
      JLAST=1
      GO TO 70
C
C     M IS EVEN
   60 LFIRST = 2
      JLAST=0
   70 DO 240 L=LFIRST,MI,2
      JJDIF=KBIT
      KBIT=KBIT/4
      KL=KBIT-2
C
C     DO FOR J=0
      DO 80 I=1,IL1,IDIF
      KLAST=I+KL
      DO 80 K=I,KLAST,2
      K1=K+KBIT
```

```
      K2=K1+KBIT
      K3=K2+KBIT
C
C     DO TWO STEPS WITH J=0
C     A(K)=A(K)+A(K2)
C     A(K2)=A(K)-A(K2)
C     A(K1)=A(K1)+A(K3)
C     A(K3)=A(K1)-A(K3)
C
C     A(K)=A(K)+A(K1)
C     A(K1)=A(K)-A(K1)
C     A(K2)=A(K2)+A(K3)*I
C     A(K3)=A(K2)-A(K3)*I
C
      T=A(K2)
      A(K2)=A(K)-T
      A(K)=A(K)+T
      T=A(K2+1)
      A(K2+1)=A(K+1)-T
      A(K+1)=A(K+1)+T
C
      T=A(K3)
      A(K3)=A(K1)-T
      A(K1)=A(K1)+T
      T=A(K3+1)
      A(K3+1)=A(K1+1)-T
      A(K1+1)=A(K1+1)+T
C
      T=A(K1)
      A(K1)=A(K)-T
      A(K)=A(K)+T
      T=A(K1+1)
      A(K1+1)=A(K+1)-T
      A(K+1)=A(K+1)+T
C
      R=-A(K3+1)
      T = A(K3)
      A(K3)=A(K2)-R
      A(K2)=A(K2)+R
      A(K3+1)=A(K2+1)-T
   80 A(K2+1)=A(K2+1)+T
      IF (JLAST) 235,235,82
   82 JJ=JJDIF    +1
C
C     DO FOR J=1
      ILAST= IL +JJ
      DO 85 I = JJ,ILAST,IDIF
      KLAST = KL+I
      DO 85 K=I,KLAST,2
      K1 = K+KBIT
      K2 = K1+KBIT
      K3 = K2+KBIT
C
C     LETTING W=(1+I)/ROOT2,W3=(-1+I)/ROOT2,W2=I,
C     A(K)=A(K)+A(K2)*I
C     A(K2)=A(K)-A(K2)*I
C     A(K1)=A(K1)*W+A(K3)*W3
C     A(K3)=A(K1)*W-A(K3)*W3
C
C     A(K)=A(K)+A(K1)
C     A(K1)=A(K)-A(K1)
C     A(K2)=A(K2)+A(K3)*I
C     A(K3)=A(K2)-A(K3)*I
C
      R =-A(K2+1)
      T = A(K2)
      A(K2) = A(K)-R
      A(K) = A(K)+R
      A(K2+1)=A(K+1)-T
      A(K+1)=A(K+1)+T
C
      AWR=A(K1)-A(K1+1)
      AWI = A(K1+1)+A(K1)
      R=-A(K3)-A(K3+1)
      T=A(K3)-A(K3+1)
      A(K3)=(AWR-R)/ROOT2
```

```
      A(K3+1)=(AWI-T)/ROOT2
      A(K1)=(AWP+R)/ROOT2
      A(K1+1)=(AWI+T)/ROOT2
      T= A(K1)
      A(K1)=A(K)-T
      A(K)=A(K)+T
      T=A(K1+1)
      A(K1+1)=A(K+1)-T
      A(K+1)=A(K+1)+T
      R=-A(K3+1)
      T=A(K3)
      A(K3)=A(K2)-R
      A(K2)=A(K2)+R
      A(K3+1)=A(K2+1)-T
   85 A(K2+1)=A(K2+1)+T
      IF(JLAST-1) 235,235,90
   90 JJ= JJ + JJDIF
C
C     NOW DO THE REMAINING J'S
      DO 230 J=2,JLAST
C
C     FETCH W'S
C     DEF- W=W**INV(J), W2=W**2, W3=W
   96 I=INV(J+1)
   98 IC=NT-I
      W(1)=S(IC)
      W(2)=S(I)
      I2=2*I
      I2C=NT-I2
      IF(I2C)120,110,100
C
C     2*I IS IN FIRST QUADRANT
  100 W2(1)=S(I2C)
      W2(2)=S(I2)
      GO TO 130
  110 W2(1)=0.
      W2(2)=1.
      GO TO 130
C
C     2*I IS IN SECOND QUADRANT
  120 I2CC = I2C+NT
      I2C=-I2C
      W2(1)=-S(I2C)
      W2(2)=S(I2CC)
  130 I3=I+I2
      I3C=NT-I3
      IF(I3C)160,150,140
C
C     I3 IN FIRST QUADRANT
  140 W3(1)=S(I3C)
      W3(2)=S(I3)
      GO TO 200
  150 W3(1)=0.
      W3(2)=1.
      GO TO 200
C
  160 I3CC=I3C+NT
      IF(I3CC)190,180,170
C
C     I3 IN SECOND QUADRANT
  170 I3C=-I3C
      W3(1)=-S(I3C)
      W3(2)=S(I3CC)
      GO TO 200
  180 W3(1)=-1.
      W3(2)=0.
      GO TO 200
C
C     3*I IN THIRD QUADRANT
  190 I3CCC=NT+I3CC
      I3CC = -I3CC
      W3(1)=-S(I3CCC)
      W3(2)=-S(I3CC)
  200 ILAST=IL+JJ
      DO 220 I=JJ,ILAST,IDIF
      KLAST=KL+I
```

```
      DO 220 K=I,KLAST,2
      K1=K+KBIT
      K2=K1+KBIT
      K3=K2+KBIT
C
C     DO TWO STEPS WITH J NOT 0
C     A(K)=A(K)+A(K2)*W2
C     A(K2)=A(K)-A(K2)*W2
C     A(K1)=A(K1)*W+A(K3)*W3
C     A(K3)=A(K1)*W-A(K3)*W3
C
C     A(K)=A(K)+A(K1)
C     A(K1)=A(K)-A(K1)
C     A(K2)=A(K2)+A(K3)*I
C     A(K3)=A(K2)-A(K3)*I
C
      R=A(K2)*W2(1)-A(K2+1)*W2(2)
      T=A(K2)*W2(2)+A(K2+1)*W2(1)
      A(K2)=A(K)-R
      A(K)=A(K)+R
      A(K2+1)=A(K+1)-T
      A(K+1)=A(K+1)+T
C
      R=A(K3)*W3(1)-A(K3+1)*W3(2)
      T=A(K3)*W3(2)+A(K3+1)*W3(1)
      AWR=A(K1)*W(1)-A(K1+1)*W(2)
      AWI=A(K1)*W(2)+A(K1+1)*W(1)
      A(K3)=AWR-R
      A(K3+1)=AWI-T
      A(K1)=AWR+R
      A(K1+1)=AWI+T
      T=A(K1)
      A(K1)=A(K)-T
      A(K)=A(K)+T
      T=A(K1+1)
      A(K1+1)=A(K+1)-T
      A(K+1)=A(K+1)+T
      R=-A(K3+1)
      T=A(K3)
      A(K3)=A(K2)-R
      A(K2)=A(K2)+R
      A(K3+1)=A(K2+1)-T
  220 A(K2+1)=A(K2+1)+T
C     END OF I AND K LOOPS
C
  230 JJ=JJDIF+JJ
C     END OF J-LOOP
C
  235 JLAST=4*JLAST+3
  240 CONTINUE
C     END OF  L  LOOP
C
  250 CONTINUE
C     END OF  ID  LOOP
C
C     WE NOW HAVE THE COMPLEX FOURIER SUMS BUT THEIR ADDRESSES ARE
C     BIT-REVERSED.  THE FOLLOWING ROUTINE PUTS THEM IN ORDER
      NTSQ=NT*NT
      M3MT=M3-MT
  350 IF(M3MT) 370,360,360
C
C     M3 GR. OR EQ. MT
  360 IGO3=1
      N3VNT=N3/NT
      MINN3=NT
      GO TO 380
C
C     M3 LESS THAN MT
  370 IGO3=2
      N3VNT=1
      NTVN3=NT/N3
      MINN3=N3
  380 JJD3 = NTSQ/N3
      M2MT=M2-MT
  450 IF (M2MT)470,460,460
C
```

```
C        M2 GR. OR EQ. MT
  460 IGO2=1
      N2VNT=N2/NT
      MINN2=NT
      GO TO 480
C
C        M2 LESS THAN MT
  470 IGO2 = 2
      N2VNT=1
      NTVN2=NT/N2
      MINN2=N2
  480 JJD2=NTSQ/N2
      M1MT=M1-MT
  550 IF(M1MT)570,560,560
C
C        M1 GR. OR EQ. MT
  560 IGO1=1
      N1VNT=N1/NT
      MINN1=NT
      GO TO 580
C
C        M1 LESS THAN MT
  570 IGO1=2
      N1VNT=1
      NTVN1=NT/N1
      MINN1=N1
  580 JJD1=NTSQ/N1
  600 JJ3=1
      J=1
      DO 880 JPP3=1,N3VNT
      IPP3=INV(JJ3)
      DO 870 JP3=1,MINN3
      GO TO (610,620),IGO3
  610 IP3=INV(JP3)*N3VNT
      GO TO 630
  620 IP3=INV(JP3)/NTVN3
  630 I3=(IPP3+IP3)*N2
  700 JJ2=1
      DO 870 JPP2=1,N2VNT
      IPP2=INV(JJ2)+I3
      DO 860 JP2=1,MINN2
      GO TO (710,720),IGO2
  710 IP2=INV(JP2)*N2VNT
      GO TO 730
  720 IP2=INV(JP2)/NTVN2
  730 I2=(IPP2+IP2)*N1
  800 JJ1=1
      DO 860 JPP1=1,N1VNT
      IPP1=INV(JJ1)+I2
      DO 850 JP1=1,MINN1
      GO TO (810,820),IGO1
  810 IP1=INV(JP1)*N1VNT
      GO TO 830
  820 IP1=INV(JP1)/NTVN1
  830 I=2*(IPP1+IP1)+1
      IF (J-I) 840,850,850
  840 T=A(I)
      A(I)=A(J)
      A(J)=T
      T=A(I+1)
      A(I+1)=A(J+1)
      A(J+1)=T
  850 J=J+2
  860 JJ1=JJ1+JJD1
C
  870 JJ2=JJ2+JJD2
C        END OF JPP2 AND JP3 LOOPS
C
  880 JJ3 = JJ3+JJD3
C        END OF JPP3 LOOP
C
  890 IF(IFSET)891,895,895
  891 DO 892 I = 1,NX
  892 A(2*I) = -A(2*I)
  895 RETURN
```

```
C       THE FOLLOWING PROGRAM COMPUTES THE SIN AND INV TABLES.
C
  900 MT=MAXO(M(1),M(2),M(3)) -2
      MT = MAXO(2,MT)
  904 IF (MT-18) 906,906,13
  906 IFERR=0
      NT=2**MT
      NTV2=NT/2
C
C       SET UP SIN TABLE
C       THETA=PIE/2**(L+1) FOR L=1
  910 THETA=.7853981633974483
C
C       JSTEP=2**(MT-L+1) FOR L=1
      JSTEP=NT
C
C       JDIF=2**(MT-L) FOR L=1
      JDIF=NTV2
      S(JDIF)=SIN(THETA)
      DO 950 L=2,MT
      THETA=THETA/2.0D0
      JSTEP2=JSTEP
      JSTEP=JDIF
      JDIF=JSTEP/2
      S(JDIF)=SIN(THETA)
      JC1=NT-JDIF
      S(JC1)=COS(THETA)
      JLAST=NT-JSTEP2
      IF(JLAST - JSTEP) 950,920,920
  920 DO 940 J=JSTEP,JLAST,JSTEP
      JC=NT-J
      JD=J+JDIF
  940 S(JD)=S(J)*S(JC1)+S(JDIF)*S(JC)
  950 CONTINUE
C
C       SET UP INV(J) TABLE
C
  960 MTLEXP=NTV2
C
C       MTLEXP=2**(MT-L). FOR L=1
      LM1EXP=1
C
C       LM1EXP=2**(L-1). FOR L=1
      INV(1)=0
      DO 980 L=1,MT
      INV(LM1EXP+1) = MTLEXP
      DO 970 J=2,LM1EXP
      JJ=J+LM1EXP
  970 TNV(JJ)=INV(J)+MTLEXP
      MTLEXP=MTLEXP/2
  980 LM1EXP=LM1EXP*2
  982 IF(IFSET)12,695,12
      END
```

```
      SUBROUTINE ICSSGU (X,Y,DY,S,N,A,B,C,D,WK)
C
C-ICSSGU--------S-------LIBRARY 1-----------------------------------------
C
C   FUNCTION            - CUBIC SPLINE DATA SMOOTHING
C   USAGE               - CALL ICSSMU(X,Y,DY,S,N,A,B,C,D,WK)
C   PARAMETERS   X      - VECTOR OF N ABSCISSA  X(1),X(2),
C                           ...,X(N). WE ASSUME X(I).GT.X(I-1)
C                           FOR I=2,3,...,N
C                Y      - VECTOR OF N FUNCTIONAL VALUES Y(1),Y(2),
C                           ...,Y(N). Y(I) IS THE FUNCTIONAL VALUE
C                           AT X(I)
C                DY     - VECTOR OF INPUT PARAMETERS DY(1),DY(2),
C                           ...,DY(N) WHERE DY(I) IS AN ESTIMATE OF
C                           THE STANDARD DEVIATION OF THE ORDINATE Y(I)
C                S      - A NON-NEGATIVE PARAMETER WHICH CONTROLS THE
C                           EXTENT OF SMOOTHING
C                N      - NUMBER OF DATA POINTS
C                A      - OUTPUT VECTOR OF SPLINE COEFFICIENTS
C                           A(1),A(2),...,A(N+1)
C                B      - OUTPUT VECTOR OF SPLINE COEFFICIENTS
C                           B(1),B(2),...,B(N+1)
C                C      - OUTPUT VECTOR OF SPLINE COEFFICIENTS
C                           C(1),C(2),...,C(N+1)
C                D      - OUTPUT VECTOR OF SPLINE COEFFICIENTS
C                           D(1),D(2),...,D(N+1)
C                           THE CUBIC SPLINE F(XX) IS CONSTRUCTED IN
C                           THE I-TH (I=1,2,...,N-1) INTERVAL BY
C                           F(XX)=((D(I+1)*H+C(I+1))*H+B(I+1))*H+A(I+1)
C                           WHERE H = XX-X(I)
C                WK     - WORK AREA OF DIMENSION .GE. 7*N+9
C   PRECISION           - SINGLE
C   LANGUAGE            - FORTRAN
C-------------------------------------------------------------------------
C   LATEST REVISION     - SEPTEMBER 29, 1972
C
      SUBROUTINE ICSSGU   (X,Y,DY,S,N,A,B,C,D,WK)
C
      DIMENSION           X(1),Y(1),DY(1),A(1),B(1),C(1),D(1),WK(1)
C                                  SET UP WORKING AREAS
      NP1=N+1
      IB1 = NP1
      IB2 = IB1+NP1
      IB3 = IB2+NP1+1
      IB4 = IB3+NP1
      IB5 = IB4+NP1
      IB6 = IB5+NP1+1
      WK(1) = 0.
      WK(2) = 0.
      WK(IB2) = 0.
      WK(IB3) = 0.
      IJK2 = IB2+NP1
      WK(IJK2)=0.
      IJK5 = IB5 + 1
      WK(IJK5)=0.
      IJK5 = IB5 + 2
      WK(IJK5)=0.
      WK(IB6) = 0.
      IJK5 = IB5+NP1
      WK(IJK5)=0.
      P=0.
      H=X(2)-X(1)
      F2=-S
      F=(Y(2)-Y(1))/H
      IF (N.LT.3) GO TO 25
      DO 5  I=3,N
         G=H
         H=X(I)-X(I-1)
         E=F
         F=(Y(I)-Y(I-1))/H
         A(I)=F-E
         IJK3 = IB3+I
         WK(IJK3)=(G+H)*.6666667
         IJK4 = IB4+I
         WK(IJK4)=H/3.
         IJK2 = IB2+I
```

```
          WK(IJK2)=DY(I-2)/G
          WK(I) = DY(I)/H
          IJK1 = IB1+I
          WK(IJK1)=-DY(I-1)/G-DY(I-1)/H
    5 CONTINUE
      DO   7 I=3,N
          IJK1=IB1+I
          IJK2=IB2+I
          B(I) = WK(I)*WK(I)+WK(IJK1)*WK(IJK1)+WK(IJK2)*WK(IJK2)
          C(I) = WK(I)*WK(IJK1+1)+WK(IJK1)*WK(IJK2+1)
          D(I) = WK(I)*WK(IJK2+2)
    7 CONTINUE
C                                        NEXT ITERATION
   10 IF (N.LT.3) GO TO 25
      DO  15   I=3,N
          IJK1 = IB1+I-1
          IJK0 = I-1
          WK(IJK1)=F*WK(IJK0)
          IJK2 = IB2+I-2
          IJK0 = I-2
          WK(IJK2)=G*WK(IJK0)
          IJK0 = I
          IJK3 = IB3+I
          WK(IJK0)=1./(P*B(I)+WK(IJK3)-F*WK(IJK1)-G*WK(IJK2))
          IJK5 = IB5+I
          IJKN = IJK5-1
          IJK0 = IJKN-1
          WK(IJK5) = A(I)-WK(IJK1)*WK(IJKN)-WK(IJK2)*WK(IJK0)
          IJK4 = IB4+I
          F=P*C(I)+WK(IJK4)-H*WK(IJK1)
          G=H
          H=D(I)*P
   15 CONTINUE
      DO  20  I=3,N
          J=N-I+3
          IJK5 = IB5+J
          IJK6 = IJK5+1
          IJK7 = IJK6+1
          IJK1 = IB1+J
          IJK2 = IB2+J
          WK(IJK5) = WK(J)*WK(IJK5)-WK(IJK1)*WK(IJK6)-WK(IJK2)*WK(IJK7)
   20 CONTINUE
   25 E=C
      H=0
                                         COMPUTE U AND ACCUMULATE E
      DO 30  I=2,N
          G=H
          IJK5 = IB5+I
          H = (WK(IJK5+1)-WK(IJK5))/(X(I)-X(I-1))
          IJK6 = IB6+I
          WK(IJK6)=(H-G)*DY(I-1)*DY(I-1)
          E=E+WK(IJK6)*(H-G)
   30 CONTINUE
      G=-H*DY(N)*DY(N)
      IJK6 = IB6+NP1
      WK(IJK6)=G
      G=F2
      F2=E*P*P
      IF(F2.GE.S .OR. F2.LE.G) GO TO 45
      F=0.
      IJK6 = IB6+2
      H = (WK(IJK6+1)-WK(IJK6))/(X(2)-X(1))
      IF(N.LT.3) GO TO 40
      DO 35  I=3,N
          G=H
          IJK6 = IB6+I
          H = (WK(IJK6+1)-WK(IJK6))/(X(I)-X(I-1)
          IJK1 = IB1+I-1
          IJK2 = IB2+I-2
          G = H-G-WK(IJK1)*WK(I-1)-WK(IJK2)*WK(I-2)
          F = F+G*WK(I)*G
          WK(I) = G
   35 CONTINUE
   40 H=E-P*F
      IF(H.LE.0) GO TO 45
C                                        UPDATE THE LAGRANGE MULTIPLIER P
```

```
C                                             FOR THE NEXT ITERATION
      P = P + (S-F2)/((SQRT(S/E)+P)*H)
      GO TO 10
C                                             IF E LESS THAN OR EQUAL TO S,
C                                             COMPUTE THE COEFFICIENTS AND RETURN.
   45 DO 50  I=2,NP1
         IJK6 = IB6+I
         A(I)=Y(I-1)-P*WK(IJK6)
         IJK5 = IB5+I
         C(I)=WK(IJK5)
   50 CONTINUE
      DO 55  I=2,N
         H=X(I)-X(I-1)
         D(I)=(C(I+1)-C(I))/(3.*H)
         B(I)=(A(I+1)-A(I))/H-(H*D(I)+C(I))*H
   55 CONTINUE
 9005 RETURN
      END
```